CONTROL AND ENERGY EFFICIENCY OPTIMIZATION OF HIGH-POWER PUMP AND FAN SYSTEMS

A thesis submitted for the degree of

Doctor of Philosophy

2014

Ing. Martin Sirový

ZÁPADOČESKÁ UNIVERZITA V PLZNI
FAKULTA ELEKTROTECHNICKÁ

ŘÍZENÍ A OPTIMALIZACE ENERGETICKÉ ÚČINNOSTI ČERPACÍCH A VENTILÁTOROVÝCH SYSTÉMŮ VELKÉHO VÝKONU

Disertační práce

k získání akademického titulu doktor

v oboru

Elektronika

Autor: Ing. Martin Sirový
Školitel: prof. Ing. Zdeněk Peroutka, Ph.D.
Datum státní doktorské zkoušky: 27. 4. 2011
Datum odevzdání práce: 10. 6. 2014

Prohlášení autora

Předkládám tímto k posouzení a obhajobě disertační práci zpracovanou na závěr doktorského studia na Fakultě elektrotechnické Západočeské univerzity v Plzni. Prohlašuji, že jsem tuto práci vypracoval samostatně s použitím odborné literatury a pramenů, uvedených v seznamu, který je součástí této práce.

V Plzni 10. 6. 2014   _____

                                                                                        Ing. Martin Sirový

Prohlášení garanta projektu

V Plzni 10. 6. 2014   _____

                                                                                  prof. Ing. Zdeněk Peroutka, Ph.D.

Acknowledgement

At this place, I would like to thank to my supervisor prof. Ing. Zdeněk Peroutka, Ph.D. for his supervising, support and exemplary attitude while working on research projects. In addition, I have to thank to the whole team I was working in – especially to Ing. Jan Michalík Ph. D. for help with a painstaking work on the user interface of software tools and to Ing. Miroslav Byrtus Ph. D. for his knowledge of mechanics and help on modeling of fan systems.

Finally, I must thank to my parents and especially to my wife and daughter for their support and joy, which they give me every day.

Martin Sirový

Abstrakt

Výkonové čerpací a ventilátorové systémy se řadí mezi nejvýznamnější spotřebiče elektrické energie. Vlivem vývoje výkonové elektroniky a frekvenčních měničů skýtají tyto systémy významný potenciál pro optimalizaci spotřeby elektrické energie plynoucí z aplikace energetické účinné otáčkové regulace na místo ztrátových, stále využívaných, zejména pasivních metod regulace průtoku. Mezi hlavní důvody, které doposud brání masivnímu prosazení výkonové elektroniky ve stávajících i nových instalacích, patří zejména náročnost spolehlivého technického a ekonomického zhodnocení přínosu, respektive exaktního vyjádření nákladů za dobu životnosti celého aplikačního řetězce. Z toho důvodu je tato práce zaměřena právě na vývoj uceleného souboru matematických modelů, metodiky a softwarových nástrojů pro zejména technické zhodnocení a optimalizaci řízení a energetické účinnosti těchto systémů s důrazem na praktickou využitelnost výsledků práce v reálných aplikacích.

Úvodní část práce je věnována motivaci výzkumu a vývoje, cílům práce a shrnutí aktuálního stavu poznaní v řešené problematice. Druhá část je zaměřena na optimalizaci hydraulických systémů s jedním čerpadlem. Je představen komplexní soubor matematických modelů pro řešení aplikačního řetězce počínaje modely hydraulického systému a čerpadla včetně souboru metod regulací průtoku přes pohon až po vstupní napájecí transformátor. Třetí část pokračuje pneumatickými systémy s jedním ventilátorem. Je popsán matematický model pneumatického systému a ventilátoru uvažující proměnnou hustotu média. Dále jsou představeny modely technik regulací průtoku jak pro radiální, tak pro axiální ventilátory. Důraz byl kladen na striktní využití standardně dostupných dat (tj. bez využití laboratorních měření). Z toho důvodu byly vyvinuty speciální aproximační techniky a metodika pro odhad energetické spotřeby systému mimo jmenovité provozní stavy, které jsou často jako jediné k dispozici. Navržené matematické modely byly následně implementovány do softwarových nástrojů pro optimalizaci energetické účinnosti hydraulických a pneumatických aplikací – MVD Pump Save 2012 a MVD Fan Save 2012. Vyvinutý software, matematické modely i metodika byly následně verifikovány na případových studiích. Součástí práce jsou i typizované výkonnostní křivky jednotlivých komponent aplikačního řetězce. Poslední část je věnována optimální strategii regulace průtoku pro čerpací aplikace s čerpadly pracujícími paralelně do společného hydraulického systému. Je představen navržený algoritmus a metodika pro řešení optimálního přerozdělení průtoku čerpadly z pohledu celkové energetické účinnosti. Pro obecné řešení optimalizační úlohy v nelineárním multidimenzionálním prostoru bylo zvoleno numerické řešení hrubou silou. Pro úlohy s omezenými stupni volnosti pak bylo odvozeno zjednodušené řešení, které výrazně snižuje výpočetní náročnost algoritmu pro speciální případy. Výsledky algoritmu jsou detailně graficky prezentovány na vypracovaných případových studiích. Na základě výchozích případových studií byla dále zpracována analýza vlivu statické složky tlaku hydraulického systému a prezentace vlivu variabilního výkonového složení skupiny čerpadel na optimální strategii regulace průtoku. Na závěr práce jsou shrnuty hlavní přínosy práce a perspektivní směry dalšího výzkumu.

Hlavními přínosy práce jsou zejména vyvinuté expertní systémy pro návrh optimálního pohonu a řízení výkonových čerpacích a ventilátorových aplikací a návrh algoritmu pro optimální řízení průtoku paralelních čerpadel pracujících do společného hydraulického sytému.

Abstract

The high-power pump and fan applications are among the main electricity appliances in a worldwide scale. Concurrently, these applications have a very significant energy-saving potential arising especially from development of high-power electronics and/or frequency converters enabling energy efficient flow control. One of the major barriers, preventing massive redesign of existing installations and use of the energy-saving potential in new applications, is the complexity of precise technical and economical evaluation of the lifetime energy savings and energy consumption of the entire application chain. Hence, the thesis has focused on a development of a complex set of mathematical models, methodology and software tools for especially technical evaluation and energy efficiency optimization of these systems with impact to practical usability of the results in real systems.

The introductory part of the work is dedicated to the state of the art, research motivation and objectives of the work. In the second part, the attention is paid to single pump systems. It is presented a set of mathematical models for a detailed evaluation of the application chain, beginning from models of hydraulic system and pump including collection of flow controls methods over drive part to power supply transformer. The third part deals with single fan systems. It describes mathematical models of pneumatic system and fan considering compressible medium. The most common flow control techniques for both radial and axial fans are also included. The impact has been put on to use strictly just commonly available data (i.e. non-laboratory measurements). Therefore, special approximation techniques and methodology has been developed to be able to estimate a system behavior out of the nominal operating state, which is commonly the only one specified. Finally, there have been developed sophisticated software tools for energy efficiency optimization of single pump and fan applications – MVD Pump Save 2012 and MVD Fan Save 2012. The performance of developed mathematical models, methodology and software tools is widely presented on evaluated case studies. A typical performance curves for application components has been also included as a referenced one to provide a complex set of relevant data for poorly specified case studies.

The last section of the thesis is dedicated to optimal control strategy of multiple pumps operating in parallel into common hydraulic system. It is presented the proposed algorithm and/or methodology for generation of an optimal control strategy of these systems. The presented algorithm is based on numerical optimization method using brute force approach, which enabled to solve the non-linear multidimensional optimization task. A special solution, which significantly speed-up the calculation process, for the cases of restricted space of freedom is also presented. The performance of the algorithm has been in detailed graphically presented on elaborated case studies. Additionally, the influence of a static head of a hydraulic system and the effect of variable sizing of pump in a pump group on an optimal control strategy have been presented.

In the conclusion, it is summarized the main contributions of the work and the very last part presents the challenges for future research.

The main contribution of this thesis is the development of the expert systems allowing optimal control design of high power pump and fan applications and proposed approach for optimal group control design of parallel pumps working into common hydraulic system.

Kurzfassung der Dissertation

Weltweit gehören Hochleistungspumpen und -lüfter zu Hochstromanwendungen mit großem Energiesparpotenzial. Die Nutzung dieser Energiesparpotenziale ist vor allem durch die Entwicklung von Hochleistungselektronik respektive Frequenzumrichtern möglich, wobei gleichzeitig eine energieeffiziente Durchsatz- und Flusskontrolle realisiert werden kann. Bei Anwendung solcher Frequenzumrichter soll andererseits eine massive Umgestaltung bestehender Anlagen verhindert werden. Generell ist bei Nutzung der Energiesparpotenziale sowohl in bestehenden, als auch in neuen Anlagen die Komplexität der genauen technischen und wirtschaftlichen Bewertung der Lebensdauer, die Energieeinsparung und der Energieverbrauch der gesamten Anwendungskette zu beachten. Daher ist die vorliegende Arbeit der Entwicklung von mathematischen Modellen, Methoden und Software-Werkzeugen für eine technische Bewertung und Optimierung der Energieeffizienz von solchen Systemen gewidmet. Außerdem werden Auswirkungen auf die praktische Verwendbarkeit der erreichten Ergebnisse in realen Systemen betrachtet.

Im einleitenden Teil der Arbeit werden der Stand der Technik, der Forschung sowie Motivation und Ziele der Arbeit beschrieben. Der zweiter Teil ist der Anwendung von Einzelpumpenanlagewidmet. Dabei werden mathematische Modelle für eine detaillierte Auswertung der Anwendungskette angegeben, beginnend mit Modellen der Hydraulik und Pumpe bei verschiedenen Ablaufsteuerungen bis zu Modellen des Antriebsteiles und Transformator. Der dritte Teil befasst sich mit Einzellüfter -Systemen. Es werden mathematische Modelle der pneumatischen Systeme und Lüfter bei Berücksichtigung komprimierbarer Medien beschrieben. Häufigsten Flusssteuerungstechniken für Radial und Axialventilatoren sind ebenfalls enthalten. Die Modelle wurden so entwickelt, dass nur allgemein verfügbare Daten genutzt werden können. Schwerpunkt sind deshalb Techniken und Methoden zur Beschreibung des Systemverhaltens in der Umgebung des Nennbetriebszustands. Schließlich wurden ausgereifte Software-Tools entwickelt, die eine Optimierung der Energieeffizienz von einzelnen Pumpen und Lüfteranwendungen - MVD Pump Save 2012 und MVD Fan Save 2012 - ermöglichen. Die Leistungsfähigkeit der entwickelten mathematischen Modelle, Methoden und Software-Werkzeuge ist weitestgehend über evaluiert Fallstudien vorgestellt. Typische Leistungskurven für Anwendungskomponenten wurden auch als Referenz erarbeitet, um eine komplexe Reihe von relevanten Daten auch für schlecht angegebenen Fallstudien zu erhalten.

Der letzte Abschnitt der Arbeit ist der optimale Steuerstrategie von mehreren Pumpen, die parallel in gemeinsamen Hydrauliksystemen betrieben werden, gewidmet. Es stellt dar den speziellen Algorithmus und / oder eine Methode zur Erzeugung eines optimalen Regelstrategie dieser Systeme. Der vorgestellte Algorithmus basiert auf numerischen Optimierungsverfahren mit Brute-Force Ansatz und ermöglicht die nicht-lineare mehrdimensionale Optimierung. Eine spezielle Lösung Beschleunigt dabei der Rechenprozess, wobei Fälle von eingeschränkten Freiheitgraden präsentiert werden. Die Leistung des Algorithmus wurde in detaillierten grafisch ausgearbeiteten Fallstudien vorgestellt. Zusätzlich wurde der Einfluß einer statischen Komponente eines hydraulischen Systems und der Wirkung der variablen Dimensionierung der Pumpe in einer Pumpengruppe auf einer optimalen Regelstrategie betrachtet.

Als Schlussfolgerung werden die Hauptbeiträge der Arbeit zusammengefasst und ein Ausblick zu Herausforderungen für die zukünftige Forschung angegeben.

Die Schwerpunkte dieser Arbeit sind die entwickelte Expertensysteme, die eine optimale Kontrolle Design von Hochleistungspumpen und -lüfter ermöglichen und vorgeschlagene Ansatz für die optimale Gruppenkontroll der parallel Pumpen, die in gemeinsamen Hydrauliksystem arbeiten.

Contents

Nomenclature

List of Symbols and Abbreviations		
Symbol	Definition	Unit
A	area	$[m^2]$
C_E	energy costs	[currency]
C_{Inflow}	cash inflow	[currency]
C_{Invest}	investment costs	[currency]
$C_{Outflow}$	cash outflow	[currency]
CFC	compared flow control	
$\cos\phi$	power factor	[-]
Δp_L	pressure loss in pipe	[Pa]
ΔP_T	transformer power losses	[kW]
ΔP_{T0}	transformer no-load power losses	[kW]
D	inside pipe diameter (e.g. (2.5)), impeller diameter (e.g. (2.19))	[m]
η	efficiency	[-]
η_{CF}	efficiency of fan control strategy	[-]
η_{CP}	efficiency of pump control strategy	[-]
η_F	fan efficiency	[-]
η_G	gearbox efficiency	[-]
η_{HC}	hydrodynamic coupling efficiency	[-]
η_M	motor efficiency	[-]
η_P	pump efficiency	[-]
η_{POP}	pump efficiency at operating point from operating profile	[-]
η_{PS}	pump efficiency at the point of intersection of pump and system curve	[-]
η_T	transformer efficiency	[-]
E	energy	[MWh]
E_c	energy consumption	[MWh]
E_{hP}	pump hydraulic energy	[MWh]
E_{hS}	system hydraulic energy	[MWh]
E_{pF}	fan pneumatic energy	[MWh]
E_{pS}	system pneumatic energy	[MWh]
f_{sM}	motor stator frequency	[Hz]
f_{rM}	motor rotor frequency (motor rotor mechanical speed)	[Hz]
$f_{rM(el)}$	Electrical rotor speed of motor ($f_{rM(el)} = f_{rM} \cdot n_{pp}$)	[Hz]
f_t	friction factor	[-]

List of Symbols and Abbreviations		
Symbol	Definition	Unit
g	acceleration of gravity (9,80665 m/s^2)	[m/s^2]
h	height	[m]
H	head	[m]
$H_{AuxCmax}$	head component of pump auxiliary curve for maximal flow under VSC	[m]
$H_{AuxCmin}$	head component of pump auxiliary curve for minimal flow under VSC	[m]
H_L	head loss in pipe	[m]
H_{Lv}	head loss in valve	[m]
H_P	pump head	[m]
H_{PmaxC}	head of auxiliary curve of maximal flow	[m]
H_{PminC}	head of auxiliary curve of minimal flow	[m]
H_S	system head	[m]
H_{SD}	system discharge head	[m]
H_{SDd}	system discharge dynamic (friction) head	[m]
H_{SDs}	system discharge static head	[m]
H_{SDsp}	system discharge surface pressure head	[m]
H_{SS}	system suction head	[m]
H_{SSd}	system suction dynamic (friction) head	[m]
H_{SSs}	system suction static head	[m]
H_{SSsp}	system suction surface pressure head	[m]
H_{ST}	system total head	[m]
H_{STs}	system total static head	[m]
$H_{STd} = H_{Sd}$	system total dynamic (friction) head	[m]
$H_{STd0} = H_{Sd0}$	system zero-flow total dynamic (friction) head	[m]
$H_{STdN} = H_{SdN}$	system nominal total dynamic (friction) head	[m]
H_{OP}	head of hydraulic system operating point	[m]
H_{OPxeqN}	equivalent of head, for head at system operating point "x" at pump nominal head-flow curve	[m]
H_{PS}	head at intersection of pump and system curve	[m]
i_R	interest rate	[-]
I_{mM}	motor magnetizing current	[A]
I_{sdM}	motor direct (flux) component of stator current	[A]
I_{sM}	motor stator current	[A]
I_{sqM}	motor quadrature (torque) component of stator current	[A]
k_ρ	gas density correction coefficient	[-]

List of Symbols and Abbreviations		
Symbol	Definition	Unit
$k_{\psi M}$	motor constant	[-]
k_{OP}	number of operating points	[-]
K	resistance coefficient	[-]
L	pipe length	[m]
L_{hM}	motor main (magnetizing) inductance	[H]
L_T	transformer per-unit load	[-]
m	mass	[g]
$m_{samples}$	number of samples	[-]
M	molar mass	[g/mole]
n	speed	[rpm]
n	number of moles	[-]
n_F	fan speed	[rpm]
n_{OP}	pump speed at pump operating points	[rpm]
n_P	pump speed	[rpm]
n_{pp}	motor pole-pairs	[-]
n_{PS}	pump speed at intersection of pump and system curve	[rpm]
n_s	specific speed	[-]
$n_{samples}$	number of samples	[-]
n_{s-orig}	original dimension-less specific speed	[-]
n_{var}	number of variants	[-]
NPV	net present value	[currency]
NPSH	net positive suction head	[m]
ω	angular speed	[rad/s]
ω_M	motor angular speed (mechanical rotor speed)	[rad/s]
OP	operating profile	[-]
ϕ	electrical angle between voltage and current	[-]
p	pressure	[Pa]
p	relative load	[-]
p_0	default pressure; $p_0 = 101300$ Pa	[Pa]
p_F	fan pressure	[Pa]
p_S	system pressure	[Pa]
p_{SDsp}	system discharge surface pressure	[Pa]
p_{SSd}	system suction dynamic (friction) pressure	[Pa]
p_{SSs}	system suction static pressure	[Pa]

List of Symbols and Abbreviations		
Symbol	Definition	Unit
p_{SSsp}	system suction surface pressure	[Pa]
$p_{ST} = p_S$	system total pressure	[Pa]
$p_{STd} = p_{Sd}$	system total dynamic (friction) pressure	[Pa]
$p_{STs} = p_{Ss}$	system total static pressure	[Pa]
P	power	[kW]
P_c	power consumption	[kW]
P_{cF}	fan power consumption	[kW]
P_{cF-OP}	fan power consumption at operating points according to operating profile	[kW]
P_{cM}	motor power consumption	[kW]
P_{cP}	pump power consumption	[kW]
P_{cP-OP}	pump power consumption at operating points according to operating profile	[kW]
P_h	hydraulic power	[kW]
P_{hS}	hydraulic power of hydraulic system	[kW]
P_p	pneumatic power	[kW]
P_{pF}	fan pneumatic power	[kW]
P_{pS}	system pneumatic power	[kW]
P_{mM}	motor mechanical (shaft) power	[kW]
P_T	transformer power	[kW]
PV	present value	[currency]
Q	flow – hydraulic systems flow – pneumatic systems	[m^3/h] [m^3/s]
$Q_{AuxCmax}$	flow component of pump auxiliary curve for maximal flow under VSC flow component of fan auxiliary curve for maximal flow under VSC	[m^3/h] [m^3/s]
$Q_{AuxCmin}$	flow component of pump auxiliary curve for minimal flow under VSC flow component of pump auxiliary curve for minimal flow under VSC	[m^3/h] [m^3/s]
Q_{cStep}	flow calculation step	[m^3/h]
Q_F	fan flow	[m^3/s]
Q_{FmaxC}	flow of fan auxiliary curve of maximal flow	[m^3/s]
Q_{FminC}	flow of fan auxiliary curve of minimal flow	[m^3/s]
Q_{FS}	flow at intersection of fan and system curve	[m^3/s]
Q_{OPxeqN}	equivalent of flow rate for flow rate at system operating point "x" at pump nominal head-flow curve equivalent of flow rate for flow rate at system operating point "x" at fan nominal head-flow curve	[m^3/h] [m^3/s]

List of Symbols and Abbreviations		
Symbol	Definition	Unit
Q_P	pump flow	[m³/h]
Q_{PmaxC}	flow of pump auxiliary curve of maximal flow	[m³/h]
Q_{PminC}	flow of pump auxiliary curve of minimal flow	[m³/h]
Q_{PS}	flow at intersection of pump and system curve	[m³/h]
Q_{PT}	total flow of pump group	[m³/h]
Q_S	system flow – hydraulic systems system flow – pneumatic systems	[m³/h] [m³/s]
ρ	density	[kg/m³]
r_G	gearbox ratio	[-]
R	resistance	[Ω]
R	universal gas constant (8,3144621)	[J/mol.K]
R_{Tsc}	transformer short circuit resistance	[Ω]
s	distance	[m]
s_M	motor slip	[-]
S	apparent power	[kVA]
$S_{\omega M}$	motor apparent power under speed control	[kVA]
S_{FC}	frequency converter apparent power	[kVA]
S_M	motor apparent power	[kVA]
S_T	transformer apparent power	[kVA]
t	time	[s]
$t_{PayBack}$	payback period	[years]
$\mathbf{T}$	temperature	[K]
T	torque	[Nm]
T_M	motor torque	[Nm]
$T_{P\text{-}OP}$	pump torque at the operating point according to operating profile	[Nm]
u_{Tsc}	transformer short circuit voltage	[-]
U	voltage or phase to phase voltage	[V]
U_p	phase to ground voltage	[V]
U_{sM}	motor stator voltage	[V]
U_T	transformer voltage	[V]
v	average fluid velocity	[m/s]
V	volume	[m³]
VFC	variable frequency control	
VSC	variable speed control	

List of Symbols and Abbreviations		
Symbol	Definition	Unit
X	reactance	[Ω]
X_σ	leakage reactance	[Ω]
X_m	main reactance	[Ω]
X_{Tsc}	transformer short circuit reactance	[Ω]
x_{Tsc}	transformer short circuit reactance	[-]
Z_L	load impedance	[Ω]
z_{Tsc}	transformer short circuit impedance	[-]

GENERAL INDICES – PUMPS		
Index	Definition	Examples
1	original state	Q_1
2	transformed state	Q_2
avg	average	
AuxC	auxiliary curve	
BEP	Best Efficiency Point	
CFC	compared flow control	
Δ	different between in-state and out-state	ΔH
eqN	equivalent to nominal value	Q_{OP1eqN}
FC	frequency converter	η_{FC}
G	gearbox	η_G
HC	hydrodynamic coupling	η_{HC}
in	at inlet, into the component	H_{in}
IGV	inlet guide vanes	
Invest	Investment	
max	maximal value	Q_{OP_max}
min	minimal value	Q_{OP_min}
minC	auxiliary curve for minimal flow	H_{PminC}
M	motor	η_M
N	nominal value	Q_N
OP	operating point	Q_{OP}
sc	short circuit	Z_{Tsc}
VFC	variable frequency control	
VS	variable speed	
VSC	variable speed control	

GENERAL INDICES – PUMPS		
Index	Definition	Examples
out	at outlet, out of the component	H_{out}
OPxeqN	equivalent nominal operating point for operating point "x"	
pu	per unit value	Q_{pu}
R	referenced value	η_R
T	transformer	η_T
T	total value	P_{hT}
wavg	weighted average	Q_{wavg}

FUNCTION DEFINITIONS		
Notation	Description	Examples
f(x)	function	$\eta=f(Q)$, $H = H(Q)$
$f_{IntersectLinIntArrays}$(**X1**,**Y1**,**X2**,**Y2**)	Find intersect of two discrete curves using linear interpolation represented by four one-dimension arrays.	
Y2 = $f_{IntLinArray}$(**X1**,**Y1**,X2)	Find linearly interpolated value for a discrete curve defined by two one-dimension arrays.	
Y2 = $f_{IntCubArray}$(**X1**,**Y1**,X2)	Find cubically interpolated value for a discrete curve defined by two one-dimension arrays.	
Z2 = $f_{IntLin2DArray}$(**X1**,**Y1**,**Z1**,X2,Y2)	Find linearly interpolated value in 2 dimensional space defined by two one-dimensional arrays representing axis (X1,Y1) and one two dimensional array defining z-component (Z1) for the point defined by X2 and Y2.	

Note 1 – Array, matrix, vector notation: Highlighted by bold font.

Note 2 – Scalar notation: Highlighted by italic font.

Note 3 – Matrices multiplication: Matrix multiplication is marked by symbol: "*", matrix and array multiplication in the meaning element by element is expressed by symbol ".*" (Mathworks Matlab notation).

Note 4 – Matrices division: Matrix division is marked by symbol: "/", matrix and array division in the meaning element by element is expressed by symbol "./" .

Note 5 – Relation between "per-unit" and "percentage" expression: $x_{percentage}[\%] = x_{per-unit}[-] \times 100$

1   Introduction

Energy efficiency topics are discussed across different technical areas still louder. The reason is plain enough – the world primary energy demand rises (see Fig. 1.1, [1]) despite of an effort to turn down this tendency and world strategic energy resources are limited. Improving energy efficiency of especially high-power technologies employed by main industrial consumers can significantly influence this negative trend. Respectively, it has significant local impact in the form of reducing operating costs and improving competitive strength among industrial companies and global impact from environmental point of view.

The topic of energy efficiency optimization in pump or fan applications has been discussed in the industry area since about 1970 – see Chapter 1.2.1. However, approximately since 2000 we can see the steeply increasing interest on energy savings in especially pumping systems. There has been founded organizations focusing specifically on research, publishing and promotion of energy saving potential in this area and the field of pump and fan applications become often discussed on worldwide energy conferences and among industrial companies and manufacturers. Why this repetitive discovery of the traditional field, which has been already in very detail explored and described? The answer is mainly in the rapid development of the field of power electronics, which has changed the traditional view on high-power industrial drives in terms of drive control possibilities. This is used right in drives for pump and fan systems where - while employing variable speed control based on variable speed electrical drive - it is possible to significantly improve the efficiency of these systems in a wide operating range in the contrast to classical fixed speed control methods using fixed speed drives or variable speed drives with traditional slip couplings.
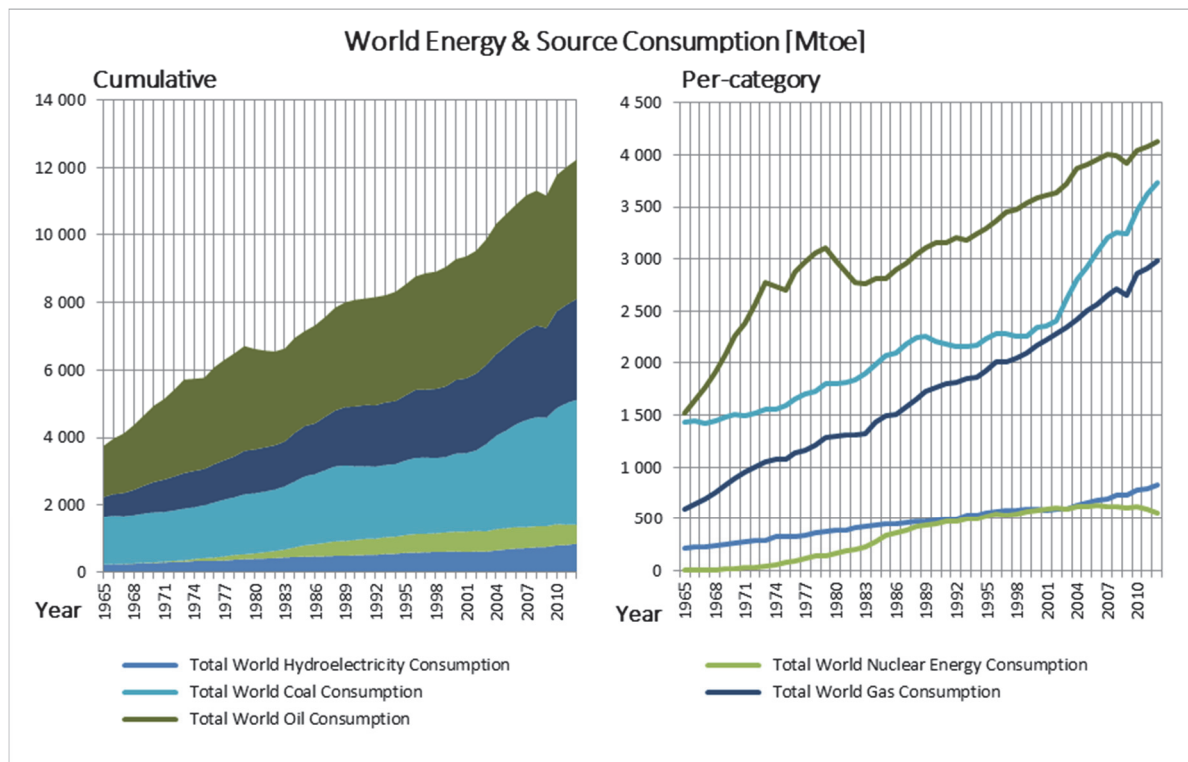

Fig. 1.1 World Energy & Source Consumption [1]

Although there is high energy-saving potential in these applications, the situation has not changed significantly over last years and both retrofit and even new applications do not use the potential in the full range often in practice. There are several main reasons:

1) The complexity of proper and reliable evaluation of pump and fan systems running under variable speed control and its comparison with other flow control technologies considering the entire application chain. It is required knowledge across several technical disciplines from hydraulics and pneumatics over mechanics to electrical machines, drives and control. State of the art tools or publications are usually focused just on a single part of the system without covering the whole application – see Chapter 1.2.2.

2) Next difficulty preventing massive enforcement of energy saving procedures in practice is typically the incomplete set of parameters and/or characteristics of application components, necessary for especially analytical modeling of the system components.

3) The unique character of each hydraulic or pneumatic system. There are hardly to find repeatable solutions that fits most cases – considering not only the point of energy efficiency but also hand in hand, the point of reliability and life cycle costs in general. A detailed analysis of the whole application chain has to be performed in order to be able to adequately estimate energy saving potential of existing installations and to optimize new installations.

4) The complexity of an optimization task of an optimal control strategy for multiple variable speed controlled pumps operating in parallel into common hydraulic system. Existing installations are usually poorly solved, based just on empiric knowledge in combination with test measurements, which is in most cases insufficient.

Since 2008, the University of West Bohemia solved the research project for ABB Switzerland, which has been focused on overcoming of these issues and on development of methodology and software tools that would assist on evaluation of a real energy saving potential of these applications from technical and economical point of view. This is finally the essential step leading to deployment of energy efficient techniques in practice and use of the energy saving potential. This thesis has been written as a part of this project.

The main objective of our research has been put on optimization of pump and fan systems in high-power industrial applications – particularly thermal and/or nuclear power plants, heating plants and pumping stations. The attention on these applications is put primarily because of high energy saving potential. However, defined methodology, proposed mathematical models and software tools that have been developed within this work could be applied to any pump or fan application in general.

1.1   Motivation

According to study elaborated by International Energy Agency (IEA), there is a significant energy saving potential of $18 - 26$ percent in manufacturing industries worldwide [2]. Another study from US Department of Energy (US DoE) presents important saving potential in the range of $10 - 25$ percent applicable in about 72 percent of process industry (see Fig. 1.2, [2] [3]).

The total worldwide electrical power consumption is of about 22 000 TWh per year (Fig. 1.3, [1]). If we consider the ratio of electricity generation from thermal power plants as presented in Fig. 1.1 and the ratio of pump (3,22%) and draft (2,20%) systems of the overall power consumption in the area of power generation in thermal or heating power plants (Fig. 1.4, [4]), then even a tiny efficiency improvement just in the area of thermal power plants involves substantial energy and cost savings and/or CO_2 emission reduction. Moreover, the median load factor of globally installed steam power plants is according to [2], [5] less than 64 percent – see Fig. 1.5. This indicates, that many of currently operating
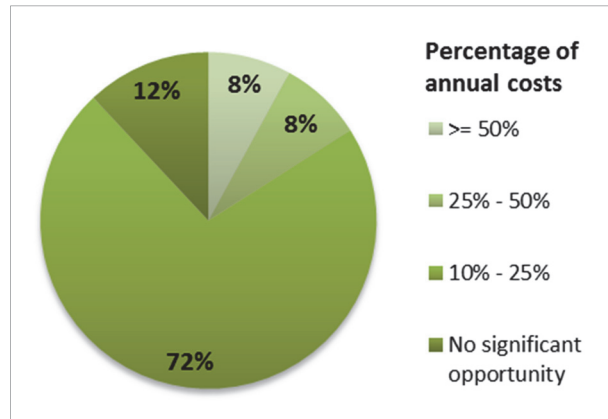
Fig. 1.2 Potential of energy savings in the field of process industry, 2004 [2] [3]
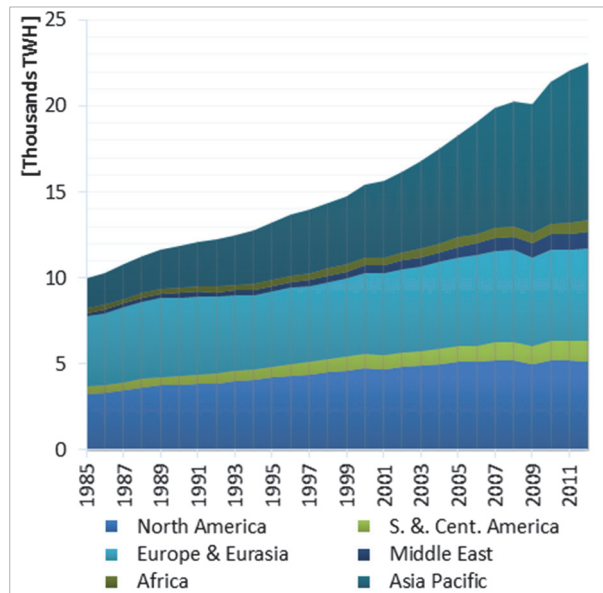
Fig. 1.3 Total World Wide Electricity Power Generation [1]
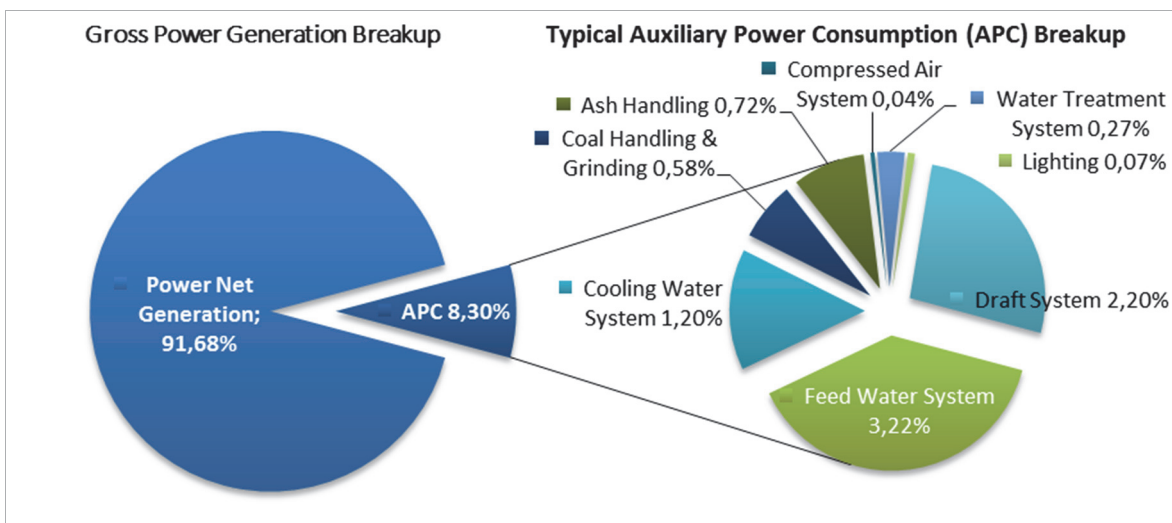
Fig. 1.4 Typical Thermal Power Plant Auxiliary Power Consumption Breakup [4]
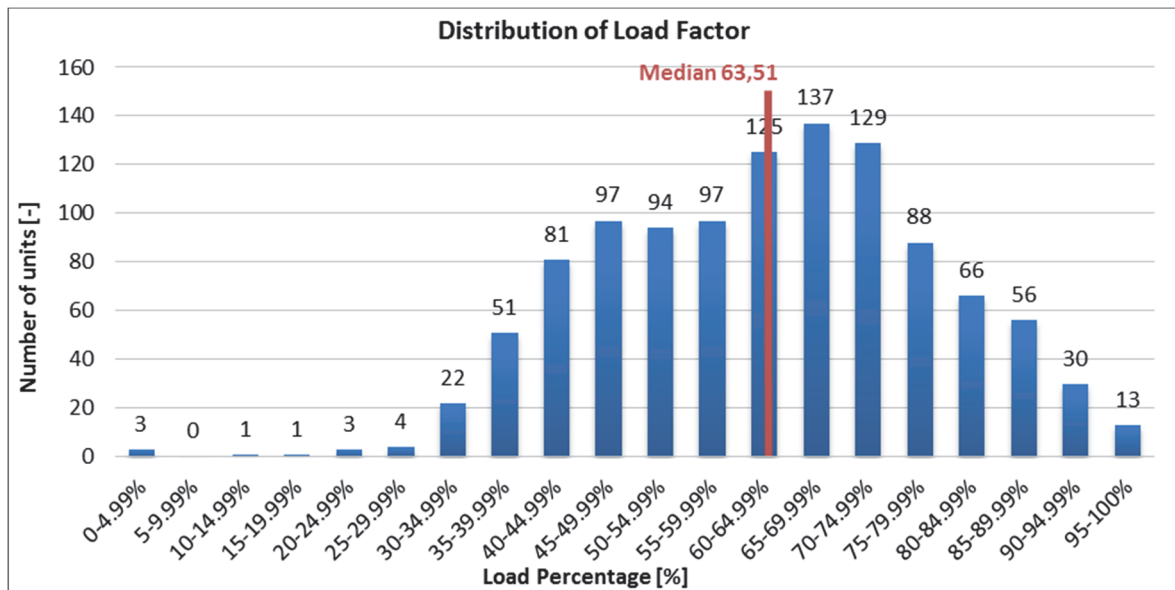
Fig. 1.5 Distribution of load factor of base loaded steam turbines, less than 500 MW, (2001 – 2006) [2] [5]

power plants are working 30-50 percent below their rated capacities [2], where especially pump and fan subsystems without variable speed flow control work significantly behind the optimal operating range from the energy efficiency point of view. Additionally, with the expansion of renewable energy resources, it is expected even higher demands on power variability of base-load power plants and good tools and methodology will be required while designing new or making retrofits of existing installations for evaluation of energy efficiency and demands of employed high-power subsystems like pump or fan applications.

Although there is apparently huge energy saving potential in the field of energy efficiency op-timization in pump and fan application known for years, the implementation in practice runs quite behind. Why? In the contrast to energy saving potential, it is especially the complexity of technical evaluation of these systems and unique character of each application. An improvement, which led to substantial savings in one application, can lead to just opposite in other application.

Hence, one of the essential motivation for this work is to provide the answer, which particular system configuration, flow control or drive topology is the most suitable one from the point of life-cycle cost & energy consumption optimization for a concrete pump or fan application based on the data usually available in real applications. Therefore, the work presents systematically methodology, procedures, mathematical models and software tools which have been developed to make process of evaluation of these systems as much as clear and reliable from both technical and economical point of view.

1.2   State of the art analysis

1.2.1   Evolution

The theory of purely pump and fan systems is very well documented and described. The baseline sources that were used in this work for pump systems and especially centrifugal pumps is [6] and for fan systems [7]. Interestingly, already in 1916, it has been introduced a two speed pump drive to optimize energy consumption [8]. However, although the basic mechanical design of pumps and fans keeps almost unchanged, especially a drive and control possibilities have rapidly developed along with rapid development of power electronics and computational power of industrial controllers.

The first serious considerations about adjustable speed drives as a tool for savings in pump, fan or compressor applications can be found in the last century in seventies – beginning with DC drives, two speed AC drives to AC drives supplied from cycloconverter-type of frequency converter (CCV). In next thirty years (until now), we can see the continual progress in promotion and employment of variable speed drives (VSDs) [9](1982), [10](1997) and sustained interest in energy savings using VSDs in a high-power pump, fan and compressor applications [11](1985) [12](1988) [13](1994) [14](1998) in all possible segments of industry – from thermal [15] [16] (1994) and nuclear power plants [17] (1994), heating plants over gas [18](1989), petroleum and chemistry industries [19](1987) [20](1999) to wastewater, sewage and air-conditioning applications in towns.

In the research and publication activity, there are two main directions of interest and their combination (i) pump and fan applications from the point of system design, evaluation and control optimization and (ii) high-power drives suitable for these applications.

Concerning high-power variable speed drives for pumps, fans and compressor applications, there are basically two options based on either fixed speed electrical motor supplemented by any type of slip coupling or electrical motor supplied from frequency converter.

Variable speed drives based on slip coupling are widely used in industry. There are two main principles based on hydrodynamic coupling or magnetic coupling and both have developed. The hydrodynamic coupling have been developed from simple fluid coupling to the advanced variable speed device based on combination of planetary gear with hydrodynamic coupling – e.g. [21]. The magnetic principle is based on eddy current coupling. The first generations have been based on electromagnets. Last generation is using the clearly mechanical principle and permanent rare earth magnets [22].

Power electronic drives had gone through intensive development from first high-power pump, fan or compressor applications in seventies of the last century, which used mainly CCVs [23]. In eighties and nineties, we can see many applications using current source inverters (CSI), under-synchronous cascades (USC) or load-commutated inverters (LCI) for variable speed drives. Since approximately 2000, the great attention is put on multilevel voltage source converters (VSI) - see [24](2001), [25](2007) and especially [26](2010) although LCI inverters still dominates in very-high power applications.

Looking at the progress of interest in the pump and fan applications from the point of systems design and control, the topic of mainly pumping systems optimizations become again widely discussed and published since about 2000 after the first wave of interest in 1970 - see [27] and group of books ([28] [29] [30]) published by organizations Pump Systems Matter and Hydraulic Institute. The reasons were increasing energy consumption together with increasing energy prices, substantial energy saving potential of these applications and intensive support from government programs, pump and fan manufacturers and especially drive manufacturers headed by manufacturers of power electronic converters, which have developed more reliable and efficient variable speed drives with reasonable payback period. The important motor of research and development is also huge demand and investments in rapidly growing regions in Asia headed by China and India together with many retrofits all over the world.

1.2.2   Challenges

Although, there is a long history of research and development in the area of pump and fan systems, there is still a huge gap between the state of the art of research and amount of optimized pump or fan installations. There are several explanations about that like poor knowledge or misunderstanding of the positive effect of variable speed control among decision makers or bad experience from older installations using power electronic converters, which had serious problems with reliability in comparison to other solutions. However, one of the major reasons according the experience from practice is the lack of tools that would be able to adequately evaluate and compare these systems and give to the investor reliable data about technical and economical parameters of an investment.

There are several software tools available. Siemens has developed online application SinaSave [31] which enables simple calculation of possible cost saving potential for pump, fan and compressor applications, ABB has developed its energy saving tools PumpSave and FanSave [32] and there are other tools available for free – e.g. PSIM published at [33]. These tools are good to get rough idea about the saving potential what is very important at the beginning. Nevertheless, they work usually above too simplified models and use very general approaches omitting individual configurations of each application. This is important especially in high-power pump o fan applications, while a tiny error in simulations leads to substantial error in real operating costs. Moreover, these tools are not able to compare satisfactorily recommended technology with alternatives from possible concurrent technologies and therefore provide to user a complex view of eligible options.

From primary point of view, there are several ways on how to improve these systems. The main trend of control optimization is in replacing of passive flow control methods like throttling, bypass or on-off control methods for pumps and especially dampers for fans for variable speed flow control. The challenging task and the objective of this work is in this case to develop mathematical models and software tools working precisely enough under variable speed control using just data for fixed speed control which are usually the only available.

The second way, which is explored in this work, deals with optimization of control of multiple variable speed controlled pumps working in parallel into common hydraulic system. The optimization commonly used is based on just empiric knowledge and measurements due to complexity of evaluation of optimal control because of optimization task of highly nonlinear and multidimensional system. Recently, there have been published several optimization approaches converting the task into mixed integer nonlinear programming problem ([34], [35]) or using dynamic programing [36]. The advantage of these approaches is especially the "real-time" character. However, the pump performance curves have to be converted into analytical representation which can lead – depending on the shape of the real pump curves - to significant total energy consumption prediction error, especially in very high-power pump applications that are the target ones.

In this thesis, it is presented the numerical optimization method using recursive brute force approach to provide solution taking into account real pump performance curves and precise-enough solution for a general case. Special attention has been also paid to selected cases with restricted space of freedom, which can be often met in real applications.

1.3   Main objectives of this thesis

Based on the state of the art analysis, the thesis focuses on overcoming of the above-defined main issues. By specific, the main objective of the work is to present systematically methodology, procedures, mathematical models and software tools which have been developed for evaluation and optimization of especially single pump and single fan systems with impact on practical usability of the results in real applications. The second main objective is to present the developed algorithm and methodology for generation of optimal control strategy of multiple pumps operating in parallel into common hydraulic system.

For the part of pump systems, the intermediate objectives are set as follows:

1. Develop a complex set of mathematical models of components of single pump applications suitable for variable speed flow control including models of hydraulic system, centrifugal pump and drive (gearbox, electrical motor, hydrodynamic coupling, frequency converter and transformer).

2. Describe the principle and quantify energy demands for pump flow-control methods – both passive (throttling, bypass, on-off) and active (variable speed control).

3. Develop approximation methods based on typical component characteristics and features to ensure basic functionality of the models in the case of poorly specified cases.

4. Implement developed mathematical models and approximation methods in expert software tool Medium Voltage Drive Pump Save.

5. Verify functionality of developed models on typical case studies.

6. Develop algorithm for optimal control strategy of multiple variable speed controlled pumps working in parallel into common hydraulic system.

For fan systems part, the intermediate objectives are set as follows:

7. Develop a complex set of mathematical models of components of single fan applications suitable for variable speed flow control including pneumatic system and both radial and axial type of fan.

8. Describe the principle and quantify energy demands for fan flow-control methods – both passive (inlet damper, outlet damper, inlet guide vanes, pitch control) and active (variable speed control).

9. Develop approximation methods based on typical component characteristics and features to ensure basic functionality of the models in the case of poorly specified cases.

10. Implement developed mathematical models and approximation methods in expert software Medium Voltage Fan Save.

11. Verify a functionality on typical case studies of fan systems.

1.4   Methodology

There have been applied two methodology approaches in this work, which also determines the structure of the work. In the first part of the work dealing with single pump and single fan systems, it has been performed basic analysis of all components of the systems including the all commonly used control techniques. After that, we have developed simplified mathematical models of particular components. The main attention in this research has been paid to development of models using just generally available initial data. Then we performed a detailed analysis and comparison of each simplified mathematical model with advanced fully specified models or with measurement results on real devices. Based on the comparison of analysis results, innovative approximation techniques have been proposed for selected model components to improve the precision and reliability of results while keeping the condition of using just commonly available initial data for model specification.

In order to evaluate efficiently a real pump and fan applications and to verify the performance and interaction of developed mathematical models in a comprehensive way, software tools, which have implemented these models and enabled fast building and/or simulation of complex pump or fan applications under various system configurations and controls, were developed. Real case studies from thermal power plants have been then elaborated to verify the functionality and present the performance of developed mathematical models, methodology and software tools under real applications.

A different approach has been applied for the optimization task of control strategy for multiple pumps working in parallel into common hydraulic system. In this task, the objective was to develop the algorithm and/or methodology enabling determination of optimal operating and/or load diagram for a group of pumps under variable speed control, respectively, to find optimal flow distribution among the pumps so that total efficiency for each operating point (i.e. total flow of the group of pumps) is maximal. The optimization task of non-linear multidimensional space has been solved numerically, based on recursive brute-force principle.

The structure of this thesis mirrors the employed and above described methodology. Except the first introductory chapter, the next chapters continues as follows:

Second chapter describes the optimization process including numerical background for single pump applications. It begins with description of models of hydraulic system and pump suitable for variable speed flow control. Then it derives evaluation of the most common flow control methods – both passive (throttling, bypass, on-off control) and active and/or variable speed flow control. Next section deals with components of drive for both fixed speed and variable speed control including gearbox, hydrodynamic coupling, electrical motor, frequency converter and transformer. Finally, two typical case studies and its variants have been processed in order to present the performance and verify behavior of proposed mathematical models and software tool on real application.

Third chapter deals with energy efficiency optimization of pneumatic systems. It builds on the common parts with hydraulic applications and extends it for chapters describing modeling of pneumatic systems and fans, which requires different methodology. There are presented mathematical models of radial and axial fans including the most common flow control methods and/or techniques

– inlet damper, outlet damper, inlet guide vanes, on-off control, variable speed control and pitch control for axial-type of fans. The methodology of modeling of flow control methods is unlike pumps based especially on empiric knowledge of these controls, which are often represented by generalized performance curves of these devices. At the end of this part, representative case studies have been elaborated to present the performance of proposed models and developed software tool in practice.

Fourth chapter solves separately the task of energy efficiency optimization of group of multiple variable speed controlled pumps working in parallel into common hydraulic system. There is described the proposed algorithm and methodology for optimal control strategy and/or optimal distribution of flow among pumps ensuring maximal total efficiency of a group of pumps for any total demanded flow. There is presented the algorithm based on numerical optimization method using brute force approach, which enabled to solve the non-linear multidimensional optimization task. A special solution, which significantly sped-up the calculation process, for the cases of restricted space of freedom is also presented. The performance of the algorithm has been finally in detailed graphically presented on elaborated case studies. Additionally, the influence of a static head of a hydraulic system and the effect of variable sizing of pump in a pump group on an optimal control strategy are presented.

Finally, the last chapter summarizes the main contribution of this thesis and defines challenges for the future research.

2   Single pump applications

This chapter describes energy efficiency optimization process for pump applications employing single pump or possibly multiple pumps working in simple parallel or series connection in the manner that allow to substitute them with a single pump head-flow and efficiency-flow curves.

The first part is dedicated to introduction of methodology and model design employed in the evaluation process. It begins with modeling of hydraulic system including typical examples of hydraulic system curves and samples of operating profiles. Next, it describes the mathematical model of a pump with impact on a model suitable for variable speed control. Then, there are described the principles and proposed mathematical models of pump flow control techniques – the passive ones as throttling, bypass and on-off control using fixed speed drives and the active one, variable speed controls, using either drive with frequency converter or fixed speed drive with hydrodynamic coupling. Next part deals with modeling of particular components of the drive with a special attention paid to approximation techniques of especially electrical motor and transformer. Due to non-linear nature of application chain components, all mathematical models are derived in the discrete form suitable for direct software implementation. Finally, it is presented the way of evaluation of main technical and economical indicators of a solved application and/or case study.

The second part is devoted to verification of mathematical models and methodology using the software tool Medium Voltage Pump Save 2012. The tool has been developed based on the presented theory to provide an advanced engineering tool for comprehensive evaluation of single pump systems. The performance of the software tool and/or developed mathematical models and methodology is presented in two typical case studies of boiler feed pump application and cooling water-circulating application. Each case study is then branched in two variants to present the influence of particular parameters of case study on the annual energy consumption and operating costs and directly compare the evaluated flow control techniques and drive configurations next to each other.

2.1   Methodology and model design

In this chapter, it is described theoretical background and procedures employed in the evaluation and energy optimization process of pump systems. There are defined mathematical models of hydraulic system, pump including the collection of flow control algorithms and components of drive suitable for simulation of both fixed speed and variable speed operation. Approximation procedures based on typical characteristics, data and behavior for all the components of pump system are also included to present the way of evaluation while having a lack of parameters and/or data for full specification of systems to be solved.

The models are developed for steady states, which is sufficient for the purposes of energy efficiency evaluation. The models are except of analytical derivation expressed especially in the form suitable for numerical calculation, which is necessary because of high non-linearity of particular component of pump systems.

From an economical point of view, investment costs can be evaluated accurately already in a planning phase. However, operating costs evaluation contains many variables, which depends right on the proper mathematical modeling and precise energy consumption and/or cost prediction. To predict energy demands and/or consumption, it is necessary to begin from load characteristics, i.e. to state pump flow distribution in time. Energy consumption is then calculated from pump operating profile and developed mathematical models of pump and each component of the pump drive under selected control. This is in general no problem if we have i) pump and control performance curves and ii) fixed speed machines where parameters and curves at nominal operating points are available. However, especially for variable speed flow control with variable speed drives, it is necessary to use sophisticated approximation techniques, which are able to estimate drive loss values at real operating points just with knowledge of model behavior under nominal conditions.

The basic expected input data for evaluation of pump application using mathematical models described in this chapter are definition of hydraulic system including control and operating profile and datasheet values and/or curves for pump and drive components. Operating data and especially the efficiency curve of each component of the drive chain are then evaluated for specific load conditions. Then it is possible to determine the annual and lifetime energy consumption, drive operating costs and other economical and technical drive indicators.

All the presented mathematical models have been implemented in the core of the software tool MVD Pump Save 2012 and tested properly on evaluated case studies. Namely, following components have been described: hydraulic system, centrifugal pump and the most common flow control algorithms including fixed speed flow control methods (throttling, bypass, on-off control) and variable speed flow control methods using either directly electrical motor supplied from frequency converter or electrical motor in combination with slip coupling. Then, there are presented models of drive chain (including clutch, hydrodynamic coupling, electrical motor, frequency converter and transformer) and methodology of evaluation of basic economical indicators.

2.1.1   Hydraulic system

Specification of hydraulic system is the key process while designing or evaluating pump application. Hydraulic system is represented by system curve, which characterizes the head required to move fluid through a hydraulic system for various flow rates. It provides also information about character of the application – static head dominated or dynamic (friction) head dominated system and determines requirements on the pump design – the pump power, operating flow range and pump head.

Hydraulic system is commonly defined as in (2.1). However, for the purposes of hydraulic system evaluation, it will be formally used definition according to (2.2) - (2.4), where hydraulic system curve is composed basically from two components – static which represents the pressure caused by external factors or elevation of fluid column and dynamic which represents the friction losses – see (2.3) and (2.4).

$$H_S = H_S(Q) \tag{2.1}$$
$$H_S(Q) = H_{ST}(Q) = H_{SD}(Q) - H_{SS}(Q)$$
$$H_{SD}(Q) = H_{SDs}(Q) + H_{SDd}(Q) + H_{SDsp}$$
$$H_{SS}(Q) = H_{SSs}(Q) - H_{SSd}(Q) + H_{SSsp}$$

$$H_S(Q) = H_{ST}(Q) = H_{STs}(Q) + H_{STd}(Q) \tag{2.2}$$

$$H_{Ss}(Q) = H_{STs}(Q) = H_{SDs}(Q) - H_{SSs}(Q) + H_{SDsp} - H_{SSsp} \tag{2.3}$$

$$H_{Sd}(Q) = H_{STd}(Q) = H_{SDd}(Q) - H_{SSd}(Q) \tag{2.4}$$

Friction losses of pipe can be evaluated according to Darcy-Weisbach equation - (2.5) or for valves and fittings according to (2.6) [6] [37]. Nevertheless, the hydraulic system can be very complex – especially in high-power pump applications e.g. in thermal power plants. Therefore, the construction of hydraulic system curve will be simplified, based on the knowledge of just nominal operating point,
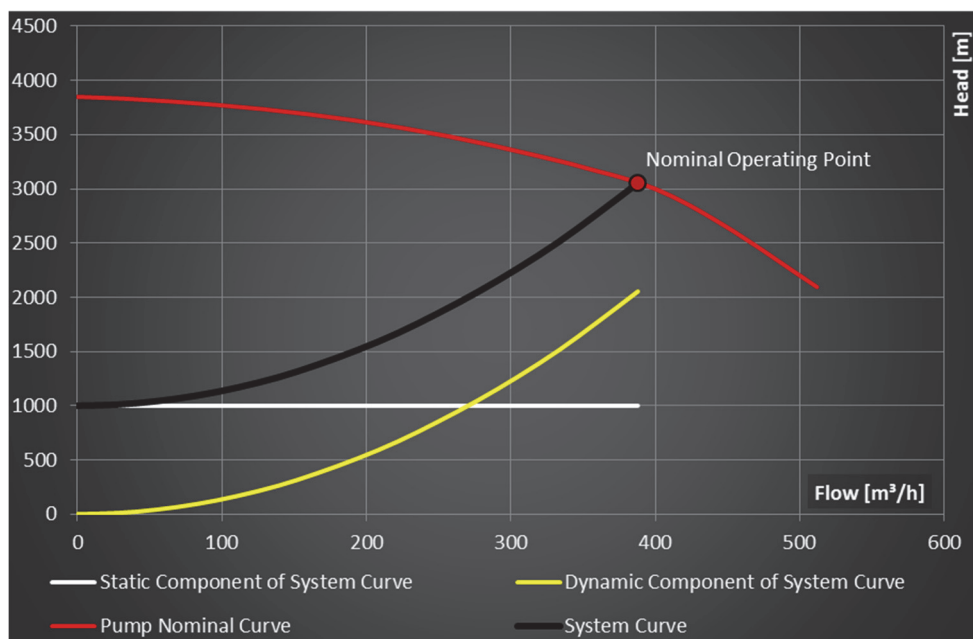
Fig. 2.1 Typical Hydraulic System Curve

zero flow point, static head curve and assumption of quadratic character of friction losses, which is sufficient for the purposes of energy consumption evaluation in most cases. The quadratic character of the friction head curve is evident from the equations (2.5) and (2.6) if we consider the red part of the equations to be constant for a particular hydraulic system. Friction head is then directly proportional to square of velocity. Based on (2.7) fluid velocity is proportional to flow (2.8) and consequently when velocity is substituted in (2.5), head caused by friction is then proportional to square of the flow (2.9) for piping system with constant pipe profile and incompressible flows.

Friction head curve is then constructed according to (2.11) where nominal friction head and zero flow friction head are calculated from (2.10). Numerical expression is in (2.12).

$$H_L = f_t \times \left(\frac{L}{D}\right) \times \frac{v^2}{2g} \tag{2.5}$$

$$H_{Lv} = K \times \frac{v^2}{2g} \tag{2.6}$$

$$v = \frac{s}{t}; s = \frac{V}{A}; Q = \frac{V}{t} \tag{2.7}$$

$$v = \frac{Q}{A} \tag{2.8}$$

$$H_L = f \times \left(\frac{L}{D}\right) \times \frac{Q^2}{2gA^2} \tag{2.9}$$

$$H_{Sd_N} = H_{S_N} - H_{Ss_N}$$
$$H_{Sd0} = 0 \tag{2.10}$$

$$H_{Sd} = H_{Sd_N} \times \left(\frac{Q_S}{Q_{S_N}}\right)^2 \tag{2.11}$$

$$\boldsymbol{Q_S} = \left[Q_{S-j}\right]^T ; j = 1, 2, \ldots, m_{samples} \tag{2.12}$$
$$Q_{S-1} = 0; \; Q_{S-m_{samples}} = Q_N$$
$$\boldsymbol{H_S} = \left[H_{S-j}\left(Q_{S-j}\right)\right]^T ; j = 1, 2, \ldots, m_{samples}$$
$$H_{S-j}\left(Q_{S-j}\right) = H_{Ss}\left(Q_{S-j}\right) + H_{Sd_N} \times \left(\frac{Q_{S-j}}{Q_{S_N}}\right)^2 ; j = 1, 2, \ldots, m_{samples}$$

In the following figures see typical examples of hydraulic system with friction dominating component (e.g. all liquid circulating applications like water cooling applications) - Fig. 2.2, hydraulic system with dominating component of static head - Fig. 2.3 and hydraulic system with linear component of static head (e.g. boiler water feed application in thermal power plants) - Fig. 2.4.

2.1.1.1 Typical examples
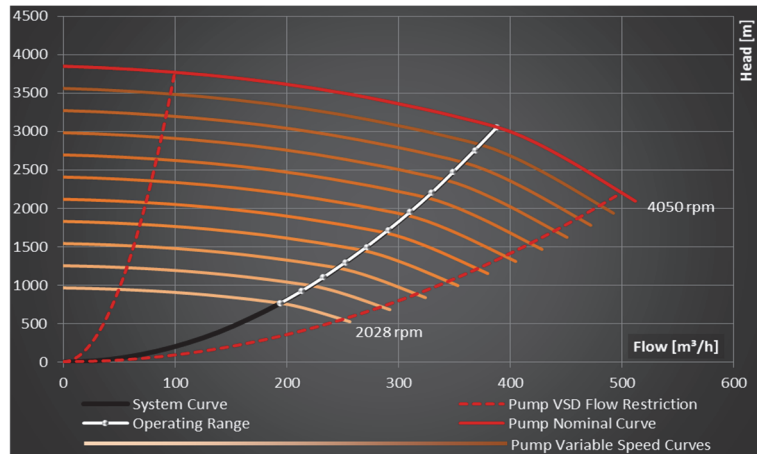
Fig. 2.2 Hydraulic system with dominating component of friction head
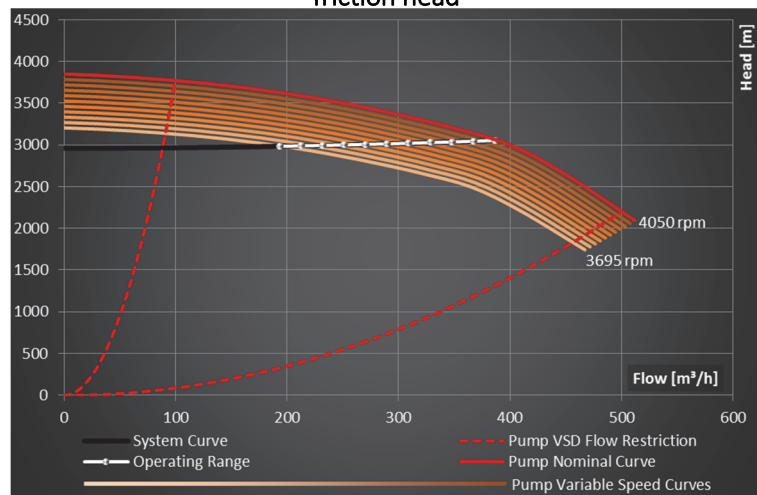
Fig. 2.3 Hydraulic system with dominating component of static head
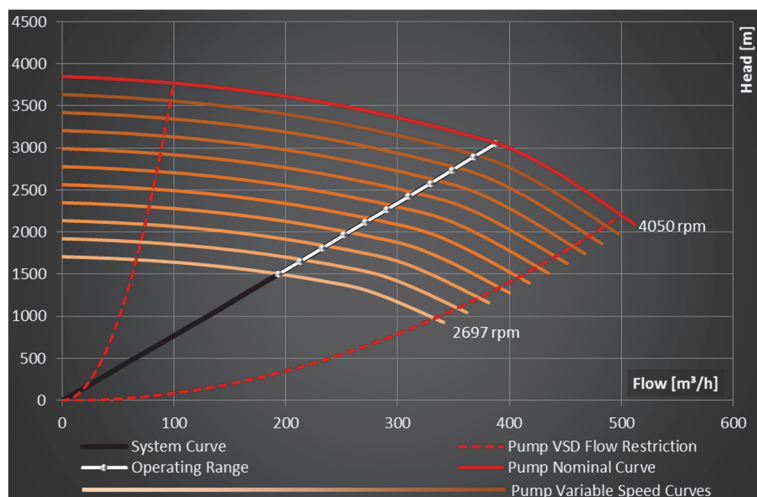
Fig. 2.4 Hydraulic system with linear component of static head

2.1.1.2   Operating Range & Profile

Operating profile is best represented by histogram, which shows graphically distribution of flow rate in time. As a function, it is expressed in (2.13) and numerical expression in (2.14).

Operating range and profile of pump application significantly influences design of whole application and/or have essential weight in decision-making which technology is the most suitable for the application.

Figures Fig. 2.5, Fig. 2.6 and Fig. 2.7 presents samples of operating profiles of hydraulic systems of various types of thermal power plants. Diagrams have been constructed based on the knowledge of workload of these power plants employed in electricity generation network of Czech Republic for the period of 07/2012 to 07/2013 [38] and assumption of directly proportional relation between power plant power and pump power and/or flow rate. Note, that this is simplified approach suitable mainly for presentation of the three different characters of operating profiles of pump applications in thermal power plants. It is always necessary to work with actual operating profile of a particular application. Nevertheless, it provides an idea about the character of these pump applications and agrees well with the place of these power plants in the daily diagram of covering of electricity consumption – from base load band covered by nuclear power plants over steam power plants to peaking combined gas and steam power plants. Notice also the typical operating range of the power plants and/or flow rate variations of particular hydraulic systems.

Weighted average of flow and weighted average of power are important statistical indicators characterizing the hydraulic application – see (2.15) and (2.16).
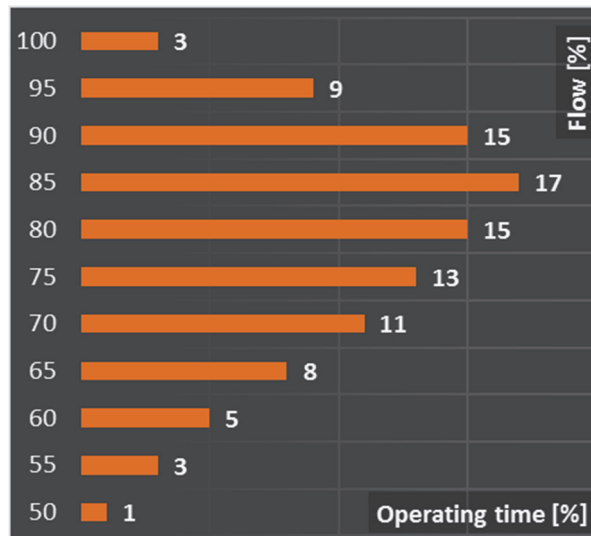
Fig. 2.5 Sample of operating profile of Conventional Steam Power Plant
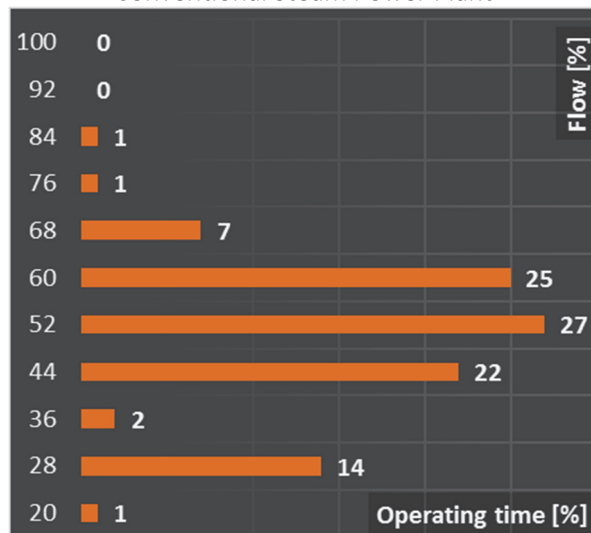
Fig. 2.6 Sample of operating profile of Combined Gas and Steam Power Plant
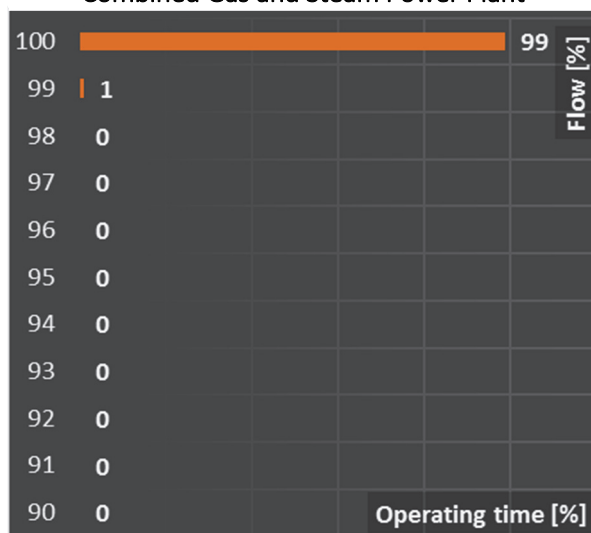
Fig. 2.7 Sample of operating profile of Nuclear Power Plant

      Physical limits of flow range are predetermined by design of pump and hydraulic system together with employed flow control methods. By selection of the pump, it has to be taken into account except of sufficient hydraulic parameters – head and flow – especially required NPSH due to risk of cavitation and minimal or maximal flow restrictions. A curve of required NPSH is supplied by pump manufacturers and varies with pump speed. Minimal and maximal flow restrictions are stated for nominal speed. In (2.17) and (2.18) it is derived the limitation curve of minimal and maximal flow for speed controlled pump using affinity rules – for details see chapter 2.1.2. For examples, see Fig. 2.2 - Fig. 2.4, red dashed curves.

$$t_{OP} = t_{OP}(Q) \tag{2.13}$$

$$\boldsymbol{OP} = [\boldsymbol{Q_{OP}}, \boldsymbol{t_{OP}}] \tag{2.14}$$

$$\boldsymbol{Q_{OP}} = \boldsymbol{Q_{S\text{-}OP}} = \left[Q_{OP1}, Q_{OP2}, ..., Q_{OPk_{OP}} \right]^T ; Q_{OP_{k_{OP}}} = Q_{OP_N}$$

$$\boldsymbol{t_{OP}} = \left[t_{OP1}(Q_{OP1}), t_{OP2}(Q_{OP2}), ..., t_{OPk_{OP}}\left(Q_{OPk_{OP}}\right) \right]^T$$

$$Q_{\text{wavg}}[\text{m}^3/\text{h}] = \frac{\sum\limits_{i=1}^{k_{OP}} Q_i[\text{m}^3/\text{h}] \times t_i[\text{h}, \%, \text{pu}]}{\sum\limits_{i=1}^{k_{OP}} t_i[\text{h}, \%, \text{pu}]} ; \quad Q_{\text{wavg}_{pu}} = \frac{\sum\limits_{i=1}^{k_{OP}} Q_{i_{pu}} \times t_{i_{pu}}}{\sum\limits_{i=1}^{k_{OP}} t_{i_{pu}}} = \sum\limits_{i=1}^{k_{OP}} Q_{i_{pu}} \times t_{i_{pu}} \tag{2.15}$$

$$P_{h\text{wavg}}[\text{kW}] = \frac{\sum\limits_{i=1}^{k_{OP}} P_{hi}[\text{kW}] \times t_i[\text{h}, \%, \text{pu}]}{\sum\limits_{i=1}^{k_{OP}} t_i[\text{h}, \%, \text{pu}]} ; \quad P_{h\text{wavg}_{pu}} = \frac{\sum\limits_{i=1}^{k_{OP}} P_{hi_{pu}} \times t_{i_{pu}}}{\sum\limits_{i=1}^{k_{OP}} t_{i_{pu}}} = \sum\limits_{i=1}^{k_{OP}} P_{hi_{pu}} \times t_{i_{pu}} \tag{2.16}$$

$$H_{P\min C} = H_{P\min C}(Q); \boldsymbol{H_{PminC}} = \left[H_{P\min Cj}\left(Q_{P\min Cj}\right) \right] \tag{2.17}$$

$$Q_{P\min Cj} = Q_{P\min N} \times \frac{n_j}{n_N}$$

$$H_{P\min Cj} = H_{P\min N}\left(Q_{P\min N}\right) \times \left(\frac{Q_{P\min Cj}}{Q_{P\min N}}\right)^2 = H_{P\min N}\left(Q_{P\min N}\right) \times \left(\frac{n_j}{n_N}\right)^2$$

$$j = 1, 2, ..., m_{samples}$$

$$H_{P\max C} = H_{P\max C}(Q); \boldsymbol{H_{PmaxC}} = \left[H_{P\max Cj}\left(Q_{P\max Cj}\right) \right] \tag{2.18}$$

$$Q_{P\max Cj} = Q_{P\max N} \times \frac{n_j}{n_N}$$

$$H_{P\max Cj} = H_{P\max N}\left(Q_{P\max N}\right) \times \left(\frac{Q_{P\max Cj}}{Q_{P\max N}}\right)^2 = H_{P\max N}\left(Q_{P\max N}\right) \times \left(\frac{n_j}{n_N}\right)^2$$

$$j = 1, 2, ..., m_{samples}$$

2.1.2   Pump

Selection of the right pump for an application is one of the most important steps. There are several types of pumps based on different principles and suitable for different hydraulic conditions. Design of a pump for a particular application is a very complex task from the field of especially fluid mechanics and it is widely described e.g. in [6]. For energy optimization purposes of pump applications, it will be used pump performance curves (see Fig. 2.8 and Fig. 2.9 for basic and derivated typical curves), which sufficiently describe the pump behavior and features and are commonly supplied by pump manufacturers together with pump. Further, it will be account with centrifugal type of pumps, which are the most common in high-power applications.

Fig. 2.8 Sample of pump datasheet performance curves for nominal speed

Nevertheless, pump performance curves are often defined only at pump nominal speed. The following equations also called affinity rules - (2.19) - (2.21) - are used to recalculate pump performance curves for variable speed, which is needed for variable speed control. The impeller diameter is considered unchanged.

It is proved in (2.22) that efficiency keeps unchanged using affinity rules. An efficiency for any speed is expressed in (2.24) and (2.25). The

Fig. 2.9 Sample of pump derivated performance curves for nominal speed

structure of pump losses is apparent from Fig. 2.10, which shows typical efficiency and losses for centrifugal pumps in the relation to pump specific speed, which is the essential parameter describing pumps expressed in (2.26). The two expressions of pump specific speed are presented to clarify the inconsistent definition of especially units in literature. The specific speed n_s matches the speed in the Fig. 2.10, the specific speed n_{s-orig} shows the original dimensionless formula including acceleration of gravity. In (2.27) it is shown that pump specific speed is independent on the pump speed using affinity rules. Pump hydraulic power, power consumption and torque on the pump shaft are then expressed in (2.28) - (2.31) . Note, that pump head is related to real head of liquid, which is being pumped in (2.29) instead of often-used equivalent in head of water column.

$$\frac{Q_1}{Q_2} = \frac{n_1 D_1}{n_2 D_2} \tag{2.19}$$

$$\frac{H_1}{H_2} = \left(\frac{n_1 D_1}{n_2 D_2}\right)^2 \tag{2.20}$$

$$\frac{P_1}{P_2} = \left(\frac{n_1 D_1}{n_2 D_2}\right)^3 \tag{2.21}$$

$$\frac{\eta_1}{\eta_2} = \left(\frac{Q_1}{Q_2}\right)\left(\frac{\Delta H_1}{\Delta H_2}\right)\left(\frac{P_2}{P_1}\right) = \left(\frac{n_1}{n_2}\right)\left(\frac{n_1}{n_2}\right)^2\left(\frac{n_2}{n_1}\right)^3 = 1 \tag{2.22}$$
$$\Delta H = H_{out} - H_{in}$$

$$Q_2 = Q_1\left(\frac{n_2}{n_1}\right); H_2 = H_1\left(\frac{n_2}{n_1}\right)^2 \tag{2.23}$$

$$\eta_{n_2} = f(Q_2); \ \eta_{n_1} = f(Q_1); \ \eta_{n_1} = \eta_{n_2} \tag{2.24}$$

$$\eta_2(Q_2) = \eta_1\left(Q_2\left(\frac{n_1}{n_2}\right)\right) \tag{2.25}$$

$$n_s = n_N[rpm] \times \frac{Q_N[m^3/s]^{1/2}}{H_N[m]^{3/4}}; \ n_{s-orig} = n_N[rpm] \times \frac{Q_N[m^3/s]^{1/2}}{\left(g[m/s^2] \times H_N[m]\right)^{3/4}} \tag{2.26}$$
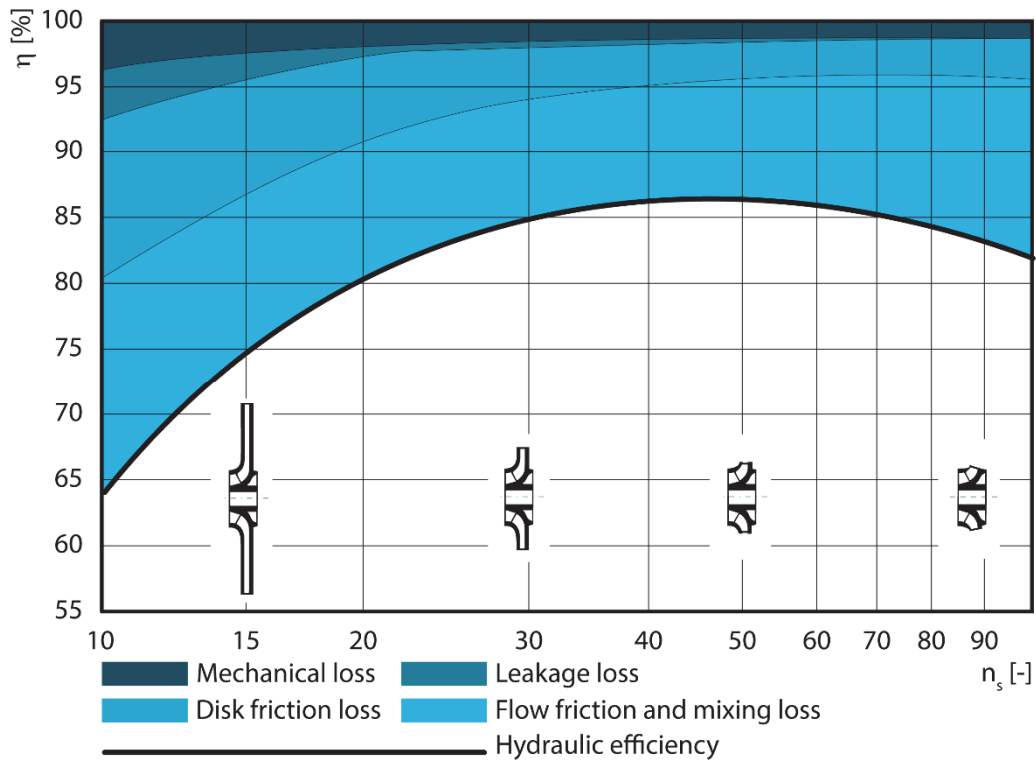
Fig. 2.10 Loss distribution in a centrifugal pump as a function of specific speed n_s [41]

$$n_{s_1} = n_{N1} \times \frac{Q_{N1}^{1/2}}{H_{N1}^{3/4}}$$

<div style="text-align: right">(2.27)</div>

$$n_{s2} = n_{N2} \times \frac{Q_{N2}^{1/2}}{H_{N2}^{3/4}} = n_{N2} \times \frac{Q_{N1}^{1/2}}{H_{N1}^{3/4}} \times \frac{\left(\frac{n_{N2}}{n_{N1}}\right)^{1/2}}{\left(\frac{n_{N2}}{n_{N1}}\right)^{3/2}} = \frac{Q_N^{1/2}}{H_N^{3/4}} \times n_{N1} = n_{s_1}$$

$$P_h[W] = Q[m^3/s] \times \Delta H[\text{Pa}] = Q[m^3/s] \times \Delta H[m] \times \rho[kg/m^3] \times g[\text{m}/\text{s}^2]$$

<div style="text-align: right">(2.28)</div>

$$P_h[\text{kW}] = \frac{Q[m^3/\text{h}]}{3600} \times \frac{\Delta H[m] \times \rho[kg/m^3] \times g[\text{m}/\text{s}^2]}{1000}$$

$$H[kPa] = \frac{h[m] \times \rho[kg/m^3] \times g[\text{m}/\text{s}^2]}{1000}$$

<div style="text-align: right">(2.29)</div>

$$P_c = \frac{P_h}{\eta}$$

<div style="text-align: right">(2.30)</div>

$$T[\text{Nm}] = \frac{P_c[\text{W}]}{\omega[rad/s]} = \frac{P_c[kW] \times 1000}{\frac{n[\text{rpm}]}{60} \times 2\pi}$$

<div style="text-align: right">(2.31)</div>

2.1.2.1   Numerical solution of pump operating points under VSC

For a precise evaluation of pump systems, it is necessary to obtain real performance curves of the pump, usually at least for nominal speed. Since every pump has a specific performance curve and the curve change slightly over the pump lifetime, there is no general analytical description available. Hence, the optimal way is to sample these curves at nominal speed and solve the complete hydraulic system numerically to obtain precise results. Nevertheless, the numerical solution requires specific methodology to be employed, which is described below.

The set of sampled data is defined in (2.32). At first, it is the stated nominal operating point, which is located at the intersection of pump nominal head-flow curve and hydraulic system curve – see (2.33). Theoretically, there could be more possible intersection points between pump and system curve, however only one stable one – see [39] page 48. The Fig. 2.11 shows sampled pump head-flow curve (red, (2.32)) and discretized hydraulic system curve (black) constructed according to (2.12). The yellow curve indicates the operating range of the system curve - (2.34). A real pump & system
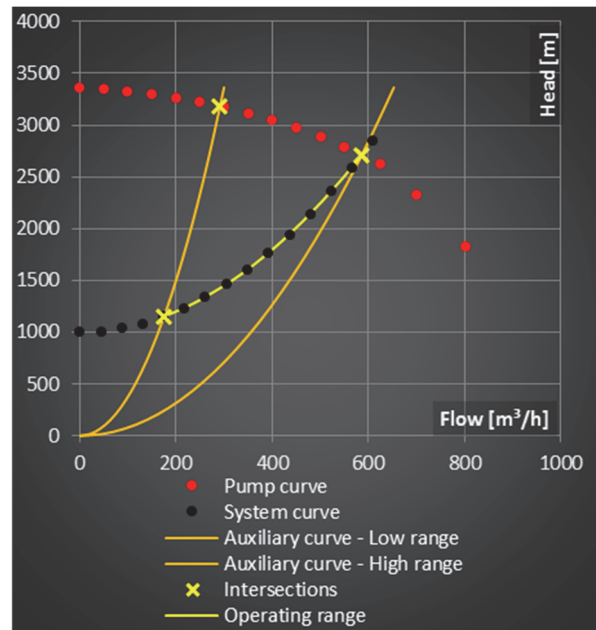
Fig. 2.11 Discrete definition of hydraulic system application

nominal operating point is then obtained as an intersection of linearly interpolated pump and hydraulic system curves - (2.35).

$$H_P = H_P(Q_P); \ \eta_P = \eta_P(Q_P) \tag{2.32}$$

$$\boldsymbol{Q}_{P_N} = \left[Q_{P_N j}\right]^T ; \ j = 1, 2, ..., m_{samples}$$

$$\boldsymbol{H}_{P_N} = \left[H_{P_N j}\left(Q_{P_N j}\right)\right]^T ; \ j = 1, 2, ..., \mathrm{m}_{samples}$$

$$\boldsymbol{\eta}_{P_N} = \left[\eta_{P_N j}\left(Q_{P_N j}\right)\right]^T ; \ j = 1, 2, ..., \mathrm{m}_{samples}$$

$$H_P = H_P(Q); \ H_S = H_S(Q) \tag{2.33}$$

$$H_P(Q) = H_S(Q)$$

$$\boldsymbol{Q}_{OP_N} = \left\{Q \mid H_P(Q) = H_S(Q); \ n_P = n_N\right\}$$

$$\boldsymbol{H}_{OP_N} = \left\{H \mid H = H_P(Q); \ Q \in \boldsymbol{Q}_{OP_N}; \ n_P = n_N\right\}$$

$$\boldsymbol{H}_{OP} = \boldsymbol{H}_{S\text{-}OP} = \left[H_S(Q)\right]^T ; Q \in \boldsymbol{Q}_{OP} \tag{2.34}$$

$$\left[\boldsymbol{Q}_{OP_N}, \boldsymbol{H}_{OP_N}\right] = f_{IntersectLinIntArrays}\left(\boldsymbol{Q}_{P_N}, \boldsymbol{H}_{P_N}, \boldsymbol{Q}_S, \boldsymbol{H}_S\right) \tag{2.35}$$

Next, it is derived pump operating speed range. The minimal speed is the speed at which pump curve crosses the system curve at the point of minimal operating flow; similarly, the maximal speed is the speed at which pump curve crosses the system curve at the point of maximal flow – see Fig. 2.11, yellow cross marks. The minimal and maximal speed can be derived from (2.19) or (2.20) if it is find an equivalent operating point for hydraulic system minimal and maximal operating points on the pump nominal curve using affinity rules – see Fig. 2.11, yellow cross marks. The minimal speed is then expressed in (2.36) and the maximal speed in (2.37). The maximal speed equals to pump nominal speed when the maximal operating point lies on the pump nominal head-flow curve at nominal speed.

To find the equal operating points on pump nominal curve, auxiliary curves have to be built - (2.38) and (2.39) for minimal and maximal operating range - see Fig. 2.11. Equivalent operating points lies on the intersection of pump nominal curve and auxiliary curves - (2.40) and (2.41). For numerical solution see (2.42) - (2.45). Distribution of pump speed covering operating range is then in (2.46).

$$n_{OP_{min}} = n_{OP_1} = n_N \times \frac{Q_{OP_1}}{Q_{OP_1 eqN}} = n_N \times \sqrt{\frac{H_{OP_1}}{H_{OP_1 eqN}}} \tag{2.36}$$

$$n_{OP_{max}} = n_{OP_{k_{OP}}} = n_N \times \frac{Q_{OP_{k_{OP}}}}{Q_{OP_{k_{OP}} eqN}} = n_N \times \sqrt{\frac{H_{OP_{k_{OP}}}}{H_{OP_{k_{OP}} eqN}}} ; \tag{2.37}$$

$$... for \ Q_{OP_{k_{OP}}} = Q_{OP_{k_{OP}} eqN} \Rightarrow n_{OP_{max}} = n_N$$

$$H_{AuxCmin} = H_{AuxCmin}(Q) = H_S(Q_{OP\_min}) \times \left(\frac{Q}{Q_{AuxCmin\_max}} \right)^2 \tag{2.38}$$

$$Q \in \left\langle 0, Q_{AuxCmin\_max} \right\rangle$$

$$Q_{AuxCmin\_max} = Q_{OP\_min} \times \sqrt{\frac{H_{AuxCmin\_max}}{H_S(Q_{OP\_min})}}$$

$$Q_{OP\_min} = \min(\boldsymbol{Q_{OP}}) = Q_{OP_l}; H_{AuxC\min\_max} = \max(\boldsymbol{H_{P_N}})$$

$$H_{AuxCmax} = H_{AuxCmax}(Q) = H_S(Q_{OP\_max}) \times \left(\frac{Q}{Q_{AuxCmax\_max}} \right)^2 \tag{2.39}$$

$$Q \in \left\langle 0, Q_{AuxC\max\_max} \right\rangle$$

$$Q_{AuxC\max\_max} = Q_{OP\_max} \times \sqrt{\frac{H_{AuxCmax\_max}}{H_S(Q_{OP\_max})}}$$

$$Q_{OP\_max} = \max(\boldsymbol{Q_{OP}}) = Q_{OP_{kOP}}; H_{AuxC\max\_max} = \max(\boldsymbol{H_{P_N}})$$

$$H_{AuxCmin}(Q) = H_{P_N}(Q) \tag{2.40}$$

$$Q_{OP_1 eqN} = \left\{ Q \mid H_{AuxCmin}(Q) = H_{P_N}(Q); \; n_p = n_N \right\}$$

$$\mathrm{H}_{OP_1 eqN} = H_{AuxCmin}(Q_{OP_1 eqN})$$

$$H_{AuxCmax}(Q) = H_{P_N}(Q) \tag{2.41}$$

$$Q_{OP_{kOP} eqN} = \left\{ Q \mid H_{AuxCmax}(Q) = H_{P_N}(Q); \; n_p = n_N \right\}$$

$$\mathrm{H}_{OP_{kOP} eqN} = H_{AuxCmin}(Q_{OP_{kOP} eqN})$$

$$\boldsymbol{Q_{AuxCmin}} = \left[Q_{AuxCmin-j} \right]^T \tag{2.42}$$

$$Q_{AuxCmin-1} = 0; \; Q_{AuxCmin-m_{samples}} = Q_{AuxCmin\_max}$$

$$\boldsymbol{H_{AuxCmin}} = \left[H_{AuxCmin-j}(Q_{AuxCmin-j}) \right]^T$$

$$H_{AuxCmin-j}(Q_{AuxCmin-j}) = H_S(Q_{OP\_min}) \times \left(\frac{Q_{AuxCmin-j}}{Q_{AuxCmin\_max}} \right)^2$$

$$j = 1, 2, ..., m_{samples}$$

$$\boldsymbol{Q_{AuxCmax}} = \left[Q_{AuxCmax-j} \right]^T \tag{2.43}$$

$$Q_{AuxCmax-1} = 0; \; Q_{AuxCmax-m_{samples}} = Q_{AuxCmax\_max}$$

$$\boldsymbol{H_{AuxCmax}} = \left[H_{AuxCmax-j}(Q_{AuxCmax-j}) \right]^T$$

$$H_{AuxCmax-j}(Q_{AuxCmax-j}) = H_S(Q_{OP\_max}) \times \left(\frac{Q_{AuxCmax-j}}{Q_{AuxCmax\_max}} \right)^2$$

$$j = 1, 2, ..., m_{samples}$$

$$\left[Q_{OP_1eqN}, H_{OP_1eqN}\right] = f_{IntersectLinIntArrays}\left(\boldsymbol{Q_{P_N}}, \boldsymbol{H_{P_N}}, \boldsymbol{Q_{AuxCmin}}, \boldsymbol{H_{AuxCmin}}\right) \tag{2.44}$$

$$\left[Q_{OPk_{OP}eqN}, H_{OPk_{OP}eqN}\right] = f_{IntersectLinIntArrays}\left(\boldsymbol{Q_{P_N}}, \boldsymbol{H_{P_N}}, \boldsymbol{Q_{AuxCmax}}, \boldsymbol{H_{AuxCmax}}\right) \tag{2.45}$$

$$\boldsymbol{n_P} = \left[n_{Pj}\right]; \; j=1,2,...,\text{m}_{curves} \tag{2.46}$$

$$n_{Pj} = n_{OP_{min}} + (j-1) \times \frac{n_{OP_{max}} - n_{OP_{min}}}{m_{curves} - 1}$$

Pump operating points - by employing variable speed control - are placed on the intersections ((2.48)) of pump curve recalculated for particular speed ((2.47)) and system curve. Finally, pump head at pump and hydraulic system operating points according to operating profile defined in ((2.14)) is obtained by linear interpolation of intersections of pump curves for variable speed with hydraulic system curve - (2.49).

See example in the Fig. 2.12 and Fig. 2.13 for detailed view, where former derived relations from (2.33) to (2.49) are presented graphically. In particular, transformation of pump curve at nominal speed for variable speed including determination of pump speed range in the Fig. 2.12 and detailed view of real pump and system operating points apparent from the Fig. 2.13.

$$\boldsymbol{Q_{Pn_i}} = \left[Q_{Pn_{i-j}}\right]; \; \boldsymbol{H_{Pn_i}} = \left[H_{Pn_{i-j}}\left(Q_{Pn_{i-j}}\right)\right] \tag{2.47}$$

$$Q_{Pn_{i-j}} = Q_{Pn_{N-j}} \times \frac{n_i}{n_N}$$

$$H_{Pn_{i-j}}\left(Q_{Pn_{i-j}}\right) = H_{Pn_{N-j}} \times \left(\frac{n_i}{n_N}\right)^2$$

$$i \in \boldsymbol{n_P}; \; j = 1,2,...,m_{samples}$$
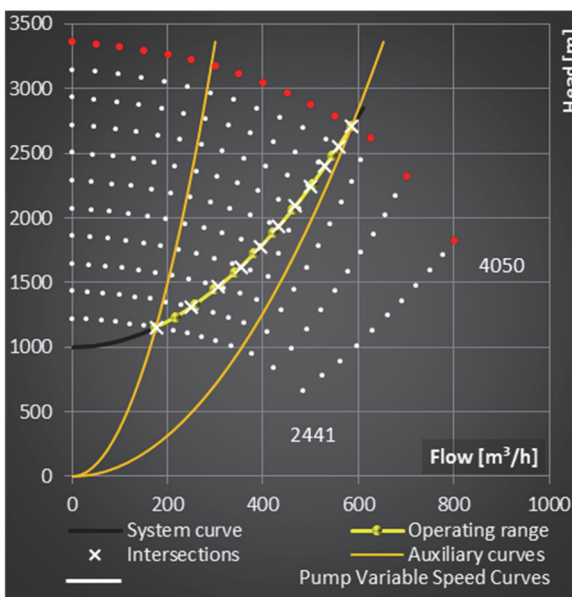
Fig. 2.12 Pump operating points employing variable speed control
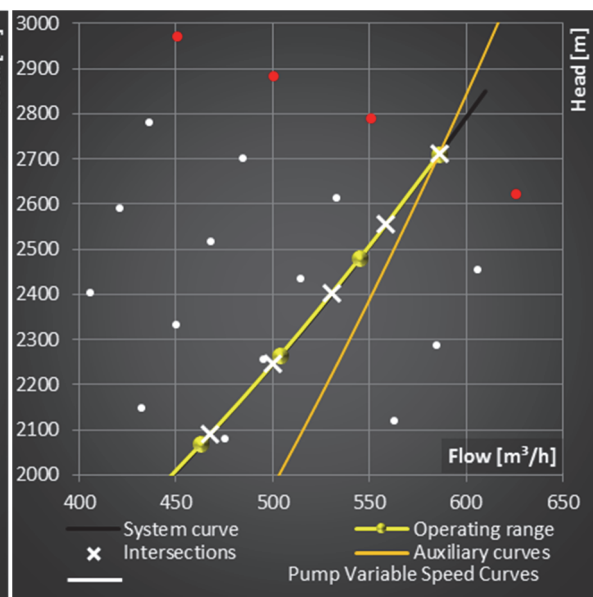
Fig. 2.13 Pump operating points employing variable speed control - detail

$$\left[Q_{PSn_i}, H_{PSn_i} \right] = f_{IntersectLinIntArrays} \left(\boldsymbol{Q_S}, \boldsymbol{H_S}, \boldsymbol{Q_{Pn_i}}, \boldsymbol{H_{Pn_i}} \right) \tag{2.48}$$

$$\boldsymbol{Q_{PS}} = \left[Q_{PSn_i} \right]; \; \boldsymbol{H_{PS}} = \left[H_{PSn_i} \right]$$

$$i \in \boldsymbol{n_P}$$

$$H_{OPi} = f_{IntLinArray} \left(\boldsymbol{Q_{PS}}, \boldsymbol{H_{PS}}, Q_{OPi} \right) \tag{2.49}$$

$$\boldsymbol{H_{OP}} = \left[H_{OPi} \right]^T$$

$$i = 1, 2, ..., k_{OP}$$

Next are expressed relations for pump hydraulic power ((2.50)), pump mechanical power and/or power consumption (2.51), pump efficiency ((2.52) and (2.53)), pump speed ((2.54)) and pump torque ((2.55)) at pump operating points. See examples in the section of case studies - Fig. 2.27 to Fig. 2.36.

$$\boldsymbol{P_{h\text{-}OP}} = \left[P_{h-OPi} \right]^T \tag{2.50}$$

$$P_{h-OPi}[\text{kW}] = \frac{Q_{OPi}[m^3/h]}{3600} \times \frac{H_{OPi}[m] \times \rho[kg/m^3] \times g[m/s^2]}{1000}$$

$$i = 1, 2, ..., k_{OP}$$

$$\boldsymbol{P_{cP\text{-}OP}} = \boldsymbol{P_{h\text{-}OP}} . / \boldsymbol{\eta_{P\text{-}OP}} \tag{2.51}$$

$$\boldsymbol{\eta_{P\text{-}OP}} = \left[\eta_{P-OPi} \right]^T \tag{2.52}$$

$$\eta_{P-OPi} = f_{IntLinArray} \left(\boldsymbol{Q_{PS}}, \boldsymbol{\eta_{PS}}, Q_{OPi} \right)$$

$$i = 1, 2, ..., k_{OP}$$

$$\eta_{PS} = \eta_{PS} \left(Q_{n_{PS}} \right) = \eta_{P_N} \left(Q_{PS} \times \frac{n_{P_N}}{n_{PS}} \right) \tag{2.53}$$

$$\boldsymbol{\eta_{PS}} = \left[\eta_{PSj} \right]^T$$

$$\eta_{PSj} = f_{IntLinArray} \left(\boldsymbol{Q_{P_N}}, \boldsymbol{\eta_{P_N}}, Q_{PSj} \times \frac{n_{P_N}}{n_{PSj}} \right); \; \boldsymbol{n_{PS}} = \boldsymbol{n_P}$$

$$j = 1, 2, ..., m_{curves}$$

$$\boldsymbol{n_{P\text{-}OP}} = \left[n_{P-OPi} \right] \tag{2.54}$$

$$n_{P-OPi} = f_{IntLinArray} \left(\boldsymbol{Q_{PS}}, \boldsymbol{n_P}, Q_{OPi} \right)$$

$$i = 1, 2, ..., k_{OP}$$

$$\boldsymbol{T_{P\text{-}OP}} = \left[T_{P-OPi} \right] \tag{2.55}$$

$$T_{P-OPi}[\text{Nm}] = \frac{P_{cP-OPi}[kW] \times 1000}{\dfrac{n_{P-OPi}[\text{rpm}]}{60} \times 2\pi}$$

$$i = 1, 2, ..., k_{OP}$$

2.1.3   Flow control algorithms

There are several flow control strategies commonly used in practice. The passive flow control strategies like throttling, bypass or on-off control, which are applied to control the flow in applications with constant pump speed and active strategy using flow control by pump variable speed control. The principle is illusrated in the Fig. 2.14. It is obvious, that passive flow control strategies are always lossy except of nominal operating point. To be able to compare and evaluate flow control algorithms among each other, following pump control efficiency is defined - (2.56). Control efficiency at pump operating points according to operating porfile is then - (2.57).

$$\eta_{CP} = \frac{P_{hS}}{P_{hP}} = \frac{P_{hS} \times t}{P_{hP} \times t} = \frac{E_{hS}}{E_{hP}} \qquad (2.56)$$

$$P_{hP} = Q_P \times \Delta H_P \left(Q_P \right)$$

$$P_{hS} = Q_S \times H_S \left(Q_S \right)$$

$$\boldsymbol{\eta_{CP\text{-}OP}} = \left[\eta_{CP-OPi} \right]^T \qquad (2.57)$$

$$\eta_{CP-OPi} = \frac{P_{hS-OPi}}{P_{hP-OPi}} = \frac{P_{hS-OPi} \times t_i}{P_{hP-OPi} \times t_i} = \frac{E_{hS-OPi}}{E_{hP-OPi}}$$

$$i = 1, 2, ..., k_{OP}$$
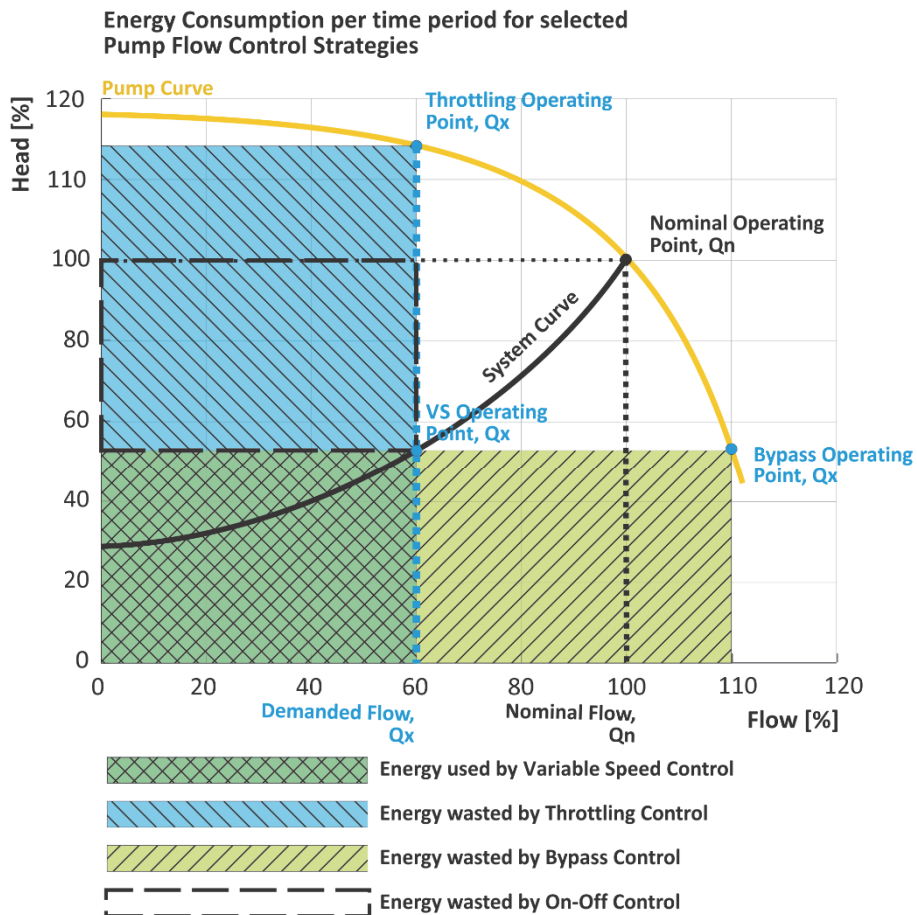
Fig. 2.14 Energy consumption per period for selected pump flow control strategies

2.1.3.1   Variable Speed Flow Control

Variable speed flow control use the change of pump speed to match demanded flow and/or operating point on hydraulic system curve. Pump flow and head match hydraulic system flow and head and therefore control efficiency under speed control equals one - (2.58). Pump efficiency under variable speed control is then - (2.59). For detailed description of pump behavior under variable speed control, see chapter 2.1.2.1.

$$Q_{P-VS-OPi} = Q_{S-OPi};\ H_{P-VS-OPi} = H_{S-OPi}\ \Rightarrow\ P_{hP-OPi} = P_{hS-OPi} \tag{2.58}$$

$$\eta_{CP-VS-OPi} = \frac{P_{hS-OPi}}{P_{hP-OPi}} = 1$$

$$i = 1,2,...,k_{OP}$$

$$\eta_{P-VS} = \eta_{P_N}\left(Q_P \times \frac{n_N}{n}\right) \tag{2.59}$$

$$\eta_{P-VS-OPi} = f_{IntLinSpline}\left(\boldsymbol{Q_{P_N}}, \boldsymbol{\eta_{P_N}}, Q_{P-OPi} \times \frac{n_N}{n_{P-OPi}}\right)$$

$$i = 1,2,...,k_{OP}$$

2.1.3.2   Throttling

Pump speed equals to pump nominal speed over the entire operating range - Eq.(2.60). Pump flow equals to system flow and pump head is a function of pump head-flow curve at nominal speed (Eq.(2.61) and Eq.(2.62)). Control efficiency for throttling control strategy is then Eq.(2.64). Pump efficiency employing throttling control strategy is then - Eq.(2.65). Head loss on control valve is expressed in Eq.(2.63). Using throttling valve change hydraulic system curve and/or nominal operating point. Hence, it is not possible to compare the control method with the others under constant hydraulic system conditions. Therefore, the pump hydraulic power and efficiency calculation is divided into two regions given by the head loss of control valve. The second region is not reachable without replacement of the pump or hydraulic system conditions, however to be able to compare it with other flow control methods, it is supposed power increase of the pump about power loss of the control valve.

$$n_{P-Throttling-OPi} = const = n_N;\ i = 1,2,...,k_{OP} \qquad \text{Eq.(2.60)}$$

$$Q_{P-Throttling-OPi} = Q_{S-OPi} = Q_{OPi};\ i = 1,2,...,k_{OP} \qquad \text{Eq.(2.61)}$$

$$H_{P-Throttling-OPi} = H_{P_N}\left(Q_{P-Throttling-OPi}\right) = f_{IntLinArray}\left(\boldsymbol{Q_{P_N}}, \boldsymbol{H_{P_N}}, Q_{P-Throttling-i}\right);\ i = 1,2,...,k_{OP} \qquad \text{Eq.(2.62)}$$

$$\Delta H_{P-ThrottlingValve-OPi} = \Delta H_{P-ThrottlingValve_N} \times \left(\frac{Q_{P-Throttling-OPi}}{Q_{P_N}}\right)^2;\ i = 1,2,...,k_{OP} \qquad \text{Eq.(2.63)}$$

$$P_{hS-OPi} = Q_{S-OPi} \times H_{S-OPi} \qquad \text{Eq.(2.64)}$$

$$P_{hP-Throttling-OPi} = Q_{P-Throttling-OPi} \times H_{P-Throttling-OPi}$$

$$\Delta P_{hP-ThrottlingValve-OPi} = Q_{P-Throttling-OPi} \times \Delta H_{P-ThrottlingValve-OPi}$$

$$\text{i. } for \left(H_{P-Throttling-OPi} - H_{S-OPi} \right) > \Delta H_{P-ThrottlingValve-OPi} \Rightarrow \eta_{CP-Throttling-OPi} = \frac{P_{hS-OPi}}{P_{hP-Throttling-OPi}}$$

$$\text{ii. } for \left(H_{P-Throttling-OPi} - H_{S-OPi} \right) \le \Delta H_{P-ThrottlingValve-OPi} \Rightarrow$$

$$\Rightarrow \eta_{CP-Throttling-OPi} = \frac{P_{hS-OPi}}{P_{hS-OPi} + \Delta P_{hP-ThrottlingValve-OPi}}$$

$$i = 1,2,...,k_{OP}$$

$$\eta_{P-Throttling-OPi} = \eta_{P_N} \left(Q_{P-Throttling-OPi} \right) = f_{IntLinArray} \left(\boldsymbol{Q}_{P_N}, \boldsymbol{\eta}_{P_N}, Q_{P-Throttling-OPi} \right) \qquad \text{Eq.(2.65)}$$

$$i = 1,2,...,k_{OP}$$

2.1.3.3 Bypass

Pump speed equals to pump nominal speed over the entire operating range (2.66). Pump flow depends on the character of pump curve and it is get from an inverse function of pump head-flow curve for head matching hydraulic system head ((2.67) and (2.68)). Control efficiency and pump efficiency are then similarly to throttling in (2.69) and (2.70).

$$n_{P-Bypass-i} = const = n_N; \ i = 1,2,...,k_{OP} \qquad (2.66)$$

$$Q_{P-Bypass-OPi} = Q_{P_N} \left(H_{P-Bypass-OPi} \right) = f_{IntLinArray} \left(\boldsymbol{H}_{P_N}, \boldsymbol{Q}_{P_N}, H_{P-Bypass-OPi} \right); i = 1,2,...,k_{OP} \qquad (2.67)$$

$$Q_{P_N} \left(H \right) = H_{P_N} \left(Q \right)^{-1}$$

$$H_{P-Bypasss-OPi} = H_{S-OPi}; \ i = 1,2,...,k_{OP} \qquad (2.68)$$

$$P_{hS-OPi} = Q_{S-OPi} \times H_{S-OPi} \qquad (2.69)$$

$$P_{hP-Bypass-OPi} = Q_{P-Bypass-OPi} \times H_{P-Bypass-OPi}$$

$$\eta_{CP-Bypass-OPi} = \frac{P_{hS-OPi}}{P_{hP-Bypass-OPi}}$$

$$i = 1,2,...,k_{OP}$$

$$\eta_{P-Bypass-OPi} = \eta_{P_N} \left(Q_{P-Bypass-OPi} \right) = f_{IntLinArray} \left(\boldsymbol{Q}_{P_N}, \boldsymbol{\eta}_{P_N}, Q_{P-Bypass-OPi} \right) \qquad (2.70)$$

$$i = 1,2,...,k_{OP}$$

2.1.3.4   On-Off Control

On-Off control is a very specific flow control, while it actually operates only at nominal operating point - (2.71). It is not possible to control flow in a real time. However, it is possible to control the flow quantity in a period (average value) - (2.72). Flow quantity is then determined by the ratio of run and stop time. Control efficiency is then - (2.73). It is apparent, that this method could be applied only for the applications, which include capacity and/or it is possible to vary flow around the set-point hysteresis range.

$$n_{P-OnOff-OPi} = const = n_N;$$

$$Q_{P-OnOff-OPi} = Q_{OP_N} = Q_{S_N}$$

$$H_{P-OnOff-OPi} = H_{OP_N} = H_{S_N}$$

$$\eta_{P-OnOff-OPi} = \eta_{P_N}\left(Q_{S_N}\right)$$

$$i = 1, 2, ..., k_{OP} \tag{2.71}$$

$$Q_{P-OnOff-OPiavg} = Q_{S_N} \times \frac{t_{OPi}}{\sum\limits_{i=1}^{k_{OP}} t_{OPi}}; \; i = 1, 2, ..., k_{OP} \tag{2.72}$$

$$P_{hS-OPi}[kW] = \frac{Q_{OPi}[m^3/h]}{3600} \times \frac{H_{OPi}[m] \times \rho[kg/m^3] \times g[m/s^2]}{1000}$$

$$\mathrm{E}_{hS-OPi}[kWh] = P_{hS-OPi}[kW] \times t_{OPi}[h]$$

$$P_{hP-OnOff-OPi}[kW] = P_{hOP_N}[kW]$$

$$E_{hP-OnOff-OPi}[kWh] = P_{hOP_N}[kW] \times t_{OPi}[h]$$

$$\eta_{CP-OnOff-OPi} = \frac{E_{hS-OPi}}{E_{hP-OnOff-OPi}}$$

$$i = 1, 2, ..., k_{OP} \tag{2.73}$$

2.1.4   Drives

High-power pump applications are usually driven by either steam-turbine drive – especially in power plants with low power variability and pump power consumption over 10 MW or electrical drives, which will be further considered in this work and developed software tool.

Based on the employed flow control, drives are divided on to i) fixed speed drives consisting of just induction machine and ii) variable speed drives consisting either of induction machine supplied from frequency converter or fixed speed induction machine supplemented by slip coupling based on hydraulic or magnetic principle. Both fixed speed and variable speed drives are possibly supplemented by power supply transformer in cases of different induction machine and power supply network voltages or by gearbox especially for pump applications working into very high head requiring high speeds over 3000 rpm.

2.1.4.1   Gearbox

For the purposes of energy efficiency evaluation of pump applications, gearbox is represented just by efficiency, which is considered constant over the entire operating range - (2.74) and gearbox ratio, which is expressed as ratio of pump and electrical motor nominal speeds - (2.75). Gearbox operating speed is considered to be the input speed on the site of a drive (2.76).

$$\boldsymbol{\eta_G} = \left[\eta_{G-OPi}\right] \tag{2.74}$$
$$\eta_{G-OPi} = \eta_{G_N}$$
$$i = 1, 2, ..., \text{k}_{OP}$$

$$r_G = \frac{n_{P_N}}{n_{M_N}} \tag{2.75}$$

$$\boldsymbol{n_G} = \left[n_{G-OPi}\right] \tag{2.76}$$
$$n_{G-OPi} = \frac{n_{P-OPi}}{r_G}$$
$$i = 1, 2, ..., \text{k}_{OP}$$

2.1.4.2 Hydrodynamic coupling

Hydrodynamic coupling works as torque/speed converter – see scheme in the Fig. 2.15. It is powered with a constant speed induction machine and output speed is controlled by the filling of the machine by oil.

It is not possible to create general model of the machine, because manufacturers adjust each machine to specific conditions of each applications. However, for the purposes of energy efficiency evaluation, pump suppliers provide the efficiency characteristic presenting the machine efficiency in the relation to output speed. In the figures Fig. 2.16 and Fig. 2.17, see sample curves for a simple and advanced hydrodynamic coupling.

Generally, hydrodynamic coupling efficiency is get by linear interpolation of hydrodynamic coupling efficiency referenced curve - (2.77). When the curve from manufacturer is not available then for simple hydrodynamic coupling it is sufficient to use linear speed – efficiency curve defined by "virtual" zero-speed efficiency offset and efficiency at nominal speed - (2.78).

1 – Primary wheel
2 – Secondary wheel
3 – Box
4 – Cover of a control bar
5 – Oil Basin
6 – Oil Pump
7 – Control bar
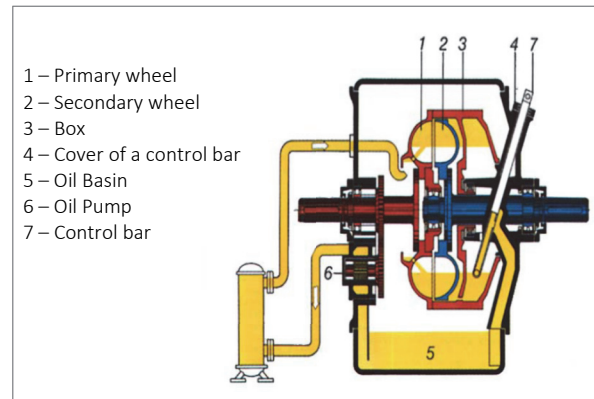
Fig. 2.15 Scheme of hydrodynamic coupling [42]
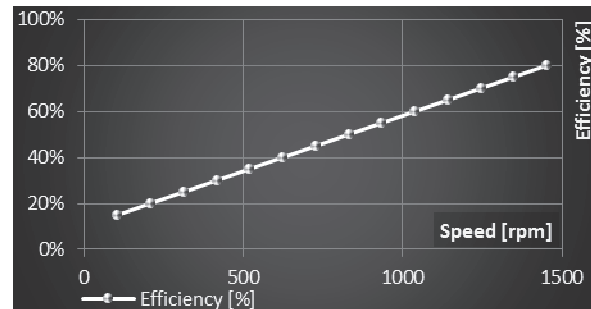
Fig. 2.16 Example of efficiency curve for simple hydrodynamic coupling
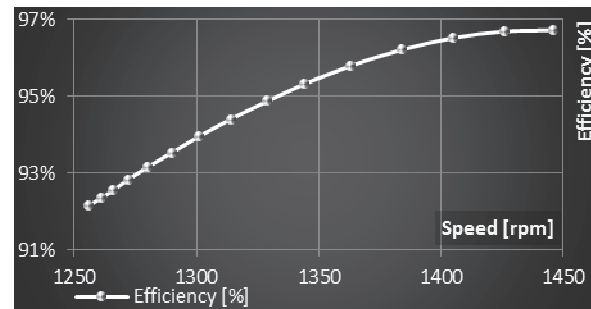
Fig. 2.17 Example of efficiency curve for advanced hydrodynamic coupling

$$\eta_{HC_R} = \eta_{HC_R}(n) \tag{2.77}$$

$$\boldsymbol{n_{HC_R}} = \left[n_{HC_R j} \right]; \boldsymbol{\eta_{HC_R}} = \left[\eta_{HC_R j}\left(n_{HC_R j} \right) \right]; j = 1, 2, ..., \mathrm{m}_{samples}$$

$$\boldsymbol{\eta_{HC\text{-}OP}} = \left[\eta_{HC-OPi} \right]; i = 1, 2, ..., k_{OP}$$

$$\eta_{HC-OPi} = f_{IntLinArray}\left(\boldsymbol{n_{HC_R}}, \boldsymbol{\eta_{HC_R}}, n_{G-OPi} \right)$$

$$\boldsymbol{\eta_{HC\text{-}OP}} = \left[\eta_{HC-OPi} \right]; \boldsymbol{n_{HC\text{-}OP}} = \left[n_{G-OPi} \right] \tag{2.78}$$

$$\eta_{HC-OPi} = \eta_{HC-OP_0} + (i-1) \times \frac{\eta_{HC-OP_N} - \eta_{HC-OP_0}}{(k_{OP}-1)}$$

$$i = 1, 2, ..., k_{OP}$$

2.1.4.3   Electrical motor

This chapter describes mathematical model of induction machine, which is the most commonly used for high-power pump and fan applications. The objective of the model is to provide induction machine efficiency and power factor based on speed and torque on the shaft of the load. The efficiency of an induction machine, when it is speed controlled, depends upon two parameters - motor stator frequency (or if you like synchronous speed) and mechanical (shaft) load. See the Fig. 2.19 for efficiency of general induction machine.

Fig. 2.19 Induction machine efficiency

Similarly, induction machine power factor depends upon stator frequency and mechanical (shaft) load, which is proportional to slip frequency – see Fig. 2.18.

Presented efficiency and power factor characteristics used for the illustration of physical background have been calculated from an equivalent induction motor circuit diagram under steady state conditions. However, this approach cannot be used in practice, where the parameters of equivalent circuit diagram are usually not available. Next, it is derived how to approximate motor efficiency and power factor from characteristics at nominal speed, which are provided by electrical motor manufacturers into the curves matching motor operating points under variable speed control.

Fig. 2.18 Induction machine power factor

Transformation of motor nominal curves into characteristics fitting for variable speed load are valid under following assumptions:

- Frequency converter is operated under fixed Volt/Hertz control. The motor is not operated in field weakening – thus, it is considered constant magnetizing current. Then, Joule's loss can be considered as dominant under motor nominal load.

- Motor flux current remains unchanged under motor fixed Volt/Hertz control. Therefore, motor current is independent on motor speed and depends only on shaft torque - (2.79).

- Motor nominal electrical loss curve does not change significantly in relation to motor per unit load ((2.83)).

- Motor mechanical losses do not significantly affect the overall efficiency. The change of mechanical losses with the speed is neglected and the nominal mechanical curve is considered

in the operating speed range unchanged (i.e. the worst case is calculated, while calculating efficiency for lower speeds).

- Motor apparent power is proportional to motor speed under motor fixed Volt/Hertz control for speeds below motor nominal speed - (2.80).

Motor efficiency is then defined by (2.81). Motor losses are expressed by (2.82) and motor relative load by (2.83). Motor power factor is then expressed in (2.84).

$$T_M = k_{\Psi M} I_{sqM} \tag{2.79}$$

$$I_{sdM} = I_{mM} = \frac{U_{sM_N} \frac{\omega}{\omega_N}}{\omega L_{hM}} = \frac{U_{sM_N}}{\omega_N L_{hM}} = const. \neq f(\omega)$$

$$I_{sM} = \sqrt{I_{sd}^2 + I_{sq}^2} \Rightarrow I_{sM} = f(T_M) = f(p)$$

$$S_{\omega M}(p) = 3 \times U_{p\omega M} \times I(p) = 3 \times U_{pM_N} \times \frac{\omega}{\omega_N} \times I(p) = S_{M_N}(p) \times \frac{\omega}{\omega_N} \Rightarrow \tag{2.80}$$

$$\Rightarrow S_{\omega M}(p) = S_{M_N}(p) \times \frac{\omega}{\omega_N}$$

$$\eta_M = \frac{P_{Mm}}{P_{Mm} + \Delta P_M}; \Delta P_M = f(p) \Rightarrow \eta_M = f(p) \tag{2.81}$$

$$\Delta P_M(p) = P_{Mm_N}(p) \times \frac{1 - \eta_{M_N}(p)}{\eta_{M_N}(p)} = P_{cM_N}(p) \times \left(1 - \eta_{M_N}(p)\right) \tag{2.82}$$

$$p = \frac{T_M}{T_{M_N}} = \frac{P_{Mm}}{P_{Mm_N} \times \frac{\omega_M}{\omega_{M_N}}} \tag{2.83}$$

$$\cos\phi_M = \frac{P_M}{S_M} = \frac{P_{Mm}}{\eta_M(p) \times S_{M_N}(p) \times \frac{\omega_M}{\omega_{M_N}}} \tag{2.84}$$

$$\cos\phi = f(p, \omega)$$

For numerical model, input efficiency and power factor characteristics at nominal speed in relation to motor mechanical power are required - (2.85). Then it is calculated the curve of motor torque and the loss curve at nominal speed - (2.86) and (2.87). Motor losses at real motor operating points are then interpolated according to (2.88) – i.e. loss curve is supposed to be independent on the speed, but only on the motor torque. Efficiency at motor operating points is finally expressed in (2.89).

For purposes of power factor evaluation, motor apparent power at nominal speed ((2.90)) and at motor operating points ((2.91) - (2.98)) is calculated. Equations (2.92) represents per unit load and (2.93) stator frequency. Motor power factor at motor operating points is then (2.95), motor nominal slip in (2.99).

$$\eta_{M_N} = \eta_{M_N}\left(P_{Mm}\right); \quad \cos\phi_{M_N} = \cos\phi_{M_N}\left(P_{Mm}\right);$$

$$\boldsymbol{\eta_{M_N}} = \left[\eta_{Mj}\left(P_{Mmj}\right)\right]^T; \quad \boldsymbol{cos\phi_{M_N}} = \left[\cos\phi_{Mj}\left(P_{Mmj}\right)\right]^T; \quad j=1,2,\ldots,m_{samples} \tag{2.85}$$

$$\boldsymbol{T_{M_N}} = \left[T_{Mj}\left(P_{Mmj}\right)\right]^T; \quad j=1,2,\ldots,m_{samples} \tag{2.86}$$

$$T_{Mj} = \frac{P_{Mj}}{\dfrac{n_{M_N}}{60}\times 2\pi}$$

$$\boldsymbol{\Delta P_{M_N}} = \left[\Delta P_{M_N j}\left(T_{M_N j}\right)\right]^T; \quad j=1,2,\ldots,m_{samples} \tag{2.87}$$

$$\Delta P_{M_N j} = \frac{P_{Mm_N j}}{\eta_{M_N j}}\left(1-\eta_{M_N j}\right) = \frac{P_{Mm_N j}}{\eta_{M_N j}} - P_{Mm_N j}$$

$$\boldsymbol{\Delta P_{M\text{-}OP}} = \left[\Delta P_{M-OPi}\left(T_{M-OPi}\right)\right]^T; \quad i=1,2,\ldots,k_{OP} \tag{2.88}$$

$$\Delta P_{M-OPi} = f_{IntLinArray}\left(\boldsymbol{T_{M_N}}, \boldsymbol{\Delta P_{M_N}}, T_{M-OPi}\right)$$

$$\boldsymbol{\eta_{M\text{-}OP}} = \left[\eta_{M-OPi}\right]^T; \quad i=1,2,\ldots,k_{OP} \tag{2.89}$$

$$\eta_{M-OPi} = \frac{P_{M-OPi}}{P_{M-OPi} + \Delta P_{M-OPi}}$$

$$\boldsymbol{S_{M_N}} = \left[S_{M_N j}\left(P_{Mm_N j}\right)\right]^T; \quad j=1,2,\ldots,m_{samples} \tag{2.90}$$

$$S_{M_N j} = \frac{P_{M_N j}}{\eta_{M_N j}\times\cos\phi_{M_N j}}$$

$$\boldsymbol{S_{M\text{-}OP}} = \left[S_{M-OPi}\right]^T; \quad i=1,2,\ldots,k_{OP} \tag{2.91}$$

$$S_{M-OPi} = f_{IntLinSplines}\left(\boldsymbol{T_{M_N}}, \boldsymbol{S_{M_N}}, p_{OPi}\times T_{M_N}\right)\times\frac{f_{sM-OPi}}{f_{sM_N}}$$

$$p_{OPi} = \frac{T_{M-OPi}}{T_{M_N}}; \quad i=1,2,\ldots,k_{OP} \tag{2.92}$$

$$f_{sM-OPi}[\text{Hz}] = f_{rm(el)-OPi}[\text{Hz}] + f_{r-OPi}[\text{Hz}] \tag{2.93}$$

$$f_{rm(el)-OPi}[\text{Hz}] = \frac{n_{M-OPi}[\text{rpm}]}{60}\times n_{pp}$$

$$f_{r-OPi} = f_{r_N}\times p_{OPi}; \quad f_{r_N} = f_{sM_N}\times s_{M_N}; \quad i=1,2,\ldots,k_{OP}$$

$$s_{M_N} = \frac{f_{s_N} - f_{m(el)_N}}{f_{s_N}} = \frac{f_{s_N}[\text{Hz}] - \dfrac{n_{M_N}[rpm]\times n_{pp}[-]}{60}}{f_{s_N}[\text{Hz}]} \tag{2.94}$$

$$\boldsymbol{cos\phi_{M\text{-}OP}} = \left[\cos\phi_{M-OPi}\right]^T; \quad i=1,2,\ldots,k_{OP} \tag{2.95}$$

$$\cos\phi_{M-OPi} = \frac{P_{Mm-OPi}}{\eta_{M-OPi}\times S_{M-OPi}}$$

2.1.4.4   Frequency converter

There are several available converter topologies (e.g. Fig. 2.20) and different power devices able to be chosen as well as possibilities of their control. Hence, it is impossible to propose general mathematical model of the converter providing a high accuracy results. The most optimal way is to obtain needed information concerning FC efficiency and power factor in demanded range of power from the FC manufacturer as an efficiency characteristic in the relation to the load apparent power. If it is not possible to get any information from FC supplier, it is possible to consider its efficiency as constant value, because it changes only about 2% in a wide power range and even less in an application with a high static head, i.e. low frequency variability. If the converter is not specified at all, the efficiency value can be chosen e.g. in a range of 96 - 98,5%. Frequency converter power factor is usually considered one.

Numerical model consists of following equations. Equation (2.96) represents input frequency converter characteristics. Frequency converter efficiency and power factor are then interpolated according to (2.97) and (2.98). Frequency converter input apparent power is then (2.99).

$$\eta_{FC} = \eta_{FC}\left(S_{FCout}\right); \quad \cos\phi_{FC} = \cos\phi_{FC}\left(S_{FCout}\right); \tag{2.96}$$
$$\boldsymbol{\eta_{FC}} = \left[\eta_{FCj}\left(S_{FCout-j}\right)\right]^{T}; \quad \boldsymbol{cos\phi_{FC}} = \left[\cos\phi_{FCout-j}\left(S_{FCout-j}\right)\right]^{T}; \quad j=1,2,...,m_{samples}$$

$$\boldsymbol{\eta_{FC\text{-}OP}} = \left[\eta_{FC-OPi}\right]^{T} \tag{2.97}$$
$$\eta_{FC-OPi} = f_{IntLinArray}\left(\boldsymbol{S_{FCout}}, \boldsymbol{\eta_{FC}}, S_{M-OPi}\right)$$
$$i=1,2,...,k_{OP}$$

$$\boldsymbol{cos\phi_{FC\text{-}OP}} = \left[\cos\phi_{FC-OPi}\right]^{T} \tag{2.98}$$
$$\cos\phi_{FC-OPi} = f_{IntLinArray}\left(\boldsymbol{S_{FCout}}, \boldsymbol{cos\phi_{FC}}, S_{M-OPi}\right)$$
$$i=1,2,...,k_{OP}$$

$$\boldsymbol{S_{FCin\text{-}OP}} = \left[S_{FCin-OPi}\right]^{T} \tag{2.99}$$
$$S_{FCin-OPi} = \frac{P_{M-OPi}}{\eta_{M-OPi} \times \eta_{FC-OPi} \times \cos\phi_{FC-OPi}}$$
$$i=1,2,...,k_{OP}$$

2.1.4.5   Transformer
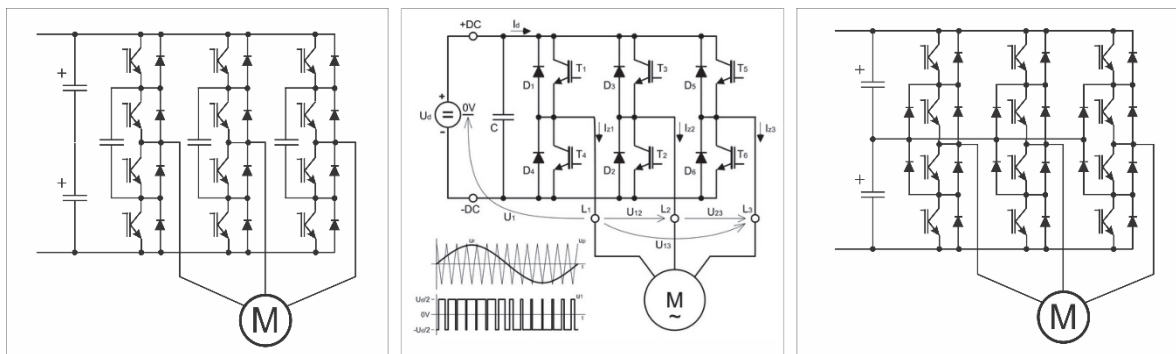
Fig. 2.20 Examples of conventional frequency converter topologies

The efficiency of a transformer is dependent upon the load of a transformer and upon the character of the load - power factor [40]. Efficiency is generally expressed by (2.100).

Losses of transformers are divided into no-load losses independent on the load and load losses. These are generally available in a transformer datasheet (2.101).
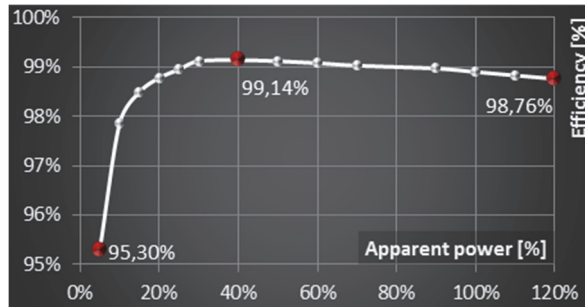
Fig. 2.21 Transformer efficiency curve

$$\eta_T = \frac{P_{Tout}}{P_{Tin}} = \frac{P_{Tout}}{P_{Tout} + \Delta P_T} = \frac{S_T \times \cos\phi_{TL}}{S_T \times \cos\phi_{TL} + \Delta P_T} \qquad (2.100)$$

$$\Delta P_T = \Delta P_{T_0} + \Delta P_{T_N} \times L_T^2 \qquad (2.101)$$

$$L_T = \frac{S_T}{S_{T_N}} \qquad (2.102)$$

From the information about the load and transformer no-load and load losses and power factor of the load, it is possible to draw the efficiency curve ((2.100)). Power factor equals usually one when supplying frequency converter.

It is also possible to derive transformer optimal load where the transformer works with best efficiency. This is important especially while dimensioning the transformer. If we differentiate the efficiency expression (2.100) with respect to the per-unit load ((2.102)), we get the relation for transformer best efficiency load point - (2.103). From (2.100) - (2.103) we get the maximal efficiency value - (2.104) [40].

$$L_{TBEP} = \sqrt{\frac{\Delta P_{T_0}}{\Delta P_{T_N}}} \qquad (2.103)$$

$$\eta_{max} = \frac{\sqrt{\Delta P_{T_0}} \times S_{T_N} \times \cos\phi_{TL}}{\sqrt{\Delta P_{T_0}} \times S_{T_N} \times \cos\phi_{TL} + 2 \times \Delta P_{T_0} \times \sqrt{\Delta P_{T_N}}} \qquad (2.104)$$

As we can see from the final efficiency curve (Fig. 2.21), it is optimal to choose the transformer size so that the real load of the transformer is within the range of 50%-80% of the transformer nominal load. Transformer final efficiency at operating points is then in (2.105). The transformer load (for apparent power and power factor) is considered frequency converter in case of VFC or electrical motor in case of CFC.

$$\eta_T = \eta_T\left(S_{TL}, \cos\phi_{TL}\right);$$

$$(2.105)$$

$$\boldsymbol{\eta_{T\text{-}OP}} = \left[\eta_{T-OPi}\left(S_{TL}, \cos\phi_{TL}\right)\right]^T$$

$$\eta_{T-OPi} = \frac{S_{TL-OPi} \times \cos\phi_{TL-OPi}}{S_{TL-OPi} \times \cos\phi_{TL-OPi} + \Delta P_{T_0} + \Delta P_{T_N} \times \dfrac{S_{TL-OPi}}{S_{T_N}}} ; \ i=1,2,...,k_{OP}$$

Concerning power factor of the transformer, it is further considered total power factor of transformer including transformer load. The derivation of transformer power factor is based on T-shape equivalent circuit diagram for steady states according to Fig. 2.22. Equations (2.106) - (2.109) express calculation of equivalent circuit parameters. Equivalent impedance of transformer including load is then in (2.110) and power factor in (2.111) or (2.112).

$$R_{Tsc} = \frac{\Delta P_{T_N}}{3 \times I_N^2} = \Delta P_{T_N} \times \left(\frac{U_{T1}}{S_{T_N}}\right)^2 ; \ R_1 = R_2' = \frac{R_{Tsc}}{2}; \ \Delta P_{T_N} = \Delta P_{CU}$$

$$(2.106)$$

$$X_{Tsc} = x_{sc} \times \left(\frac{U_{T1_N}^2}{S_{T_N}}\right) = \sqrt{z_{Tsc}^2 - \left(\frac{\Delta P_{T_N}}{S_{T_N}}\right)^2} \times \left(\frac{U_{T1_N}^2}{S_{TN}}\right); z_{Tsc} = u_{Tsc}$$

$$(2.107)$$

$$X_{\sigma 1} = X_{\sigma 2}' = \frac{X_{Tsc_N}}{2}$$

$$R_{FE} = \frac{U_{T1_N}^2}{\Delta P_{T_0}}; \Delta P_{T_0} = \Delta P_{FE}$$

$$(2.108)$$

$$X_m = \frac{U_{T1_N}^2}{i_0 \times S_{T_N}}$$

$$(2.109)$$

$$\overline{Z}_{eq} = \left(R_1 + \frac{AC + BD}{C^2 + D^2}\right) + j\left(X_{\sigma 1} + \frac{BC - AD}{C^2 + D^2}\right)$$

$$(2.110)$$

$$A = R_{FE}\left(R_2' + R_L\right) - X_m\left(X_{\sigma 2}' + X_m\right)$$

$$B = R_{FE}\left(X_{\sigma 2}' + X_L\right) + X_m\left(R_2' + R_L\right)$$

$$C = R_2' + R_L + R_{FE}$$

$$D = X_{\sigma 2}' + X_L + X_m$$
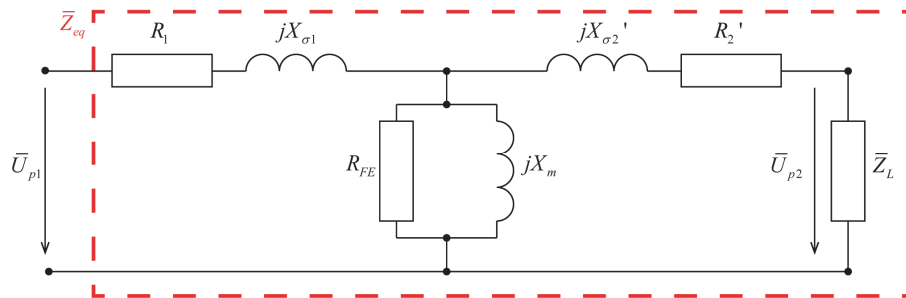
Fig. 2.22 Transformer equivalent circuit diagram

$$\cos\phi_T = \cos\left(\tan^{-1}\left(\frac{Im\left(\overline{Z}_{eq}\right)}{Re\left(\overline{Z}_{eq}\right)}\right)\right) \tag{2.111}$$

$$\cos\phi_T = \cos\phi_T\left(\overline{Z}_{eq}\left(R_1, X_{\sigma1}, R_2', X_{\sigma2}', R_{FE}, X_m, \overline{Z}_L\right)\right); \tag{2.112}$$

$$\boldsymbol{cos\phi_{TOP}} = \left[\cos\phi_{T-OPi}\left(\overline{Z}_{eq}\left(\overline{Z}_{L-OPi}\right)\right)\right]^T$$

$$Z_{L-OPi} = \frac{U_{L-OPi}^2}{S_{L-OPi}}; \ i=1,2,...,k_{OP}$$

2.1.5   Total evaluation

For total energy consumption evaluation, it is required hydraulic power of pump, evaluated efficiency of pump and complete drive chain and operating time for each operating point. Total efficiency is get according to (2.113) from particular efficiencies of evaluated application components (brackets denotes optional components of evaluated application). Total power consumption in operating points including auxiliary power consumption is then in (2.114) and (2.115). Total annual energy consumption based on application operating profile is finally in (2.116) and accordingly CO_2 emissions in (2.117).

$$\eta_{Total} = \eta_P \times \eta_{PC} \times[\eta_G]\times[\eta_{HC}]\times\eta_M \times[\eta_{FC}]\times[\eta_T] \tag{2.113}$$

$$\boldsymbol{\eta_{Total\text{-}OP}} = \boldsymbol{\eta_{P\text{-}OP}}\times\boldsymbol{\eta_{PC\text{-}OP}}\times[\boldsymbol{\eta_{G\text{-}OP}}]\times[\boldsymbol{\eta_{HC\text{-}OP}}]\times\boldsymbol{\eta_{M\text{-}OP}}\times[\boldsymbol{\eta_{FC\text{-}OP}}]\times[\boldsymbol{\eta_{T\text{-}OP}}]$$

$$P_{cTotal} = \frac{P_{hP}}{\eta_{Total}} + P_{Aux} \tag{2.114}$$

$$\boldsymbol{P_{cTotal\text{-}OP}} = \boldsymbol{P_{hP\text{-}OP}}./\boldsymbol{\eta_{Total\text{-}OP}} + P_{Aux}$$

$$P_{Aux} = [P_{AuxHC}]+[P_{AuxFC}]+P_{AuxM}+[P_{AuxT}] \tag{2.115}$$

$$\boldsymbol{E_{c\text{-}OP}} = \boldsymbol{P_{hP\text{-}OP}}./\boldsymbol{\eta_{Total\text{-}OP}}\times\boldsymbol{t_{OP}} \tag{2.116}$$

$$E_{cTotal}[\text{MWh/ year}] = \frac{\sum_{i=1}^{k_{OP}}\left(\frac{P_{hP-OPi}[\text{kW}]}{\eta_{Total-OPi}[-]}\times t_{OPi}[\text{h}]\right)+\sum_{i=1}^{k_{OP}}t_{OPi}[\text{h}]\times P_{Aux}[\text{kW}]}{1000}$$

$$CO_{2-Total}[\text{t/ year}] = k_{CO_2}[\text{kg/ kWh}]\times E_{cTotal}[\text{MWh/ year}] \tag{2.117}$$

From economical indicators, it is evaluated net present value of an investment according to (2.118) and payback period generally defined as in (2.119). It is considered one-time investment at the beginning and constant interest rate and annual savings over the whole service life.

$$NPV = PV - C_{Invest} \tag{2.118}$$

$$NPV = \sum_{k=1}^{n_{years}}\left(C_{AnSavings}\times\frac{1}{\left(1+i_R\right)^k}\right) - C_{Invest}$$

$$C_{AnSavings}[\text{currency}] = E_{cSavings}[\text{MWh}]\times1000\times C_E[\text{currency/ kWh}]$$

$$t_{PayBack} = t_{PayBack} \mid \sum_{k=1}^{t_{PayBack}} \left(C_{Inflow-k} - C_{Outlow-k} \right) - C_{Invest} > 0$$

(2.119)

$$C_{Inflow} = E_{cSavings} \times C_E$$

$$C_{Outflow} = C_{Invest} \times i_R$$

For economical comparison of two variants of flow control technique (CFC and VFC) differential and/or relative values are substituted in former relations according to (2.120) to get relative comparison.

$$E_{cSavings} = \Delta E_{cSavings}$$

(2.120)

$$\Delta E_{cSavings-CFC} = E_{cTotal-CFC} - E_{cTotal-VFC} ; \Delta E_{cSavings-VFC} = E_{cTotal-VFC} - E_{cTotal-CFC}$$

$$C_{Invest} = \Delta C_{Invest}$$

$$\Delta C_{Invest-CFC} = C_{Invest-CFC} - C_{Invest-VFC} ; \Delta C_{Invest-VFC} = C_{Invest-VFC} - C_{Invest-CFC}$$

2.2   Model verification - Case studies

In this chapter, two typical case studies of hydraulic systems are presented to show complex pump optimization process employing variable speed flow control in comparison to other flow control techniques for typical high-power pump applications and to verify developed mathematical models on particular applications. Simultaneously, it is presented the performance and functionality of software tool Medium-Voltage Drive Pump Save 2012, which has been developed within this work, based on the mathematical models described in the Chapter 2.1. In the Fig. 2.23, see the main screenshot of the software tool. More in-detail information about the software tool and its features have been published especially in following international conferences: [A4, A5, A6, A7] and research reports [A39, A41, A42, A43, A44, A45]. Brief summary is available in Appendix 1 – MVD Pump Save 2012.

The case studies below have been selected considering to present not only typical high-power pump applications suitable for variable speed flow control, but also to present selected important case study factors, that might fundamentally influence technical and economical parameters and/or payback period of the installations. Therefore, every case study is presented in two variants, where in each variant one particular change has been made, to present the influence of the change directly next to each other. In the first case study of boiler feed pump application, it is presented identical case once with hydraulic system with constant pressure control and second with hydraulic system with linear pressure control. The second case study show the water circulating pump application with high flow variability with weighted average of flow about 53% in the first variant and weighted average of flow about 78% in the second variant.
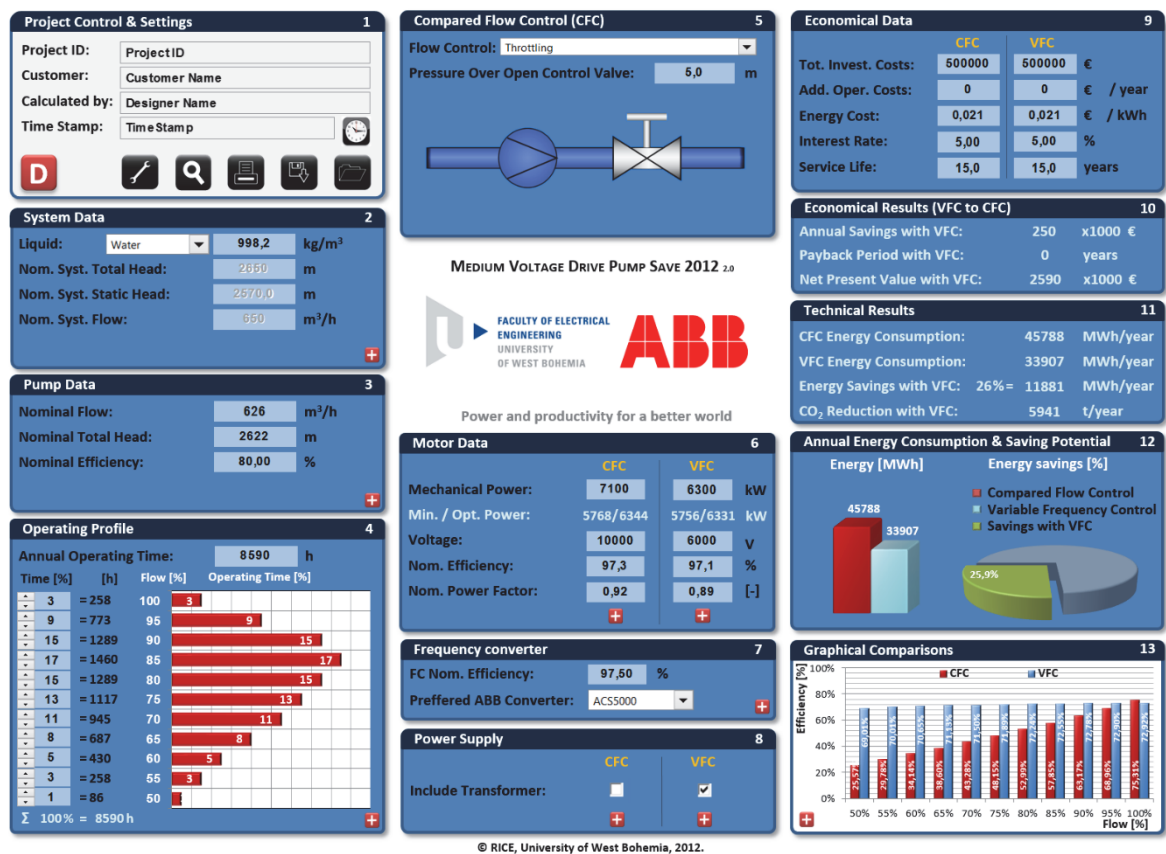
Fig. 2.23 Medium-Voltage Drive Pump Save 2012 – Main screen

2.2.1   Case study 1 – Hydraulic system with high ratio of static head

This case study presents a boiler feed pump application in thermal power plant – i.e. a pump application with a high ratio of head versus flow. The case study is presented in two variants to present the behavior and suitability or no suitability of evaluated flow control methods for this type of pump applications in relation to static head control and to present the performance of developed mathematical models under different load conditions. The first variant represents the hydraulic system with a control on a constant static head and the second variant represents the identical hydraulic system with a linear control of static head.

2.2.1.1   Hydraulic system & Operating profile

The case study hydraulic system parameters are summarized in the Table 2.1. The Fig. 2.24 shows the operating profile – statistical distribution of flow in time. Figures Fig. 2.25 and Fig. 2.26 presents the hydraulic system curves including operating range and/or operating points.

Table 2.1 – Case study 1, Hydraulic system

Hydraulic system	Value - Var. 1	Value – Var. 2	Unit
Hydraulic system			
Nominal flow	650	650	m³/h
Nominal total head	2650	2650	m
Nominal dynamic head	80	80	m
Nominal static head	2570	2570	m
Zero flow static head	2570	0	m
Static / referenced head control	constant	linear	
Liquid density	998,2	998,2	kg/m³
System operating data			
Annual running time	8590	8590	h
Flow operating range	50 - 100	50 - 100	%
Weighted average of flow	79,30	79,30	%
Weighted average of hydraulic system power	78,59	63,87	%
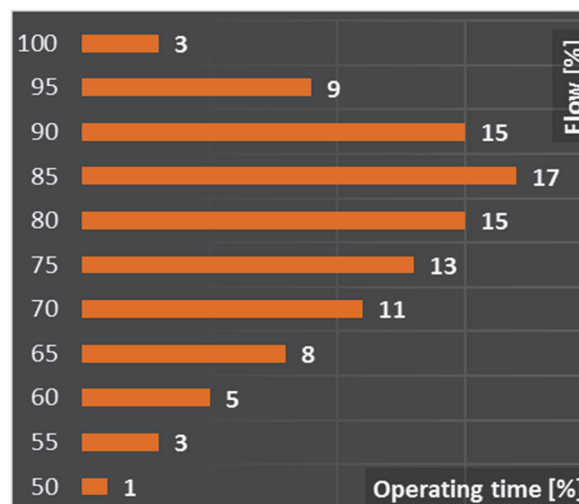
Fig. 2.24 – Case study 1 – V1 and V2,
Operating profile

2.2.1.2   Pump

It is employed centrifugal pump with the parameters according to Table 2.2. Pump calculated real operating point (see Table 2.3) is very close to Pump Best Efficiency Operating Point (BEP). Fig. 2.25 and Fig. 2.26 present approximated pump performances curves from nominal speed to speed range covering demanded flow range employing Variable Speed Control (VSC) for the case study variants. See also the operating ranges and points for VSC and passive flow control methods. Notice, that throttling operating range keeps practically unchanged, however operating range for bypass flow control, changes dramatically in relation to static head control. Bypass flow operating range also exceeds recommended pump operating range and it is clearly not suitable for this combination of pump of hydraulic system and pump. Notice the significantly lower speed variation for the variant of hydraulic system with high constant static head against the variant with linear static head control - Fig. 2.27 and Fig. 2.28. Also, see a slightly different real nominal operating point for both variants resulting from the change of hydraulic system curve - Table 2.3

Table 2.2 – Case study 1, Pump

Pump	Value – Var. 1,2	Unit
Pump		
Nominal speed	4 050	rpm
Minimal flow operating range at nominal speed	$156,5 - 782,5$	m^3/h
Pump BEP		
Flow	626	m^3/h
Head	2 622	m
Efficiency	80	%
Hydraulic power	4 463	kW
Mechanical / shaft power	5 579	kW
Torque	13 154	Nm

Table 2.3 – Case study 1, Real nominal operating points

Pump & Hydraulic system	Value – Var. 1	Value – Var. 2	Unit
Real nominal operating point			
Flow	614	633	m^3/h
Head	2641	2 579	m
Efficiency	79,83	79,90	%
Hydraulic power	4 407	4 442	kW
Mechanical / shaft power	5 520	5 559	kW
Torque	13 015	13 108	Nm
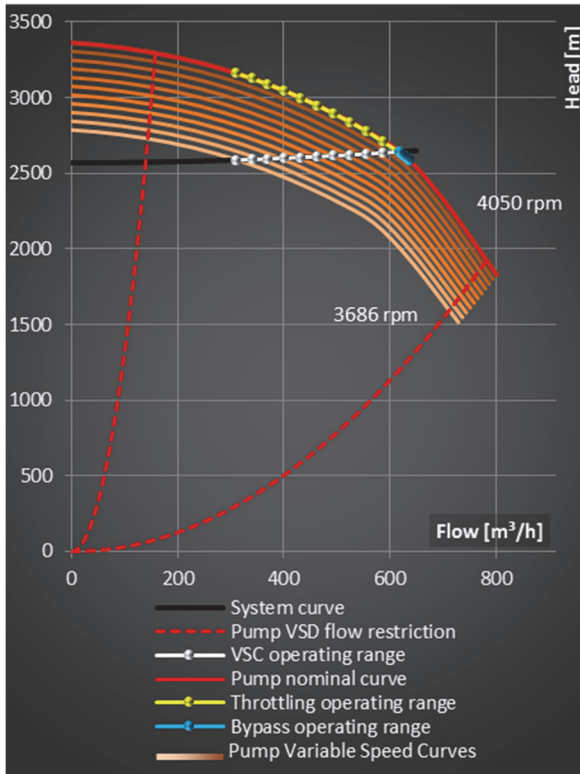
Fig. 2.25 Case study 1 – V1,
Pump & Hydraulic system curves
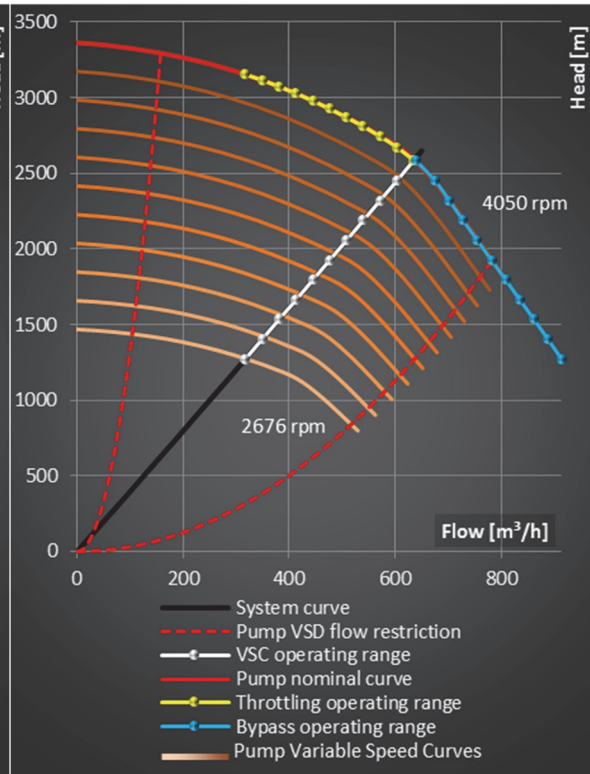
Fig. 2.26 Case study 1 – V2,
Pump & Hydraulic system curves
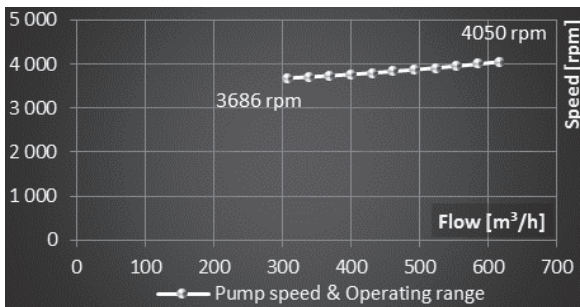
Fig. 2.27 Case study 1 – V1,
Pump VSC speed range
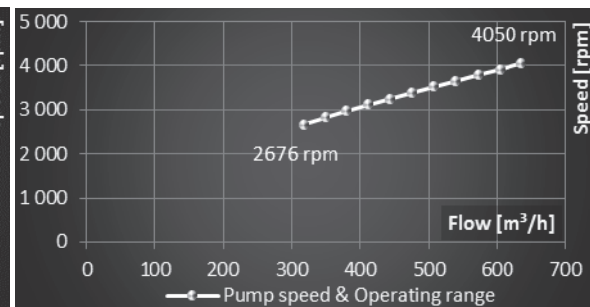
Fig. 2.28 Case study 1 – V2,
Pump VSC speed range

Pump performance curves and operating points under VSC

Fig. 2.29 - Fig. 2.36 show approximated pump performance curves – torque, efficiency, hydraulic power and mechanical power or power consumption – from curves at nominal speed to curves at variable speed according to VSC. See especially the positive effect of variable speed control for high-speed ranges - Fig. 2.32 – where the efficiency keeps close to nominal operating point efficiency against the efficiency of pump with low operating range - Fig. 2.31 (hydraulic system with constant, high static head). Derivation of pump torque (Fig. 2.29 and Fig. 2.30) and mechanical or shaft power (Fig. 2.35 and Fig. 2.36) at pump operating points is important for further proper approximation of especially electrical motor efficiency.
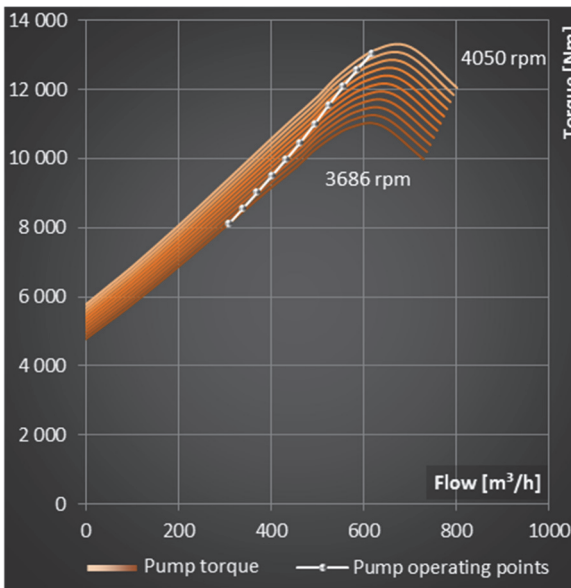
Fig. 2.29 Case study 1 – V1, Pump VSC torque
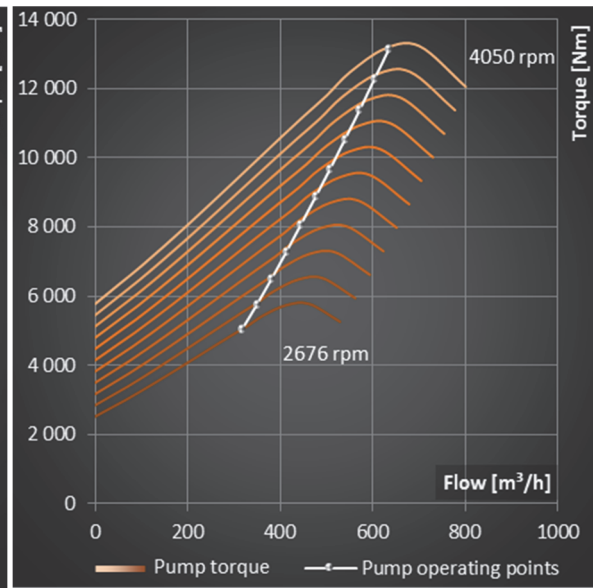
Fig. 2.30 Case study 1 – V2, Pump VSC torque
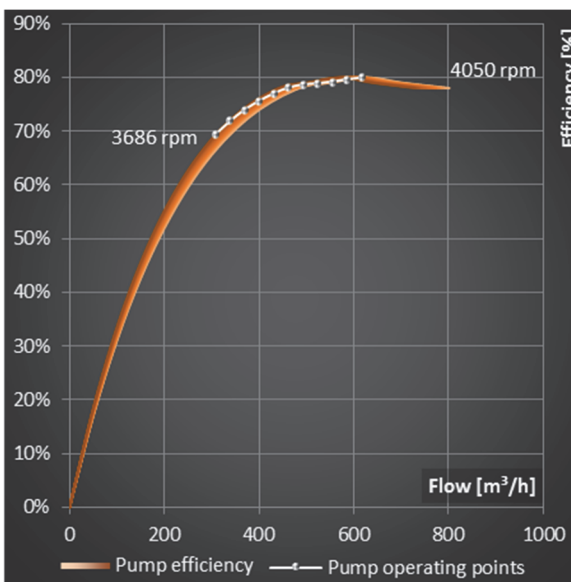
Fig. 2.31 Case study 1 – V1, Pump VSC efficiency
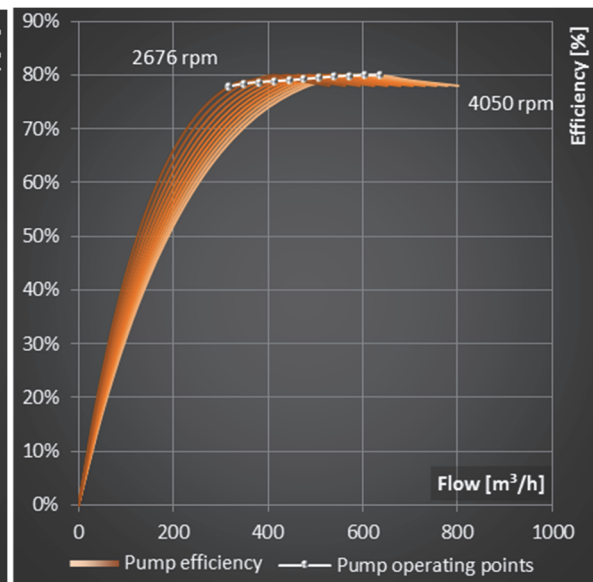
Fig. 2.32 Case study 1 – V2, Pump VSC efficiency
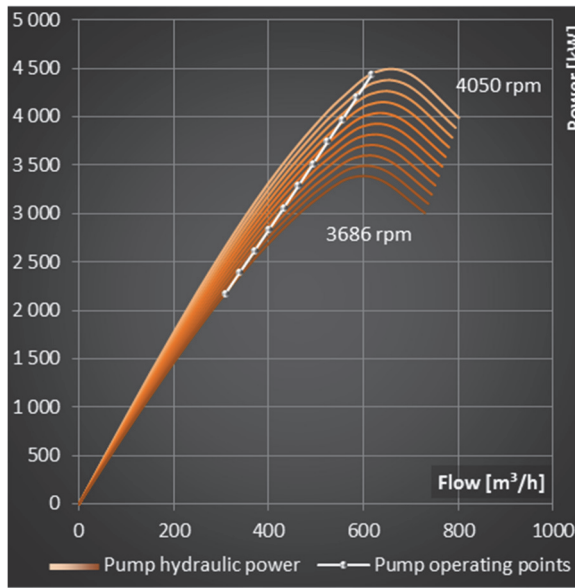
Fig. 2.33 Case study 1 – V1,
Pump VSC hydraulic power
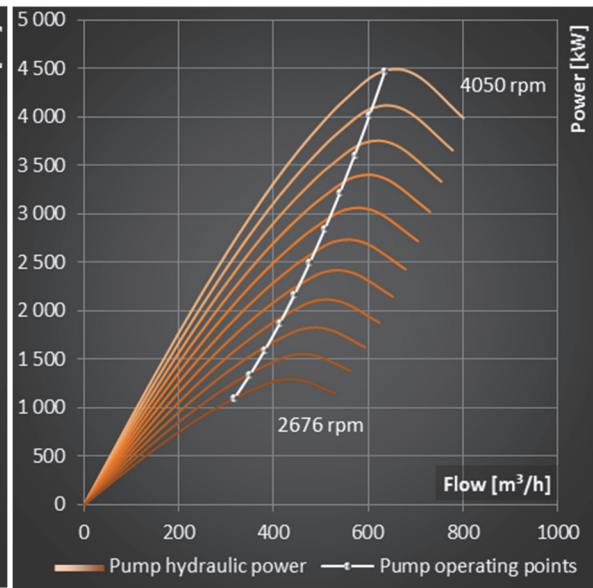
Fig. 2.34 Case study 1 – V2,
Pump VSC hydraulic power
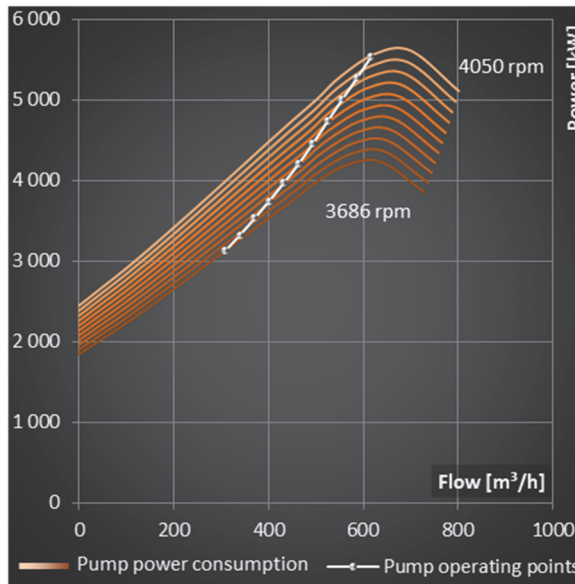
Fig. 2.35 Case study 1 – V1,
Pump VSC power consumption
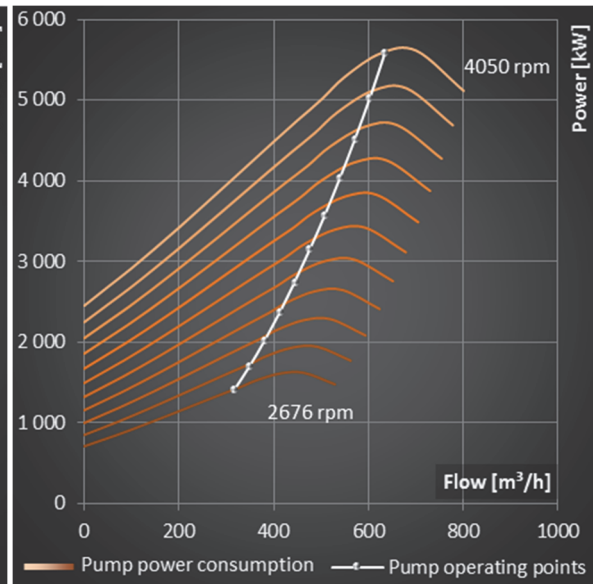
Fig. 2.36 Case study 1 – V2,
Pump VSC power consumption

2.2.1.3   Flow control

Below see the parameters of throttling valve (Table 2.4) and hydrodynamic coupling (Table 2.5), employed in the case study. Note, that inclusion of throttling valve into hydraulic system shifts the nominal operating point, which does not allow reaching exactly comparable hydraulic parameters in relation to other flow control techniques. However, the loss on control valve is included in the control efficiency and therefore final comparison to other flow control techniques is still relevant.

Hydrodynamic coupling efficiency curve (Fig. 2.37) is set to simple linear curve just as a sample device. Nevertheless, it should be always used hydrodynamic performance curve generated directly from manufacturer for specific load conditions, when available.

Throttling valve

<center>Table 2.4 – Case study 1, Throttling</center>

Throttling	Value – Var. 1	Value – Var. 2	Unit
Throttling valve			
Pressure drop at nominal flow	5	5	m
Nominal operating point			
Nominal flow	617	633	m³/h
Nominal head	2637	2574	m

Hydrodynamic coupling

<center>Table 2.5 – Case study 1, Hydrodynamic coupling</center>

Hydrodynamic coupling	Value – Var. 1,2	Unit
Nominal speed	2989	rpm
Nominal efficiency	94,0	%
Auxiliary losses	0	kW
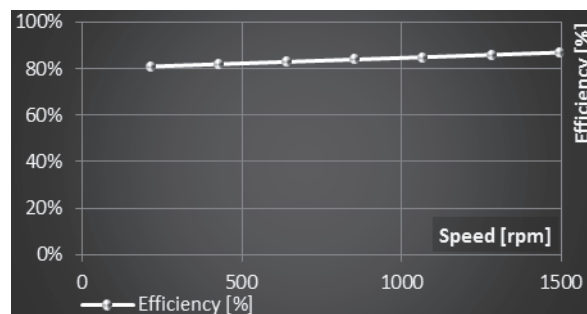
<center>Fig. 2.37 Case study 1 – V1 and V2,
Efficiency curve for hydrodynamic coupling</center>

2.2.1.4 Electrical motor & Gearbox

Electrical motors are specified separately for drive with frequency converter (VFC) and fixed speed drive due to different demand on power and voltages. Electrical motor for Compared Flow Control (CFC) methods has to be designed to higher power to cover additional losses. However, purposely has been chosen power plant with bus voltage of 10 kV to be able to take the advantage of connection of fixed speed electrical motor directly do electrical bus in contrast to electrical drive with frequency converter, which requires an additional transformer. Nominal parameters of both electrical motors are summarized in Table 2.6, below.

   Two gearboxes are employed with different gearbox ratio due to use of different electrical motors, however the efficiency is set for both identical – 97 % (Table 2.7). In real gearboxes, the efficiency would likely slightly vary. However, in relation to efficiency of other drive chain components, this effect could be neglected.

Table 2.6 – Case study 1, Electrical motor

Electrical motor	CFC Value - Var. 1,2	VFC Value - Var. 1,2	Unit
Nominal parameters			
Mechanical power	7 100	6 300	kW
Voltage	10 000	6 000	V
Current	458	701	A
Frequency	50	50	Hz
Speed	2989	1492	rpm
Number of poles	2	4	-
Efficiency	97,3	97,1	%
Power factor	0,92	0,89	-
Apparent power	7 932	7 290	kVA
Shaft Torque	22 683	40 322	Nm
Slip	0,004	0,005	-
Other			
Auxiliary losses	0	0	kW

Table 2.7 – Case study 1, Gearbox

Gearbox	CFC Value - Var. 1,2	VFC Value - Var. 1,2	Unit
Gearbox ratio	1,355	2,714	-
Gearbox efficiency	97,0	97,0	%

Electrical motor for Variable Frequency Control (VFC) – VSC with Frequency Converter

Electrical motor datasheet efficiency and power factor for nominal speed are specified in the Fig. 2.38. Fig. 2.39 and Fig. 2.40 show then detailed view on approximated motor efficiency and power factor for the operating speed range according the algorithms described in the chapter 2.1.4.3. Especially for the case of higher operating range, the difference between performance curves for nominal speed and variable speed is very noticeable and using just performance curves for nominal speed can clearly lead to significant error in final evaluation.

Fig. 2.41 - Fig. 2.44 characterize motor load at evaluated operating points. Fig. 2.41 and Fig. 2.42 present load or motor mechanical power and torque and Fig. 2.43 and Fig. 2.44 show the speed progress over the operating range.
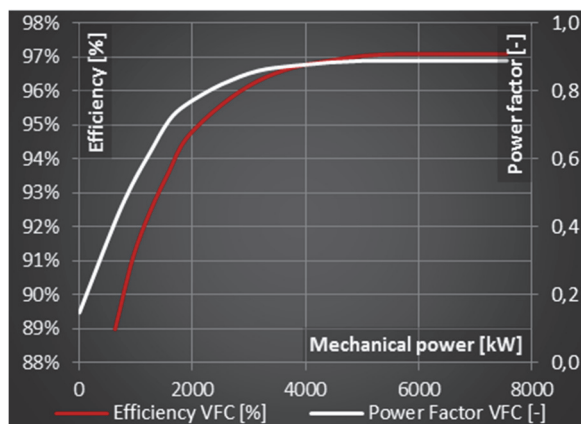
Fig. 2.38 Case study 1 - V1 and V2,
VFC motor - nominal-speed curves
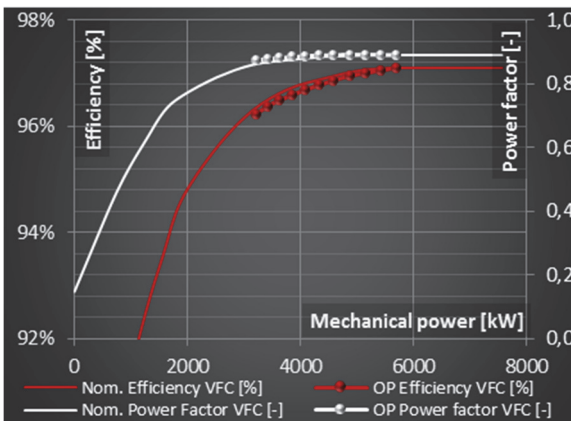
Fig. 2.39 Case study 1 – V1,
VFC motor – variable speed curves and OP range
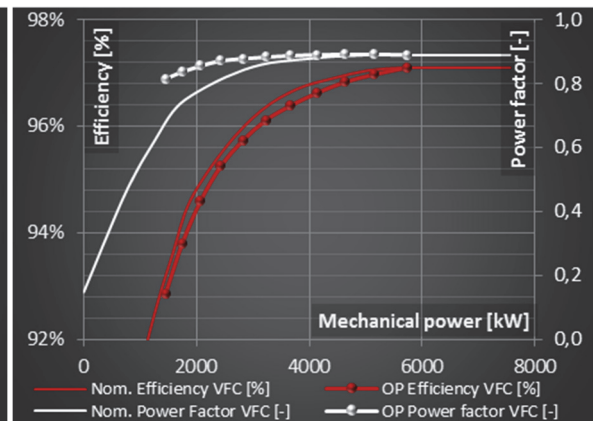
Fig. 2.40 Case study 1 – V2,
VFC motor – variable speed curves and OP range
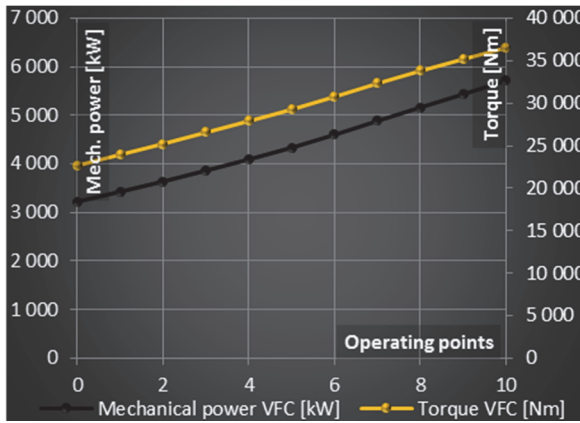
Fig. 2.41 Case study 1 – V1,
VFC motor - mechanical power and torque for evaluated OP
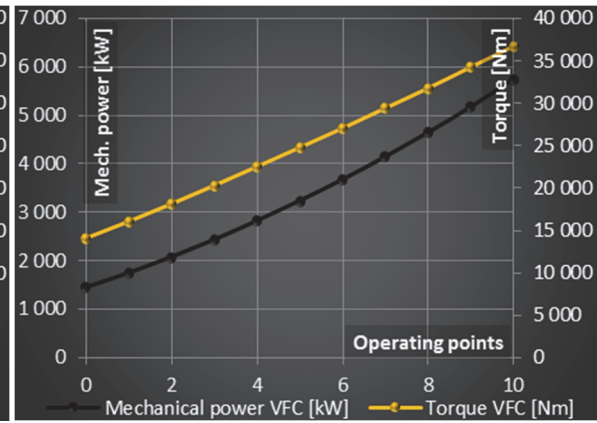
Fig. 2.42 Case study 1 – V2,
VFC motor - mechanical power and torque for evaluated OP
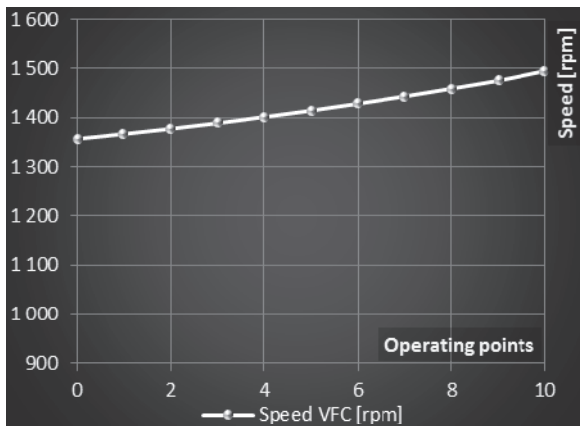
Fig. 2.43 Case study 1 – V1,
VFC motor - speed curve for evaluated OP
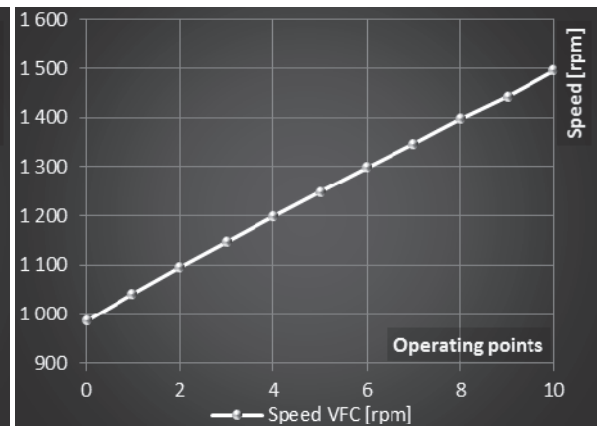
Fig. 2.44 Case study 1 – V2,
VFC motor - speed curve for evaluated OP

Electrical motor for Compared Flow Control (CFC) – VSC with Hydrodynamic Coupling, Throttling, Bypass and On-Off control

For Compared Flow Control methods (CFC) – VSC with Hydrodynamic Coupling, Throttling, Bypass and On-Off control identical electrical fixed speed motor with following nominal speed efficiency and power factor curves is considered - see Fig. 2.45. The motors speed is considered constant over the entire operating range - Fig. 2.46.

Fig. 2.47 - Fig. 2.50 show motor performance curves – efficiency, power factor and torque and mechanical power - while driving variable speed controlled pump with hydrodynamic coupling. It is possible to observe similar performance curves to VSC with frequency converter due to the character of VSC. However, see the difference in motor efficiency and power factor – VFC motor efficiency shifted slightly down in opposite to VFC power factor (Fig. 2.39 and Fig. 2.40) compared to CFC motor (Fig. 2.47 - Fig. 2.48).

Fig. 2.51 - Fig. 2.54 show motor performance curves – efficiency, power factor and torque and mechanical power - while driving fixed speed pump with flow control by throttling. See the practically identical performance curves independent on the change of hydraulic system static head control (variant 1 compared to variant 2). The tiny different is given just by a slightly different nominal operating point.

Fig. 2.56 - Fig. 2.58 are related to bypass pump flow control. See especially the Fig. 2.57, which shows the paradox of increasing power consumption with decreasing of flow (for lower operating points). This is caused because of the derivative of pump curve at the operating range, and clearly indicates the no suitability of this technique of flow control in combination with selected pump and hydraulic system.

On-Off control operates just at nominal operating point common e.g. with nominal operating point of bypass control, therefore it is not explicitly presented.
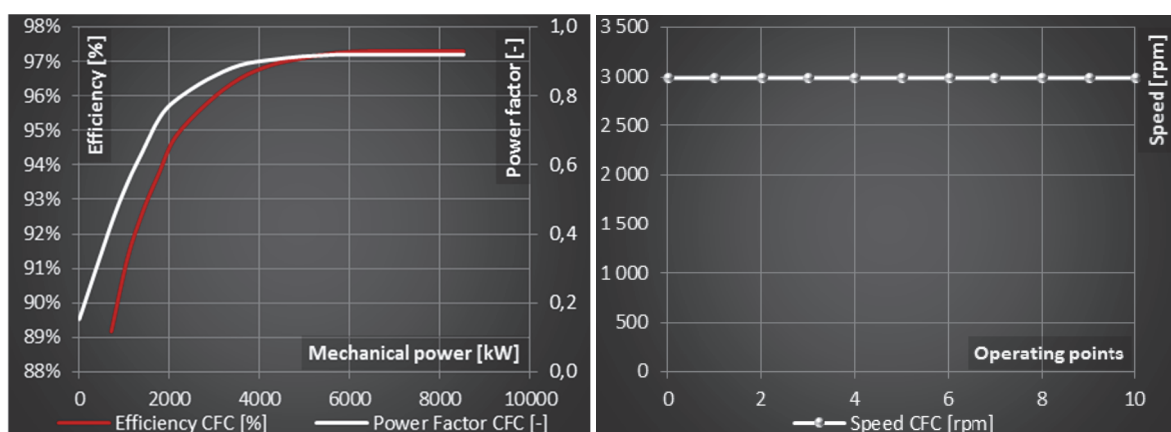
Fig. 2.45 Case study 1 - V1 and V2, CFC motor - nominal-speed efficiency and power factor curves

Fig. 2.46 Case study 1 - V1 and V2, CFC motor speed for OP range
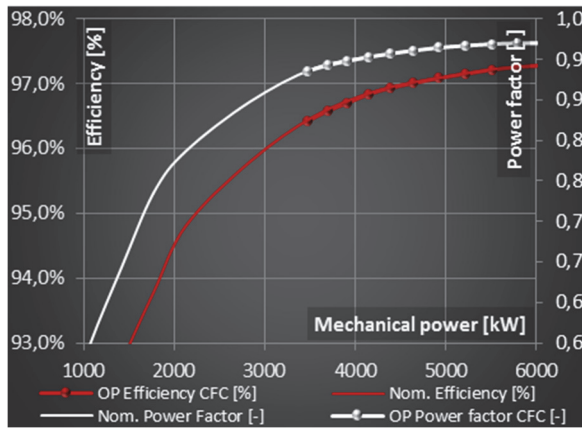
Fig. 2.47 Case study 1 – V1,
CFC motor efficiency and power factor curves for
HC OP range
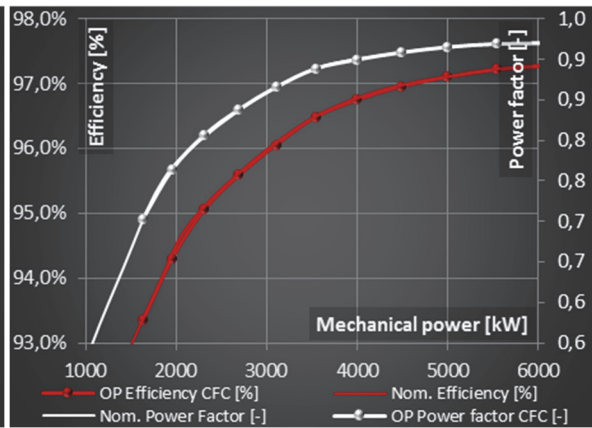
Fig. 2.48 Case study 1 – V2,
CFC motor efficiency and power factor curves for
HC OP range
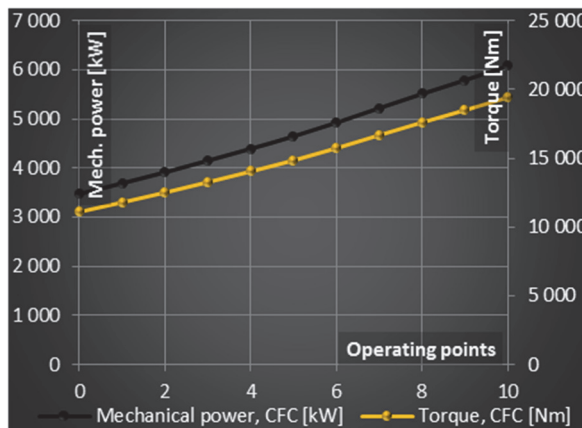
Fig. 2.49 Case study 1 – V1,
CFC motor power and torque curves for
HC OP range
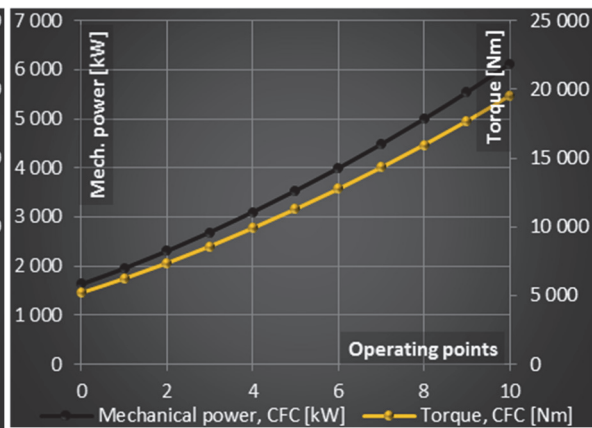
Fig. 2.50 Case study 1 – V2,
CFC motor power and torque curves for
HC OP range
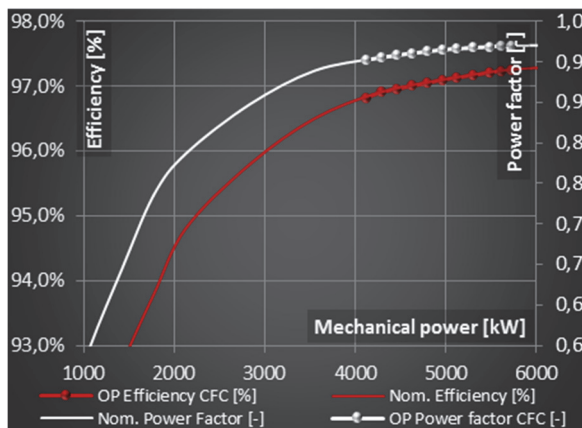
Fig. 2.51 Case study 1 – V1,
CFC motor efficiency and power factor curves for
Throttling OP range
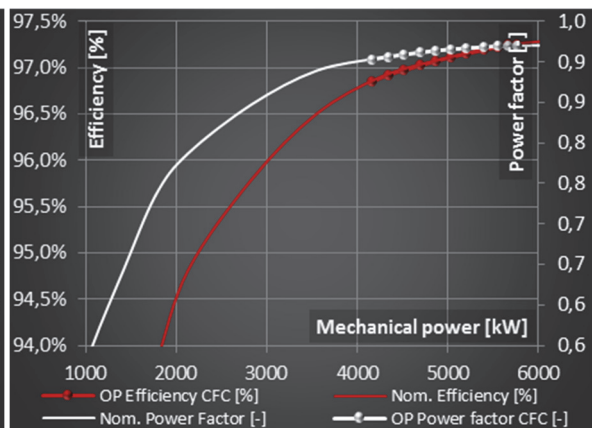
Fig. 2.52 Case study 1 – V2,
CFC motor efficiency and power factor curves for
Throttling OP range
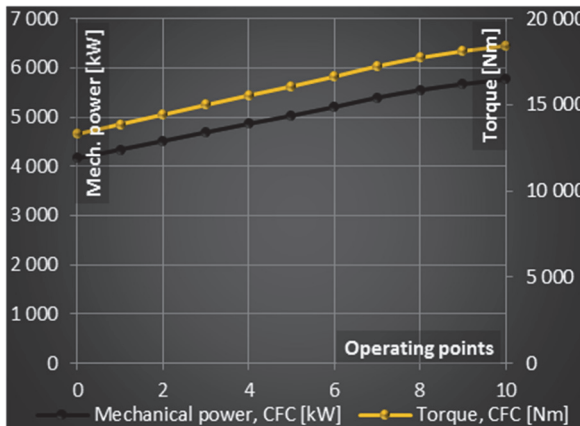
Fig. 2.53 Case study 1 – V1,
CFC motor power and torque curves for
Throttling OP range
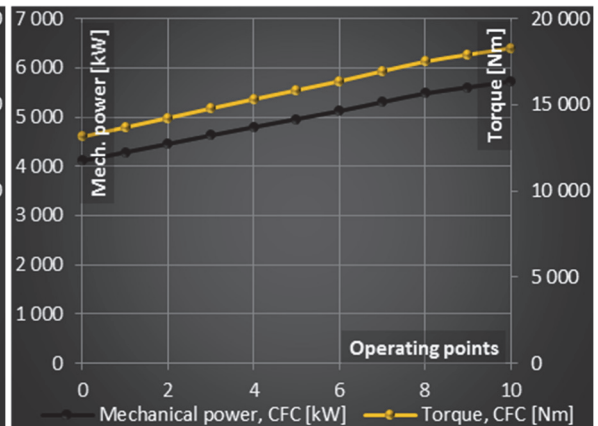
Fig. 2.54 Case study 1 – V2,
CFC motor power and torque curves for
Throttling OP range
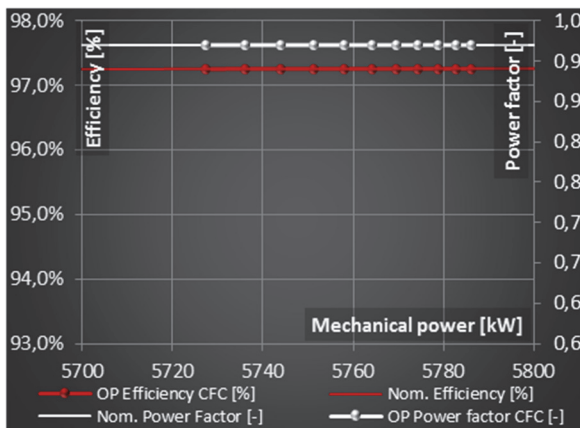
Fig. 2.55 Case study 1 – V1,
CFC motor efficiency and power factor curves for
Bypass OP range
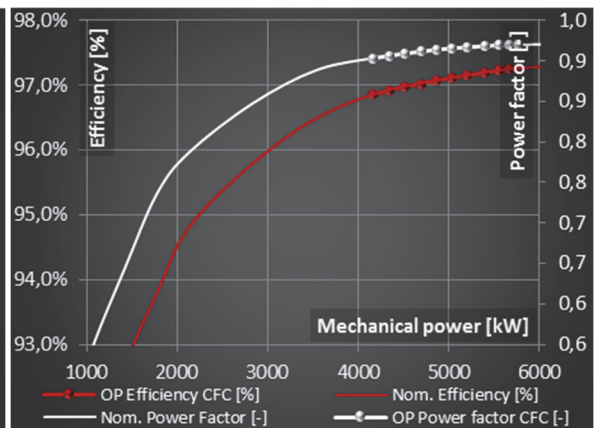
Fig. 2.56 Case study 1 – V2,
CFC motor efficiency and power factor curves for
Bypass OP range
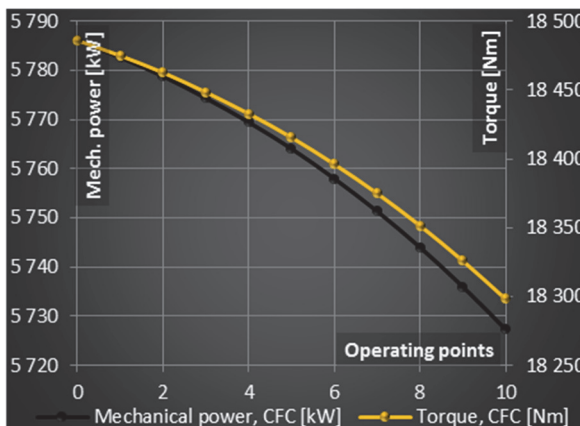
Fig. 2.57 Case study 1 – V1,
CFC motor power and torque curves for
Bypass OP range
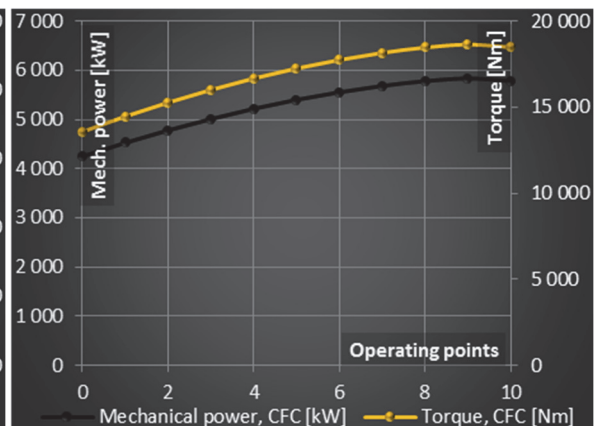
Fig. 2.58 Case study 1 – V2,
CFC motor power and torque curves for
Bypass OP range

2.2.1.5   Frequency converter

For the purposes of the test case study, frequency converter is considered with constant efficiency and power factor over the entire operating range – see Fig. 2.59 and Table 2.8 for details.

<div align="center">Table 2.8 – Case study 1, Frequency converter</div>

Frequency converter	Value – Var. 1,2	Unit
Input nominal FC parameters		
Input voltage	6 000	V
Power supply frequency	50	Hz
Efficiency	97,5	%
Nominal power factor	1	-
Apparent power	8 923	kVA
Current	859	A
Output FC parameters		
Nominal continuous apparent power	8 700	kVA
Frequency range	$1 - 66$	Hz
Other		
Auxiliary losses	0	kW
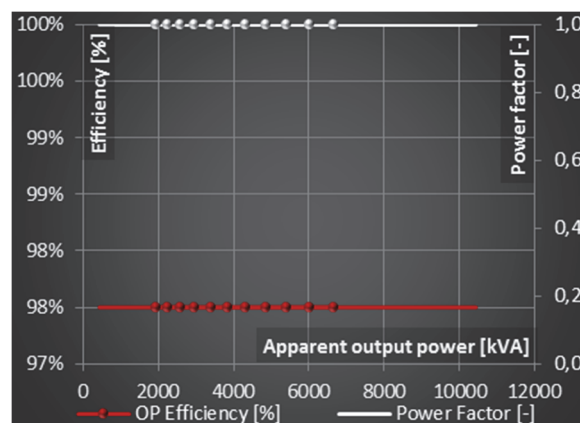
<div align="center">Fig. 2.59 Case study 1 – V1 and V2,
Frequency converter efficiency and power factor</div>

2.2.1.6   Transformer

Transformer is included in both case study variants just for VFC to adapt 10 kV bus voltage to input voltage 6 kV of frequency converter. Transformer parameters are summarized in the Table 2.9. Real operating points have been then calculated from the knowledge of equivalent circuit diagram (see chapter 2.1.4.5) and apparent power and power factor of the load – i.e. electrical motor for VFC. Fig. 2.60 and Fig. 2.61 show the transformer operating points supplying electrical motor at operating points according to Fig. 2.39 respectively Fig. 2.40.

Table 2.9 – Case study 1, Transformer

Transformer	Value – Var. 1,2	Unit
Nominal parameters		
Primary voltage	10 000	V
Secondary voltage	6 000	V
Frequency	50	Hz
Efficiency	99,8	%
Nominal power factor	0,999	-
Other parameters		
Short circuit voltage	6	%
No load current	0,5	%
No load losses	22	kW
Load losses	90	kW
Other		
Auxiliary losses	0	kW
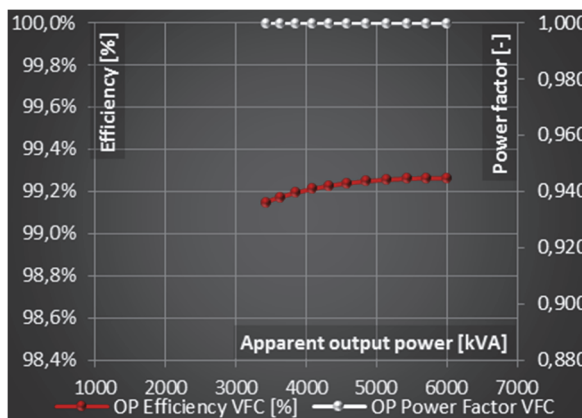
Fig. 2.60 Case study 1 – V1, VFC Transformer efficiency and power factor operating range
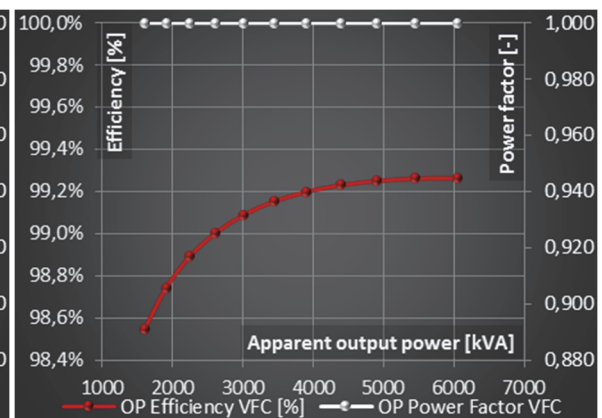
Fig. 2.61 Case study 1 – V2, VFC Transformer efficiency and power factor operating range

2.2.1.7   Technical evaluation

This chapter summarizes the results of technical evaluation of both variants of the case study. For each variant of case study, it has been processed evaluation of energy consumption and/or energy savings, total energy efficiency comparison with variable frequency drive and detailed breakup of energy efficiency chain for all throttling, bypass, on-off control, VSC with hydrodynamic coupling and VSC with frequency converter at each operating point according the operating profile.

Considering throttling flow control against VSC with frequency converter, the savings differ very significantly based on the type of static head control – see Fig. 2.62 and Fig. 2.63. We can see that VSC with frequency converter have a clear advantage in the second variant with linear static head control, especially for lower operating points, due to higher speed variability. At nominal operating point, the efficiency of VFC is worse due to additional loss in frequency converter and transformer against the fixed speed CFC. See that energy consumption of throttling flow control are almost identical for both variants of hydraulic system. This explains the principle of throttling flow control - see chapter 2.1.3 – and confirms that hydraulic system static head control doesn't influence the energy consumption although total control efficiency gets naturally lower and advantage of VFC increases for hydraulic systems with zero or linear static head control.

Bypass flow control results are summarized in Fig. 2.64 and Fig. 2.65. It has been stated already in design phase, that bypass flow control is not suitable for this combination of pump and hydraulic system neither for variant with constant hydrostatic head nor for variant with linear static head control. Similarly like in variant with throttling, bypass provide good results just around nominal operating point for both variants.

On-Off is not usable for boiler feed pump, however have been included in the case study to see the behavior on a general hydraulic system with a high static head. Results for both variants of hydraulic systems are summarized in Fig. 2.66 and Fig. 2.67. Interestingly, for hydraulic system with a high static head performs on-off control significantly better than other both passive and active flow controls while having the least investment costs. However, the advantage is lost at hydraulic systems with zero or linear static head curve. Moreover, on-off control is usable just in systems with a capacity and/or tank and allows controlling of just the average flow quantity, not the real time flow quantity.

Finally, VSC with hydrodynamic coupling and VSC with frequency converter are to be compared. Variant of VSC with HC is summarized in Fig. 2.68 and Fig. 2.69 and variant of VSC with FC is summarized in Fig. 2.70 and Fig. 2.71. We can see that independently on the type of hydraulic system static head control, both controls performed well. Control efficiency equals to one, hence the main difference is especially in the efficiency of hydrodynamic coupling. Although variant with VFC has additional transformer and frequency converter, it is still more efficient variant than variant with hydrodynamic coupling. However, it is necessary to mention, that for reliable conclusion, hydrodynamic coupling would have to be designed directly by manufacturer for this specific case and therefore this result cannot be generalized.

Throttling
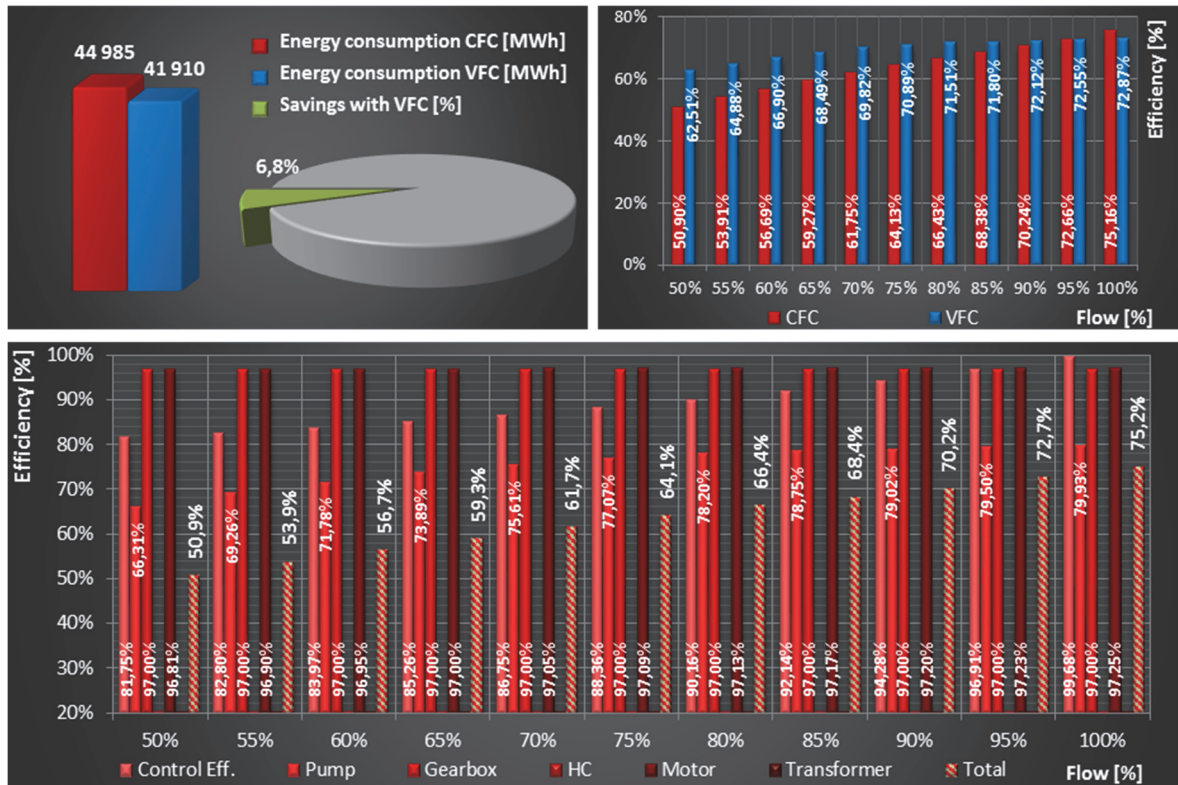
Fig. 2.62 Summary of results – V1 – Throttling, Energy consumption and savings – top left, Efficiency compared to VFC – top right, Efficiency break up – bottom.
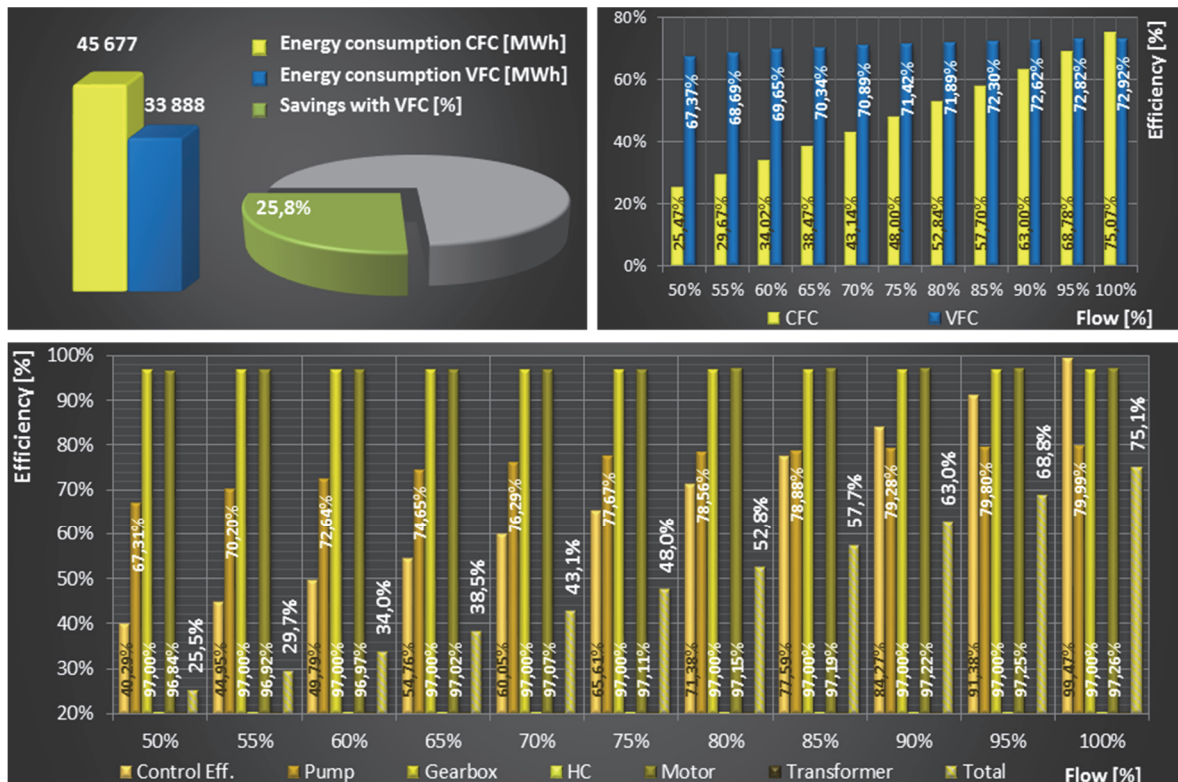
Fig. 2.63 Summary of results – V2 – Throttling, Energy consumption and savings – top left, Efficiency compared to VFC – top right, Efficiency break up – bottom.

Bypass
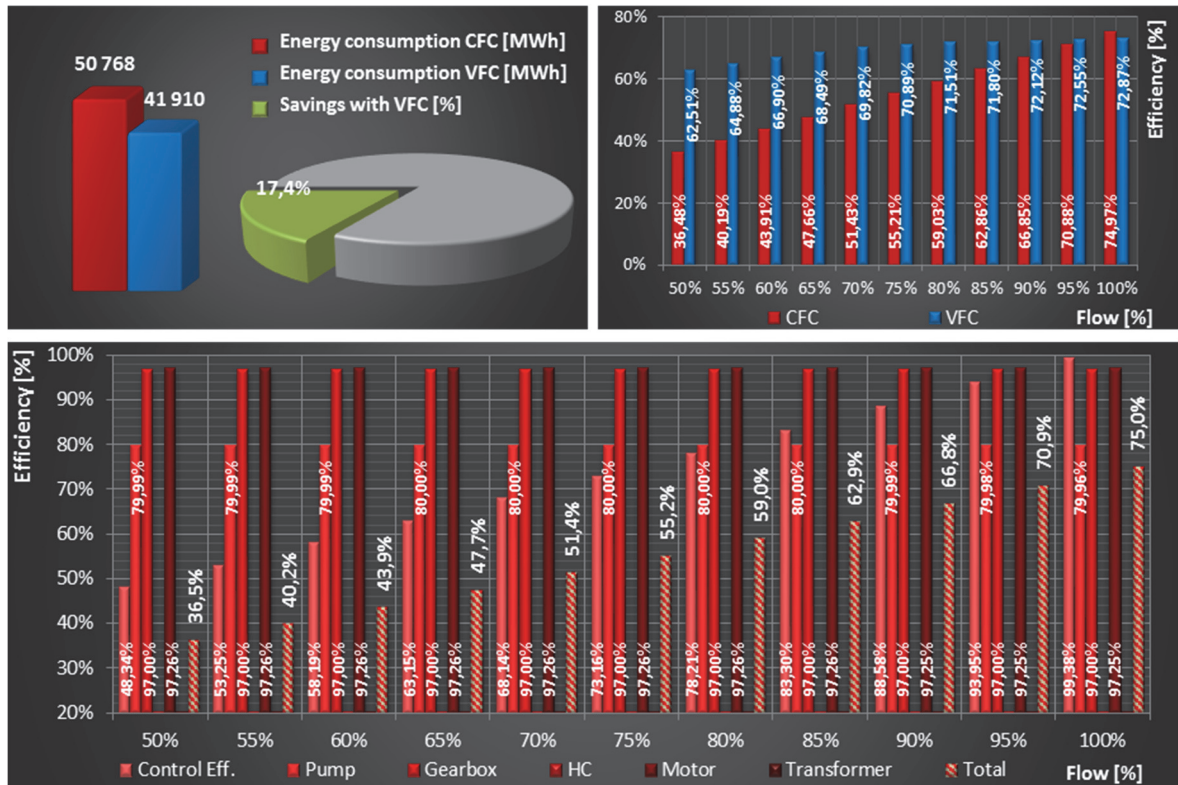
Fig. 2.64 Summary of results – V1 – Bypass, Energy consumption and savings – top left, Efficiency compared to VFC – top right, Efficiency break up – bottom.
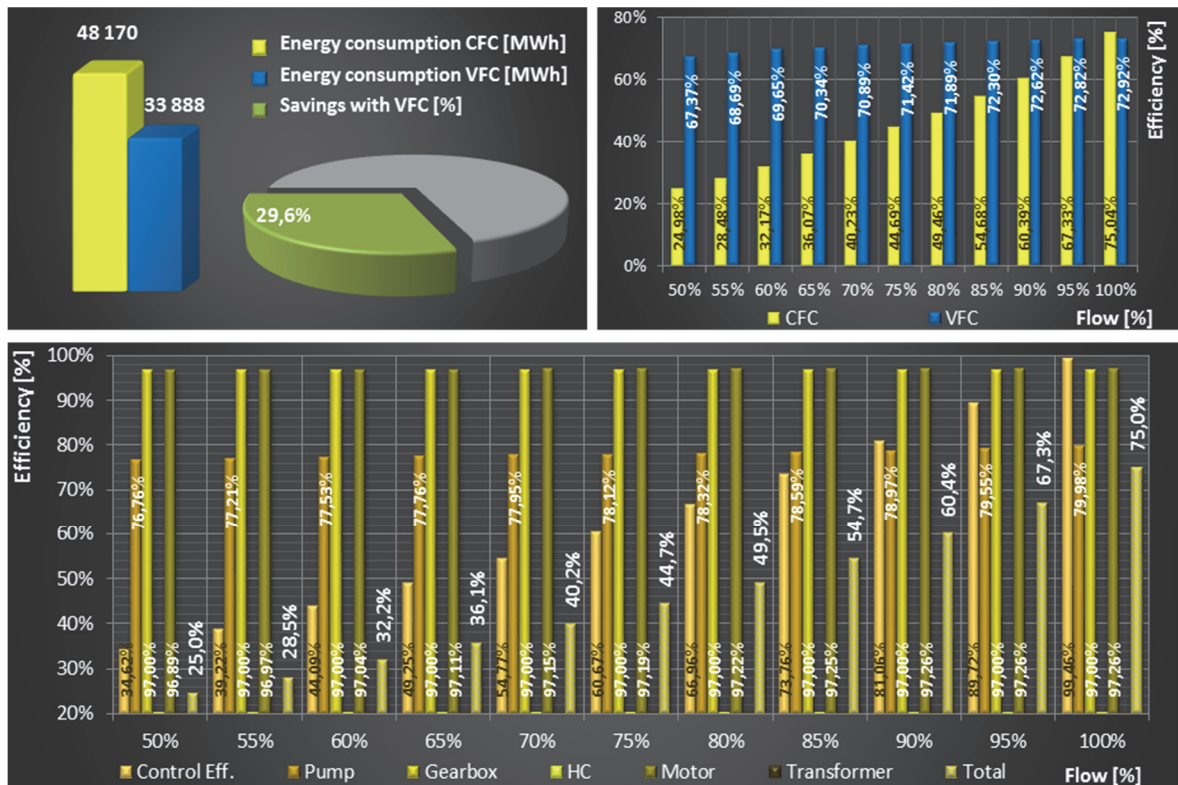
Fig. 2.65 Summary of results – V2 – Bypass, Energy consumption and savings – top left, Efficiency compared to VFC – top right, Efficiency break up – bottom.

On-Off control
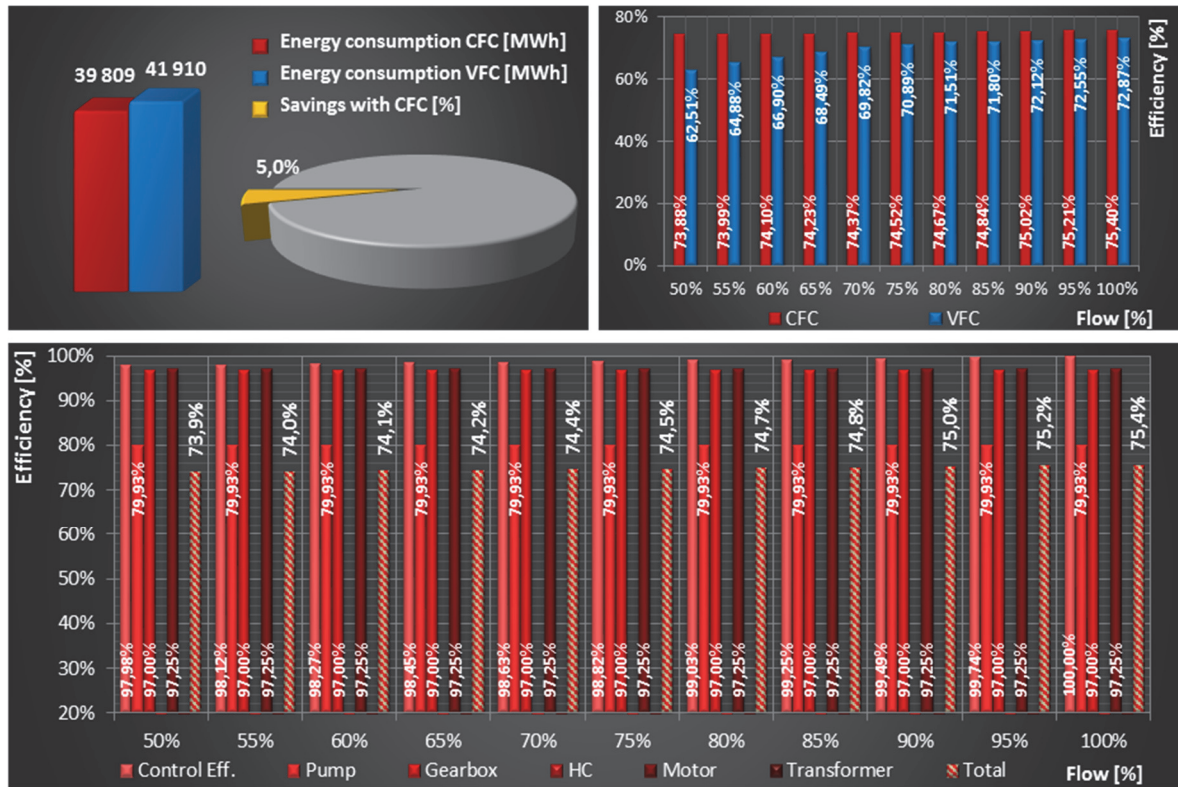
Fig. 2.66 Summary of results – V1 – On-Off control, Energy consumption and savings – top left, Efficiency compared to VFC – top right, Efficiency break up – bottom.
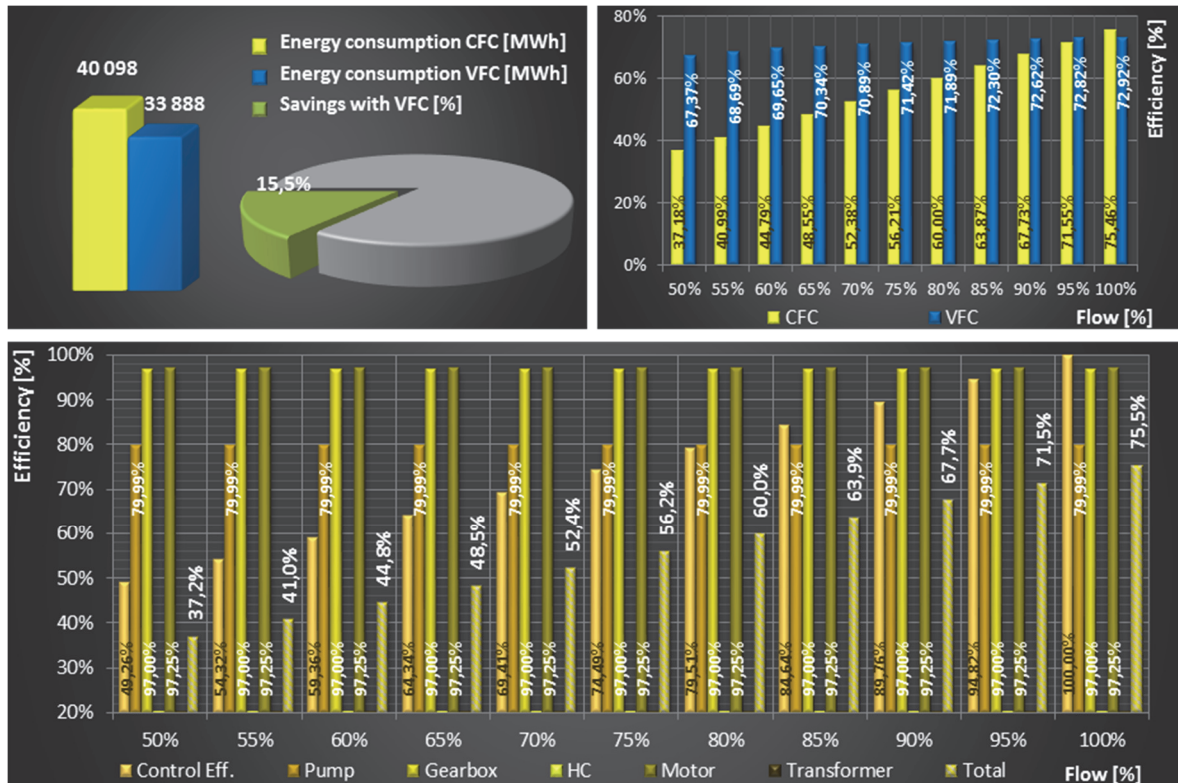
Fig. 2.67 Summary of results – V2 – On-Off control, Energy consumption and savings – top left, Efficiency compared to VFC – top right, Efficiency break up – bottom.

Variable speed flow control with Hydrodynamic coupling
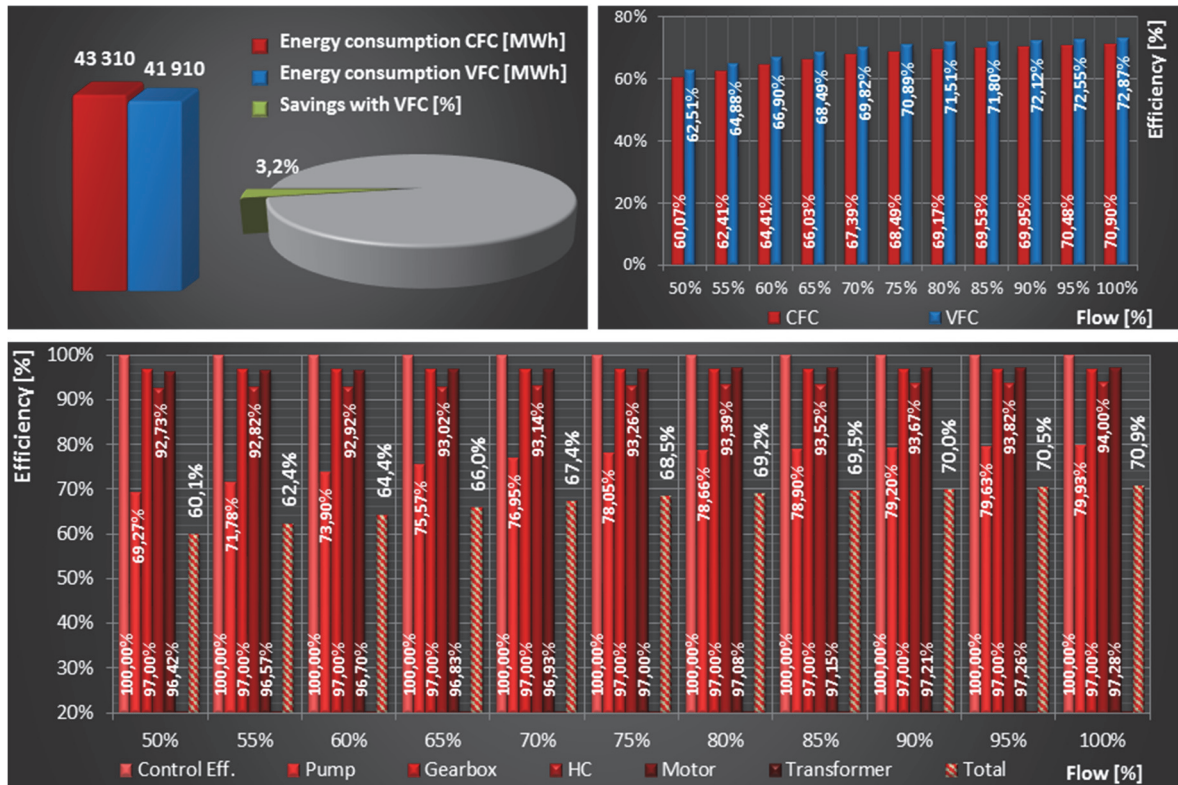
Fig. 2.68 Summary of results – V1 – VSC with HC, Energy consumption and savings – top left, Efficiency compared to VFC – top right, Efficiency break up – bottom.
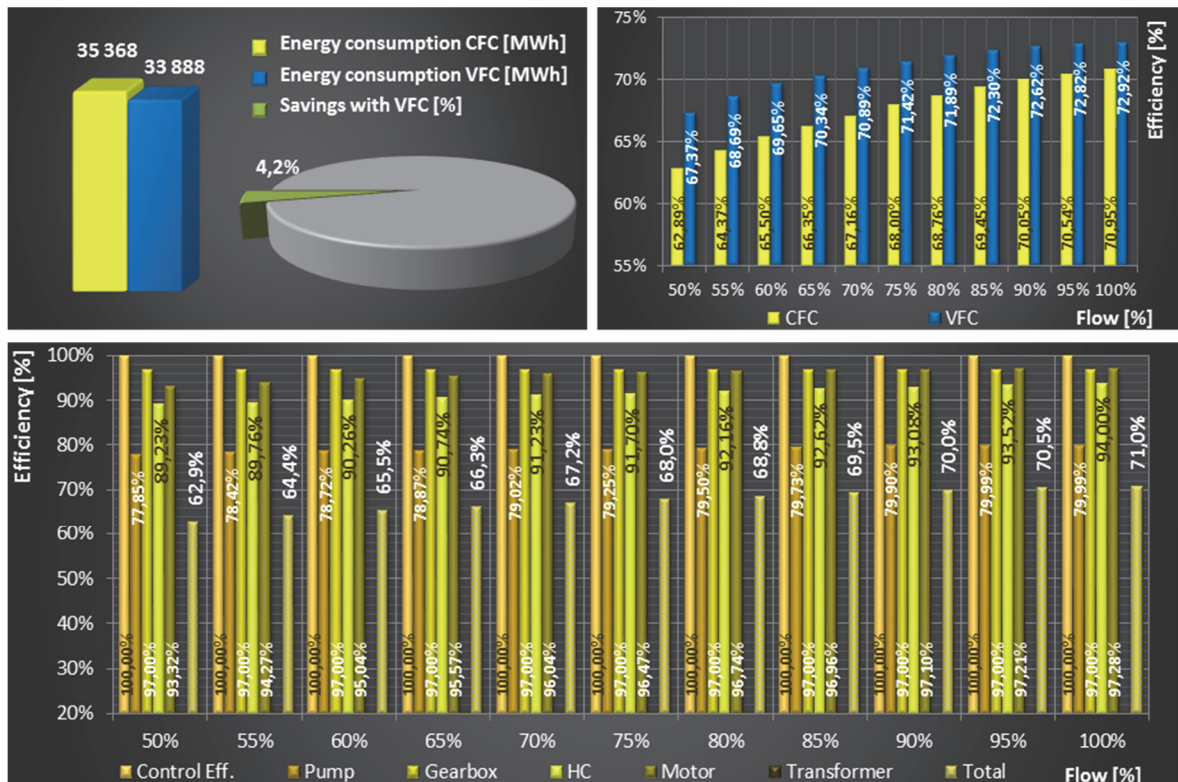
Fig. 2.69 Summary of results – V2 – VSC with HC, Energy consumption and savings – top left, Efficiency compared to VFC – top right, Efficiency break up – bottom.

Variable speed flow control with Frequency converter

Flow [%]	50%	55%	60%	65%	70%	75%	80%	85%	90%	95%	100%
Control Eff.	100,00%	100,00%	100,00%	100,00%	100,00%	100,00%	100,00%	100,00%	100,00%	100,00%	100,00%
Pump	69,27%	71,78%	73,90%	75,57%	76,95%	78,05%	78,66%	78,90%	79,20%	79,63%	79,93%
Gearbox	97,00%	97,00%	97,00%	97,00%	97,00%	97,00%	97,00%	97,00%	97,00%	97,00%	97,00%
Motor	96,23%	96,38%	96,49%	96,59%	96,68%	96,77%	96,86%	96,95%	97,00%	97,05%	97,10%
FC	97,50%	97,50%	97,50%	97,50%	97,50%	97,50%	97,50%	97,50%	97,50%	97,50%	97,50%
Transformer	99,15%	99,17%	99,19%	99,21%	99,23%	99,24%	99,25%	99,26%	99,26%	99,26%	99,26%
Total	62,51%	64,88%	66,90%	68,49%	69,82%	70,89%	71,51%	71,80%	72,12%	72,55%	72,87%

Fig. 2.70 Summary of results – V1 – VSC with FC.

Flow [%]	50%	55%	60%	65%	70%	75%	80%	85%	90%	95%	100%
Control Eff.	100,00%	100,00%	100,00%	100,00%	100,00%	100,00%	100,00%	100,00%	100,00%	100,00%	100,00%
Pump	69,27%	71,78%	73,90%	75,57%	76,95%	78,05%	78,66%	78,90%	79,20%	79,63%	79,93%
Gearbox	97,00%	97,00%	97,00%	97,00%	97,00%	97,00%	97,00%	97,00%	97,00%	97,00%	97,00%
Motor	96,23%	96,38%	96,49%	96,59%	96,68%	96,77%	96,86%	96,95%	97,00%	97,05%	97,10%
FC	97,50%	97,50%	97,50%	97,50%	97,50%	97,50%	97,50%	97,50%	97,50%	97,50%	97,50%
Transformer	99,15%	99,17%	99,19%	99,21%	99,23%	99,24%	99,25%	99,26%	99,26%	99,26%	99,26%
Total	62,51%	64,88%	66,90%	68,49%	69,82%	70,89%	71,51%	71,80%	72,12%	72,55%	72,87%

Fig. 2.71 Summary of results – V2 – VSC with FC.

2.2.1.8   Summary

Table 2.10 and Table 2.11 summarize the main technical and economical indicators. The investment costs are commonly the subject of business secret and therefore, could not be included in the calculation. Energy cost, interest rate and service life have been set to constant for both VFC and CFC to present comparison under identical conditions, however especially the service life and additional operating costs may significantly differ and has to be accounted when evaluating a commercial case study.

From technical results, it is presented energy consumption and savings of energy and CO_2 of variant with frequency converter (VFC) in comparison to other flow control techniques.

From economical parameters, annual savings and Net Present Value (NPV) of variant with frequency converter against other variant have been calculated. Payback period is zero due to no investment costs included in the submission.

Excepting the on-off control technique in the second variant, which couldn't be applied in real boiler feed pump application, combination of VSC with drive with frequency converter performed best from evaluated flow control methods. The net present value of variant with VSC reach in this high-power pump application hundreds of thousands euro, based just on the energy savings against especially passive flow control methods. This safely covers all the investment and other operating costs and would be the most suitable choice from both technical and economical point of view for the both case study variants.

Focusing on VS flow control, it is clearly observable the steeply increasing advantage of VS flow control with increasing of flow and/or speed range against all passive flow control methods. The speed range is highly influenced by static head control as presented in the case study variants – see Fig. 2.43 and Fig. 2.44 and Fig. 2.76 from second case study for zero static head having identical flow range 50% - 100% of flow. This is caused mainly due to significantly higher efficiency of pump employing VSC – see Fig. 2.31 and Fig. 2.32 - which has the essential weight in the whole application. Nevertheless, variable speed control has clearly negative effect on efficiency of induction machine against fixed speed machine (Fig. 2.39 and Fig. 2.40). Moreover, the positive effect of VSC is especially close to nominal operating point degraded by additional losses caused by frequency converter and transformer – see in detail results of efficiency progress over the operating range for all drive chain components and control techniques (Chapter 2.2.1.7).

Table 2.10 – Case study 1, Summary V1

	Throttling	Bypass	On-Off	VSC with HC	VFC	Unit
Economical Data						
Total investment costs	0	0	0	0	0	€
Additional operating cost	0	0	0	0	0	€/year
Energy cost	0,021	0,021	0,021	0,021	0,021	€/kWh
Interest rate	5,0	5,0	5,0	5,0	5,0	%
Service life	15	15	15	15	15	years
Technical Results						
Energy consumption	44 985	50 768	39 809	43 310	41 910	MWh/year
Energy savings with VFC	3 075	8 858	-2 101	1 400	-	MWh/year
CO_2 Reduction with VFC	1 538	4 429	-1 050,5	700	-	t/year
Economical Results – VFC to CFC						
Annual savings	64,6	186,0	-44,1	29,4	-	x1000 €
Payback period	0	0	0	0	-	years
Net Present Value	670	1 931	-458	305	-	x1000 €

Table 2.11 – Case study 1, Summary V2

	Throttling	Bypass	On-Off	VSC with HC	VFC	Unit
Economical Data						
Total investment costs	0	0	0	0	0	€
Additional operating cost	0	0	0	0	0	€/year
Energy cost	0,021	0,021	0,021	0,021	0,021	€/kWh
Interest rate	5,0	5,0	5,0	5,0	5,0	%
Service life	15	15	15	15	15	years
Technical Results						
Energy consumption	45 677	48 170	40 098	35 368	33 888	MWh/year
Energy savings with VFC	11 789	14 282	6 348	1 480	-	MWh/year
CO_2 Reduction with VFC	5 894	7 141	6 210	740	-	t/year
Economical Results – VFC to CFC						
Annual savings	247,6	299,9	130,4	31,1	-	x1000 €
Payback period	0	0	0	0	-	years
Net Present Value	2 570	3 113	1 354	323	-	x1000 €

2.2.2   Case study 2 - Hydraulic system with zero static head

This case study presents cooling water pump application – i.e. a pump application with a low ratio of head versus flow and zero static head. The case study is presented brief form compared to the first case study to present the second most typical high-power application and especially the influence of flow range variability in systems with zero static head on suitability or no suitability of evaluated flow control methods. Flow range of the first variant is from 50% to 100% of flow with weighted average of flow 79,3% of nominal flow and weighted average of hydraulic system power 53,07% of nominal power. In the second variant, flow range is from 80% to 100% of flow with weighted average of flow 91,72% of nominal flow and weighted average of hydraulic system power 77,94% of nominal power.

2.2.2.1   *Hydraulic system & Operating profile*

The case study hydraulic system parameters are summarized in the Table 2.12. The Fig. 2.72 and Fig. 2.73 shows the operating profile for the case study variants. Fig. 2.74 and Fig. 2.75 present the hydraulic system curves including operating range and/or operating points.

Table 2.12 – Case study 2, Hydraulic system

Hydraulic system	Value - Var. 1	Value – Var. 2	Unit
Hydraulic system			
Nominal flow	11 632	11 632	m³/h
Nominal total head	17	17	m
Nominal dynamic head	17	17	m
Nominal static head	0	0	m
Static / referenced head control	constant	constant	
Liquid density	998,2	998,2	kg/m³
System operating data			
Annual running time	8590	8590	h
Flow operating range	50 - 100	80 - 100	%
Weighted average of flow	79,30	91,72	%
Weighted average of hydraulic system power	53,07	77,94	%
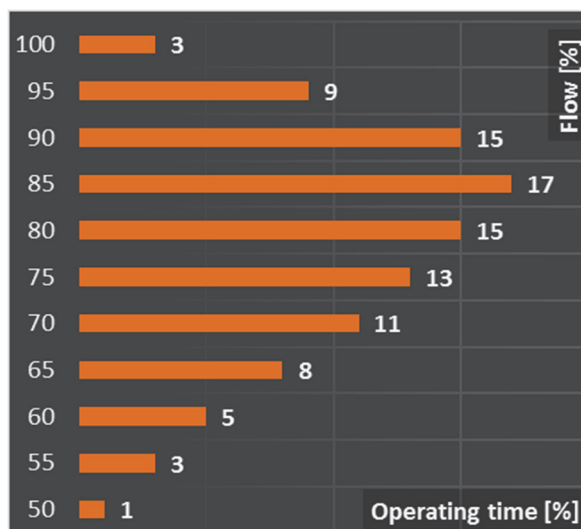
Fig. 2.72 Case study 2 – V1, Operating profile
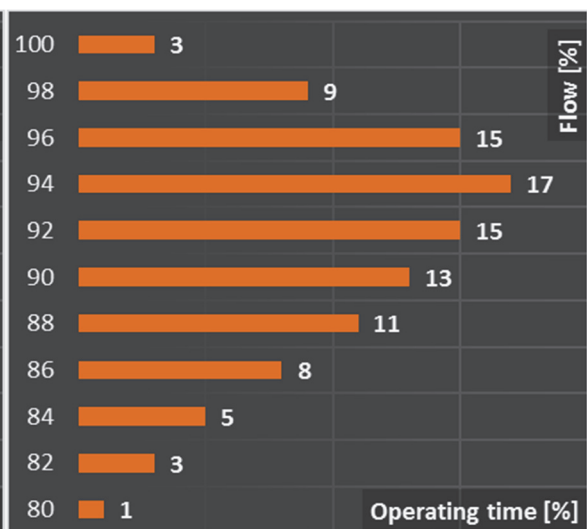
Fig. 2.73 Case study 2 – V2, Operating profile

2.2.2.2   Pump

It is employed centrifugal pump with the parameters according to Table 2.13. Pump Best Efficiency Operating Point (BEP) equals to hydraulic system nominal operating point - see Table 2.14. Fig. 2.74 and Fig. 2.75 present approximated pump performances curves from nominal speed, to speed range covering demanded flow range employing Variable Speed Control (VSC) for the case study variants. See also the operating ranges and points for VSC and passive flow control methods. Bypass flow control exceeds pump recommended maximum flow, however have been included to present the behavior under identical pump and hydraulic system conditions. Nevertheless, in real applications, it is not likely to use identical pump for both throttling and bypass. Fig. 2.76 and Fig. 2.77 show the speed operating range for the operating profile flow range. We can see, that in hydraulic systems with zero static head, the speed is simple directly proportional to flow beginning from zero point in contrast to former hydraulic system with a positive component of static head, where in zero flow point certain pump speed producing pump head equal to system static head is required.

Table 2.13 – Case study 2, Pump

Pump	Value – Var. 1,2	Unit
Pump		
Nominal speed	370	rpm
Flow operating range at nominal speed	5 816 – 11 632	m³/h
Pump BEP		
Flow	11 632	m³/h
Head	17	m
Efficiency	79,60	%
Hydraulic power	538	kW
Mechanical / shaft power	676	kW
Torque	17 434	Nm

Table 2.14 – Case study 2, Real nominal operating points

Pump & Hydraulic system	Value – Var. 1,2	Unit
Real nominal operating point		
Flow	11 632	m³/h
Head	17	m
Efficiency	79,60	%
Hydraulic power	538	kW
Mechanical / shaft power	676	kW
Torque	17 434	Nm
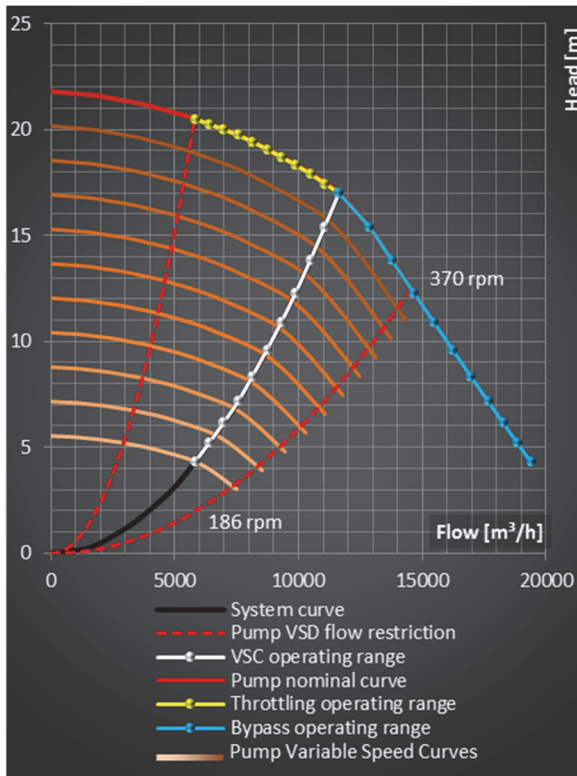
Fig. 2.74 Case study 2 – V1,
Pump & Hydraulic system curves
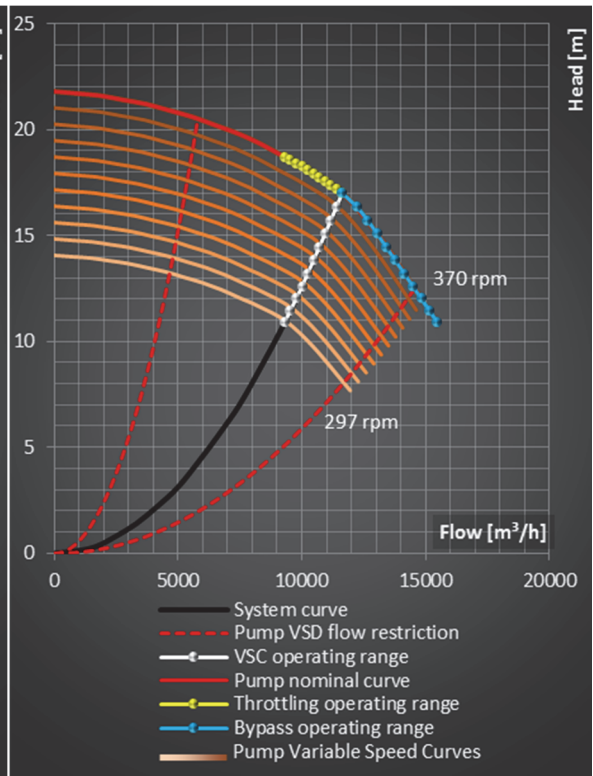
Fig. 2.75 Case study 2 – V2,
Pump & Hydraulic system curves
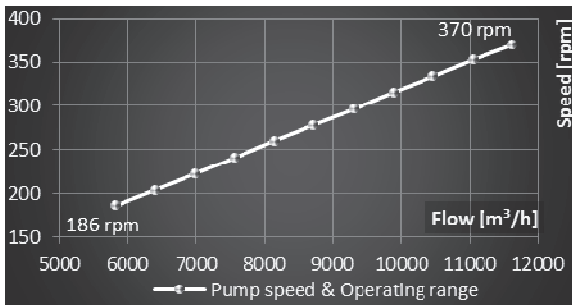
Fig. 2.76 Case study 2 – V1,
Pump VSC speed range
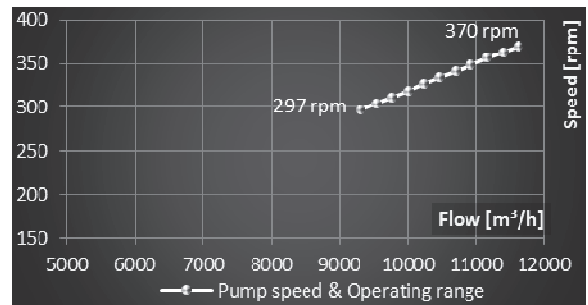
Fig. 2.77 Case study 2 – V2,
Pump VSC speed range

Pump performance curves and operating points under VSC

Fig. 2.78 - Fig. 2.81 show approximated pump performance curves for pump efficiency and hydraulic power from curves at nominal speed, to curves at variable speed according to VSC. See, that pump efficiency keeps constant and/or nominal over the entire operating range, employing VSC in hydraulic systems with zero static head independently on the speed range.
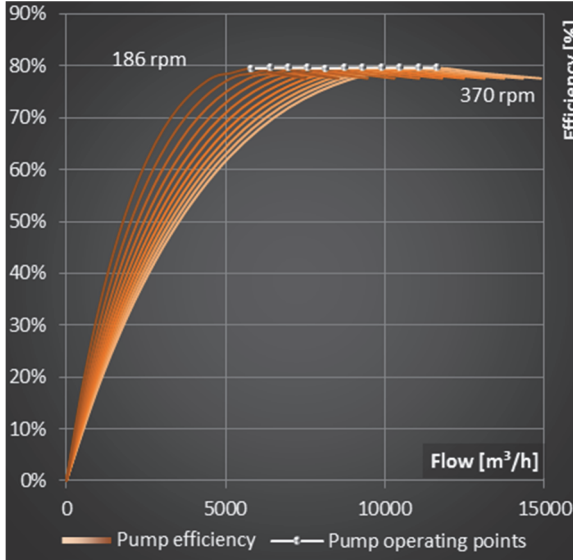
Fig. 2.78 Case study 2 – V1, Pump VSC efficiency   Fig. 2.79 Case study 2 – V2, Pump VSC efficiency
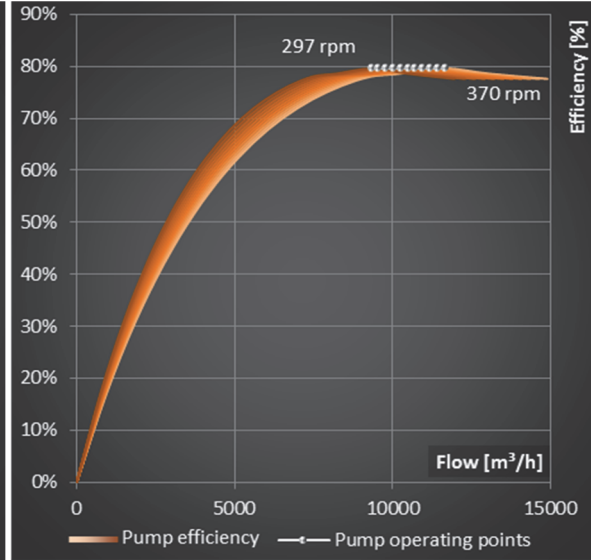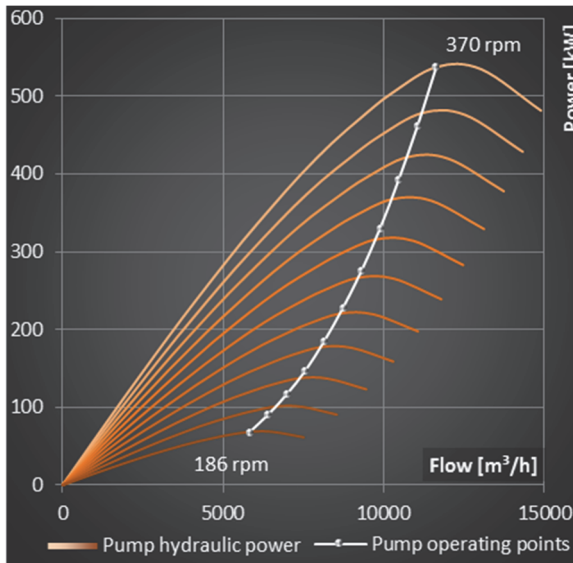
Fig. 2.80 Case study 2 – V1,
Pump VSC hydraulic power
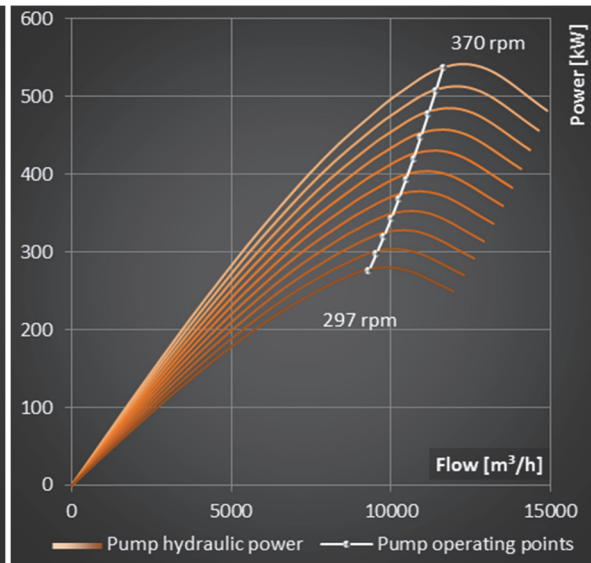
Fig. 2.81 Case study 2 – V2,
Pump VSC hydraulic power

2.2.2.3   Flow control

Below see the parameters of the throttling valve (Table 2.15) and the hydrodynamic coupling (Table 2.16), employed in the case study. Note, that inclusion of throttling valve into hydraulic system shifts the nominal operating point, which does not allow reaching exactly comparable hydraulic parameters in relation to other flow control techniques. However, the loss on control valve is included in the control efficiency and therefore final comparison to other flow control techniques is still relevant.

Hydrodynamic coupling efficiency curve (Fig. 2.82) is set to simple linear curve just as a sample device. Nevertheless, it should be always used hydrodynamic performance curve generated directly from manufacturer for specific load conditions, when available.

Throttling valve

Table 2.15 – Case study 2, Throttling

Throttling	Value – Var. 1,2	Unit
Throttling valve		
Pressure drop at nominal flow	0,5	m
Nominal operating point		
Nominal flow	11 632	m³/h
Nominal head	16,5	m

Hydrodynamic coupling

Table 2.16 – Case study 2, Hydrodynamic coupling

Hydrodynamic coupling	Value – Var. 1,2	Unit
Nominal speed	495	rpm
Nominal efficiency	94	%
Auxiliary losses	0	kW
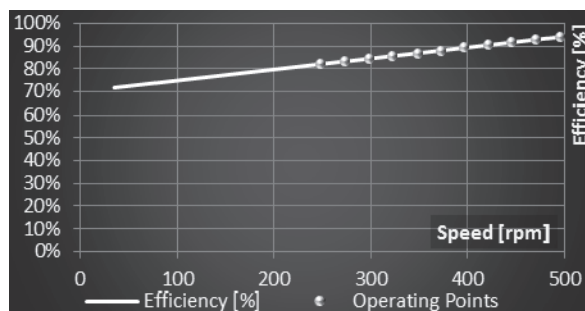
Fig. 2.82 Case study 2 – V1 and V2,
Efficiency curve for hydrodynamic coupling

2.2.2.4   *Electrical motor & Gearbox*

Electrical motors are specified separately for drive with frequency converter (VFC) and fixed speed drive due to different demand on power and voltages. Electrical motor for Compared Flow Control (CFC) methods has to be designed to higher power to cover additional losses. However, purposely has been chosen power plant with bus voltage of 10 kV to be able to take the advantage of connection of fixed speed electrical motor directly do electrical bus in contrast to electrical drive with frequency converter which needs an additional transformer. Nominal parameters of both electrical motors are summarized in Table 2.17, below.

Pumps for high flow rates in relation to pump pressure head are in general designed for lower speed rates than pumps with a high-pressure head in relation to the flow rate. This is advantage for variable speed controlled pumps with frequency converter, where no additional gearbox is needed to drive pump at pump nominal speed – usually for speeds below 3 000 rpm for 50 Hz power supply network. Nevertheless, it has to be account the worse electrical motor efficiency while operating significantly below the nominal speed – see Fig. 2.85 and Fig. 2.86. Gearbox for CFC methods is defined in the Table 2.18.

Table 2.17 – Case study 2, Electrical motor

Electrical motor	CFC Value - Var. 1,2	VFC Value - Var. 1,2	Unit
Nominal parameters			
Mechanical power	900	800	kW
Voltage	10 000	6 000	V
Current	68	104	A
Frequency	50	50	Hz
Speed	495	494	rpm
Number of poles	12	12	-
Efficiency	94,7	95,1	%
Power factor	0,81	0,78	-
Apparent power	1 173	1 078	kVA
Shaft Torque	17 362	15 464	Nm
Slip	0,010	0,012	-
Other			
Auxiliary losses	0	0	kW

Table 2.18 – Case study 2, Gearbox

Gearbox	CFC Value - Var. 1,2	VFC Value - Var. 1,2	Unit
Gearbox ratio	0,747	-	-
Gearbox efficiency	97,0	-	%

Electrical motor performance curves

Electrical motor datasheet efficiency and power factor curve for nominal speed are for the both case study variants presented in Fig. 2.83 for VFC and in Fig. 2.84 for CFC. Fig. 2.85 and Fig. 2.86 show approximated motor efficiency and power factor for the operating speed range using VFC. Fixed speed operating points for other flow control methods are evaluated similarly as it has been already presented in former case study – i.e. lies directly on motor performance curves at nominal speed.
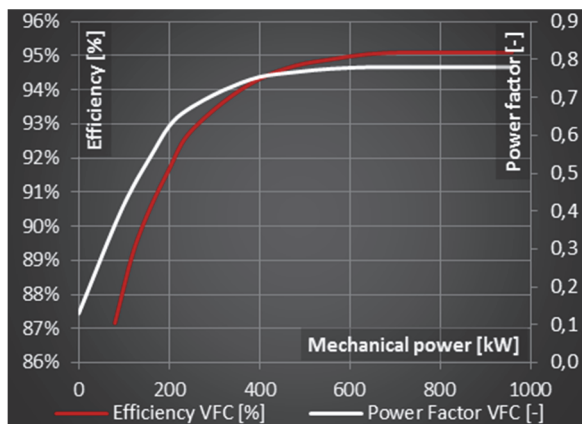
Fig. 2.83 Case study 2 - V1 and V2,
VFC motor - nominal-speed
curves efficiency and power factor curves
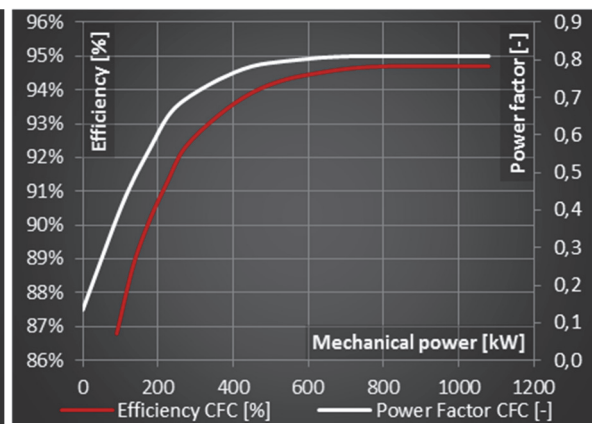
Fig. 2.84 Case study 2 - V1 and V2,
CFC motor - nominal-speed
efficiency and power factor curves
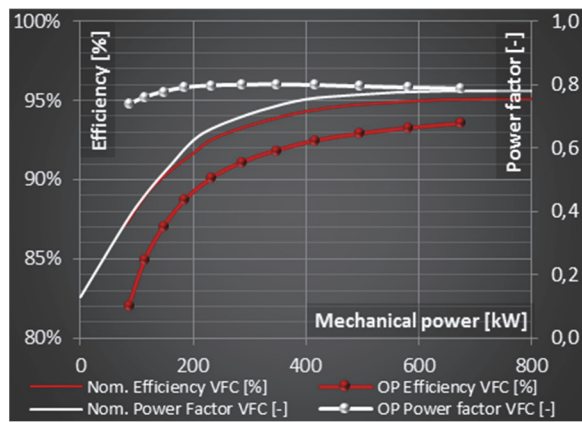
Fig. 2.85 Case study 2 – V1,
VFC motor – variable speed curves and OP range
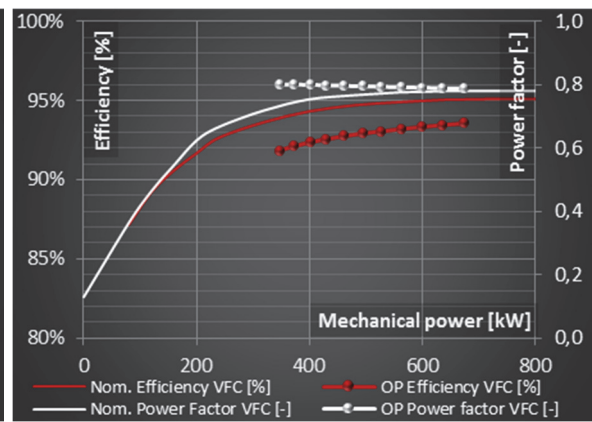
Fig. 2.86 Case study 2 – V2,
VFC motor – variable speed curves and OP range

2.2.2.5   Frequency converter

For the purposes of this case study, frequency converter is considered with constant efficiency and power factor over the entire operating range, which is sufficient in relation to total application efficiency – see Fig. 2.87 and Table 2.19 for details. For a precise comparison, the performance curves would have to be supplied directly from frequency converter manufacturer, generated for specific load conditions.

Table 2.19 – Case study 2, Frequency converter

Frequency converter	Value – Var. 1,2	Unit
Input nominal FC parameters		
Input voltage	6 000	V
Power supply frequency	50	Hz
Efficiency	97,5	%
Nominal power factor	1	-
Apparent power	1 641	kVA
Current	158	A
Output FC parameters		
Nominal continuous apparent power	1 600	kVA
Frequency range	1 – 66	Hz
Other		
Auxiliary losses	0	kW

Fig. 2.87 Case study 2 – V1 and V2,
Frequency converter efficiency and power factor

2.2.2.6   Transformer

Transformer is included in both case study variants just for VFC to adapt 10 kV bus voltage to 6 kV input voltage of frequency converter. Transformer parameters are summarized in the Table 2.20. Real operating points have been then calculated from the knowledge of equivalent circuit diagram (see chapter 2.1.4.5) and apparent power and power factor of the load – i.e. load of frequency converter supplying electrical motor for VFC. Fig. 2.88 and Fig. 2.89 show the transformer operating points.

Table 2.20 – Case study 2, Transformer

Transformer	Value – Var. 1,2	Unit
Nominal parameters		
Primary voltage	10 000	V
Secondary voltage	6 000	V
Frequency	50	Hz
Efficiency	99,08	%
Nominal power factor	0,999	-
Other parameters		
Short circuit voltage	6	%
No load current	0,5	%
No load losses	2,2	kW
Load losses	15,5	kW
Other		
Auxiliary losses	0	kW
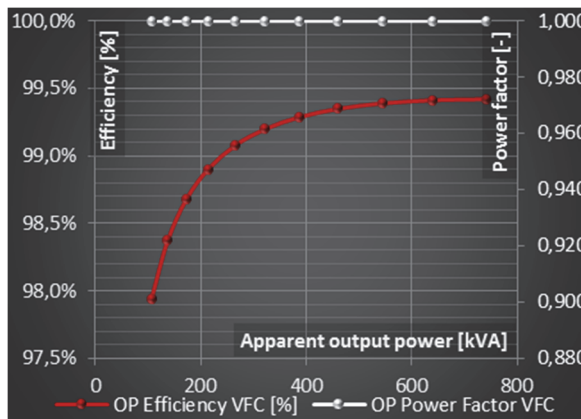
Fig. 2.88 Case study 2 – V1, VFC Transformer efficiency and power factor operating range
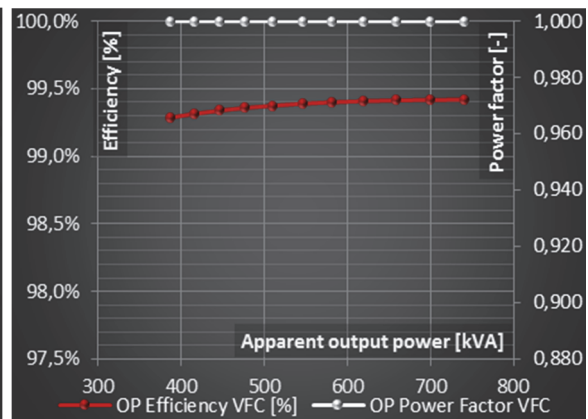
Fig. 2.89 Case study 2 – V2, VFC Transformer efficiency and power factor operating range

2.2.2.7   Technical evaluation

This chapter summarizes the results of technical evaluation of both variants of the case study. For each variant of case study, it has been processed evaluation of energy consumption and/or energy savings and total energy efficiency comparison with variable frequency drive at each operating point according the operating profile.

Considering throttling flow control, it is the least and second least suitable flow control method for this pump application and first and second variants and/or flow control ranges. See Fig. 2.94 and Fig. 2.95 for comparison against VSC with frequency converter. It is clearly observable, that operating profile and/or flow very significantly influence the potential of energy saving by employing VSC.

Bypass flow control results are summarized in Fig. 2.92 and Fig. 2.93. The results are similar to throttling flow control – bypass flow control efficiency rapidly decreases with extending of flow control range. The savings while employing VSC are almost double for operating range of 50% - 100% against the operating range of 80% - 100% of flow.

On-Off control provided best results from passive flow control methods, however especially in the first case study variant, it is still extremely uneconomical against VSC – see Fig. 2.94 and Fig. 2.95. Moreover, on-off control is usable just in systems with a capacity and/or tank, which allows controlling of just the average flow quantity instead of the real time flow quantity.

Finally, VSC with hydrodynamic coupling and VSC with frequency converter are to be compared. Fig. 2.96 and Fig. 2.97 show the comparison of these two variable speed controls. It is evident, that VSC is the best possible flow control option for hydraulic systems with zero static head. When considering VSC with HC against VSC with FC, variant with frequency converter provided best results in both cases. However, the result is very influenced by HC efficiency curve, which would have to be provided directly by HC manufacturer for reliable conclusion. Nevertheless, the advantage for VFC is also no gearbox in drive chain, which is not necessary while supplying pump from variable frequency drive. Although VSC with FC required power supply transformer, it provided clearly best results against all flow control techniques and has been the best choice even at nominal operating point in contrast to former case study, where passive flow control techniques have been more efficient close to nominal operating point.

Throttling
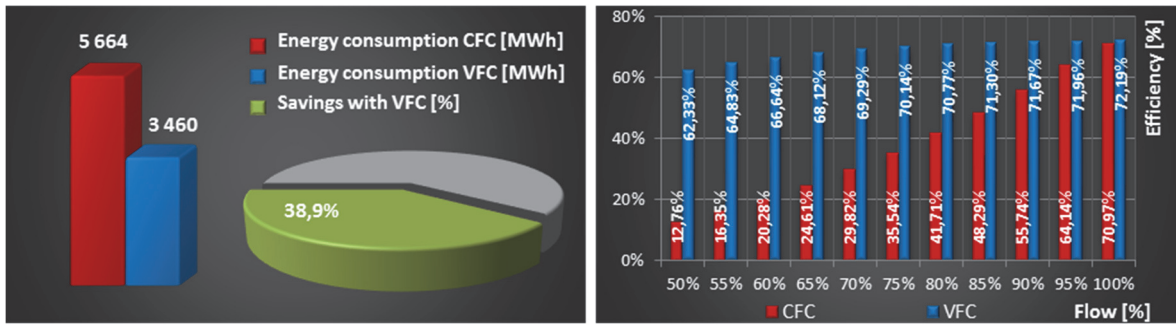
Fig. 2.90 Summary of results – V1 – Throttling,
Energy consumption and saving potential to VFC – left, Efficiency compared to VFC – right.
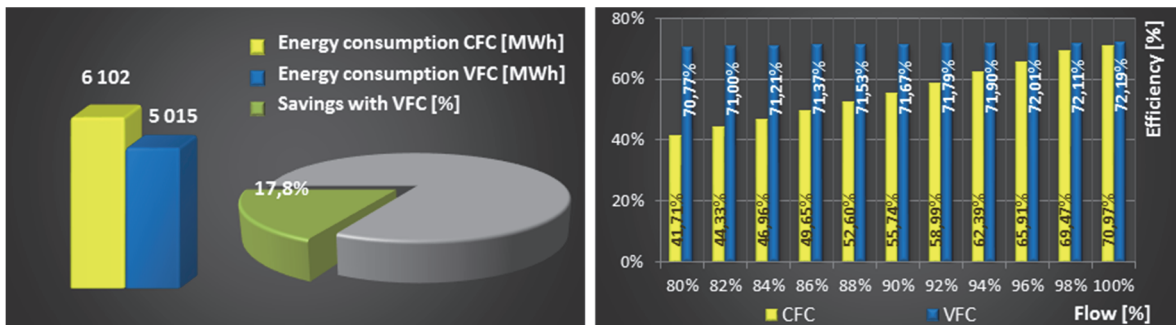
Fig. 2.91 Summary of results – V2 – Throttling,
Energy consumption and saving potential to VFC – left, Efficiency compared to VFC – right.

Bypass
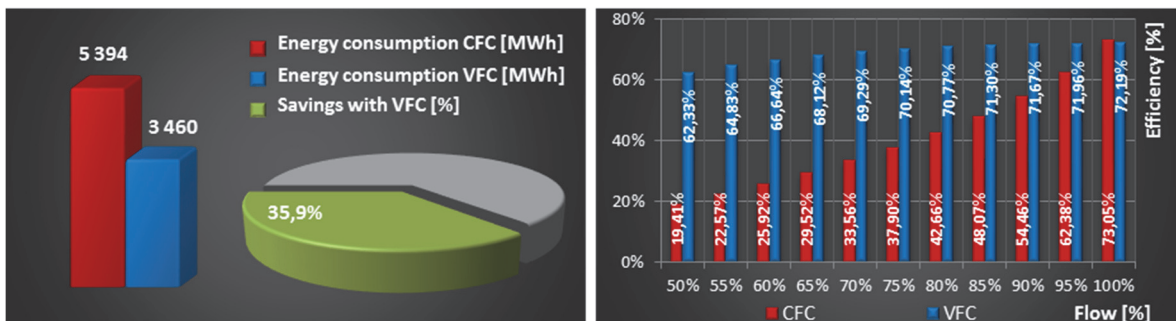
Fig. 2.92 Summary of results – V1 – Bypass,
Energy consumption and saving potential to VFC – left, Efficiency compared to VFC – right.
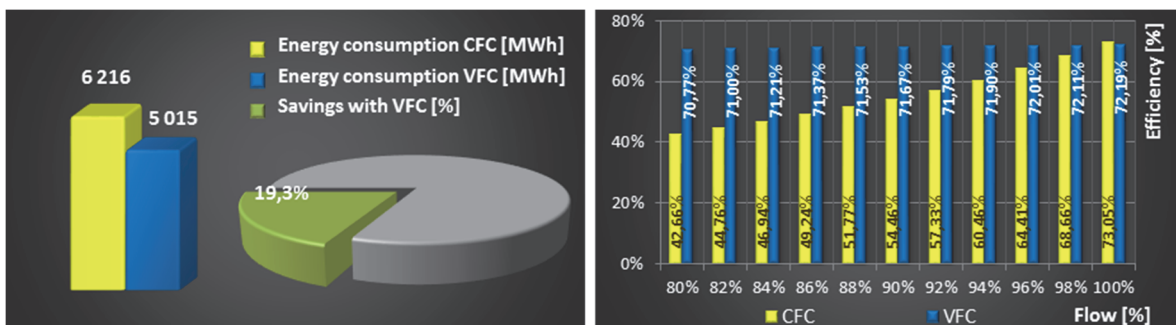
Fig. 2.93 Summary of results – V2 – Bypass,
Energy consumption and saving potential to VFC – left, Efficiency compared to VFC – right.
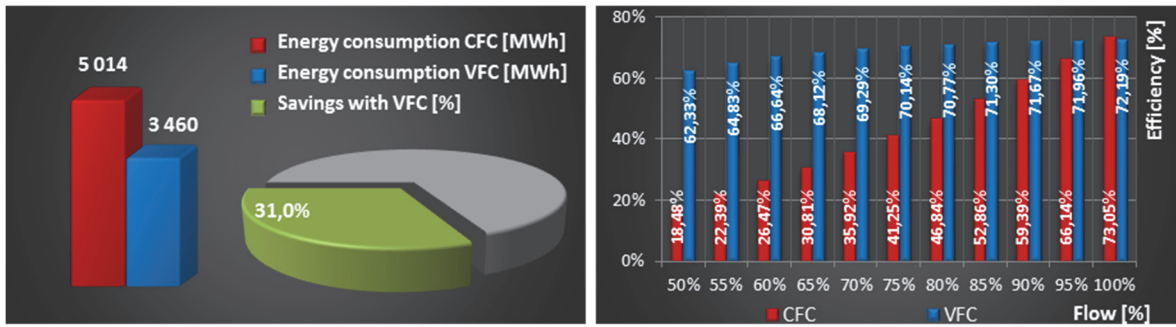
On-Off control

Fig. 2.94 Summary of results – V1 – On-Off control,
Energy consumption and saving potential to VFC – left, Efficiency compared to VFC – right.
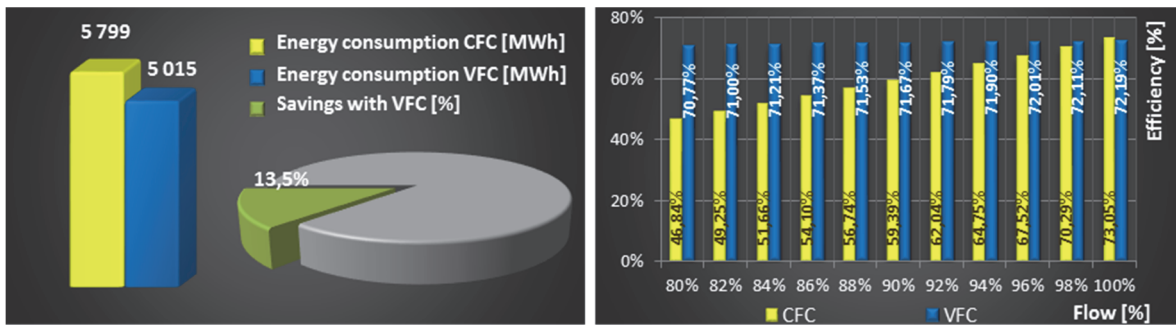
Fig. 2.95 Summary of results – V2 – On-Off control,
Energy consumption and saving potential to VFC – left, Efficiency compared to VFC – right.

Variable speed flow control with Hydrodynamic coupling
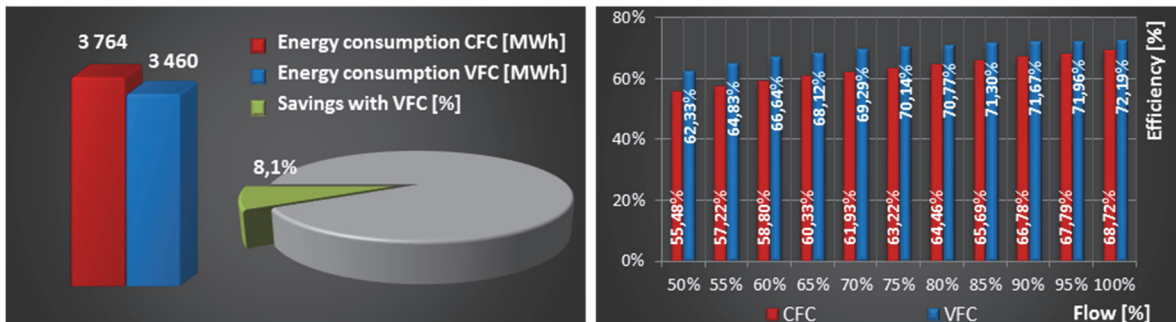
Fig. 2.96 Summary of results – V1 – VSC with HC,
Energy consumption and saving potential to VFC – left, Efficiency compared to VFC – right.
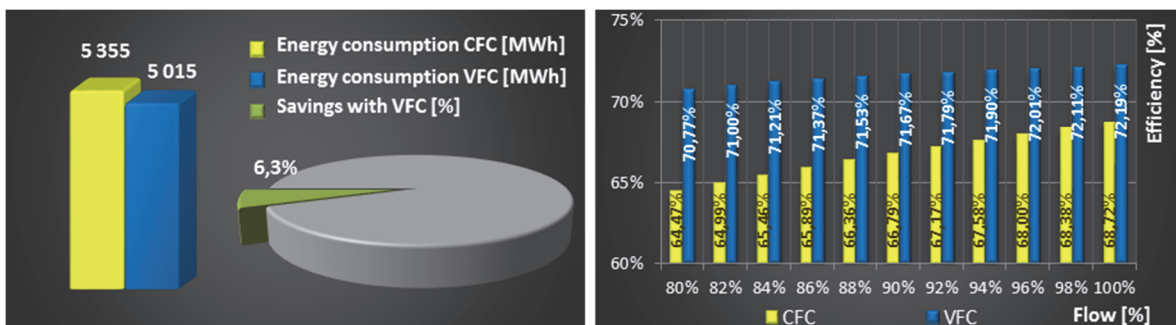
Fig. 2.97 Summary of results – V2 – VSC with HC,
Energy consumption and saving potential to VFC – left, Efficiency compared to VFC – right.

2.2.2.8   Summary

Table 2.21 and Table 2.22 summarize the main technical and economical indicators. The investment costs are commonly the subject of business secret and therefore, could not be included in the calculation. Energy cost, interest rate and service life have been set to constant for both VFC and CFC to present comparison under identical conditions, however especially the service life and additional operating cost may significantly differ and has to be accounted when evaluating commercial case study.

From technical results, it is presented energy consumption and savings of energy and CO_2 of variant with frequency converter (VFC) in comparison to other flow control techniques.

From economical parameters, annual savings and Net Present Value (NPV) of variant with frequency converter against other variants have been calculated. Payback period is zero due to no investment costs included in the submission.

The summary clearly shows the advantage of VSC with FC against all the other options for both the case study variants. It is clearly observable the trend of increasing saving potential of VSC with extending of flow range in relation to passive flow control techniques.

Further, if we compare the annual saving potential of VFC to annual energy consumption for VFC we can see that the ratio is significantly higher compared to former case study. This confirms the suitability of variable speed controlled pumps in hydraulic systems with zero static head similar to the case study.

Table 2.21 – Case study 2, Summary V1

	Throttling	Bypass	On-Off	VSC with HC	VFC	Unit
Economical Data						
Total investment costs	0	0	0	0	0	€
Additional operating cost	0	0	0	0	0	€/year
Energy cost	0,021	0,021	0,021	0,021	0,021	€/kWh
Interest rate	5,0	5,0	5,0	5,0	5,0	%
Service life	15	15	15	15	15	years
Technical Results						
Energy consumption	5 664	5 394	5 014	3 764	3 460	MWh/year
Energy savings with VFC	2 204	1934	1 554	304	-	MWh/year
CO_2 Reduction with VFC	1 102	967	777	152	-	t/year
Economical Results – VFC to CFC						
Annual savings	46,3	40,6	32,6	6,4	-	x1000 €
Payback period	0	0	0	0	-	years
Net Present Value	480	422	339	66	-	x1000 €

Table 2.22 – Case study 2, Summary V2

	Throttling	Bypass	On-Off	VSC with HC	VFC	Unit
Economical Data						
Total investment costs	0	0	0	0	0	€
Additional operating cost	0	0	0	0	0	€/year
Energy cost	0,021	0,021	0,021	0,021	0,021	€/kWh
Interest rate	5,0	5,0	5,0	5,0	5,0	%
Service life	15	15	15	15	15	years
Technical Results						
Energy consumption	6 102	6 216	5 799	5 355	5015	MWh/year
Energy savings with VFC	1 087	1 200	784	340	-	MWh/year
CO_2 Reduction with VFC	554	600	392	170	-	t/year
Economical Results – VFC to CFC						
Annual savings	22,8	25,2	16,5	7,1	-	x1000 €
Payback period	0	0	0	0	-	years
Net Present Value	237	262	171	74	-	x1000 €

2.3   Conclusion for single pump applications

In this part, it has been comprehensively presented the developed methodology, mathematical models and performance of developed software tools for energy efficiency optimization of especially high-power single pump applications. It has been systematically described the way of evaluation of these applications including in detailed elaboration of typical sample case studies. The mathematical models of all application components have been presented due to high nonlinearity and empiric character of particular components in numerical form suitable for direct software implementation. The impact – while designing the mathematical models and methodology - has been put on to use strictly just commonly available (i.e. non laboratory measurement) input data despite of lower precision and necessity of development of special approximation techniques with respect to practical use in real applications.

In the first part, there have been described models of hydraulic system and centrifugal pump including derivation of operating points and behavior under variable speed flow control. Thereafter, mathematical models representing passive flow control methods – throttling, bypass and on-off control have been evaluated.

In the second part, there have been derived mathematical models of drive components for both CFC and VSC flow control methods – from gearbox, over electrical motor to hydrodynamic coupling, frequency converter and transformer. Special attention has been put to approximation techniques of especially induction machine and transformer.

Finally, the presented mathematical models and methodology have been implemented in the software tool Medium-Voltage Drive Pump Save 2012 and the performance have been presented on real case studies which have been in detailed processed. In the first case study, it has been evaluated boiler feed pump application in thermal power plant. The case study has been elaborated for two variants of static head control to present the effect of the change on both technical and economical case study indicators. The second case study has represented a cooling water circulating pump application. It has been evaluated again in two modifications to enumerate the influence of shape of operating profile and /or weighted flow average on final economy for selected flow control methods. Typical performance and energy saving potential employing VSC of these applications have been described and generalized for hydraulic systems with similar conditions.

3   Single fan applications

This chapter continues on former part dealing with single pump systems. It describes energy efficiency evaluation and/or optimization process of single fan applications. The evaluation process is especially in the drive part identical to processing of pump applications, which has been described already in detail. Hence, this chapter will focus mainly on differences arising from the employment of compressible medium and specific fan types and flow control techniques.

The first part describes methodology and model design employed in evaluation of pneumatic part of fan applications. It begins with mathematical models of pneumatic system and fans including both basic fan types - axial and radial – derived for variable speed flow control. Next, methodology, typical performance curves and mathematical representation of other commonly used flow control techniques for both axial and radial fans are included – namely, flow control with inlet guide vanes, inlet damper, outlet damper and on-off control. The active flow control algorithms include variable speed control via fixed speed electrical motor with hydrodynamic coupling and variable speed control with electrical motor supplied from frequency converter. In addition, it is included a model of pitch control for axial fans.

The second part is devoted to verification of mathematical models and methodology using the software tool Medium-Voltage Fan Save 2012. The tool has been developed based on the presented theory to provide an advanced engineering tool for evaluation of these systems. The performance of the software tool and/or developed mathematical models and methodology is presented in two typical case studies. The first case study is focused on sample application employing radial fan for gas recirculation fan in heating power plant, the second case study presents the performance of model of axial fan employed in cooling tower of a thermal power plant. Both case studies present the technical and economical results and comparison among possible flow control techniques.

3.1   Methodology and Model design

This chapter describes methodology and mathematical models employed in the evaluation and energy consumption optimization process of fan systems. The attention is paid to mathematical model of pneumatic system considering compressible medium and mathematical model of fan (common for both axial and radial type) derived for variable speed flow control. Next, it is presented methodology for evaluation of other commonly used flow control techniques and/or referenced typical performance characteristics for inlet guide vanes, inlet damper and outlet damper. Special attention is paid to approximation techniques for pitch-controlled axial fans.

The mathematical models are developed for steady states, which is sufficient for the purposes of energy efficiency evaluation. The models are expressed especially in the form suitable for numerical calculation, which is necessary because of high non-linearity of pneumatic system components. Models of flow control techniques are represented mainly by referenced typical performance curves due to unique character of each application and high complexity of analytical derivation of models of fan and flow control components. Performance curves tuned directly for particular application are usually supplied directly by fan manufacturer.

The general evaluation procedure for fan systems is equivalent to evaluation procedure of pump systems described in former chapters – i.e. the all application components are supposed to be specified under nominal speed conditions. Operating data and especially the efficiency curve of each component of the drive chain are then approximated for specific load conditions at operating points according to operating profile.

Presented mathematical models have been implemented in the core of the software tool MVD Fan Save 2012 and verified on elaborated case studies.

3.1.1   Pneumatic system

Specification of pneumatic system is the key process while designing or evaluating fan application. Similarly to pump systems, pneumatic system is represented by system curve, which characterizes the pressure required to move gas through the system for various flow rates. In the contrast to pump applications, gas pressure in SI units is used directly, instead of equivalent in meter of fluid head. Pneumatic system is then defined as in (3.1), static component is expressed in (3.2) and dynamic and/or friction component in (3.3).

$$p_S(Q) = p_{ST}(Q) = p_{STs}(Q) + p_{STd}(Q) \tag{3.1}$$

$$p_{Ss}(Q) = p_{STs}(Q) = p_{SDs}(Q) - p_{SSs}(Q) + p_{SDsp} - p_{SSsp} \tag{3.2}$$

$$p_{Sd}(Q) = p_{STd}(Q) = p_{SDd}(Q) - p_{SSd}(Q) \tag{3.3}$$

Friction losses are influenced except of gas flow speed and/or volume flow rate additionally by gas density, which varies according to pressure loss ((3.4)) in the pneumatic system [41], [42] in the contrast to incompressible fluids derived in Chapter 2.1.1. The red part is supposed to be constant for a particular application. Gas density is according to ideal gas equation proportional to gas pressure while considering constant gas temperature - (3.5) and (3.6).

   System pressure curve including gas density and/or pressure correction factor (red) is expressed in (3.7) and numerical equivalent in (3.8). The correction factor is introduced to increase the precision of the system curve and/or calculation of energy demand especially for pneumatic systems with both high friction losses and high operating speed range.

$$\Delta p_L = f \times \left(\frac{L}{D}\right) \times \frac{\rho}{2} \times v^2 \tag{3.4}$$

$$p \times V = n \times R \times T \tag{3.5}$$

$$n = \frac{m}{M}; \rho = \frac{m}{V}$$

$$p = \rho \times \frac{R}{M} \times T$$

$$\frac{\rho_2}{\rho_1} = \frac{p_2}{p_1} \tag{3.6}$$

$$p_S = p_{Ss} + p_{Sd} \times k_\rho \tag{3.7}$$

$$p_S = p_{Ss} + \left[p_{Sd_N} \times \left(\frac{Q_S}{Q_{S_N}}\right)^2 \right] \times \frac{p_S + p_0}{p_{S_N} + p_0} \Rightarrow$$

$$p_S = \frac{p_{Ss}\left(p_{S_N} + p_0\right) + p_0 \times p_{Sd_N} \times \left(\frac{Q_S}{Q_{S_N}}\right)^2}{p_{S_N} + p_0 - p_{Sd_N} \times \left(\frac{Q_S}{Q_{S_N}}\right)^2}$$

$$p_{Sd_N} = p_{S_N} - p_{Ss_N}$$

$$\boldsymbol{Q_S} = \left[Q_{S-j} \right]^T \; ; \; j = 1, 2, \ldots, m_{samples} \tag{3.8}$$

$$Q_{S-1} = 0; \; Q_{S-m_{samples}} = Q_N$$

$$\boldsymbol{p_S} = \left[p_{S-j} \left(Q_{S-j} \right) \right]^T \; ; \; j = 1, 2, \ldots, m_{samples}$$

$$p_{S-j} \left(Q_{S-j} \right) = \frac{p_{Ss-j} \left(p_{S_N} + p_0 \right) + p_0 \times \left(p_{S_N} - p_{Ss_N} \right) \times \left(\dfrac{Q_{S-j}}{Q_{S_N}} \right)^2}{p_{S_N} + p_0 - \left(p_{S_N} - p_{Ss_N} \right) \times \left(\dfrac{Q_{S-j}}{Q_{S_N}} \right)^2} \; ; \; j = 1, 2, \ldots, m_{samples}$$

3.1.2   Fan

The methodology of fan model design is analogous to pump model design, which has been described in the former part. Fan performance curves are defined for fan nominal speed and then approximated for variable speed using affinity rules. The difference is arising from adjusted affinity laws for compressible medium – see equations (3.9) and (3.10). Equation (3.11) confirms that efficiency keeps unchanged while using fan affinity laws. Fan approximated flow, pressure and efficiency for any operating point and speed are express in equations (3.12) - (3.15).

$$\frac{Q_1}{Q_2} = \left(\frac{n_1}{n_2}\right) \times \left(\frac{D_1}{D_2}\right)^3 \tag{3.9}$$

$$\frac{p_1}{p_2} = \left(\frac{n_1}{n_2}\right)^2 \times \left(\frac{D_1}{D_2}\right)^2 \times \left(\frac{\rho_1}{\rho_2}\right) \tag{3.10}$$

$$\frac{\rho_1}{\rho_2} = \frac{p_1 + p_0}{p_2 + p_0}$$

$$\frac{\eta_1}{\eta_2} = \left(\frac{Q_1}{Q_2}\right) \times \left(\frac{\Delta p_1}{\Delta p_2}\right) \times \left(\frac{P_{p2}}{P_{p1}}\right) = \left(\frac{n_1}{n_2}\right) \times \left(\frac{n_1}{n_2}\right)^2 \times \left(\frac{\rho_1 \times \rho_2}{\rho_2 \times \rho_1}\right) \times \left(\frac{n_2}{n_1}\right)^3 = 1 \tag{3.11}$$

$$\Delta p = p_{out} - p_{in}$$

$$Q_2 = Q_1 \left(\frac{n_2}{n_1}\right) \tag{3.12}$$

$$p_2 = p_1 \times \left(\frac{n_2}{n_1}\right)^2 \times \frac{p_0}{p_1 \times \left[1 - \left(\frac{n_2}{n_1}\right)^2\right] + p_0} \tag{3.13}$$

$$\eta_2 = \eta_{n_2} = f(Q_2); \ \eta_1 = \eta_{n_1} = f(Q_1); \ \eta_{n_1} = \eta_{n_2} \tag{3.14}$$

$$\eta_2(Q_2) = \eta_1\left(Q_2\left(\frac{n_1}{n_2}\right)\right) \tag{3.15}$$

Fan pneumatic power is expressed in (3.16). Note that in this form, gas density is not explicitly included in the opposite to pump hydraulic power formula, which uses a meter of head instead of directly pressure in SI units. Fan power consumption and torque are then in (3.17) and (3.18).

$$P_p[\text{kW}] = Q[m^3/s] \times \Delta p[\text{kPa}] \tag{3.16}$$

$$P_c = \frac{P_p}{\eta} \tag{3.17}$$

$$T[\text{Nm}] = \frac{P_c[\text{W}]}{\omega[rad/s]} = \frac{P_c[kW] \times 1000}{\frac{n[\text{rpm}]}{60} \times 2\pi} \tag{3.18}$$

3.1.2.1   Numerical solution of fan operating points under VSC

Since every fan has specific performance curves and the curves change slightly over the fan lifetime, there is no general analytical description available. Hence, it is needed to sample the curves of fan and solve the entire pneumatic system numerically to obtain precise results. The most suitable way is to obtain the performance curves of both fan and control directly from fan manufacturer for application operating range. However, this approach is especially in retrofit applications not possible. Therefore, the below introduced methodology can be employed to approximate fan behavior and/or performance curves from the curves at nominal speed to performance curves at variable speed.

The set of sampled data is defined in (3.19). At first, it will be identified nominal operating point, which is located at the intersection of fan nominal pressure-flow curve and pneumatic system curve – see (3.20). Theoretically there could be more possible intersection points between fan and system curve, however similarly to pump systems only one is stable. The Fig. 3.1 shows sampled fan pressure-flow curve (red, (3.19)) and discretized pneumatic system curve (black) constructed according to (3.8). The yellow curve indicates the operating range of the system curve - (3.21). Nominal operating point is then obtained as an intersection of linearly interpolated fan and pneumatic system curves - (3.22). Note, that auxiliary curves for speed range calculation ((3.29) and (3.30)) are merged into one for systems with a zero static head component.

$$p_F = p_F\left(Q_F\right); \; \eta_F = \eta_F\left(Q_F\right) \tag{3.19}$$

$$\boldsymbol{Q_{F_N}} = \left[Q_{F_N j}\right]^T ; \; j = 1,2,...,m_{samples}$$

$$\boldsymbol{p_{F_N}} = \left[p_{F_N j}\left(Q_{F_N j}\right)\right]^T ; \; j = 1,2,...,m_{samples}$$

$$\boldsymbol{\eta_{F_N}} = \left[\eta_{F_N j}\left(Q_{F_N j}\right)\right]^T ; \; j = 1,2,...,m_{samples}$$

$$p_F = p_F(Q); \; p_S = p_S(Q) \tag{3.20}$$

$$p_F(Q) = p_S(Q)$$

$$\boldsymbol{Q_{OP_N}} = \left\{Q \mid p_F(Q) = p_S(Q); \; n_F = n_N\right\}$$

$$\boldsymbol{p_{OP_N}} = \left\{p \mid p = p_F(Q); \; Q \in \boldsymbol{Q_{OP_N}}; \; n_F = n_N\right\}$$

$$\boldsymbol{p_{OP}} = \boldsymbol{p_{S\text{-}OP}} = \left[p_S(Q)\right]^T ; Q \in \boldsymbol{Q_{OP}} \tag{3.21}$$

$$\left[\boldsymbol{Q_{OP_N}}, \boldsymbol{p_{OP_N}}\right] = f_{IntersectLinIntArrays}\left(\boldsymbol{Q_{F_N}}, \boldsymbol{p_{F_N}}, \boldsymbol{Q_S}, \boldsymbol{p_S}\right) \tag{3.22}$$

Next, it will be derived fan operating speed range. The minimal speed is the speed at which fan curve crosses the system curve at the point of minimal operating flow, similarly, the maximal speed is the speed at which fan curve crosses the system curve at the point of maximal flow – see Fig. 3.1, yellow cross marks. The minimal and maximal speed can be derived from (3.9) or (3.10) if we find an equivalent operating point for minimal and maximal operating points on the fan nominal curve using affinity rules. The minimal speed is then expressed in (3.23) and the maximal speed in (3.24). The maximal speed equals to fan nominal speed when the maximal operating point lies on the fan nominal head-flow curve at nominal speed.
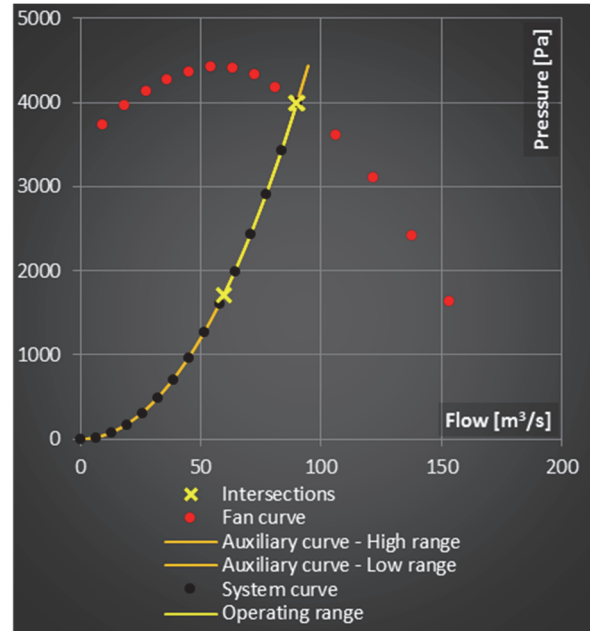
Fig. 3.1 Discrete definition of pneumatic system application

To find the equal operating points on fan nominal curve, auxiliary curves have to be build – see (3.25) and (3.26) for minimal and maximal operating range. Equivalent operating point is then find on the intersection of fan nominal curve and auxiliary curves - (3.27) and (3.28). For numerical solution see (3.29) - (3.32). Distribution of fan speed covering operating range is then in (3.33).

$$n_{OP_{\min}} = n_{OP_1} = n_N \times \frac{Q_{OP_1}}{Q_{OP_1 eqN}} = n_N \times \sqrt{\frac{p_{OP_1} \times \rho_{OP_1 eqN}}{p_{OP_1 eqN} \times \rho_{OP1}}} \tag{3.23}$$

$$n_{OP_{\max}} = n_{OP_{kOP}} = n_N \times \frac{Q_{OP_{kOP}}}{Q_{OP_{kOP} eqN}} = n_N \times \sqrt{\frac{p_{OP_{kOP}} \times \rho_{OP_{kOP} eqN}}{p_{OP_{kOP} eqN} \times \rho_{OP_{kOP}}}} ; \tag{3.24}$$

$$...for \ Q_{OP_{kOP}} = Q_{OP_{kOP} eqN} \Rightarrow n_{OP_{\max}} = n_N$$

$$p_{AuxCmin} = p_{AuxCmin}(Q) = \frac{p_S(Q_{OP\_\min}) \times \left(\dfrac{Q}{Q_{AuxCmin\_\max}}\right)^2 \times p_0}{p_S(Q_{OP\_\min}) \times \left[1 - \left(\dfrac{Q}{Q_{AuxCmin\_\max}}\right)^2\right] + p_0} \tag{3.25}$$

$$Q \in \left\langle 0, Q_{AuxCmin\_\max} \right\rangle$$

$$Q_{AuxCmin\_\max} = Q_{OP\_\min} \times \sqrt{\frac{p_{AuxCmin\_\max} \times \left(p_S(Q_{OP\_\min}) + p_0\right)}{p_S(Q_{OP\_\min}) \times \left(p_{AuxCmin\_\max} + p_0\right)}}$$

$$Q_{OP\_\min} = \min(\boldsymbol{Q_{OP}}) = Q_{OP_1}; p_{AuxCmin\_\max} = \max(\boldsymbol{p_{F_N}})$$

$$p_{AuxCmax} = p_{AuxCmin}(Q) = \frac{p_S(Q_{OP\_max}) \times \left(\dfrac{Q}{Q_{AuxCmax\_max}}\right)^2 \times p_0}{p_S(Q_{OP\_max}) \times \left[1 - \left(\dfrac{Q}{Q_{AuxCmax\_max}}\right)^2\right] + p_0}$$

(3.26)

$$Q \in \left\langle 0, Q_{AuxCmax\_max} \right\rangle$$

$$Q_{AuxCmax\_max} = Q_{OP\_max} \times \sqrt{\frac{p_{AuxCmax\_max} \times \left(p_S(Q_{OP\_max}) + p_0\right)}{p_S(Q_{OP\_max}) \times \left(p_{AuxCmax\_max} + p_0\right)}}$$

$$Q_{OP\_max} = \max(\boldsymbol{Q_{OP}}) = Q_{OP_{kOP}}; \ p_{AuxC\max\_max} = \max(\boldsymbol{p_{F_N}})$$

$$p_{AuxCmin}(Q) = p_{F_N}(Q)$$

(3.27)

$$Q_{OP_1eqN} = \left\{Q \mid p_{AuxCmin}(Q) = p_{F_N}(Q); \ n_F = n_N\right\}$$

$$p_{OP_1eqN} = p_{AuxCmin}(Q_{OP_1eqN})$$

$$p_{AuxCmax}(Q) = p_{F_N}(Q)$$

(3.28)

$$Q_{OP_{kOP}eqN} = \left\{Q \mid p_{AuxCmax}(Q) = p_{F_N}(Q); \ n_F = n_N\right\}$$

$$p_{OP_{kOP}eqN} = p_{AuxCmin}(Q_{OP_{kOP}eqN})$$

$$\boldsymbol{Q_{AuxCmin}} = \left[Q_{AuxCmin-j}\right]^T$$

(3.29)

$$Q_{AuxCmin-1} = 0; \ Q_{AuxCmin-m_{samples}} = Q_{AuxCmin\_max}$$

$$\boldsymbol{p_{AuxCmin}} = \left[p_{AuxCmin-j}\left(Q_{AuxCmin-j}\right)\right]^T$$

$$p_{AuxCmin-j}\left(Q_{AuxCmin-j}\right) = \frac{p_S(Q_{OP\_min}) \times \left(\dfrac{Q_{AuxCmin-j}}{Q_{AuxCmin\_max}}\right)^2 \times p_0}{p_S(Q_{OP\_min}) \times \left[1 - \left(\dfrac{Q_{AuxCmin-j}}{Q_{AuxCmin\_max}}\right)^2\right] + p_0}$$

$$j = 1, 2, \ldots, m_{samples}$$

$$\boldsymbol{Q_{AuxCmax}} = \left[Q_{AuxCmax-j}\right]^T$$

(3.30)

$$Q_{AuxCmax-1} = 0; \ Q_{AuxCmax-m_{samples}} = Q_{AuxCmax\_max}$$

$$\boldsymbol{p_{AuxCmax}} = \left[p_{AuxCmax-j}\left(Q_{AuxCmax-j}\right)\right]^T$$

$$p_{AuxCmax-j}\left(Q_{AuxCmax-j}\right) = \frac{p_S(Q_{OP\_max}) \times \left(\dfrac{Q_{AuxCmax-j}}{Q_{AuxCmax\_max}}\right)^2 \times p_0}{p_S(Q_{OP\_max}) \times \left[1 - \left(\dfrac{Q_{AuxCmax-j}}{Q_{AuxCmax\_max}}\right)^2\right] + p_0}$$

$$j = 1, 2, \ldots, m_{samples}$$

$$\left[Q_{OP_1eqN}, p_{OP_1eqN}\right] = f_{IntersectLinIntArrays}\left(\boldsymbol{Q_{F_N}}, \boldsymbol{p_{F_N}}, \boldsymbol{Q_{AuxCmin}}, \boldsymbol{p_{AuxCmin}}\right)$$

(3.31)

$$\left[Q_{OPk_{OP}eqN}, p_{OPk_{OP}eqN} \right] = f_{IntersectLinIntArrays} \left(\boldsymbol{Q}_{F_N}, \boldsymbol{p}_{F_N}, \boldsymbol{Q}_{AuxCmax}, \boldsymbol{p}_{AuxCmax} \right) \tag{3.32}$$

$$\boldsymbol{n}_F = \left[n_{Fj} \right]; \ j=1,2,\ldots,m_{curves} \tag{3.33}$$

$$n_{Fj} = n_{OP_{min}} + (j-1) \times \frac{n_{OP_{max}} - n_{OP_{min}}}{m_{curves} - 1}$$

Fan operating points are placed - by employing variable speed control - on the intersections ((3.35)) of fan curve recalculated for particular speed ((3.34)) and system curve. Finally, fan pressure at common fan and pneumatic system operating points - according to operating profile - are obtained by linear interpolation of intersections of fan curves at variable speed with system curve - (3.36).

$$\boldsymbol{Q_{Fn_i}} = \left[Q_{Pn_{i-j}} \right]; \ \boldsymbol{p_{Fn_i}} = \left[p_{Fn_{i-j}} \left(Q_{Fn_{i-j}} \right) \right] \tag{3.34}$$

$$Q_{Fn_{i-j}} = Q_{Fn_{N-j}} \times \frac{n_i}{n_N}$$

$$p_{Fn_{i-j}} \left(Q_{Fn_{i-j}} \right) = p_{Fn_{N-j}} \times \left(\frac{n_i}{n_N} \right)^2 \times \frac{p_0}{p_{Fn_{N-j}} \times \left[1 - \left(\frac{n_i}{n_N} \right)^2 \right] + p_0}$$

$$i \in \boldsymbol{n}_F; \ j = 1,2,\ldots,m_{samples}$$

$$\left[Q_{FSn_i}, p_{FSn_i} \right] = f_{IntersectLinIntArrays} \left(\boldsymbol{Q_S}, \boldsymbol{p_S}, \boldsymbol{Q_{Fn_i}}, \boldsymbol{p_{Fn_i}} \right) \tag{3.35}$$

$$\boldsymbol{Q_{FS}} = \left[Q_{FSn_i} \right]; \ \boldsymbol{p_{FS}} = \left[p_{FSn_i} \right]$$

$$i \in \boldsymbol{n}_F$$

$$p_{OPi} = f_{IntLinArray} \left(\boldsymbol{Q_{FS}}, \boldsymbol{p_{FS}}, Q_{OPi} \right) \tag{3.36}$$

$$\boldsymbol{p_{OP}} = \left[p_{OPi} \right]^T$$

$$i = 1,2,\ldots,k_{OP}$$

Next are expressed relations for fan pneumatic power ((3.37)), fan mechanical power and/or power consumption (3.38), fan efficiency ((3.39) and (3.40)), fan speed ((3.41)) and fan torque ((3.42)) at fan operating points.

$$\boldsymbol{P_{p\text{-}OP}} = \left[P_{p-OPi} \right]^T \tag{3.37}$$

$$P_{p-OPi}[\text{kW}] = Q_{OPi}[m^3/\text{s}] \times p_{OPi}[\text{kPa}]$$

$$i = 1,2,\ldots,k_{OP}$$

$$\boldsymbol{P_{cF\text{-}OP}} = \boldsymbol{P_{p\text{-}OP}} / \boldsymbol{\eta_{F\text{-}OP}} \tag{3.38}$$

$$\boldsymbol{\eta_{F\text{-}OP}} = \left[\eta_{F-OPi} \right]^T \tag{3.39}$$

$$\eta_{F-OPi} = f_{IntLinArray} \left(\boldsymbol{Q_{FS}}, \boldsymbol{\eta_{FS}}, Q_{OPi} \right)$$

$$i = 1,2,\ldots,k_{OP}$$

$$\eta_{FS} = \eta_{FS}\left(Q_{n_{FS}}\right) = \eta_{F_N}\left(Q_{FS} \times \frac{n_{F_N}}{n_{FS}}\right)$$

(3.40)

$$\boldsymbol{\eta_{FS}} = \left[\eta_{FSj}\right]^T$$

$$\eta_{FSj} = f_{IntLinArray}\left(\boldsymbol{Q_{F_N}}, \boldsymbol{\eta_{F_N}}, Q_{FSj} \times \frac{n_{F_N}}{n_{FSj}}\right); \; \boldsymbol{n_{FS}} = \boldsymbol{n_F}$$

$$j = 1, 2, \ldots, m_{curves}$$

$$\boldsymbol{n_{F\text{-}OP}} = \left[n_{F-OPi}\right]$$

(3.41)

$$n_{F-OPi} = f_{IntLinArray}\left(\boldsymbol{Q_{FS}}, \boldsymbol{n_F}, Q_{OPi}\right)$$

$$i = 1, 2, \ldots, k_{OP}$$

$$\boldsymbol{T_{F\text{-}OP}} = \left[T_{F-OPi}\right]$$

(3.42)

$$T_{F-OPi}[\text{Nm}] = \frac{P_{cF-OPi}[kW] \times 1000}{\dfrac{n_{F-OPi}[\text{rpm}]}{60} \times 2\pi}$$

$$i = 1, 2, \ldots, k_{OP}$$

3.1.2.2   Typical performance curves

Evaluation of particular flow control methods – namely inlet guide vanes, inlet damper and pitch control - described in next chapter - is based purely on flow control typical performance curves, which are closely related to specific fan due to no-existing general analytical solution. Hence, to be able to evaluate these flow control techniques in cases of incomplete case study data available, following set of data for both radial and axial type of fans expressed in per unit values have been sampled as referenced ones. Fig. 3.2 shows fan flow – pressure curves and Fig. 3.3 flow – efficiency curves for axial type of fan and radial type of fan with straight, forward, and backward curved blades. Expression of fan curves in physical units is then in (3.43). Efficiency in Fig. 3.3 is not presented in per-unit values to prevent reader from confusion from values higher than 100 %.

The set of curves were sampled from [41] and compared and/or verified with measurements of real industrial fans published by the world's leading industrial fan manufacturers – especially with products of ZVVZ Machinery a.s. company, which supply fans for wide range of industrial applications.

$$Q_{F_N} = Q_{F_N} \times Q_{F_{R\text{-}pu}}; Q_{F_{R\text{-}pu}} = \frac{Q_{F_R}}{Q_{F_{R-N}}}$$

$$(3.43)$$

$$p_{F_N} = p_{F_N} \times p_{F_R}; p_{F_{R\text{-}pu}} = \frac{p_{F_R}}{p_{F_{R-N}}}$$

$$\eta_{F_N} = \frac{\eta_{F_N}}{\eta_{F_{R-N}}} \times \eta_{F_R}$$
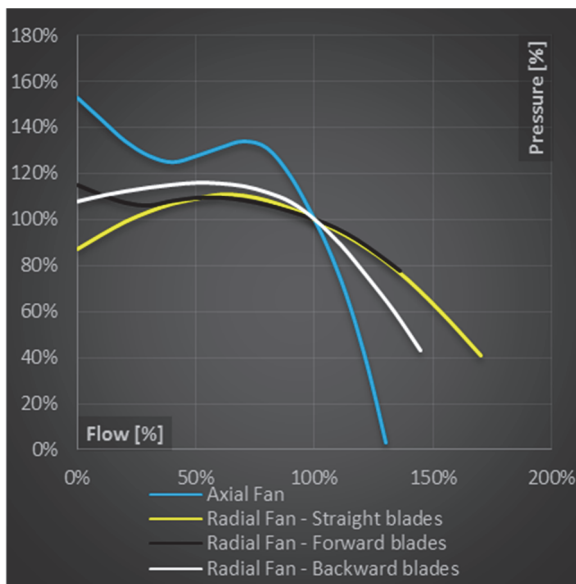
Fig. 3.2 Referenced fan pressure – flow curves   Fig. 3.3 Referenced fan efficiency – flow curves
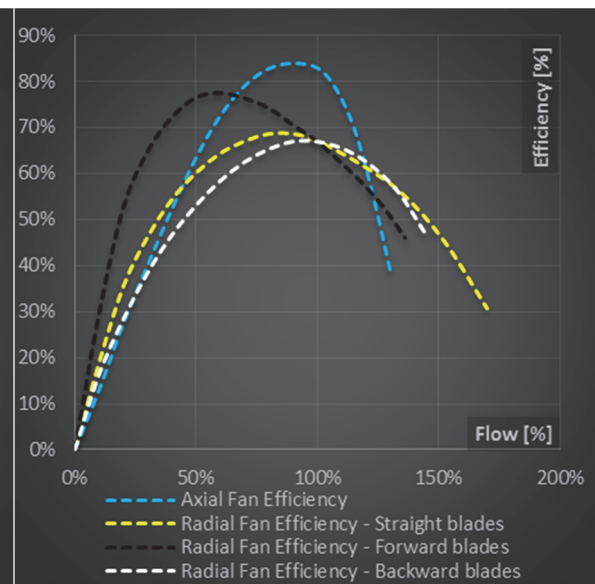
3.1.3   Flow control algorithms

Evaluation of flow control algorithms for fan systems differ significantly from pump systems. The difference steams from two basic topologies of fans – radial and axial, which are used in combination with additional fan-type specific devices to control the flow. Variable speed flow control, on-off control and outlet dumper flow control could be solved similarly to pump systems based on fan affinity rules and analytical description of flow control principles. However, mathematical models for flow control realized by inlet guide vanes, inlet damper and pitch control couldn't be generalized enough and therefore are usually represented just by final efficiency performance curve supplied directly by fan manufacturer together with fan. Hence, typical set of radial fan performance curves with forward curved blades, backward curved blades and straight blades and axial fan and control techniques performance curves have been sampled as a referenced ones to be able to approximate fan performance even with incomplete definition of all components of fan systems. Special attention has been paid to approximation procedures for pitch flow control of axial fan.

Similarly to pump systems, control efficiency is defined to be able to compare and evaluate flow control algorithms among each other – see (3.44) and (3.45).

$$\eta_{CF} = \frac{P_{pS}}{P_{pF}} = \frac{P_{pS} \times t}{P_{pF} \times t} = \frac{E_{pS}}{E_{pF}} \tag{3.44}$$

$$P_{pF} = Q_F \times \Delta p_F \left(Q_F \right)$$

$$P_{pS} = Q_S \times p_S \left(Q_S \right)$$

$$\boldsymbol{\eta_{CF\text{-}OP}} = \left[\eta_{CF-OPi} \right]^T \tag{3.45}$$

$$\eta_{CF-OPi} = \frac{P_{pS-OPi}}{P_{pF-OPi}} = \frac{P_{pS-OPi} \times t_i}{P_{pP-OPi} \times t_i} = \frac{E_{pS-OPi}}{E_{pF-OPi}}$$

$$i = 1, 2, ..., k_{OP}$$

3.1.3.1   Variable Speed Flow Control

Variable speed flow control use the change of fan speed to match demanded flow and/or operating point on pneumatic system curve. Fan flow and outlet pressure match pneumatic system flow and pressure and therefore control efficiency under speed control equals one - (3.46). Fan efficiency under variable speed control is then - (3.47). This is valid for both axial and radial type of fans. For detailed derivation of mathematical model of fan for variable speed control see Chapter 3.1.2.1.

$$Q_{F-VS-OPi} = Q_{S-OPi}; \; p_{F-VS-OPi} = p_{S-OPi} \; \Rightarrow \; P_{pF-OPi} = P_{pS-OPi} \tag{3.46}$$

$$\eta_{CF-VS-OPi} = \frac{P_{pS-OPi}}{P_{pF-OPi}} = 1$$

$$i = 1,2,...,k_{OP}$$

$$\eta_{F-VS} = \eta_{F_N}\left(Q_F \times \frac{n_N}{n}\right) \tag{3.47}$$

$$\eta_{F-VS-OPi} = f_{IntLinArray}\left(\boldsymbol{Q_{F_N}}, \boldsymbol{\eta_{F_N}}, Q_{F-OPi} \times \frac{n_N}{n_{F-OPi}}\right)$$

$$i = 1,2,...,k_{OP}$$

3.1.3.2   Inlet Guide Vanes & Inlet Damper

The principles of evaluation of Inlet Guide Vanes (IGV) and Inlet Damper flow control techniques are equal. The equations below are written for IGV however are identical for inlet damper by substituting IGV for Inlet Damper in the notation. Both techniques are used in combination with fixed speed fan ((3.48)). There is no general mathematical model available, therefore, manufacturer usually supply both the fan and inlet guide vanes or inlet damper together with measured performance curves. This is the most optimal way. Evaluation of efficiency is then simple linear approximation of fan and inlet guide vanes or inlet damper efficiency curve for system flow - (3.49) and (3.50). However, especially at retrofit applications not all necessary curves are usually available. Hence, typical fan and control performance curves have been sampled based on presented curves from [41] to be able to get an approximate idea about expected behavior in comparison to other flow control methods. For referenced fan efficiency curves see Fig. 3.3. Referenced efficiency curve for inlet guide vanes and inlet damper are in Fig. 3.4. Total efficiency from referenced curves is then evaluated according to (3.51) and (3.52).

$$n_{F-IGV-OPi} = const = n_N ; \ i = 1,2,...,k_{OP} \tag{3.48}$$

$$Q_{F-IGV-OPi} = Q_{S-OPi} = Q_{OPi} ; \ i = 1,2,...,k_{OP} \tag{3.49}$$

$$\eta_{F+IGV-OPi} = \eta_{F+IGV}\left(Q_{S-OPi}\right) = f_{IntLinArray}\left(\boldsymbol{Q_{F+IGV}}, \boldsymbol{\eta_{F+IGV}}, Q_{S-OPi}\right) \tag{3.50}$$
$$i = 1,2,...,k_{OP}$$

$$\eta_{F+IGV-OPi} = \eta_{F-OPi}\left(Q_{S-OPi}\right) \times \eta_{CF-IGV-OPi}\left(Q_{S-OPi}\right) \tag{3.51}$$
$$\eta_{F-OPi} = f_{IntLinArray}\left(\boldsymbol{Q_{F_N}}, \boldsymbol{\eta_{F_N}}, Q_{S-OPi}\right)$$
$$\eta_{CF-IGV-OPi} = f_{IntLinArray}\left(\boldsymbol{Q_{CF-IGV}}, \boldsymbol{\eta_{CF-IGV}}, Q_{S-OPi}\right)$$
$$i = 1,2,...,k_{OP}$$

$$\boldsymbol{Q_{CF-IGV}} = Q_{CF-IGV_N} \times \boldsymbol{Q_{CF-IGV_{R-pu}}} ; \boldsymbol{Q_{CF-IGV_{R-pu}}} = \frac{\boldsymbol{Q_{CF-IGV_R}}}{Q_{CF-IGV_{R-N}}} \tag{3.52}$$

$$\boldsymbol{\eta_{CF-IGV}} = \frac{\eta_{CF-IGV_N}}{\eta_{CF-IGV_{R-N}}} \times \boldsymbol{\eta_{CF-IGV_R}}$$
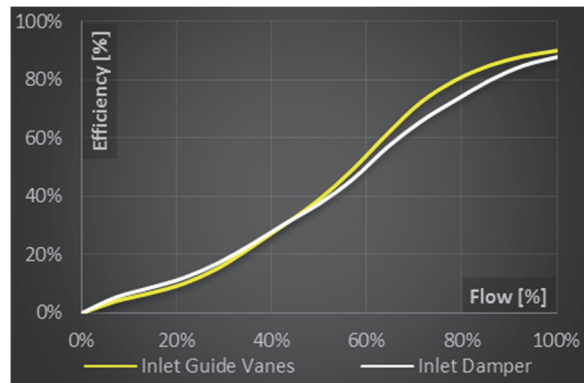
Fig. 3.4 Inlet Guide Vanes and Inlet Damper – Efficiency curve

3.1.3.3   Outlet Damper

Employing outlet damper to control fan flow is similar to throttling flow control in pump systems. Fan speed equals to fan nominal speed over the entire operating range - (3.53). Fan and damper flow equals to system flow and fan outlet pressure is a function of fan pressure-flow curve at nominal speed ((3.54) and (3.55)). Pressure loss over outlet damper is expressed in (3.56). Control efficiency for outlet damper is (3.57). Fan efficiency employing flow control strategy is then in (3.58). Using outlet damper changes pneumatic system curve and/or nominal operating point. Hence, it is not possible to compare the control method with the others under constant pneumatic system conditions. Therefore, the fan pneumatic power and efficiency calculation is divided into two regions given by the pressure loss over the damper ((3.57)). The second region is not reachable without replacement of the fan or pneumatic system conditions, however to be able to compare it with other flow control techniques, it is supposed the power increase of the fan about power loss on the damper.

$$n_{F-OutletDamper-OPi} = const = n_N; \ i = 1,2,...,\mathrm{k}_{OP} \tag{3.53}$$

$$Q_{F-OutletDamper-OPi} = Q_{OutletDamper-OPi} = Q_{S-OPi} = Q_{OPi}; \ i = 1,2,...,\mathrm{k}_{OP} \tag{3.54}$$

$$p_{F-OutletDamper-OPi} = p_{F_N}\left(Q_{F-OutletDamper-OPi}\right) = f_{IntLinArray}\left(\boldsymbol{Q}_{F_N}, \boldsymbol{p}_{F_N}, Q_{F-OutletDamper-i}\right) \tag{3.55}$$
$$i = 1,2,...,\mathrm{k}_{OP}$$

$$\Delta p_{OutletDamper-OPi} = \frac{\Delta p_{OutletDamper_N} \times \left(\dfrac{Q_{OutletDamper-OPi}}{Q_{F_N}}\right)^2 \times p_0}{\Delta p_{OutletDamper_N} \times \left(1 - \dfrac{Q_{OutletDamper-OPi}}{Q_{F_N}}\right)^2 + p_0}; \ i = 1,2,...,\mathrm{k}_{OP} \tag{3.56}$$

$$P_{pS-OPi} = Q_{S-OPi} \times p_{S-OPi} \tag{3.57}$$
$$P_{pF-OutletDamper-OPi} = Q_{F-OutletDamper-OPi} \times p_{F-OutletDamper-OPi}$$
$$\Delta P_{p-OutletDamper-OPi} = Q_{OutletDamper-OPi} \times \Delta p_{OutletDamper-OPi}$$
$$\mathrm{i}.\, for \ \left(p_{F-OutletDamper-OPi} - p_{S-OPi}\right) > \Delta p_{OutletDamper-OPi} \Rightarrow$$
$$\eta_{CF-OutletDamper-OPi} = \frac{P_{pS-OPi}}{P_{pF-OutletDamper-OPi}}$$
$$\mathrm{ii}.\, for \ \left(p_{F-OutletDamper-OPi} - p_{S-OPi}\right) \le \Delta p_{OutletDamper-OPi} \Rightarrow$$
$$\Rightarrow \eta_{CF-OutletDamper-OPi} = \frac{P_{pS-OPi}}{P_{pS-OPi} + \Delta P_{p-OutletDamper-OPi}}$$
$$i = 1,2,...,\mathrm{k}_{OP}$$

$$\eta_{F-OutletDamper-OPi} = \eta_{F_N}\left(Q_{F-OutletDamper-OPi}\right) = f_{IntLinArray}\left(\boldsymbol{Q}_{F_N}, \boldsymbol{\eta}_{F_N}, Q_{F-OutletDamper-OPi}\right) \tag{3.58}$$
$$i = 1,2,...,\mathrm{k}_{OP}$$

3.1.3.4   Pitch Control

Pitch control is typically the most efficient way of flow control employing fixed speed ((3.59)) drive because the flow is adjusted just by pitch of fan blades without additional devices. Fan flow and outlet pressure equals to demanded system flow and pressure and therefore control efficiency equals similarly to variable speed flow control to one - see (3.60). Pitch of fan blades shifts fan flow-pressure curve and fan flow-efficiency curve. Fan efficiency is therefore dependent in contrast to other flow control techniques by two variables. Respectively, the efficiency is represented by surface related to both fan flow and fan outlet pressure. Fan total efficiency for specific operating range is then obtained as a two dimensional interpolation of fan efficiency space for pneumatic system flow and pressure – see (3.61). Usually fan manufacturer supply directly the efficiency curve for specific system conditions. In this case, operating range is calculated by simple interpolation of supplied efficiency curve - (3.62).

However, based on experience from especially retrofit case studies, just the fan efficiency curve for one fan blade position is often available. Next, it is described approximation procedure based on referenced axial fan with pitch control to estimate fan efficiency in case of lack of initial data.

Fig. 3.5 and Fig. 3.6 present efficiency surface and interpolated efficiency curve for referenced axial fan with pitch flow control. Efficiency surface for pitch-controlled fan has been sampled from presented case in [41] and reshaped to per unit values as well as corresponding interpolated efficiency curve and fan pressure flow curve. Per unit expression of fan efficiency allow to use the fan as a referenced one without direct relation to fan power. The approximation technique is based on adjusting of fan efficiency surface based on the change of user fan in per unit values in comparison to referenced fan in per unit values.

Referenced fan efficiency surface and related interpolated 1D efficiency curve is expressed in (3.63). Approximated fan efficiency surface is then generated according to (3.64). Adjustment of referenced efficiency surface is done via efficiency correction matrix. Matrix elements are obtained as
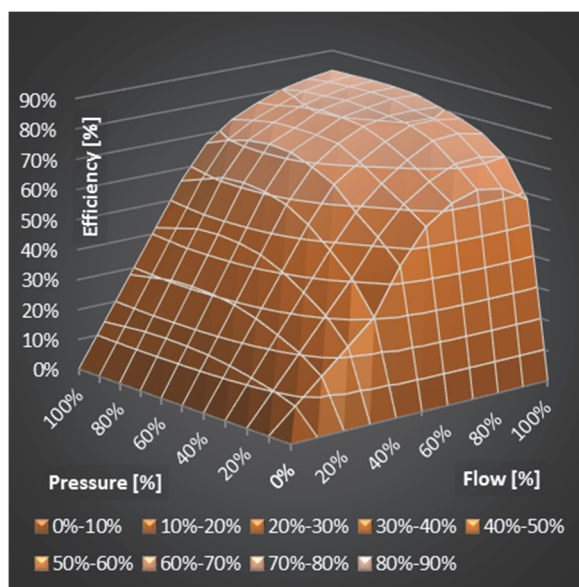
Fig. 3.5 Efficiency surface of referenced axial fan with pitch control
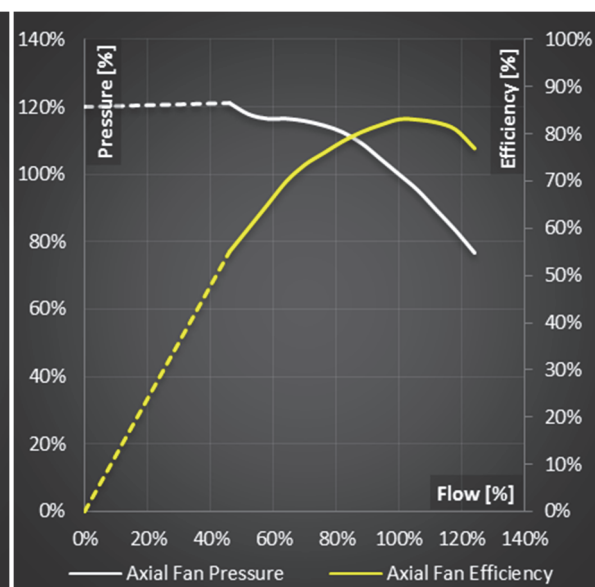
Fig. 3.6 Referenced axial fan

a ratio of interpolated efficiencies of user and referenced fans. Efficiency at fan operating points is then calculated from (3.61).

$$n_{F-Pitch-OPi} = const = n_N; \ i = 1, 2, ..., k_{OP} \tag{3.59}$$

$$Q_{F-Pitch-OPi} = Q_{S-OPi} = Q_{OPi}; \ p_{F-Pitch-OPi} = p_{S-OPi} \ \Rightarrow \ P_{pF-Pitch-OPi} = P_{pS-OPi} \tag{3.60}$$

$$\eta_{CF-Pitch-OPi} = \frac{P_{pS-OPi}}{P_{pF-Pitch-OPi}} = 1$$
$$i = 1, 2, ..., k_{OP}$$

$$\eta_{F-Pitch-OPi} = \eta_{F-Pitch2D}\left(Q_{F-Pitch-OPi}, p_{F-Pitch-OPi}\right) = \tag{3.61}$$
$$= f_{IntLin2DArray}\left(\boldsymbol{Q_{F\text{-}Pitch}}, \boldsymbol{p_{F\text{-}Pitch}}, \boldsymbol{\eta_{F\text{-}Pitch2D}}, Q_{S-OPi}, p_{S-OPi}\right)$$
$$i = 1, 2, ..., k_{OP}$$

$$\eta_{F-Pitch-OPi} = \eta_{F-Pitch1D}\left(Q_{F-Pitch-OPi}\right) = f_{IntLinArray}\left(\boldsymbol{Q_{F\text{-}Pitch}}, \boldsymbol{\eta_{F\text{-}Pitch1D}}, Q_{S-OPi}\right) \tag{3.62}$$
$$i = 1, 2, ..., k_{OP}$$

$$\boldsymbol{\eta_{F\text{-}Pitch2D_R}} = \begin{bmatrix} \eta_{2D_R-11} & \eta_{2D_R-12} & \cdots & \eta_{2D_R-1q} \\ \eta_{2D_R-21} & \eta_{2D_R-22} & \cdots & \eta_{2D_R-2q} \\ \vdots & \vdots & \ddots & \vdots \\ \eta_{2D_R-p1} & \eta_{2D_R-p2} & \cdots & \eta_{2D_R-pq} \end{bmatrix} \tag{3.63}$$

$$\boldsymbol{Q_{F\text{-}Pitch_R}} = \begin{bmatrix} Q_q \end{bmatrix}$$

$$\boldsymbol{p_{F\text{-}Pitch_R}} = \begin{bmatrix} p_p \end{bmatrix}$$

$$q = 1, 2, ..., m_{samples}; \ p = 1, 2, ..., m_{samples}$$

$$Q_1 = p_1 = 0; \ Q_{m_{samples}} = p_{m_{samples}} = 1$$

$$\boldsymbol{\eta_{F\text{-}Pitch1D_R}} = \begin{bmatrix} \eta_{F-Pitch1D_R-OP_i} \end{bmatrix}$$

$$\eta_{F-Pitch1D_R-OP_i} = f_{IntLin2DArray}\left(\boldsymbol{Q_{F\text{-}Pitch_R}}, \boldsymbol{p_{F\text{-}Pitch_R}}, \boldsymbol{\eta_{F\text{-}Pitch2D_R}}, Q_{S_R-OPi}, p_{S_R-OPi}\right)$$

$$i = 1, 2, ..., k_{OP_R}$$

$$\boldsymbol{\eta_{F\text{-}Pitch2D}} = \begin{bmatrix} \eta_{2D_R-11} & \eta_{2D_R-12} & \cdots & \eta_{2D_R-1q} \\ \eta_{2D_R-21} & \eta_{2D_R-22} & \cdots & \eta_{2D_R-2q} \\ \vdots & \vdots & \ddots & \vdots \\ \eta_{2D_R-p1} & \eta_{2D_R-p2} & \cdots & \eta_{2D_R-pq} \end{bmatrix} .\times \begin{bmatrix} c_{\eta-1} & c_{\eta-2} & \cdots & c_{\eta-q} \\ c_{\eta-1} & c_{\eta-2} & \cdots & c_{\eta-q} \\ \vdots & \vdots & \ddots & \vdots \\ c_{\eta-1} & c_{\eta-2} & \cdots & c_{\eta-q} \end{bmatrix} .\times \frac{\eta_{F-Pitch_N}}{\eta_{F-Pitch_{R-N}}} \tag{3.64}$$

$$\boldsymbol{c_\eta} = \begin{bmatrix} c_{\eta-q} \end{bmatrix}$$

$$c_{\eta-q} = \frac{f_{IntLinArray}\left(\boldsymbol{Q_{F\text{-}Pitch-q}} ./ Q_{F-Pitch_N}, \boldsymbol{\eta_{F\text{-}Pitch1D}} ./ \eta_{F-Pitch_N}, Q_q[pu]\right)}{f_{IntLinArray}\left(\boldsymbol{Q_{F\text{-}Pitch_R-q}} ./ Q_{F-Pitch_{R-N}}, \boldsymbol{\eta_{F\text{-}Pitch1D_R}} ./ \eta_{F-Pitch_{R-N}}, Q_q[pu]\right)}$$

$$q = 1, 2, ..., m_{samples}$$

3.1.3.5   On-Off Control

On-Off control is a very specific flow control while it actually operates only at nominal operating point - (3.65). It is not possible to control flow in a real time. However, it is possible to control the flow quantity in a time period (average value) - (3.66). Flow quantity is then determined by the ratio of run and stop time. Hence, control efficiency for on-off control is then expressed via energy - (3.67). It is apparent, that this method could be applied only for the application that includes capacity and it is possible to vary flow around the set-point hysteresis range.

$$n_{F-OnOff-OPi} = const = n_N \tag{3.65}$$

$$Q_{F-OnOff-OPi} = Q_{OP_N} = Q_{S_N}$$

$$p_{F-OnOff-OPi} = p_{OP_N} = p_{S_N}$$

$$\eta_{F-OnOff-OPi} = \eta_{F_N}\left(Q_{S_N}\right)$$

$$i = 1, 2, ..., k_{OP}$$

$$Q_{F-OnOff-OPiavg} = Q_{S_N} \times \frac{t_{OPi}}{\sum\limits_{i=1}^{k_{OP}} t_{OPi}}; \quad i = 1, 2, ..., k_{OP} \tag{3.66}$$

$$P_{pS-OPi} = Q_{S-OPi} \times p_{S-OPi} \tag{3.67}$$

$$E_{pS-OPi} = P_{pS-OPi} \times t_{OPi}$$

$$P_{pF-OnOff-OPi} = P_{pF-OP_N} = Q_{F-OP_N} \times p_{F-OP_N}$$

$$E_{pF-OnOff-OPi} = P_{pF-OP_N} \times t_{OPi}$$

$$\eta_{CP-OnOff-OPi} = \frac{E_{pS-OPi}}{E_{pF-OnOff-OPi}}$$

$$i = 1, 2, ..., k_{OP}$$

3.2   Model verification - Case studies

In this chapter, two case studies of typical fan systems are presented to show the performance and verify developed mathematical models and methodology presented in the chapter 3.1 on particular applications. The case studies have been evaluated in the software tool Medium-Voltage Drive Fan Save 2012, which has been developed - based on the introduced mathematical models and methodology - for advanced evaluation of these systems. In the Fig. 3.7, see the main screenshot of the software tool. More in-detail information about the software tool and its features have been published especially in the following international conferences: [A2, A3] and research reports [A38, A44, A45, A46, A47, A48]. Brief summary is available in Appendix 2 – MVD Fan Save 2012 .

The first case study is focused on a radial fan and associated flow control techniques. It is elaborated in two variants to compare directly the technical and economical indicators of the flow control techniques in relation to operating flow and/or speed range. The second case study presents fan application with pitch-controlled axial fan and compares it with variable speed flow control and other commonly used flow control techniques. The drive part developed for fan systems is identical to drives for pump systems and the performance has been widely presented in the case study section of pump applications, therefore this chapter will focus especially on presentation of pneumatic part and total flow control comparison among each other on presented cases.
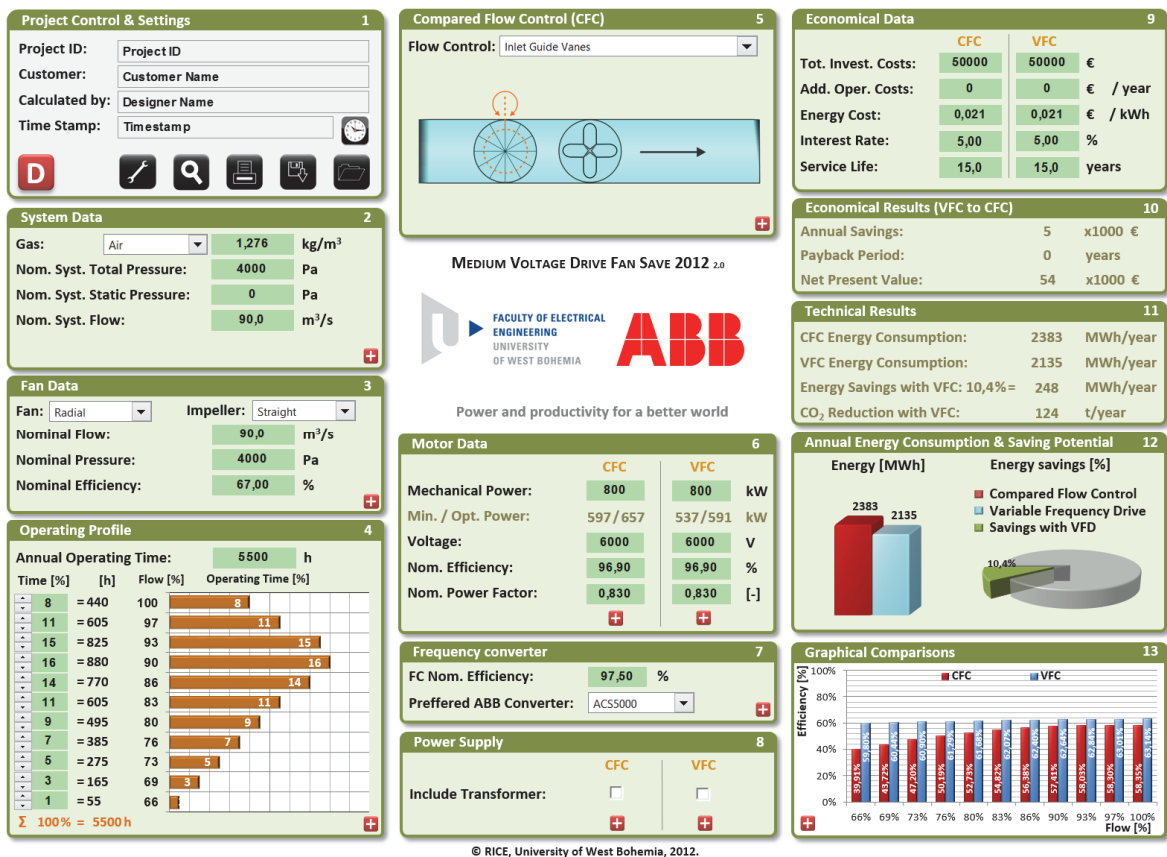
Fig. 3.7 Medium-Voltage Drive Fan Save 2012 – Main screen

3.2.1 Case study 1 – Radial fan

This case study presents the performance of radial-type fan with associated flow control techniques on gas recirculation application in thermal power plant. The case study is presented in two variants to compare the suitability of flow control methods in relation to operating flow and or speed range. The first variant varies flow range from 75% to 100 % of nominal flow with weighted average of flow 89,65% and weighted average of system pneumatic power 79,49%. The second variant varies the flow from 90% to 100% of nominal flow with weighted average of flow 95,86% and weighted average of system pneumatic power 88,04%.

3.2.1.1 Pneumatic system & Operating profile

The case study pneumatic system parameters are summarized in the Table 3.1.The Fig. 3.8 and Fig. 3.9 show the operating profile for the case study variants. Fig. 3.10 and Fig. 3.11 present the pneumatic system curves including operating range and/or operating points.

Table 3.1 – Case study 1, Pneumatic system

Pneumatic system	Value - Var. 1	Value – Var. 2	Unit
Pneumatic system			
Nominal flow	96	96	m^3/s
Nominal total head	4 000	4 000	Pa
Nominal dynamic head	4 000	4 000	Pa
Nominal static head	0	0	Pa
Static / referenced head control	constant	constant	
Gas density	0,585	0,585	kg/m^3
System operating data			
Annual running time	8590	8590	h
Flow operating range	75 - 100	90 - 100	%
Weighted average of flow	89,65	95,86	%
Weighted average of pneumatic system power	79,49	88,04	%
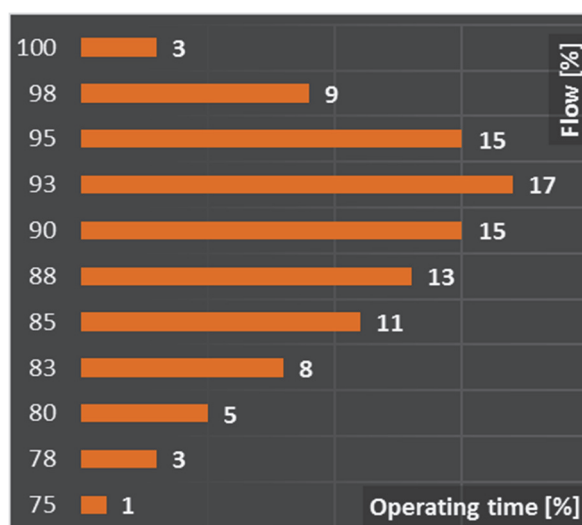
Fig. 3.8 Case study 1 – V1, Operating profile
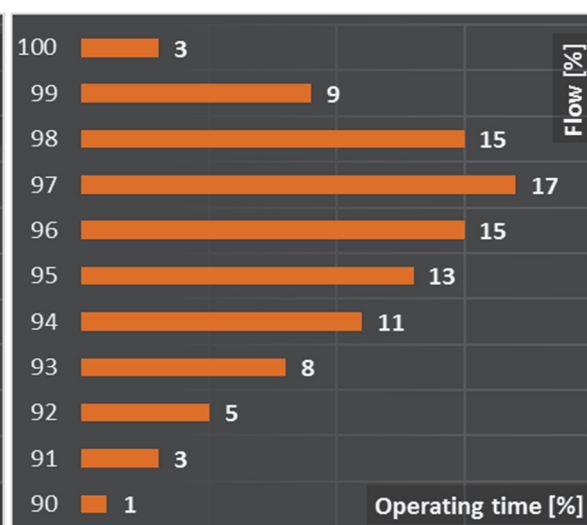
Fig. 3.9 Case study 1 – V2, Operating profile

3.2.1.2   Fan

It is employed radial fan with the specification according to Table 3.2. See, that fan nominal operating point is not located at the fan Best Efficiency Operating Point. Best Efficiency Point is located close to real fan and system nominal operating point – see Table 3.3. Fig. 3.10 and Fig. 3.11 present approximated fan performances curves from nominal speed, to speed range covering demanded flow range employing Variable Speed Control (VSC) for the case study variants. Fig. 3.12 and Fig. 3.13 show the speed operating range for the operating profile flow range.

Table 3.2 – Case study 1, Fan

Fan	Value – Var. 1,2	Unit
Fan		
Nominal speed	994	rpm
Flow operating range at nominal speed	$69,3 - 116,82$	m^3/s
Fan Nominal Operating Point		
Flow	99	m^3/s
Pressure	3 797	Pa
Efficiency	66,0	%
Pneumatic power	376	kW
Mechanical / shaft power	570	kW
Torque	5 472	Nm

Table 3.3 – Case study 1, Real nominal operating points

Fan & Pneumatic system	Value – Var. 1,2	Unit
Real nominal operating point		
Flow	94,9	m^3/s
Pressure	3 908	Pa
Efficiency	66,92	%
Pneumatic power	371	kW
Mechanical / shaft power	554	kW
Torque	5 323	Nm
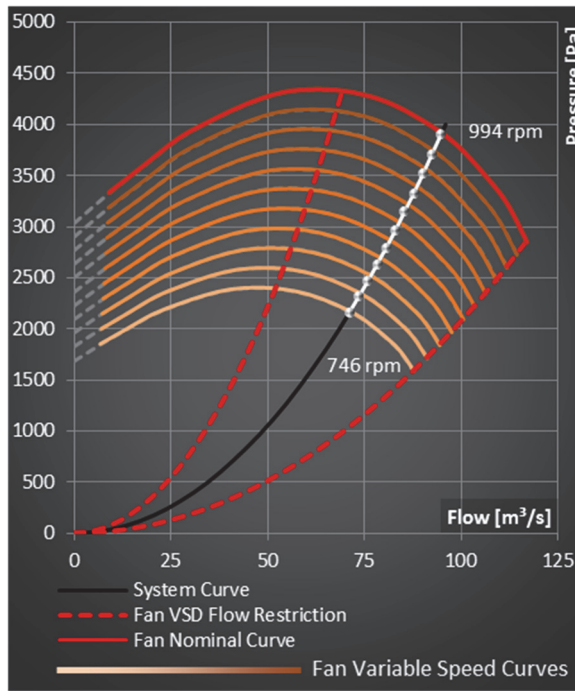
Fig. 3.10 Case study 1 – V1,
Fan & Pneumatic system curves
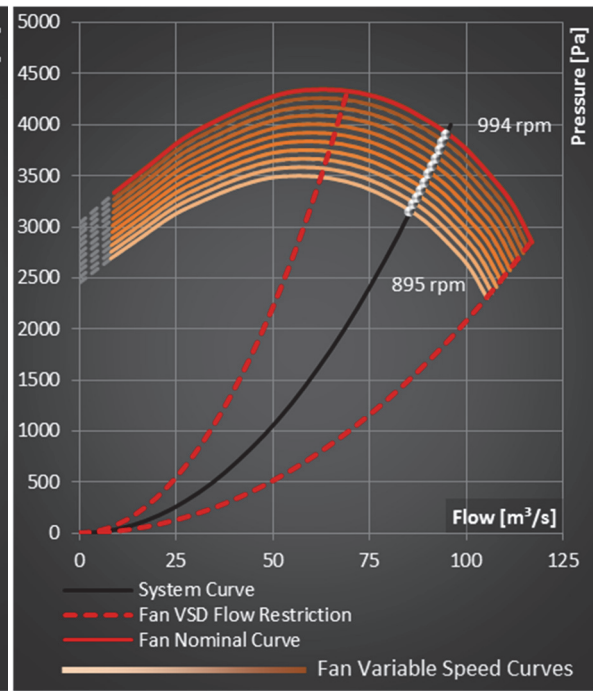
Fig. 3.11 Case study 1 – V2,
Fan & Pneumatic system curves
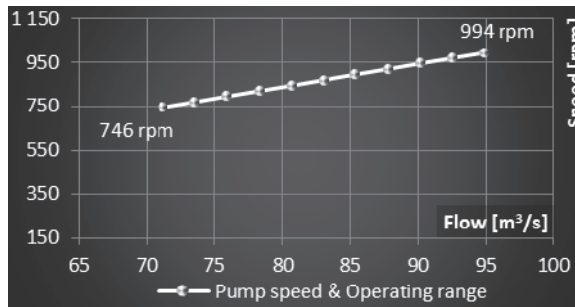
Fig. 3.12 Case study 1 – V1,
Fan VSC speed range
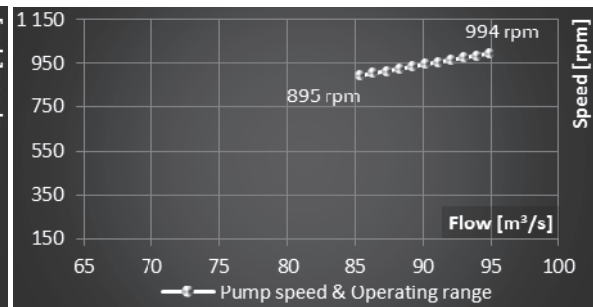
Fig. 3.13 Case study 1 – V2,
Fan VSC speed range

Fan performance curves and operating points under VSC

Fig. 3.14 - Fig. 3.17 show approximated fan performance curves for fan efficiency and pneumatic power from curves at nominal speed to curves at variable speed according to VSC. See, that similarly to pump systems, fan efficiency keeps constant and/or nominal over the entire operating range employing VSC in pneumatic systems with zero static pressure independently on the speed range.
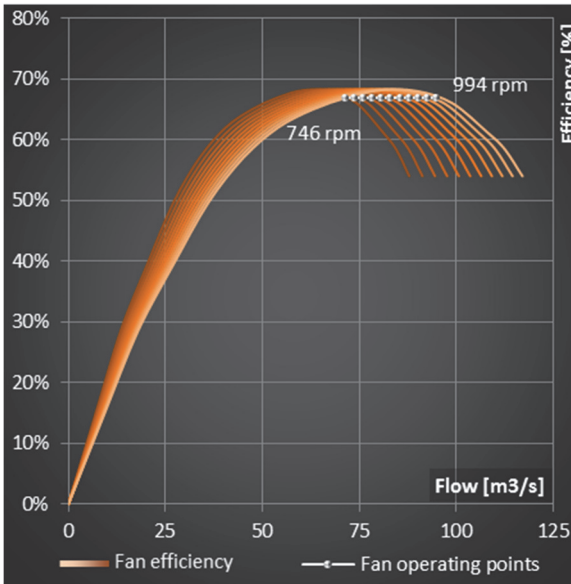
Fig. 3.14 Case study 1 – V1, Fan VSC efficiency   Fig. 3.15 Case study 1 – V2, Fan VSC efficiency
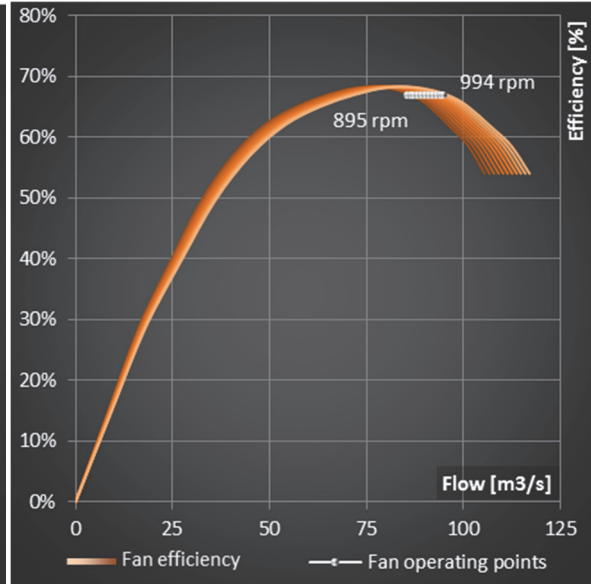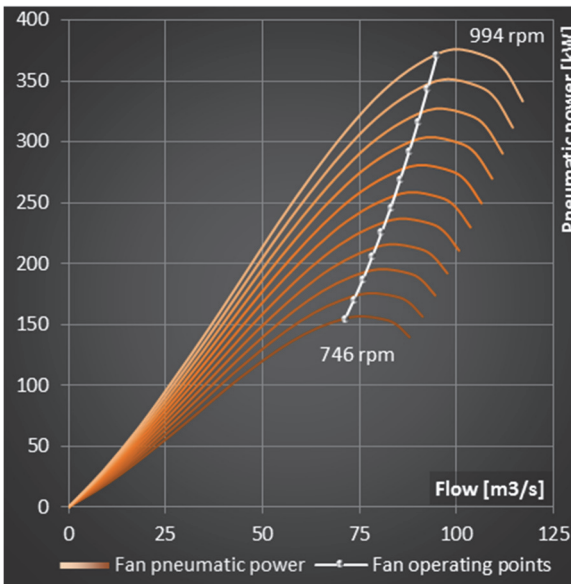
Fig. 3.16 Case study 1 – V1,   Fig. 3.17 Case study 1 – V2,
Fan VSC pneumatic power   Fan VSC pneumatic power
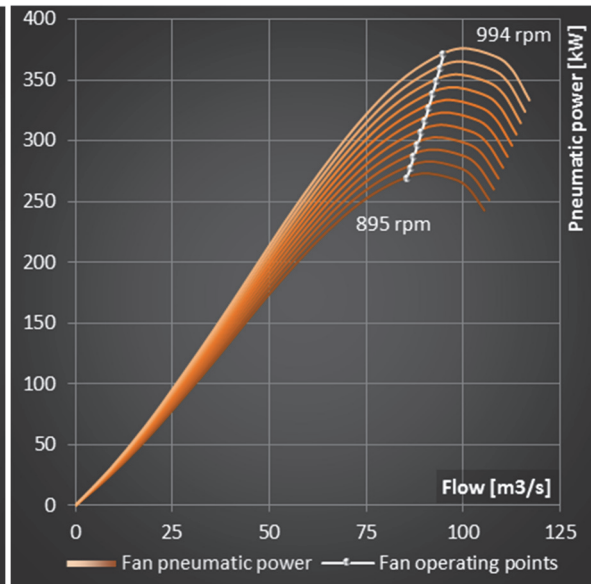
3.2.1.3   Flow control

Inlet Guide Vanes & Inlet Damper

Representation of flow control by inlet guide vanes or inlet damper is done purely by control efficiency curves. For nominal operating point efficiency see Table 3.4, efficiency curves for both variants are shown in Fig. 3.18 and Fig. 3.19. The curves have been generated based on referenced efficiency curves, nevertheless each device is usually unique and it would be necessary to obtain particular curve directly from manufacturer for precise evaluation. In general, flow control with IGV is more efficient within the usual operating range than Inlet Damper.

Table 3.4 – Case study 1, IGV & Inlet Damper

Inlet Guide Vanes & Inlet Damper	Value – Var. 1,2	Unit
Nominal efficiency		
Inlet Guide Vanes	92,0	%
Inlet Damper	90,0	%
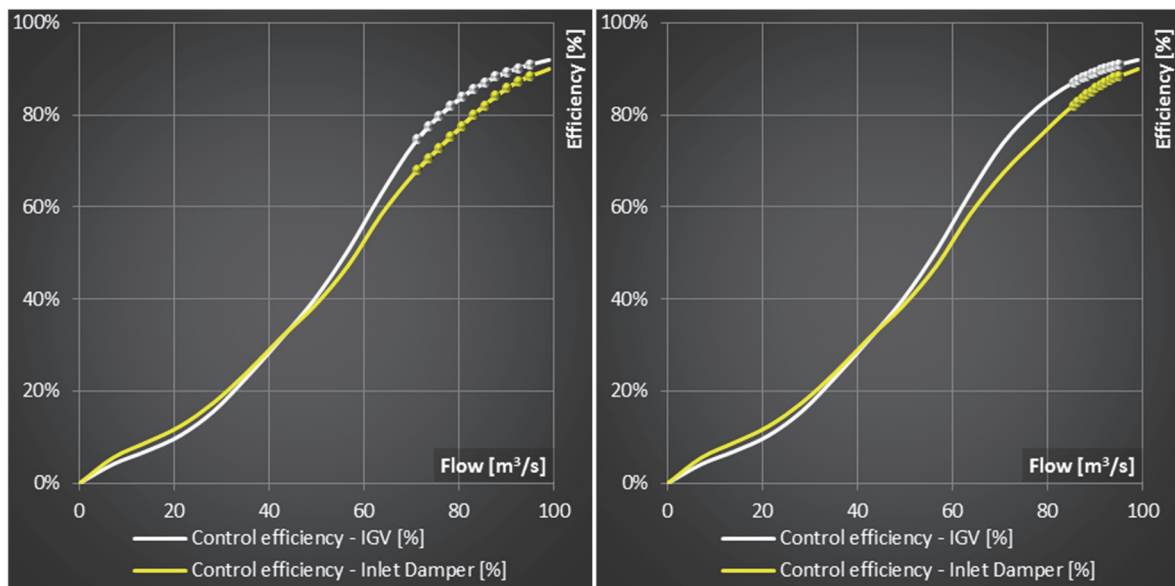
Fig. 3.18 Case study 1 – V1, Efficiency curve for Inlet Guide Vanes and Inlet Damper

Fig. 3.19 Case study 1 – V2, Efficiency curve for Inlet Guide Vanes and Inlet Damper

Outlet Damper

In the Table 3.5, see the parameters of outlet damper. Note, that employing outlet damper into pneumatic system shifts the nominal operating point, what does not allow reaching exactly comparable pneumatic conditions to other flow control techniques. Nevertheless, the energy loss on outlet damper is included in the control efficiency and therefore final comparison is still relevant.

Table 3.5 – Case study 1, Outlet Damper

Outlet Damper	Value – Var. 1,2	Unit
Pressure drop at nominal flow	380	Pa
Nominal operating point		
Nominal flow	94,9	m³/s
Nominal head	3528	m

Hydrodynamic coupling

Hydrodynamic coupling parameters are summarized in the Table 3.6. Efficiency curve is set to linear, which is adequate for simple hydrodynamic coupling used in the industry. However, for precise evaluation, it has to be always used hydrodynamic coupling performance curve generated directly by manufacturer for specific load conditions. It is considered the identical hydrodynamic coupling for both case study variants, which differ just by speed operating range – see Fig. 3.20 and Fig. 3.21.

Table 3.6 – Case study 1, Hydrodynamic coupling

Hydrodynamic coupling	Value – Var. 1,2	Unit
Nominal speed	994	rpm
Nominal efficiency	89,0	%
Auxiliary losses	0	kW
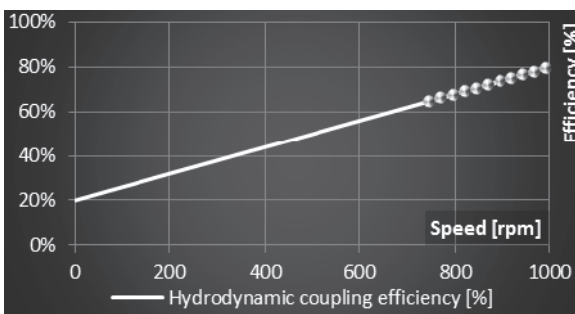
Fig. 3.20 Case study 1 – V1,
Efficiency curve for hydrodynamic coupling
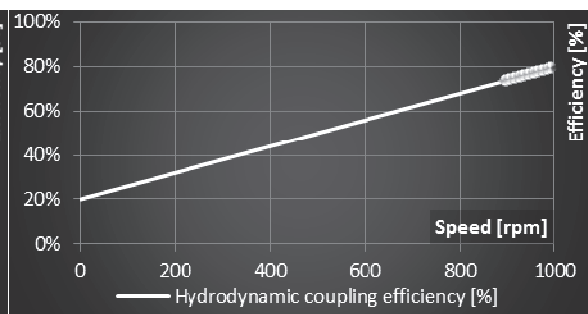
Fig. 3.21 Case study 1 – V2,
Efficiency curve for hydrodynamic coupling

Summary

To be able to compare just pneumatic part including fan and flow control techniques see following figures Fig. 3.22 and Fig. 3.23, which summarizes fan and control efficiency in one figure to see the relative differences without the effect of drive and power supply.
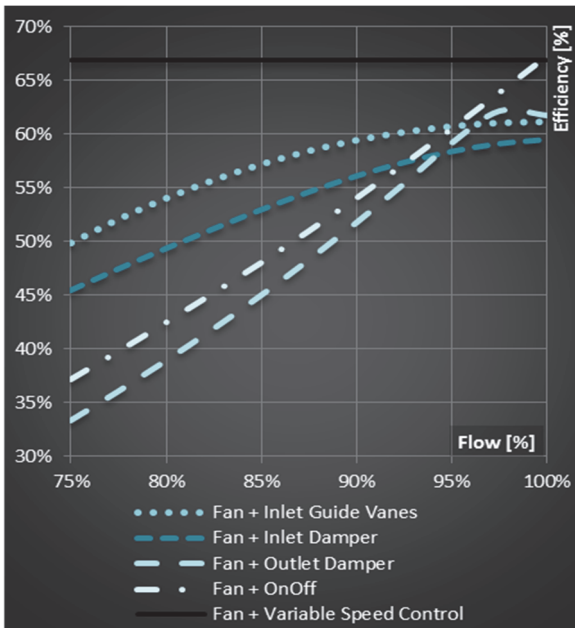
Fig. 3.22 Case study 1 – V1,
Summary of pneumatic system efficiency
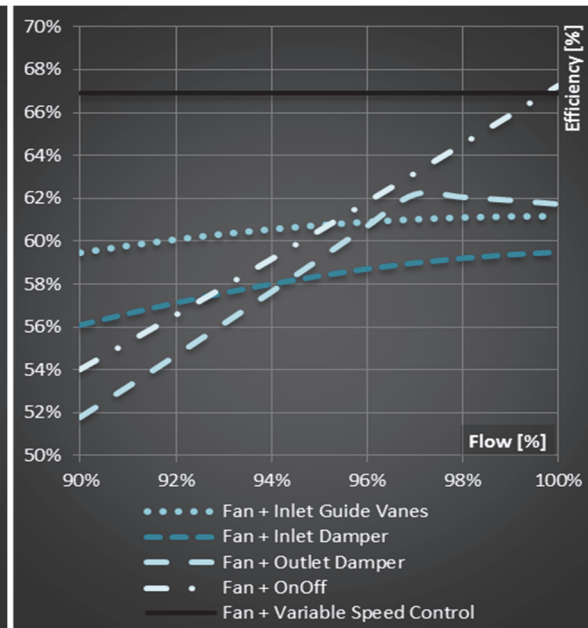
Fig. 3.23 Case study 1 – V2,
Summary of pneumatic system efficiency

3.2.1.4   Electrical motor

Electrical motor for both CFC and VFC is supposed to be identical, specified according to Table 3.7. Note, that the motor is slightly overpowered - for most of flow control methods, it would be sufficient 650 kW electrical motor. Nevertheless, to simplify the case study, single motor covering all possible variants has been selected. There is a neglectable effect in energy consumption due to higher efficiency of 800 kW typical induction machine against 650 kW machine, which compensates the shape of efficiency curve lowering with the power. Naturally, from investment costs point of view, 650 kW machine would be preferred. No gearbox is needed due to fan speed matching the common speed range of induction machines. Electrical motor nominal performance curves and approximated performance curves for VSC are in the Fig. 3.24 and Fig. 3.25 for both variants.

<div align="center">Table 3.7 – Case study 2, Electrical motor</div>

Electrical motor	CFC Value - Var. 1,2	VFC Value - Var. 1,2	Unit
Nominal parameters			
Mechanical power	800	800	kW
Voltage	6 000	6 000	V
Current	96	96	A
Frequency	50	50	Hz
Speed	994	994	rpm
Number of poles	6	6	-
Efficiency	96,90	96,90	%
Power factor	0,830	0,830	-
Apparent power	995	995	kVA
Shaft Torque	7 686	7 686	Nm
Slip	0,0060	0,0060	-
Other			
Auxiliary losses	0	0	kW
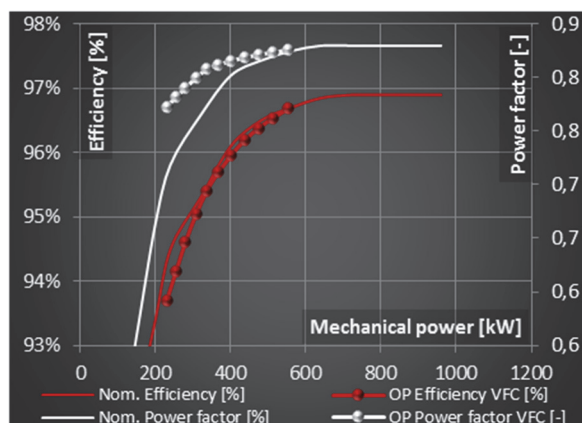
Fig. 3.24 Case study 1 – V1,
Electrical motor performance curves
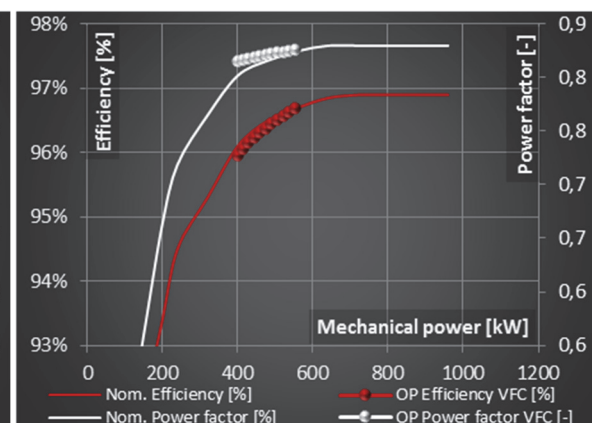
Fig. 3.25 Case study 1 – V2,
Electrical motor performance curves

3.2.1.5   Frequency converter

For the purposes of this case study, frequency converter is considered with a constant efficiency and power factor over the entire operating range, which is sufficient in relation to the total application efficiency. See Table 3.8, Fig. 3.26 and Fig. 3.27 for details. Frequency converter is supplied directly from plant 6 kV distribution network – i.e. no transformer is included.

Table 3.8 – Case study 2, Frequency converter

Frequency converter	Value – Var. 1,2	Unit
Input nominal FC parameters		
Input voltage	6 000	V
Power supply frequency	50	Hz
Efficiency	97,5	%
Nominal power factor	1	-
Apparent power	1 641	kVA
Current	158	A
Output FC parameters		
Nominal continuous apparent power	1 600	kVA
Frequency range	1 – 66	Hz
Other		
Auxiliary losses	0	kW

Fig. 3.26 Case study 1 – V1,
Frequency converter performance curves
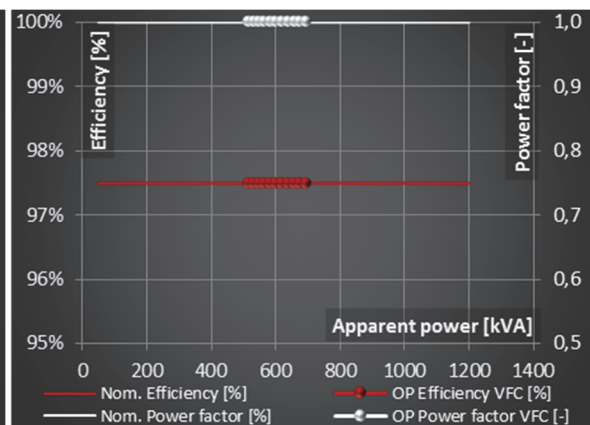
Fig. 3.27 Case study 1 – V2,
Frequency converter performance curves

3.2.1.6 Technical evaluation

This chapter summarizes the results of technical evaluation of both variants of the case study. For each variant of case study, it has been processed evaluation of energy consumption and/or energy savings and total energy efficiency comparison of each flow control technique with variable speed flow control with VSD at each operating point according the operating profile.

Variable speed flow control is clearly the most efficient option in the comparison to other flow control techniques and both case study variants. However, see the comparison of energy savings based on the case study variants and/or weighted flow rates.

Inlet guide vanes is clearly the most efficient passive flow control technique in this case – see Fig. 3.28 and Fig. 3.29. Comparing the both case study variants, reduction of weighted average of flow of 6,21% resulted in reduced saving of VSC about 27,5% from 9,1% to 6,6%.

Inlet damper is the second behind inlet guide vanes from energy consumption point of view – see Fig. 3.30 and Fig. 3.31. Comparing the both case study variants, the reduction of weighted average of flow of 6,21% resulted in reduced savings of VSC about 28,5% from 14% to 10% - i.e. similar to inlet guide vanes.

Considering outlet damper, the energy consumption is highly dependent on the operating flow range and/or weighted average of flow – see Fig. 3.32 and Fig. 3.33. The energy savings difference of VSC between the case study variants is almost 60 % in contrast to difference of weighted average of flow 6,21 %. Hence, employing of outlet damper is usually suitable just for pneumatic systems with low flow rate variations.

The greatest variation of energy savings of VSC between the two variants is notable in comparison of On-Off control – see Fig. 3.34 and Fig. 3.35. The reduction of weighted average flow rate resulted in reduction of relative savings of VSC about 68%. Hence similarly to outlet damper, on-off control is not suitable for applications working within a high operating range. Moreover, the applications have to be flow cycling suitable.

Finally, VSC with hydrodynamic coupling and VSC with frequency converter are to be compared – see Fig. 3.36 and Fig. 3.37. The control efficiency equals one for both variants, hence the energy consumption difference is influenced only by the drive. VSC with frequency converted performed better in both variants, however result is very influenced by HC efficiency curve, which would have to be provided directly by HC manufacturer for reliable conclusion. In this case study, VSC with HC performed even worse than passive flow control using IGV.

Inlet Guide Vanes
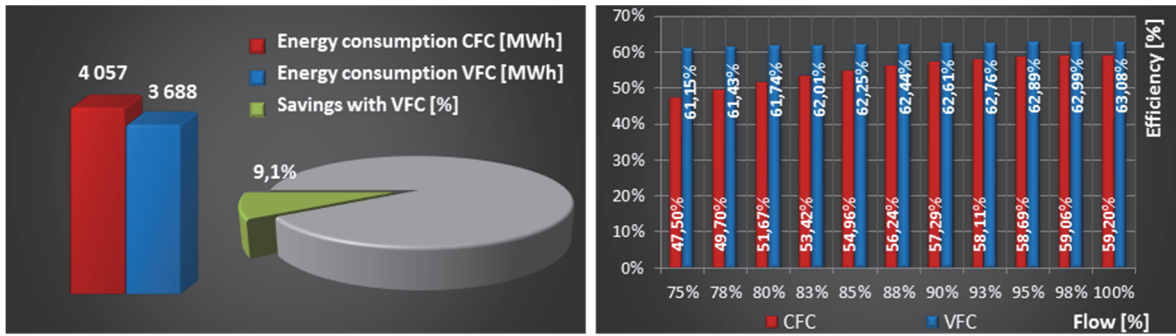
Fig. 3.28 Summary of results – V1 – Inlet Guide Vanes,
Energy consumption and saving potential to VFC – left, Efficiency compared to VFC – right.
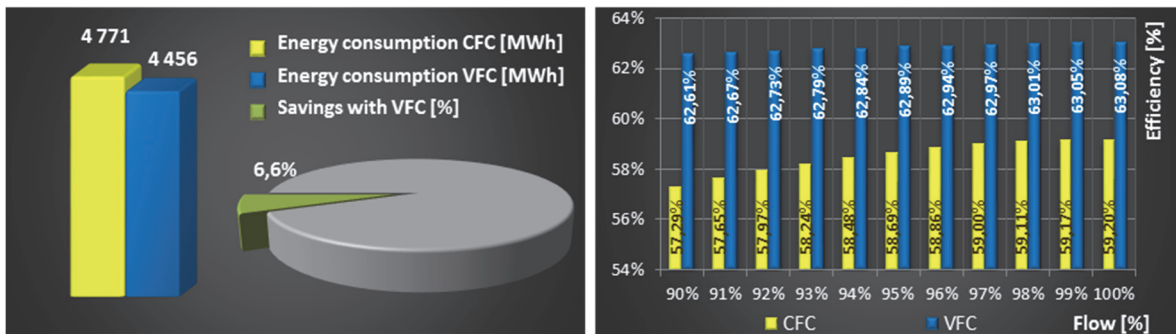
Fig. 3.29 Summary of results – V2 – Inlet Guide Vanes,
Energy consumption and saving potential to VFC – left, Efficiency compared to VFC – right.

Inlet Damper
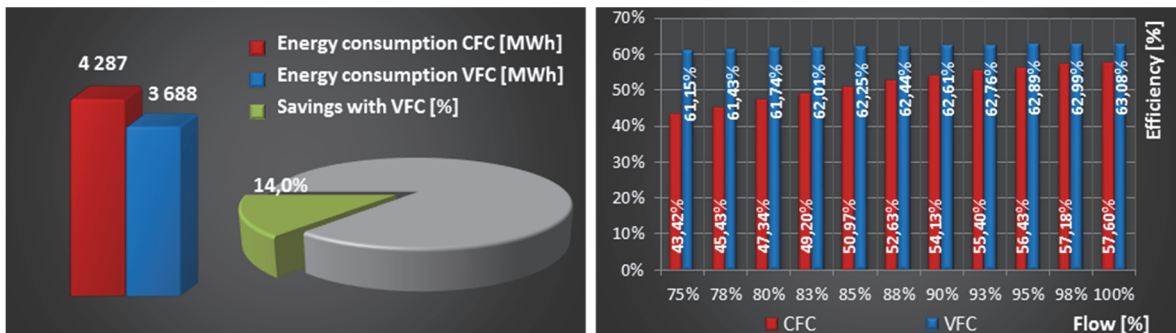
Fig. 3.30 Summary of results – V1 – Inlet Damper,
Energy consumption and saving potential to VFC – left, Efficiency compared to VFC – right.
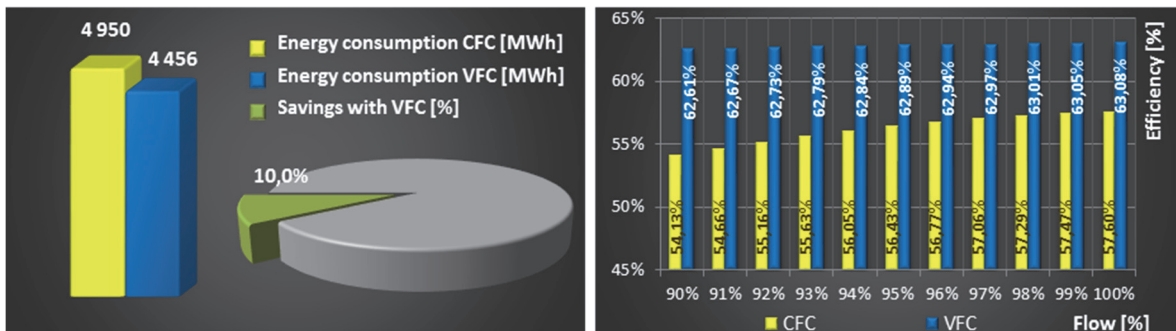
Fig. 3.31 Summary of results – V2 – Inlet Damper,
Energy consumption and saving potential to VFC – left, Efficiency compared to VFC – right.

Outlet Damper
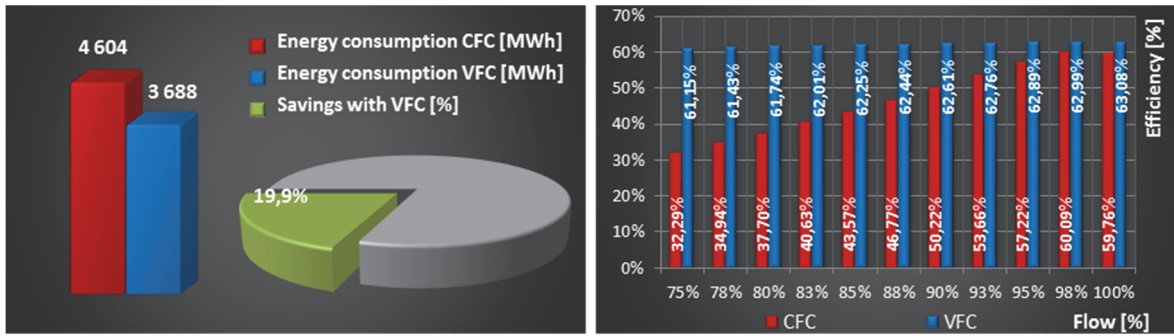
Fig. 3.32 Summary of results – V1 – Outlet Damper,
Energy consumption and saving potential to VFC – left, Efficiency compared to VFC – right.
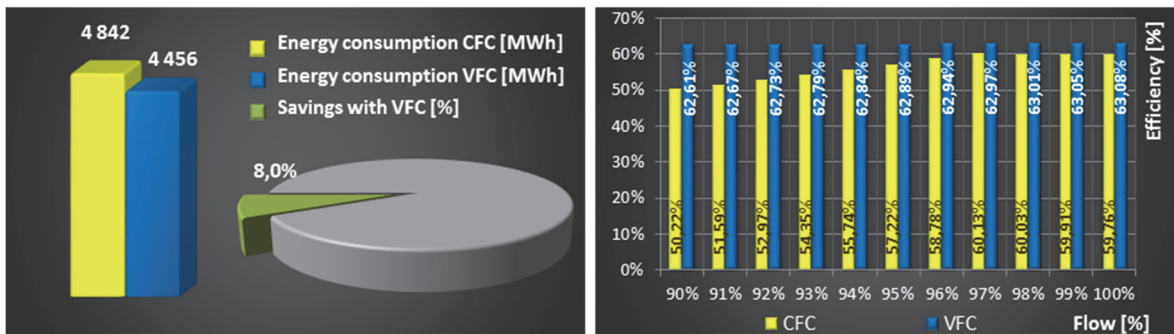
Fig. 3.33 Summary of results – V2 –Outlet Damper,
Energy consumption and saving potential to VFC – left, Efficiency compared to VFC – right.
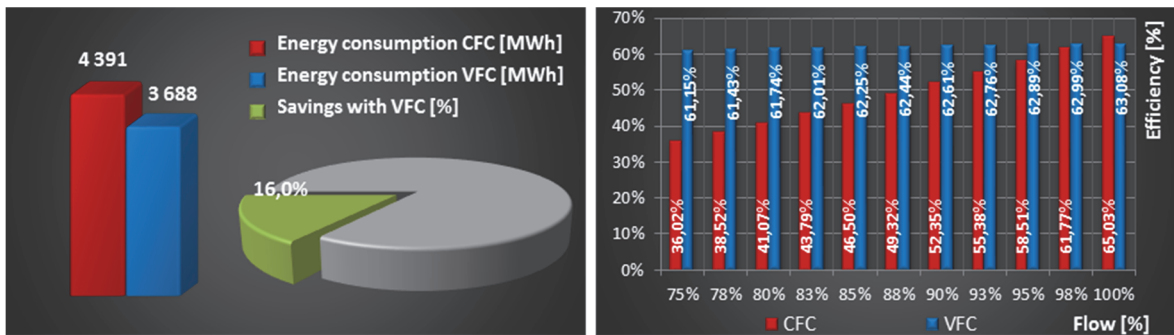
On-Off Control

Fig. 3.34 Summary of results – V1 – On-Off control,
Energy consumption and saving potential to VFC – left, Efficiency compared to VFC – right.
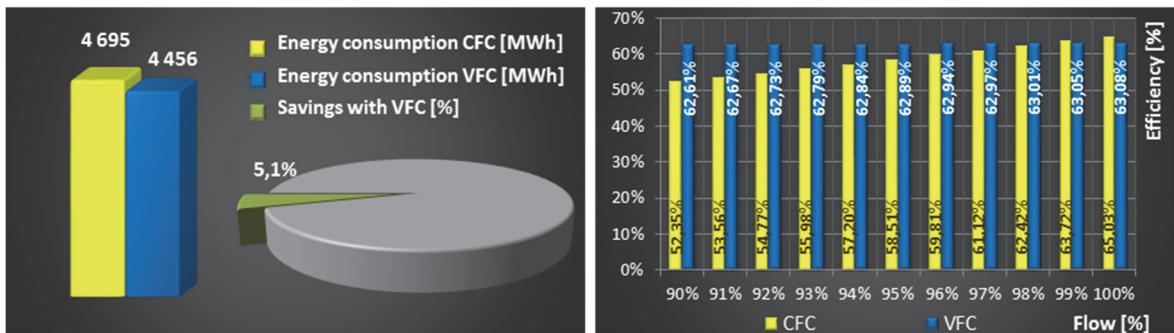
Fig. 3.35 Summary of results – V2 – On-Off control,
Energy consumption and saving potential to VFC – left, Efficiency compared to VFC – right.

Variable speed flow control with Hydrodynamic coupling
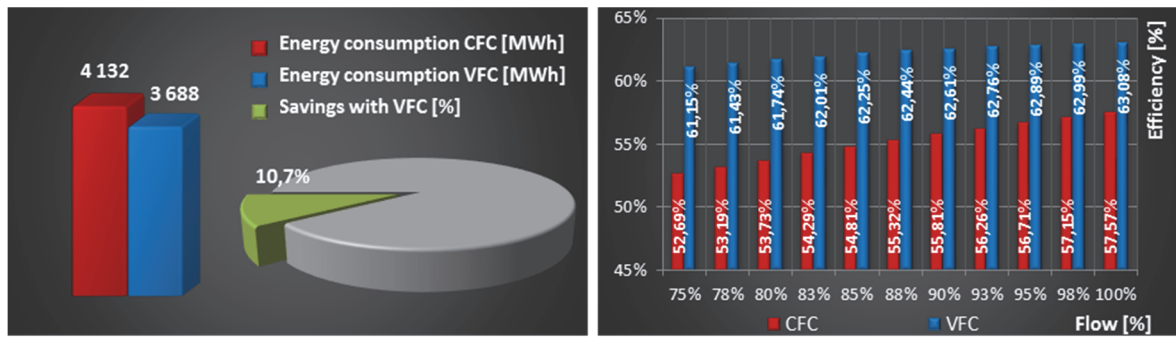
Fig. 3.36 Summary of results – V1 –VSC with HC,
Energy consumption and saving potential to VFC – left, Efficiency compared to VFC – right.
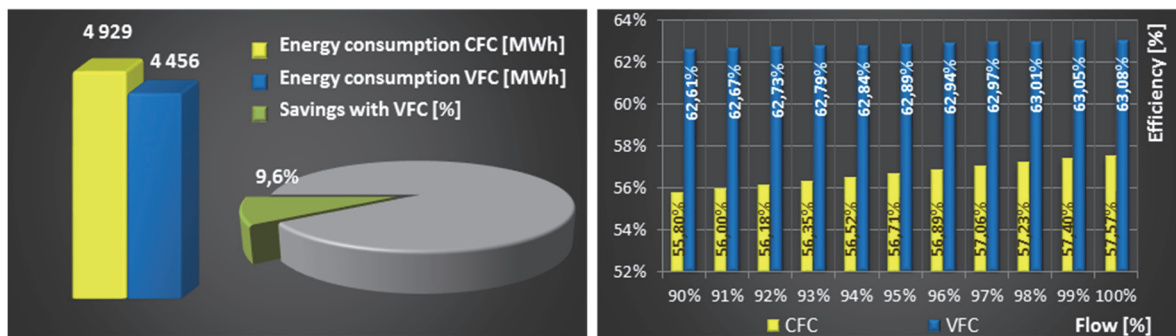
Fig. 3.37 Summary of results – V2 – VSC with HC,
Energy consumption and saving potential to VFC – left, Efficiency compared to VFC – right.

3.2.1.7 Summary

Table 3.9 and Table 3.10 summarize the main technical and economical indicators. The investment costs are commonly the subject of business secret and therefore, could not be included in the calculation. Energy cost, interest rate and service life have been set to constant for both VFC and CFC to present comparison under identical conditions, however especially the service life and additional operating cost may significantly differ and have to be accounted when evaluating commercial case study.

From technical results, it is presented energy consumption and savings of energy and CO_2 of variant with frequency converter (VFC) in comparison to other flow control techniques.

From economical parameters, annual savings and Net Present Value (NPV) of variant with frequency converter against other variants have been calculated. Payback period is zero due to no investment costs included in the submission.

The summary clearly shows the advantage of VSC with FC against all the other options for both the case study variants. It is clearly observable the trend of increasing saving potential of VSC with extending of flow range in relation to passive flow control techniques.

Table 3.9 – Case study 1, Summary V1

	IGV	Inlet Damper	Outlet Damper	On-Off	VSC - HC	VSC - FC	Unit
Economical Data							
Total investment costs	0	0	0	0	0	0	€
Additional operating cost	0	0	0	0	0	0	€/year
Energy cost	0,021	0,021	0,021	0,021	0,021	0,021	€/kWh
Interest rate	5,0	5,0	5,0	5,0	5,0	5,0	%
Service life	15	15	15	15	15	15	years
Technical Results							
Energy consumption	4 057	4 287	4 604	4 391	4 132	3 688	MWh/year
Energy savings with VFC	369	599	916	703	444	-	MWh/year
CO_2 Reduction with VFC	185	300	458	352	222	-	t/year
Economical Results – VFC to CFC							
Annual savings	7,7	12,6	19,2	14,8	9,3	-	x1000 €
Payback period	0	0	0	0	0	-	years
Net Present Value	80	131	200	153	97	-	x1000 €

Table 3.10 – Case study 1, Summary V2

	IGV	Inlet Damper	Outlet Damper	On-Off	VSC - HC	VSC - FC	Unit
Economical Data							
Total investment costs	0	0	0	0	0	0	€
Additional operating cost	0	0	0	0	0	0	€/year
Energy cost	0,021	0,021	0,021	0,021	0,021	0,021	€/kWh
Interest rate	5,0	5,0	5,0	5,0	5,0	5,0	%
Service life	15	15	15	15	15	15	years
Technical Results							
Energy consumption	4 771	4 950	4 842	4 695	4 929	4 456	MWh/year
Energy savings with VFC	315	494	386	239	473	-	MWh/year
CO_2 Reduction with VFC	158	247	193	120	237	-	t/year
Economical Results – VFC to CFC							
Annual savings	6,6	10,4	8,1	5,0	9,9	-	x1000 €
Payback period	0	0	0	0	0	-	years
Net Present Value	69	108	84	52	103	-	x1000 €

3.2.2   Case study 2 - Axial fan

The second case study solves axial-type fan for power plant cooling tower. The methodology of evaluation of conventional flow control techniques (inlet guide vanes, inlet damper, outlet damper and on-off control) for axial fan is identical to radial-type fan and the performance has been already presented in former case study. Therefore, this case study will focus explicitly on presentation of pitch-flow control, which is specific for axial fans.

In the case study, pitch flow control will be evaluated and compared to variable speed flow control, which is the most competing alternative from efficiency and energy demand point of view. The case study is focused specifically to pneumatic part of fan application – the evaluation of drive part has been widely presented in former case studies. The electrical motor is considered identical for both pitch and variable speed flow control variants.

3.2.2.1   *Pneumatic system & Operating profile*

The case study pneumatic system parameters are summarized in the Table 3.11. For operating profile see Fig. 3.38.

Table 3.11 – Case study 2, Pneumatic system

Pneumatic system	Value	Unit
Pneumatic system		
Nominal flow	480	m^3/s
Nominal total head	150	Pa
Nominal dynamic head	150	Pa
Nominal static head	0	Pa
Static / referenced head control	constant	
Gas density	1,150	kg/m^3
System operating data		
Annual running time	8590	h
Flow operating range	70 - 100	%
Weighted average of flow	88,73	%
Weighted average of pneumatic system power	71,25	%
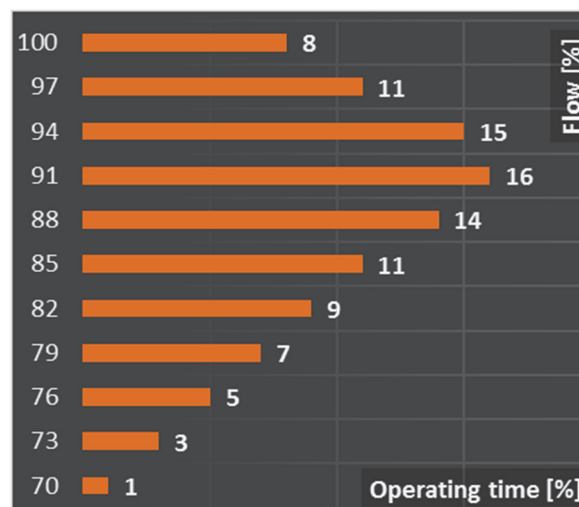
Fig. 3.38 Case study 2,
Operating profile

3.2.2.2   Fan

It is employed axial fan with nominal parameters according to Table 3.12. Fan pressure-flow and efficiency-flow performance curves approximated for variable speed within the operating range are presented in Fig. 3.39 and Fig. 3.40. Fan and pneumatic system nominal operating points are identical in this case.

Table 3.12 – Case study 2, Fan

Fan	Value – Var. 1,2	Unit
Fan		
Nominal speed	176	rpm
Flow operating range at nominal speed	336 – 600	m³/s
Fan Nominal Operating Point		
Flow	480	m³/s
Pressure	150	Pa
Efficiency	83,0	%
Pneumatic power	72	kW
Mechanical / shaft power	87	kW
Torque	4 707	Nm
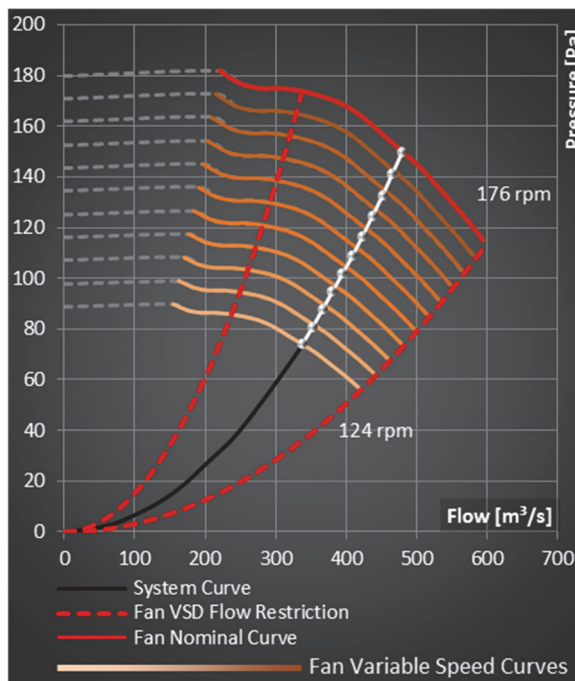
Fig. 3.39 Case study 2,
Fan & Pneumatic system curves
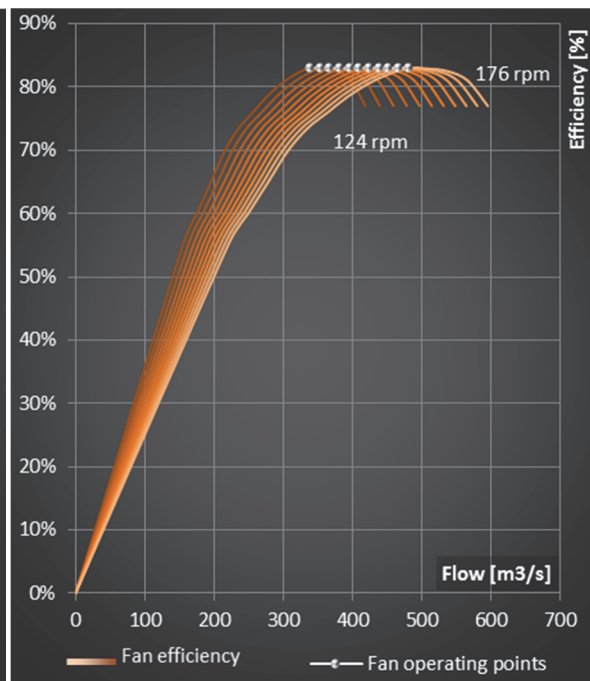
Fig. 3.40 Case study 2,
Fan VSC efficiency curves

3.2.2.3   Flow control

Approximated efficiency surface for pitch-controlled fan is presented in the Fig. 3.41. The white path marks the efficiency for the pneumatic system obtained as a two dimensional interpolation of fan efficiency space by pneumatic system curve. Nevertheless, it has been used efficiency curve generated directly from fan datasheet for the system curve and/or flow and pressure. The difference between automatically generated efficiency curve, based just on a nominal efficiency value, and real efficiency curve from fan datasheet is noticeable in the Fig. 3.43 – white and grey curves. See also in detail the efficiency progress for variable speed and pitch control compared to fan efficiency at fan nominal speed, which is often incorrectly used. In the Fig. 3.42, see the efficiency comparison of the pneumatic part for the all-possible flow control techniques. The variable speed control provide the best results considering just the pneumatic part, however pitch control stays in the worst case just 3% behind. The pneumatic efficiency of other flow control techniques – inlet guide vanes, inlet damper, outlet damper and on-off control is about 10 % lower at nominal operating point and steeple decreases with the flow. Outlet damper would be the worst choice in this case.
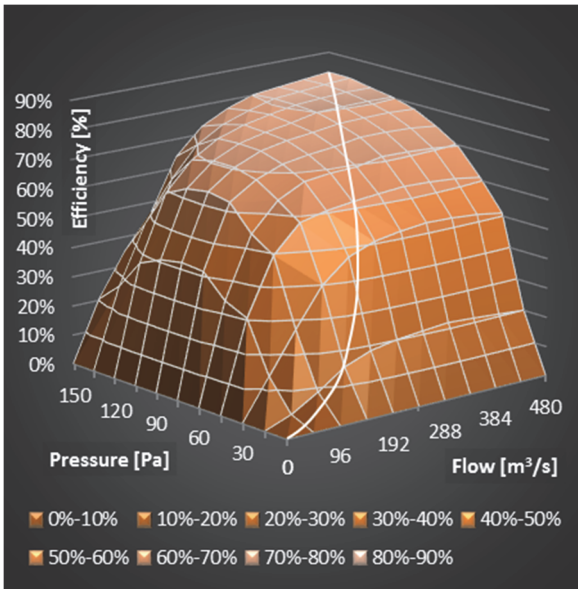
Fig. 3.41 Case study 2,
Fan efficiency for pitch control
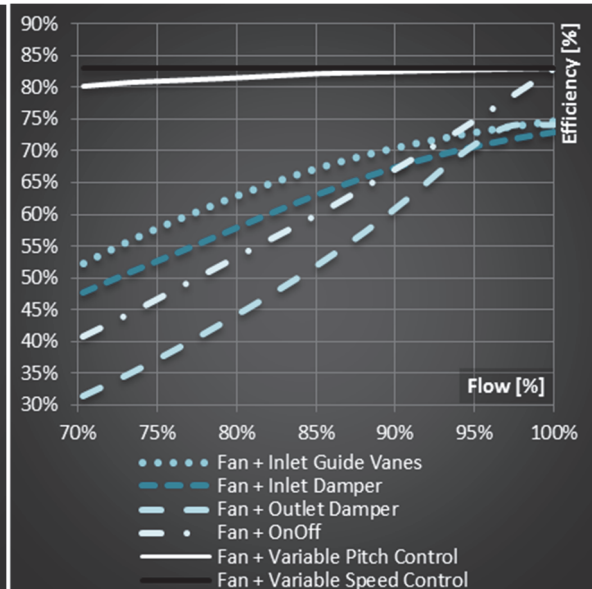
Fig. 3.42 Case study 2,
Efficiency comparison of fan & controls
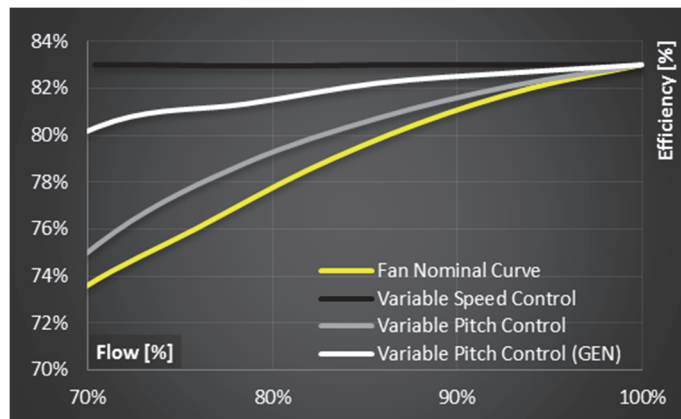
Fig. 3.43 Fan nominal efficiency curve versus efficiency for
variable speed and pitch controlled fan.

3.2.2.4   Technical evaluation

Below, it is summarized the results of technical evaluation of both variable speed and pitch controlled variant for the case study. In Fig. 3.44 top, see the comparison of total energy consumption and energy efficiency for Pitch control versus VSC, below see in detail efficiency chain breakup for pitch control variant. In detailed breakup for VSC is available in Fig. 3.45.
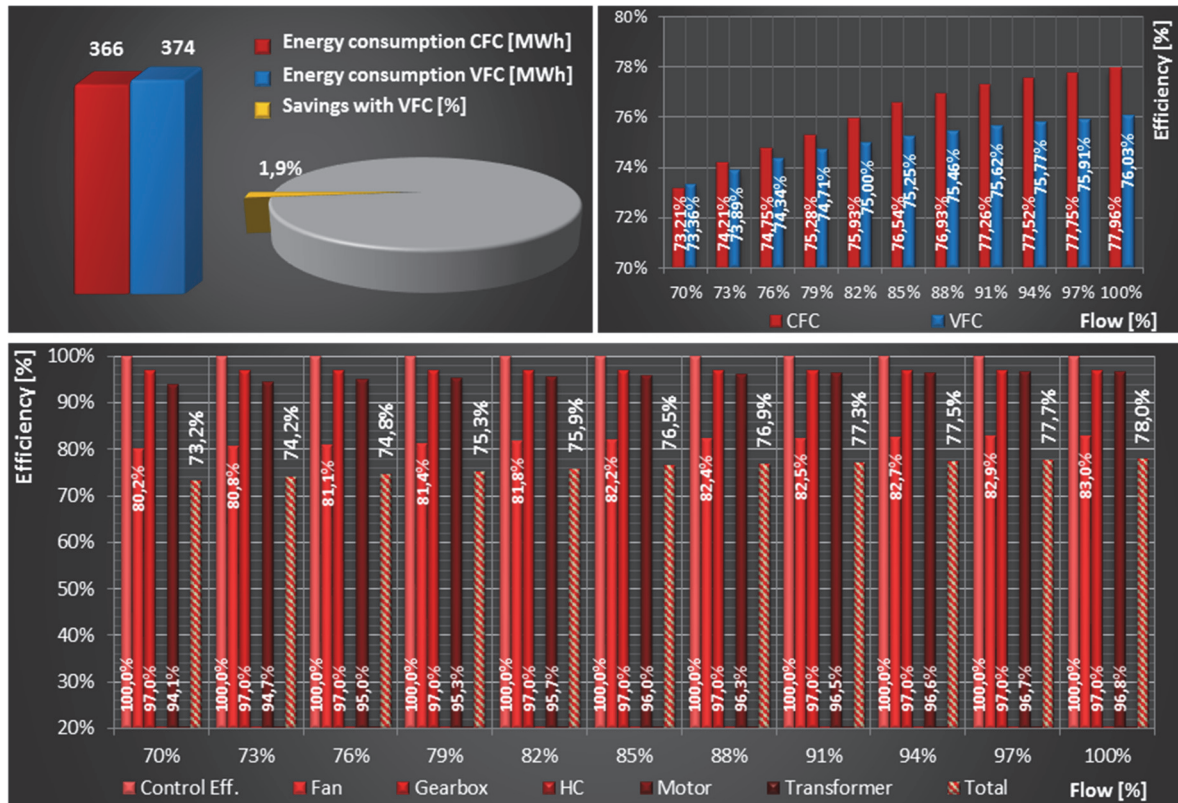
Fig. 3.44 Summary of results - Pitch Control versus Variable Speed Control,
Energy consumption and saving potential to VFC – top left, Efficiency compared to VFC – top right,
Efficiency chain breakup for Pitch Control – down.
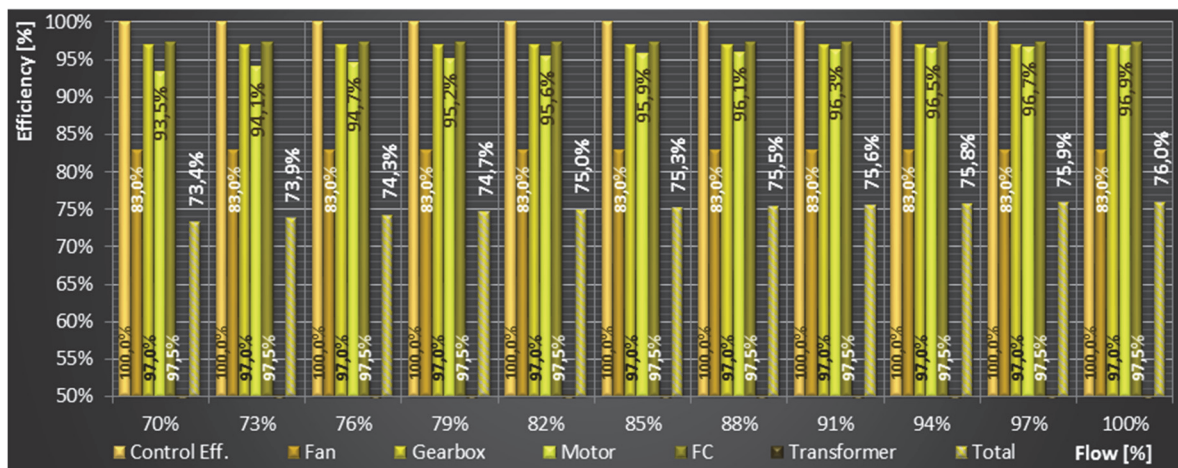
Fig. 3.45 Summary of results, Efficiency chain break up for VSC

The results confirm the almost equal performance at high flow rates. Although the pure pneumatic efficiency is higher over the whole operating range (see Fig. 3.43) the final VSC efficiency of the whole drive chain is lower than by pitch-controlled fan. The lower efficiency is given especially by lower

variable speed controlled electrical motor and additional losses in frequency converter – see Fig. 3.44, bottom. The efficiency tipping point is at the 70% of flow where VSC becomes more efficient.

3.2.2.5 Summary

Main technical and economical indicators are summarized in the Table 3.13. The investment costs are commonly the subject of a business secret and therefore, could not be included in the calculation. Energy cost, interest rate and service life have been set to constant in both cases to present comparison under identical conditions, however especially the service life and additional operating cost may significantly differ and has to be accounted when evaluating a commercial case study.

From technical results, it is presented energy consumption and savings of energy and CO_2. From economical parameters, annual savings and Net Present Value (NPV) of variant with frequency converter against pitch controlled variant have been calculated. Payback period is zero due to no investment costs included in the submission.

The summary shows the tiny advantage for pitch controlled variant in this case, considering energy consumption and/or savings. The investment costs are supposed to be lower as well. Nevertheless, the result is valid specifically for this case – mainly due to high weighted flow rate at almost 90% of nominal flow.

Table 3.13 – Case study 2, Summary

		Pitch control	VSC - FC	Unit
Economical Data				
Total investment costs		0	0	€
Additional operating cost		0	0	€/year
Energy cost		0,021	0,021	€/kWh
Interest rate		5,0	5,0	%
Service life		15	15	years
Technical Results				
Energy consumption		366	374	MWh/year
Energy savings with VFC		-	- 8	MWh/year
CO_2 Reduction with VFC		-	- 4	t/year
Economical Results – VSC to Pitch Control				
Annual savings		0,2	-	x1000 €
Payback period		0	-	years
Net Present Value		1,6	-	x1000 €

3.3   Conclusion for single fan applications

In the part of single fan applications, it has been systematically presented the way of evaluation of the pneumatic part of fan applications. It has been in detailed described developed methodology and mathematical models of pneumatic system and fan considering compressible medium. The most common fan flow control techniques have been also included, to be able to compare them among each other on a particular application – namely: flow control by inlet guide vanes, inlet damper, outlet damper, on-off control and variable flow speed control employed for both axial and radial type of fans. Furthermore, methodology for pitch-controlled axial fan has been also presented. All the mathematical models have been expressed due to non-linear character in a numerical form suitable for direct software implementation.

One of the main difficulties - while evaluating and compare flow control techniques in real case studies - is the lack of publicly available complex set of data and/or performance curves for fans and flow control techniques. Hence, the necessary typical performance curves of fans and control techniques obtained from credible sources and/or manufacturers has been included as a referenced ones to provide the complex set of relevant data in case evaluation of poorly defined case studies.

Finally, the presented mathematical models and methodology have been implemented in the sophisticated software tool Medium-Voltage Drive Fan Save 2012. The tool has been developed to provide a support in evaluation process of the high-power - especially industrial - fan applications in the future and to verify the performance of mathematical models and methodology behind the tool on real case studies. The first case study is focused on presentation of radial-type fan and related common flow control techniques on a gas recirculation application in thermal power plant. The second case study was evaluated to present specifically the performance of axial pitch-controlled and variable speed controlled fan used in power plant cooling towers. The attention while presenting the case studies has been put mainly to proper specification and presentation of pneumatic part and total comparison of flow control techniques and its technical and economical indicators, while the methodology and mathematical models of drive part has been widely presented in the former section of single pump application.

4   Multiple pump applications with parallel control

This chapter focuses specifically to optimization of control of a group of variable speed controlled pumps working in parallel into common hydraulic system. The optimization commonly used is based on just empiric knowledge in combination with check measurements due to complexity of evaluation of optimal operation arising from solution of optimization task of highly nonlinear and multidimensional systems. Recently, there have been published several optimization approaches converting the task into mixed integer nonlinear programming problem ([34], [35]) or using dynamic programing [36]. The advantage of these approaches is especially the "real-time" character. However, the pump performance curves have to be converted into analytical representation which can lead – depending on the shape of the real pump curves - to significant total energy consumption prediction error, especially in high-power pump applications that are the target ones. The tiny error in control efficiency estimation in these applications can lead to substantial energy losses over the pumps lifetime.

In this chapter, it is presented a solution of the optimization task based on the numerical optimization method using recursive brute force approach to provide solution taking into account real pump performance curves and precise-enough solution for a general case. Special attention has been then paid to the case of group of pumps consisting from subgroups of identical pumps, which is the very often case in parallel pump applications.

In the first part, it is described the developed algorithm for calculation of optimal and/or most efficient flow distribution among pumps for general hydraulic system operating point and number of pumps. Then it is presented a performance of the algorithm on case studies based on real applications that have been solved using this algorithm. Sensitivity analysis of system static head on optimal operating profile has been done as well to present the influence of system static head on optimal control for a special case of identical pumps, which is often met in practice. The algorithm has been implemented in the Mathworks Matlab R2012b that has been used to evaluate the presented case study results.

4.1   Optimal control algorithm

The objective of the algorithm for optimal control is to find the optimal operating profile – the function of a single pump flow on total hydraulic system flow - for each pump in a group - which will ensure maximal total efficiency and/or minimal possible power consumption of the group of pumps for any hydraulic system operating point. To provide a clear idea about the purpose of the algorithm, expected results and developed methodology at the beginning of the description, following simple two pump case study results are included as an illustrative example (Fig. 4.1).

The algorithm is based on a brute-force exploring of the entire operating space. In the first phase, all operating states and/or flow vectors are generated (Fig. 4.1 A,B – white points). The number of operating points and/or combinations increases exponentially with the number of pumps – as the space dimension order equals to number of pumps order. In the second phase, obtained data are analyzed to search an optimal control path based on set of weight criterions – see the resulting path in Fig. 4.1 A,B (the black part indicates the operating range, the grey-dashed part indicates the connection of non-continuous sections).

A

Diagram of optimal flow distribution

B

Diagram of optimal flow distribution

C

D
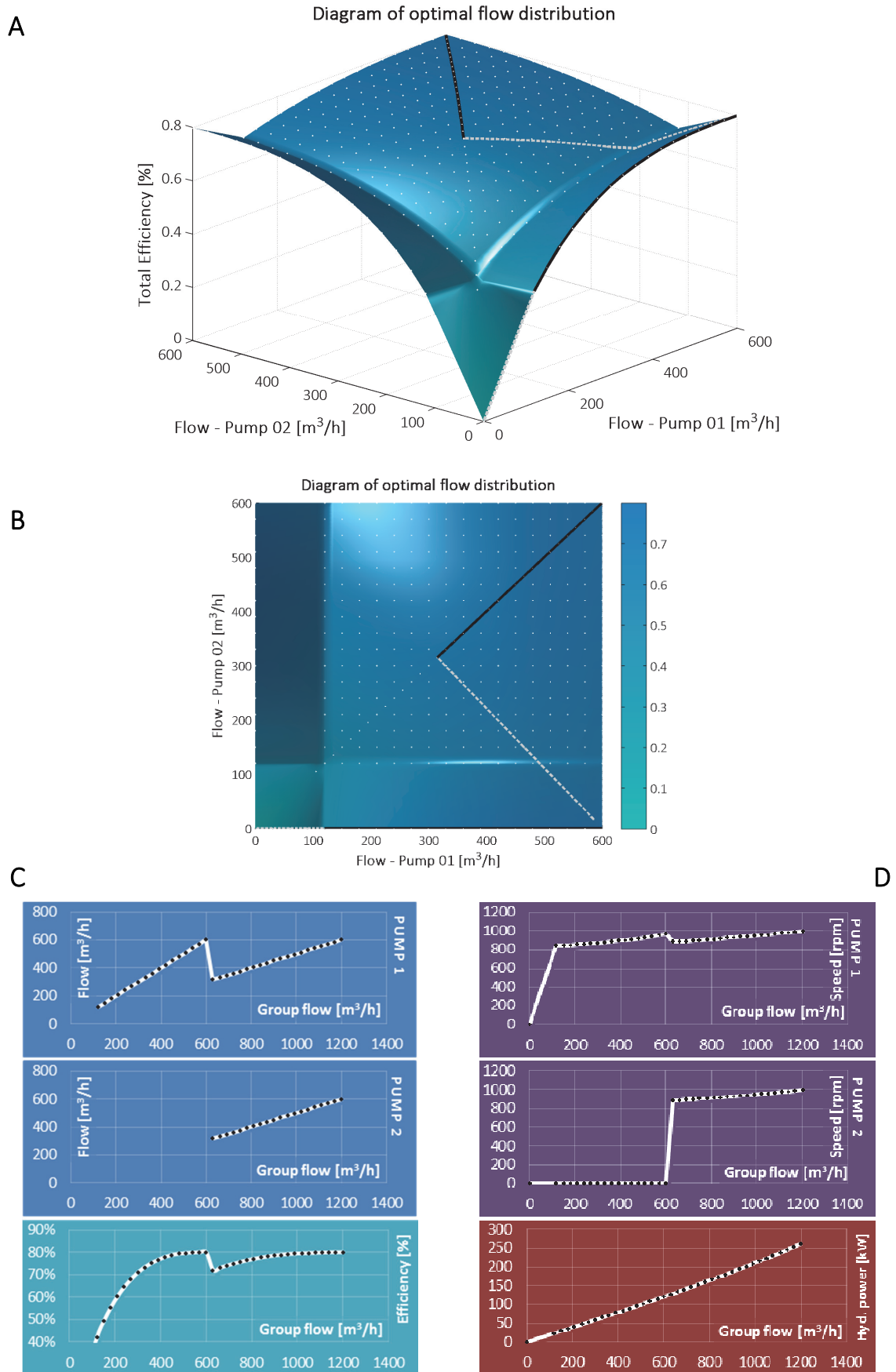
Fig. 4.1 Illustrative sample of a simple case study with 2 identical pumps, (Hn = 80m, Hst = 72m)
3D view on operating space (A), 2D projection of operating space (B), pump flow diagrams and to-
tal/group efficiency (C), pump speed diagrams and total hydraulic power (D)

Based on the optimal control path, final operating flow and speed diagrams in relation to total hydraulic system flow are generated (Fig. 4.1 C,D) including additional performance characteristics – e.g. total efficiency and total hydraulic power.

The overview flow chart diagram of the algorithm is presented in the Fig. 4.2, a detailed description is given below.

4.1.1   Flow chart diagram

4.1.1.1   The main block

The main block is used as a container including functions for processing of input data and/or parameters, launching of core of the algorithm and for processing of returned results.

Following input parameters are considered for the calculation:

- Hydraulic system
    - Static head [m]
    - Nominal head [m]
    - Nominal total flow [m^3/h]
- Pump
    - Number of pumps in parallel
    - Pump Q-H performance curves for each pump
    - Pump Q-η performance curves for each pump
    - Operating range and/or minimal flow restriction for each pump
- Calculation
    - Resolution and/or flow discretization step [m^3/h]

Pump performance curves are sampled in a custom resolution, cubic interpolation is then employed for data processing.

Calculation of flow state vectors is processed via function *getFlowStates* and its child functions, which are described later. The returned result represent the entire flow state space including other derived state parameters and/or variables for each flow state vector – total flow, total head, total efficiency and partial flow, speed and efficiency of each pump.

To get the optimal control way and/or the optimal flow and speed operating diagrams – the flow state vector with highest total efficiency in relation to total flow is selected from the flow state space for each unique total flow via sorting and filtering according to following criteria:

A. Sorting (according to priority)
    1. Total flow (from low to high)
    2. Total efficiency (from high to low)
    3. Flow states with flow distribution ratio equal to nominal flow ratio
    4. Number of active pumps (high to low)
    5. Pump partial flow (Pump 1, Pump 2, …, number of pumps)
B. Filtering (filtering of the first unique value of each total flow operating state – the first unique flow state matches best the above sorting criteria)

Multiple pump applications with parallel control
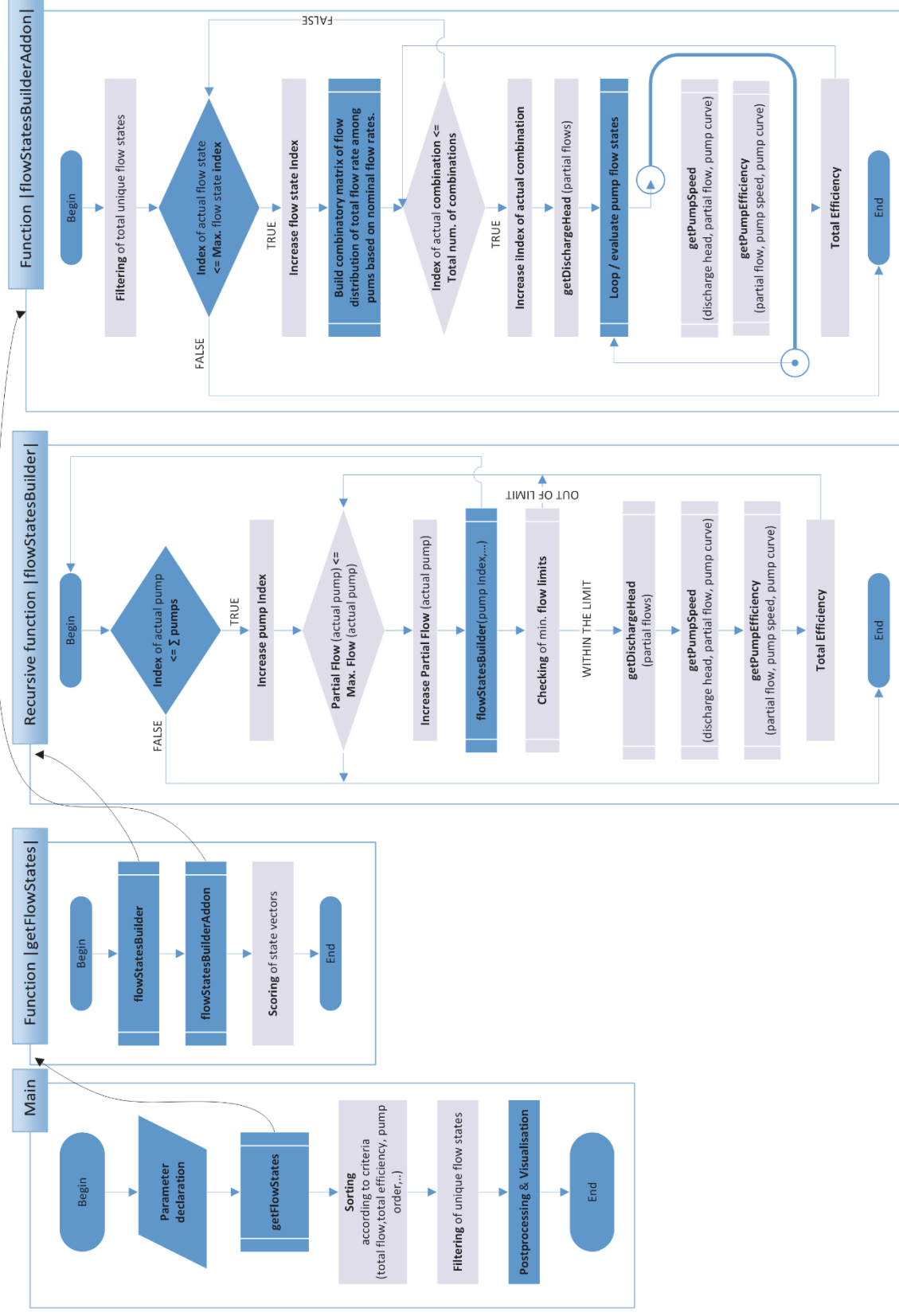
Fig. 4.2 Overview flow chart of algorithm for calculation of optimal control of parallel group of pumps

The resulted optimal control path and/or flow vectors are considered as ideal ones in the discretized space – in this form can be directly interpreted and visualized, however for a final implementation further post processing is needed. The post processing is not a part of this work, due to specific approach based on a concrete applications, however following procedures have to be done:

1. The optimal control path is usually divided by several discontinuities, which would case hazard state for the pumps. This can be solved by employing hysteresis and/or by generating two operating profiles for the direction up and down.

2. The result is generated in discrete form. For a simple applications or applications with restricted space of freedom, linear approximation of obtained results is usually sufficient. Nevertheless for complex applications more sophisticated multidimensional curve fitting methodology is usually required. The alternative to curve fitting process is to refine the flow state grid and use linear multidimensional interpolation, however, this can be especially for more than 4-pump applications very computer-power demanding due to exponential character of calculation power demand.

4.1.1.2   Exploring of a flow state space

To explore a general n-dimensional space a recursive function approach has been used in the algorithm. The building of the flow state space is covered via function *getFlowStates* in the Fig. 4.2. The function initializes and runs the recursive function *flowStatesBuilder,* which generates the flow state space and related flow states characteristics and function *flowStatesBuilderAddon,* which refine the flow state grid for a special cases.

The recursive function *flowStatesBuilder* is the core function generating the *n*-dimensional flow state space of all combination or variations (order dependent) of partial flow states including calculation of state characteristics of pumps and/or hydraulic system at each flow state. The *n* represents the number of parallel pumps in the group working into common hydraulic system. Total number of variations is dependent upon the calculation step and nominal flow rate of pumps – see (4.1).

The following quantities are calculated for each flow state vector:

1. Total flow rate and partial flow rate for each pump
2. Total discharge head and/or system head
3. Speed rate for each pump
4. Efficiency for each pump
5. Total efficiency of the pump group

Total flow rate is expressed in (4.2), hydraulic system total head and/or pump group total discharge head in (4.3). Common hydraulic system is considered – i.e. pumps in the group are linked via the outlet and/or system pressure that is common for the whole group. Single pump speed and efficiency is then in (4.4) and (4.5). Total efficiency for a group of pumps is then expressed in (4.6). Following minimal flow condition has to be fulfilled to ensure operation within pump operating range

- see (4.7). For in detailed derivation of hydraulic system curve and model of single pump for variable speed control see chapters 2.1.1 and 2.1.2.

$$n_{\text{var}} = \prod_{i=1}^{n_{Pumps}} \frac{Q_{P_N - i}}{Q_{cStep}} \tag{4.1}$$

$$Q_{PT-j} = \sum_{i=1}^{n_{Pumps}} Q_{Pi-j} \text{; j...group state; i...single pump state} \tag{4.2}$$

$$H_{ST-j} = H_{STs_N} + H_{STd_N} \times \frac{Q_{PT-j}}{Q_{ST_N}} \text{; j...group state; i...single pump state} \tag{4.3}$$

$$\mathbf{H}_{AuxC} = H_{Pi-j}.\times \left(\mathbf{Q}_{Pi_{N-curve}}./Q_{Pi-j} \right)^{.2} \tag{4.4}$$

$$\mathbf{Q}_{AuxC} = \mathbf{Q}_{Pi_{N-curve}}$$

$$\left[Q_{PeqNi-j}, H_{PeqNi-j} \right] = f_{IntersetLinIntArray} \left(\mathbf{Q}_{Pi_{N-curve}}, H_{Pi_{N-curve}}, \mathbf{Q}_{AuxC}, \mathbf{H}_{AuxC} \right)$$

$$n_{Pi-j} = n_{P_N i} \times \sqrt{\frac{H_{Pi-j}}{H_{PeqNi-j}}}$$

j...group state; i...single pump state

$$\eta_{Pi-j} = f_{IntCubArray} \left(\mathbf{Q}_{Pi_{N-curve}}, \boldsymbol{\eta}_{Pi_{N-curve}}, Q_{Pi-j} \times \frac{n_{Pi_N}}{n_{Pi-j}} \right) \text{; j...group state; i...single pump state} \tag{4.5}$$

$$P_{hT-j}[\text{kW}] = \frac{\sum_{i=1}^{n_{Pumps}} Q_{Pi-j}[m^3/\text{h}] \times H_{S-j}[m] \times \rho[kg/m^3] \times g[m/s^2]}{1000} \tag{4.6}$$

$$P_{cT-j}[\text{kW}] = \sum_{i=1}^{n_{Pumps}} \frac{Q_{Pi-j}[m^3/\text{h}] \times H_{S-j}[m] \times \rho[kg/m^3] \times g[m/s^2]}{\eta_{Pi-j}[-]}$$

$$\eta_{T-j} = \frac{P_{hT}}{P_{cT}} = \frac{\sum_{i=1}^{n_{Pumps}} Q_{Pi-j}}{\sum_{i=1}^{n_{Pumps}} \frac{Q_{Pi-j}}{\eta_{Pi-j}}}$$

j...group state; i...single pump state

$$Q_{Pi-j} \geq Q_{Pmin-i-j} \tag{4.7}$$

$$Q_{Pmin-i-j} = Q_{Pi-min_N} \times \frac{n_{Pi-j}}{n_{Pi_N}}$$

j...group state; i...single pump state

Function *flowStatesBuilderAddon* in the Fig. 4.2 refine the basic flow state grid about additional flow state vectors obtained according to (4.8). Within the testing of the basic algorithm, it has been observed that for identical pumps with the typical centrifugal pump flow-efficiency curves, the optimal flow distribution is determined exactly by the ratio of pump nominal flow rates. Hence, adding the specific flow vectors into the basic flow state space smooth the optimal operating diagrams with no

necessity of decreasing calculation discretization step. The number of variations of flow distribution for one flow state vector is expressed in (4.9). The total number of additional flow state vectors is then in (4.10). Nevertheless, it must be emphasized, that the positive effect is observable just in the pump applications consisting of identical pumps and/or pump subgroups – which is however a very often case. Alternatively, it can be observed also for pumps differently sized however with proportionally shaped pump-flow efficiency curves in flow-axis direction - but this is only a theoretical case – see chapter 4.2.2.4.

The characteristic quantities for additional flow states are evaluated in the same way like in the function *flowStatesBuilder.*

$$Q_{Pi_a-j} = \frac{\sum_{i_a=1}^{n_{aPumps-j}} Q_{Pi_a-j}}{\sum_{i_a=1}^{n_{aPumps-j}} Q_{P_N-i_a}} \times Q_{P_N-i_a}; \quad \sum_{i_a=1}^{n_{aPumps-j}} Q_{Pi_a-j} = Q_{T-j} \tag{4.8}$$

j...group state; i_a ... active single pump

$$n_{var-j} = \overline{V}^2_{n_{Pumps}} - 1 = 2^{n_{Pumps}} - 1 \tag{4.9}$$

j...group state

$$n_{var} = \frac{\sum_{i=1}^{n_{Pumps}} Q_{P_N-i}}{Q_{cStep}} \times n_{var-j} \tag{4.10}$$

4.2   Algorithm verification - Case studies

In this chapter, it is presented the performance of designed algorithm of optimal distribution of hydraulic system total flow among pumps in a group. To present the results in a clear way, two case studies have been evaluated. The first – basic one – consists of a group of just two pumps that enable to present the operating space and optimal control path in an easy to imagine way in the form of 3D figures. The second case study solves then a more complex application consisting of a group of four pumps. Both presented case studies are based on a real application, which has been solved using this algorithm. However, to show the performance under conditions that are more complex and to show several remarkable tendencies, which can be observed and/or generalized for similar applications, additional derived variants of case studies have been evaluated.

4.2.1   Case study 1 – Two pump application

4.2.1.1   Specification

It is considered a two-pump application working in parallel into common hydraulic system. It has been elaborated three variants of the application differing by particular changes in the configuration to be able to make relevant comparison among each other. The specification of hydraulic system and pump group parameters and configurations is summarized in the Table 4.1. In the Fig. 4.3, see the default pump performance characteristics expressed in per unit values that have been used for pump modelling.

The first variant presents the influence of a ratio of hydraulic system static and dynamic head on a variable speed controlled group of pumps. Pumps are considered identical. The second variant presents the effect of variable sizing of pump in the group considering identical and/or similar efficiency curves. The last variant then present the effect of both variable sizing of pumps in the group including variable efficiency curves, which is the most probable case.

Table 4.1 – Case study 1, Specification of hydraulic system & pumps

Hydraulic system	Var. 1	Var. 2	Var. 3	Unit
Hydraulic system				
Nominal flow	1200	1200	1200	m³/h
Nominal total head	80	80	80	m
Nominal dynamic head	[72, 8]	[72, 8]	[72, 8]	m
Nominal static head	[8, 72]	[8, 72]	[8, 72]	m
Static / referenced head control	constant	constant	constant	
Pumps				
Number of pumps in parallel	2	2	2	
Identical pumps	yes	no	no	
Nominal total head	80	[80, 80]	[80, 80]	m
Nominal flow	600	[600, 800]	[600, 800]	m³/h
Nominal efficiency	80	[80, 80]	[68, 84]	%
Nominal speed minimal flow	120	[80, 160]	[80, 160]	m³/h
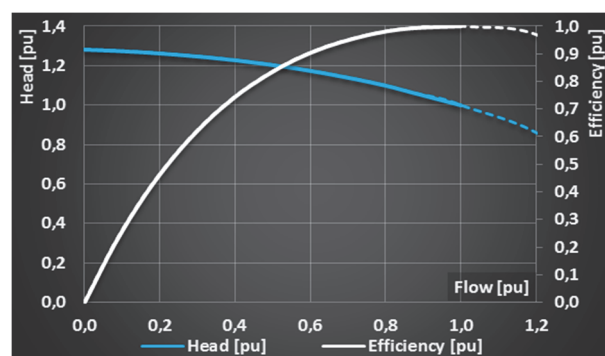
Fig. 4.3 Referenced pump performance curves in per-unit expression

4.2.1.2   Results

The first case presents especially the influence of the ratio of hydraulic system static and dynamic head on the optimal control. The results of the first case study variant are summarized in the Fig. 4.4 and Fig. 4.5. See the symmetrical operating space determined by the employment of identical pumps and compare especially the shift of switching point in the flow diagrams and the total efficiency curve. It is notable, that the switching point is shifting with increasing ratio of static head, what changes the operation character from purely parallel operation in hydraulic system with zero static head to parallel cascade in hydraulic system with high ratio of static head. Similar tendency is confirmed also later on the static head sensitivity analysis in the second case study of four-pump application – chapter 4.2.2.3. The total efficiency curve is notable smoother in the first variant, which is given by the employment of variable speed control, and high-speed operating range in hydraulic systems with a low static head.

The second variant solves the identical hydraulic system with a different composition of pump sizes of 400 m^3/h and 800 m^3/h instead of two identical pumps of 600 m^3/h of nominal flow. See results in the Fig. 4.6 and Fig. 4.7 for low and high ratio of hydraulic system static head. Comparing the first sub variant (Fig. 4.6) with a low static head former variant (Fig. 4.4), no significant improvement in the total efficiency curve is mark able, beside the little higher efficiency at very low flows, which are usually out of the common operating range. Comparing the second sub variant solving the high-static head hydraulic system (Fig. 4.7), decomposition to variable sizes improved the efficiency progress both in the low and middle flow range in comparison to Fig. 4.5. See that in spite of different pump sizing, the best efficiency area lies on the diagonal of pump flow axis for the ranges of parallel operation – this confirms the assumption according to (4.8). Nevertheless, the both pumps are supposed to have ideal, identically and/or similarly shaped efficiency curves in relation to pump nominal flow.

The third variant reflects the same hydraulic system taking into account also the real efficiencies of pumps. See that the optimal operating path is not on the diagonal of flows and both flow operating diagrams and total efficiency curves are more complex in both sub variants compared to former ones - see Fig. 4.8 and Fig. 4.9. This confirms the necessity of proper evaluation of each individual case study taking into account the real pump performance curves to ensure the most efficient operation in the entire operating range.
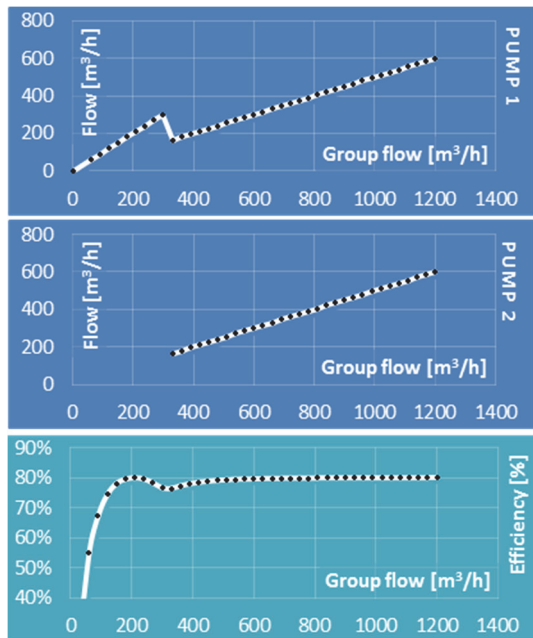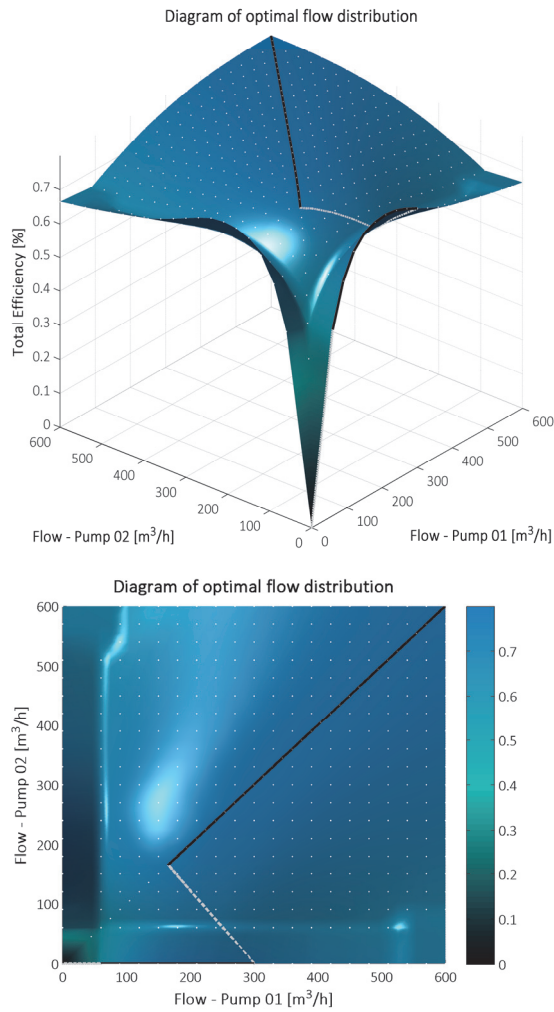
Fig. 4.4 Case study 1 – from top to bottom: 3D and 2D projection of operating space, pump flow diagrams and total efficiency diagram. Q_N = [600, 600] m³/h; η_N = [80, 80] %; H_{STN} = 80 m; H_{STsN} = 8 m;
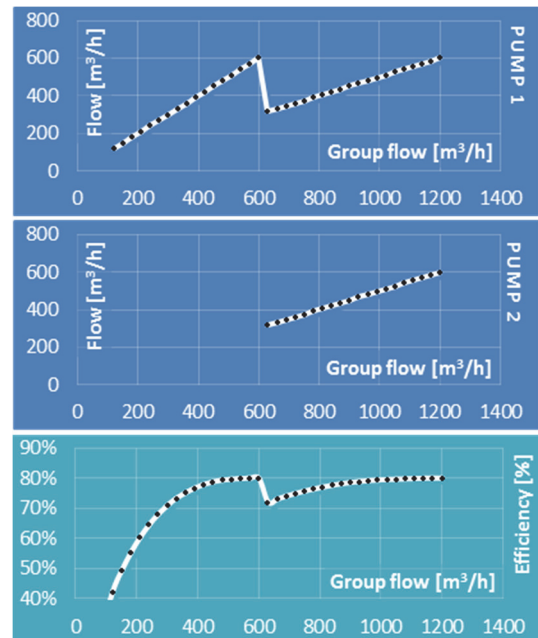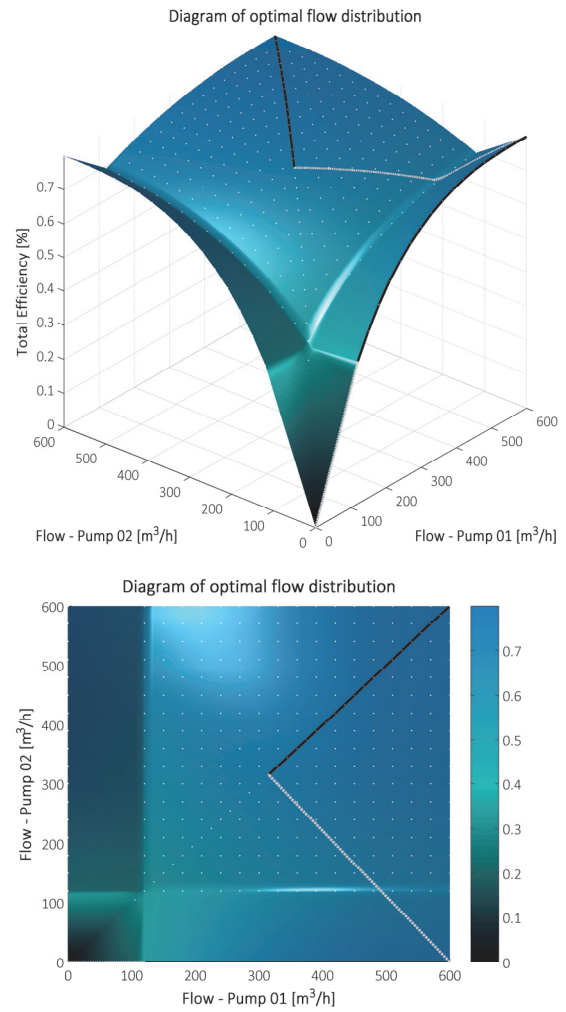
Fig. 4.5 Case study 1 – from top to bottom: 3D and 2D projection of operating space, pump flow diagrams and total efficiency diagram. Q_N = [600, 600] m³/h; η_N = [80, 80] %; H_{STN} = 80 m; H_{STsN} = 72 m;
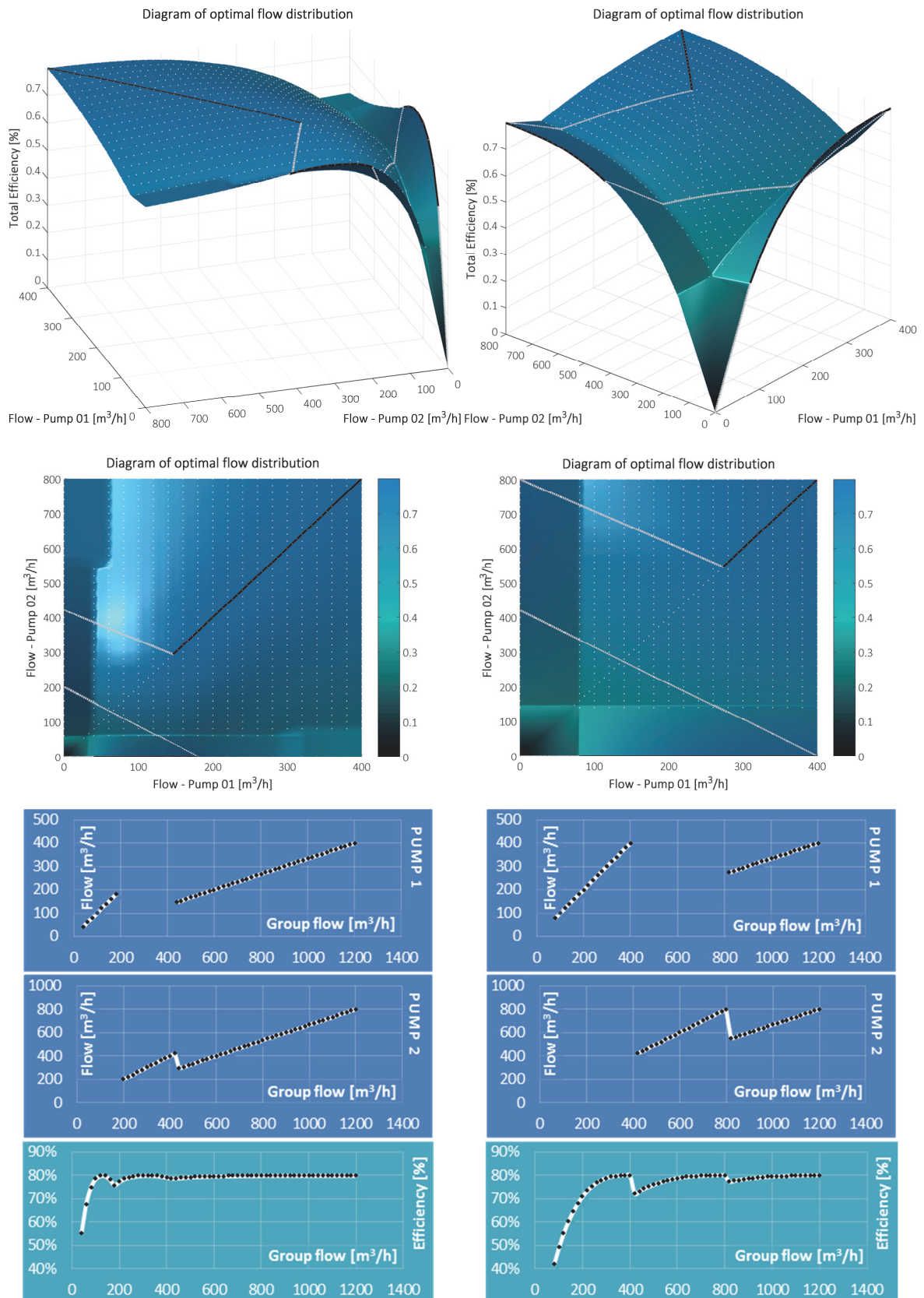
Fig. 4.6 Case study 1 – from top to bottom:
3D and 2D projection of operating space, pump
flow diagrams and total efficiency diagram.
Q_N = [400, 800] m³/h; η_N = [80, 80] %;
H_{STN} = 80 m; H_{STsN} = 8 m;

Fig. 4.7 Case study 1 – from top to bottom:
3D and 2D projection of operating space, pump
flow diagrams and total efficiency diagram.
Q_N = [400, 800] m³/h; η_N = [80, 80] %;
H_{STN} = 80 m; H_{STsN} = 72 m;
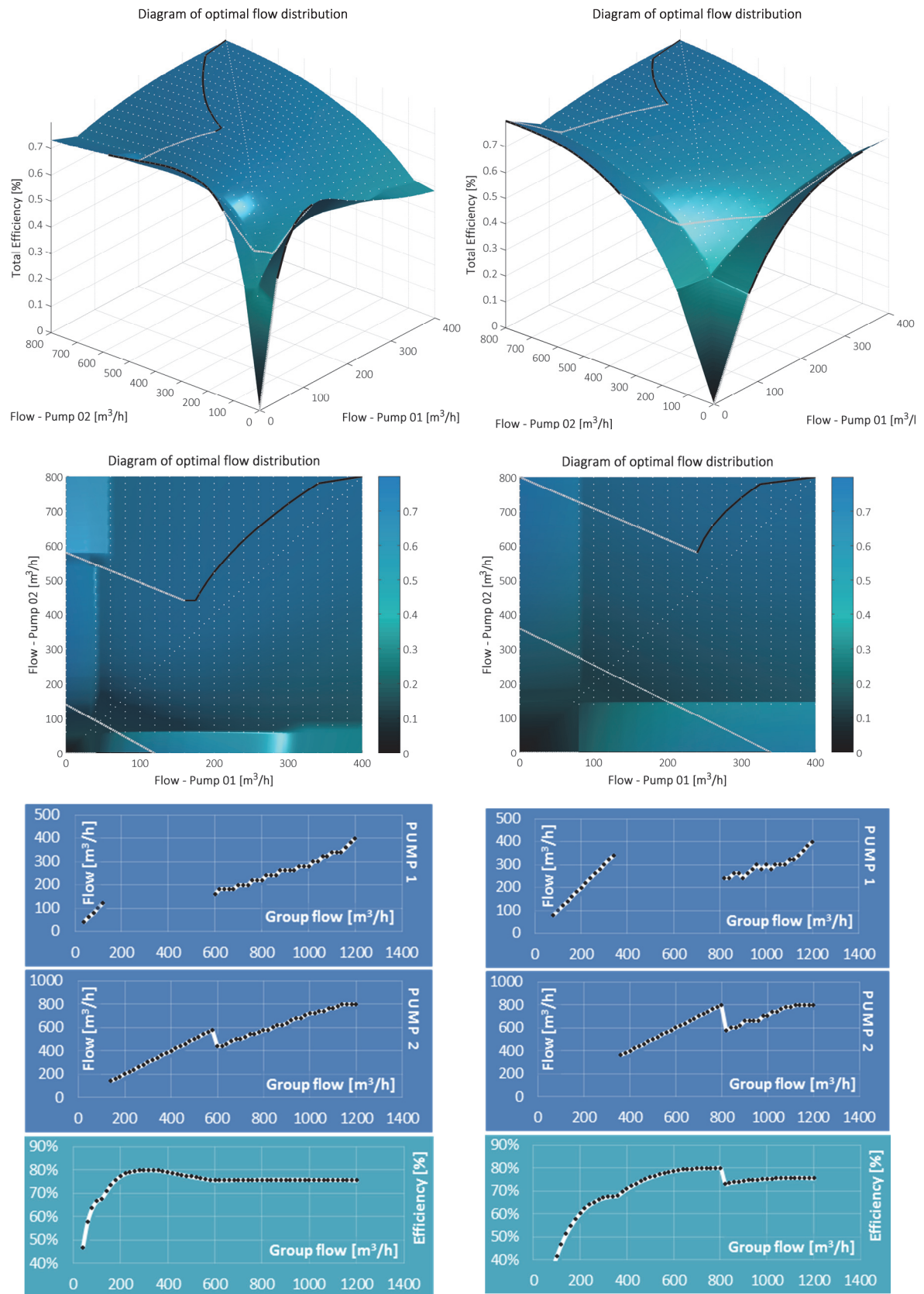
Fig. 4.8 Case study 1 – from top to bottom: 3D and 2D projection of operating space, pump flow diagrams and total efficiency diagram.
$Q_N = [400, 800]$ m³/h; $\eta_N = [68, 80]$ %;
$H_{STN} = 80$ m; $H_{STSN} = 8$ m;

Fig. 4.9 Case study 1 – from top to bottom: 3D and 2D projection of operating space, pump flow diagrams and total efficiency diagram.
$Q_N = [400, 800]$ m³/h; $\eta_N = [68, 80]$ %;
$H_{STN} = 80$ m; $H_{SsTTN} = 72$ m;

4.2.2   Case study 2 – Four pump application

4.2.2.1   *Specification*

It is considered a four-pump application working in parallel into common hydraulic system. Three variants of the application have been elaborated, differing by particular changes in the configuration to be able to make relevant comparison among each other. The specification of hydraulic system and pump group parameters and configurations is summarized in the Table 4.2. Pump performance characteristics used for the modelling are based on the identical referenced pump curves expressed in per unit values as in the former case study – see the Fig. 4.3.

The first variant presents the comparison of variable speed controlled pumps (VSC) to fixed speed controlled group of pumps in the case of hydraulic system with a zero static head. In the second variant, static head sensitivity analysis has been performed in the range of 0% to 90% of the ratio of static head on the total hydraulic system head to present the major impact of this factor and relation to optimal control and/or total efficiency curve. The last variant then presents the solution of hydraulic system with a high static head via the differently sized group of pumps with ideal and real efficiency curves.

Table 4.2 – Case study 2, Specification of hydraulic system & pumps

Hydraulic system	Var. 1	Var. 2	Var. 3	Unit
Hydraulic system				
Nominal flow	3200	3200	3200	m^3/h
Nominal total head	80	80	80	m
Nominal dynamic head	80	[80, 72, 40, 8]	8	m
Nominal static head	0	[0, 8, 40, 72]	72	m
Static / referenced head control	constant	constant	constant	
Pumps				
Number of pumps in parallel	4	4	4	
Identical pumps	yes	yes	no	
Nominal total head	80	80	80	m
Nominal flow	800	800	[400, 400, 1200, 1200]	m^3/h
Nominal efficiency	80	80	[80, 80] [68, 84]	%
Nominal speed minimal flow	160	160	[80, 240]	m^3/h

4.2.2.2   Results – Variable speed control versus throttling

Below see the comparison of variable speed controlled group of pumps (Fig. 4.10) to fixed speed group of pumps controlled via throttling (Fig. 4.11). It is clearly observable the advantage of VSC group of pumps in hydraulic systems with a zero static head – i.e. liquid circulating applications. The speed is controlled in a full range and efficiency keeps nominal in an ideal case in the contrast to fixed speed control, where the efficiency is just flow dependent. Moreover, the total efficiency in the throttling case, takes into account just the efficiency of the pump without the control efficiency.
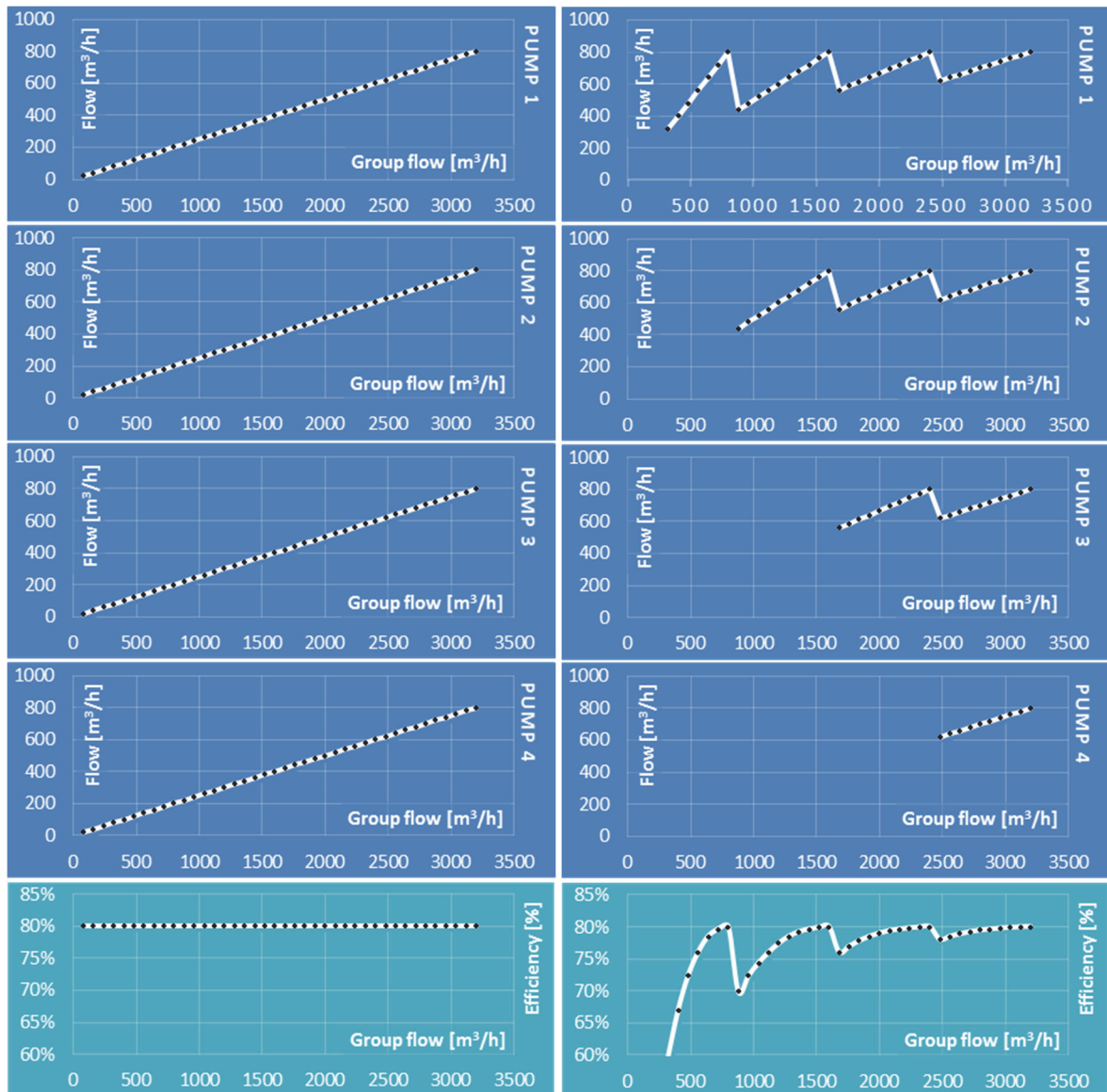
Fig. 4.10 Case study 2 – VSC,
pump operating diagrams of flow and
total efficiency.
Q_N = [800, 800, 800, 800] m³/h;
η_N = [80, 80, 80, 80] %;
H_{STN} = 80 m; H_{STsN} = 0 m;

Fig. 4.11 Case study 2 – Throttling,
pump operating diagrams of flow and
total efficiency.
Q_N = [800, 800, 800, 800] m³/h;
η_N = [80, 80, 80, 80] %;
H_{STN} = 80 m; H_{STsN} = 0 m;

4.2.2.3   Results – Static head sensitivity analysis

In this case, a static head sensitivity analysis has been performed in the range of 0% to 90% of the ratio of static head on total head – see Fig. 4.12 to Fig. 4.15. Two major effects are observed. The shifting of pump switching point from purely parallel operation to parallel cascade with the points of discontinuity close to pump nominal operating range for the highest ratio of static head. In parallel, the deformation of total efficiency curve is increasing with the ratio of static head which is caused by decreasing of speed range. Note, that although pump efficiency curve is highly no-linear, the final optimal operating diagrams shows, that simple purely parallel operation is the most efficient one for all active pumps for a case of identical pumps in a group. However, the remaining challenge is to find the optimal flow switching points in these cases.
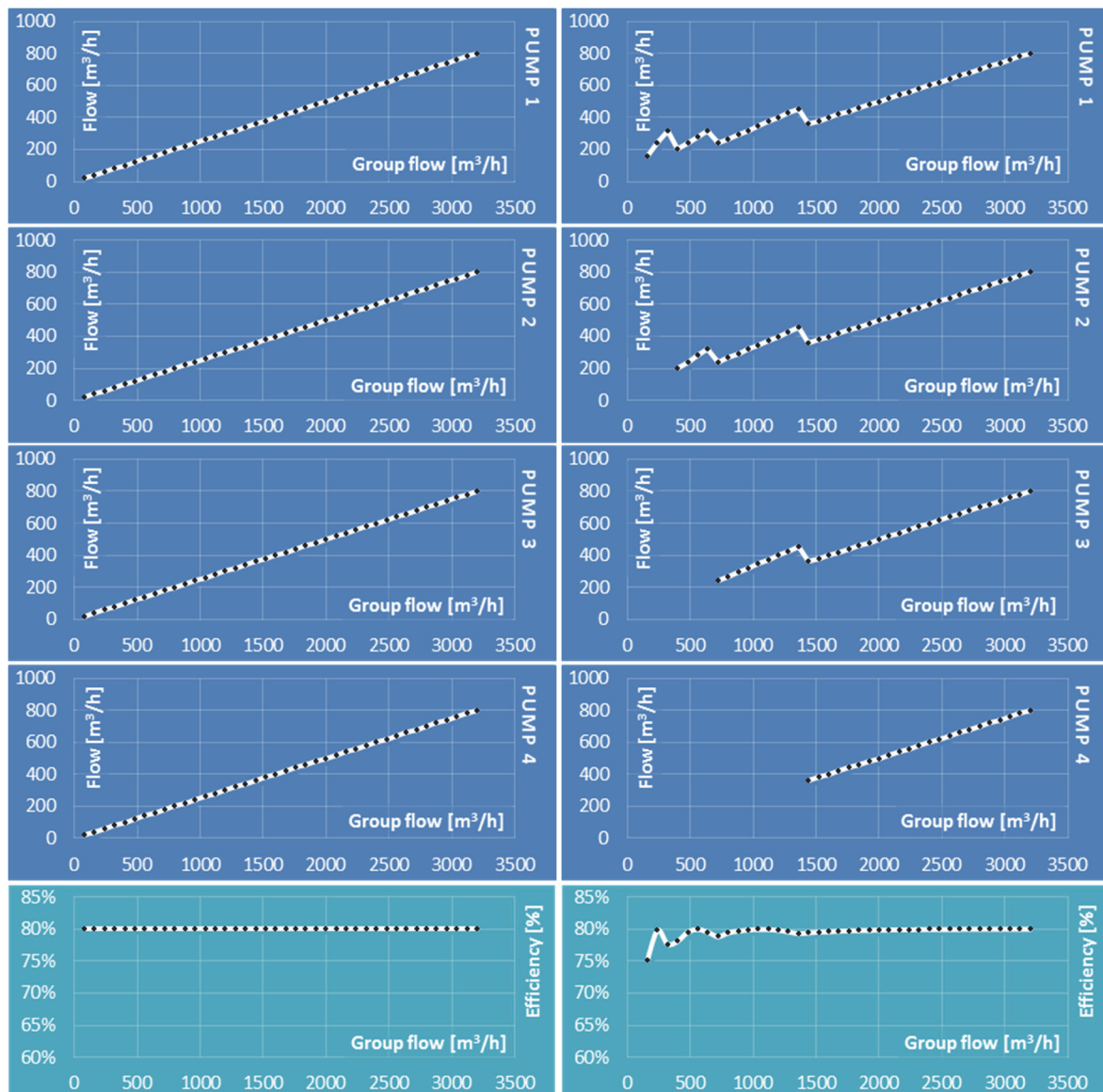
Fig. 4.12 Case study 2 – VSC,
pump operating diagrams of flow and
total efficiency.
Q_N = [800, 800, 800, 800] m³/h;
η_N = [80, 80, 80, 80] %;
H_{STN} = 80 m; H_{STSN} = 0 m;

Fig. 4.13 Case study 2 – VSC,
pump operating diagrams of flow and
total efficiency.
Q_N = [800, 800, 800, 800] m³/h;
η_N = [80, 80, 80, 80] %;
H_{STN} = 80 m; H_{STSN} = 8 m;
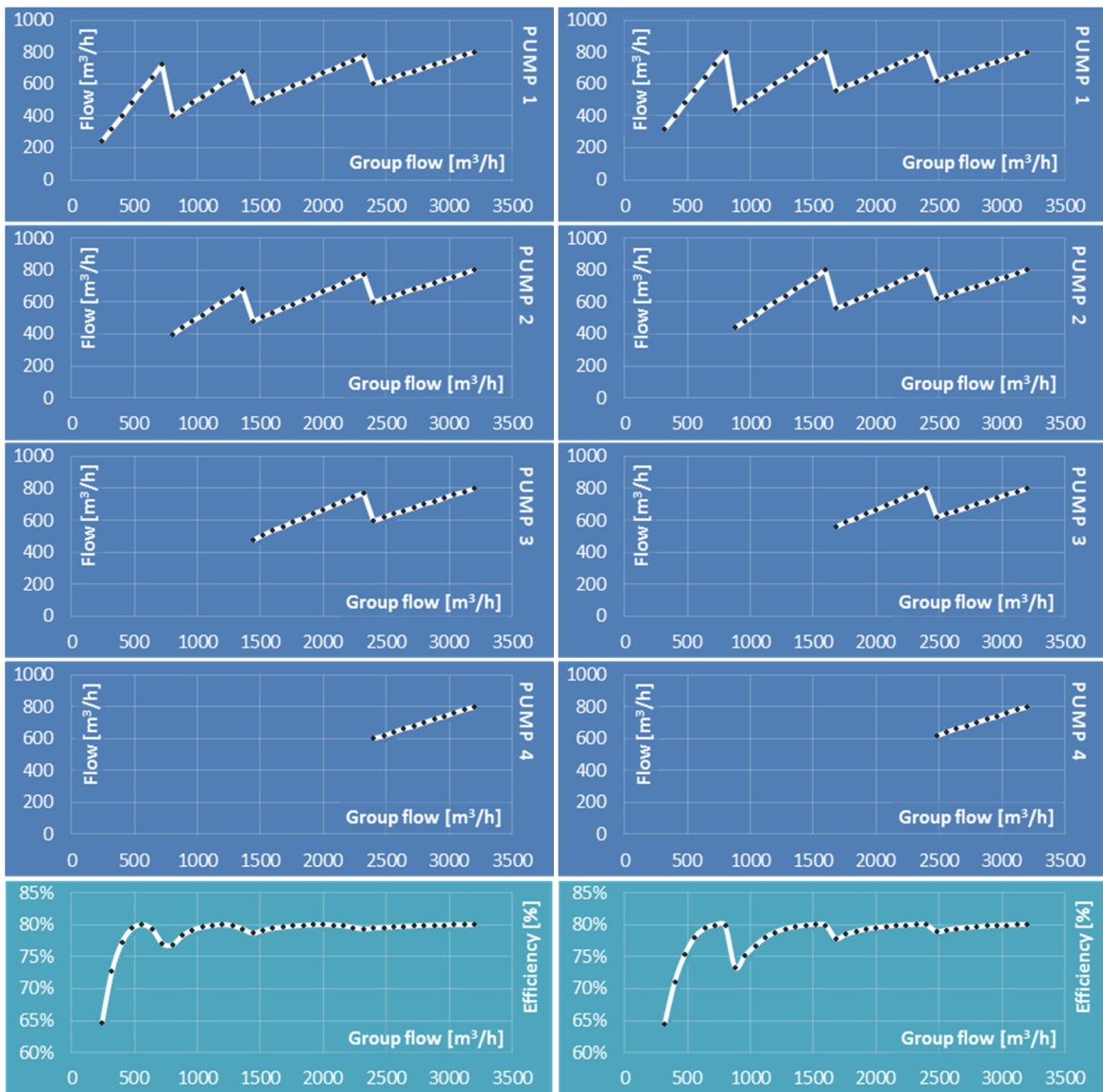
Fig. 4.14 Case study 2 – VSC,
pump operating diagrams of flow and
total efficiency.
Q_N = [800, 800, 800, 800] m³/h;
η_N = [80, 80, 80, 80] %;
H_{STN} = 80 m; H_{STsN} = 40 m;

Fig. 4.15 Case study 2 – VSC,
pump operating diagrams of flow and
total efficiency.
Q_N = [800, 800, 800, 800] m³/h;
η_N = [80, 80, 80, 80] %;
H_{STN} = 80 m; H_{STsN} = 72 m;

4.2.2.4   Results – Variation of pump group composition

The last case study variation show the effect of employment of variable sized pumps in the group. As a sample case, it has been selected the identical hydraulic system from former variant with a high static head. Instead of four identical pumps with the nominal flow rate of 800 m³/h, two subgroups of pumps with the nominal flow rate of 400 m³/h and 1200 m³/h were used. Comparing the result of variable sized pumps in the Fig. 4.16 with the former case in the Fig. 4.15, the total efficiency curve is significantly smoother with lower drops. Nevertheless, identically shaped efficiency curves with nominal value of 80% were used. In the Fig. 4.17, see the identical case with variable efficiencies of 68% or 84% for the low and high flow rate pumps.
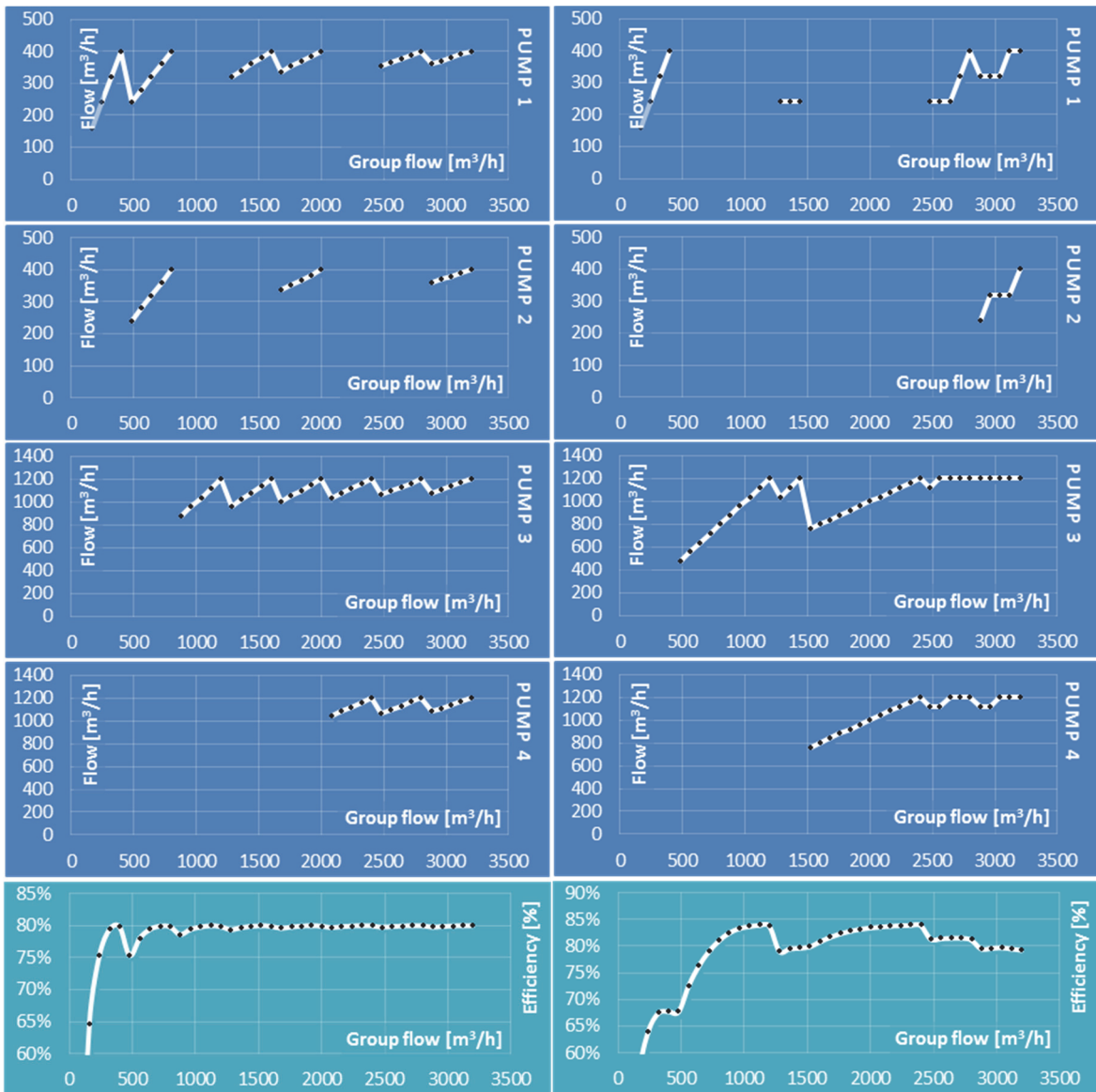
Fig. 4.16 Case study 2 – VSC,
pump operating diagrams of flow and
total efficiency.
Q_N = [400, 400, 1200, 1200] m³/h;
η_N = [80, 80, 80, 80] %;
H_{STN} = 80 m; H_{STSN} = 72 m;

Fig. 4.17 Case study 2 – VSC,
pump operating diagrams of flow and
total efficiency.
Q_N = [400, 400, 1200, 1200] m³/h;
η_N = [68, 68, 84, 84] %;
H_{STN} = 80 m; H_{STSN} = 72 m;

4.3   Conclusion for multiple pump applications with parallel control

In this part, it has been presented the developed methodology and/or algorithm for generation of an optimal control of variable speed controlled pumps working in parallel into common hydraulic system. The presented algorithm is based on numerical optimization method using brute force approach, which enabled to solve the highly non-linear multidimensional optimization task in a reasonable precision.

In the first part, it has been described the optimal control algorithm itself, including flow chart-diagram and mathematical background for evaluation of flow state space and related quantities – especially vector of pump speeds and total efficiency for each generated flow state vector. Due to exponential demand on calculation power increasing with the number of pumps and/or flow state dimension, special attention has been paid to cases of group of pumps consisting from subgroups of identical pumps, which is the very often case in practice. A simplified solution has been observed in these restricted cases, which sped-up the calculation process and/or enable to decrease the density of grid of flow states.

In the second part, the performance of developed algorithm has been presented on two case studies based on a successful application that has been solved using this algorithm. Moreover several derived variants of the cases have been evaluated and in detailed graphically presented to show especially the influence of a static head of a hydraulic system and variable sizing of pump in a pump group on an optimal control in the form of flow control diagrams. The generated optimal flow control diagrams are considered as ideal ones and further individual post processing is needed for final implementation - the points of discontinuity (pump on/off switching points) are solved by the hysteresis range and multidimensional curve fitting methodology is employed for final implementation.

5   Conclusion

The high-power pump and fan applications are among the major electricity consumers in a world-wide scale. Concurrently, these applications have a very significant energy-saving potential arising especially from development of high-power electronics and/or frequency converters allowing to employ energy-efficient variable speed flow control in contrast to especially passive flow control methods. Nevertheless, the positive effect of VSC cannot be generalized and a change causing energy or cost savings in one application can lead to just opposite in the other. One of the major barriers, preventing massive redesign of existing applications and use of the energy-saving potential in new applications, is the complexity of technical and economical evaluation of the lifetime energy savings and/or energy consumption including the entire application chain. Hence, this thesis has focused on the development of a complex set of mathematical models, methodology and software tools for especially technical evaluation and energy efficiency optimization of these systems. The impact, while designing the mathematical models and methodology, has been put on to use strictly just commonly available data (i.e. non laboratory measurement) with respect to practical use in real applications – i.e. special approximation techniques has been developed to be able to estimate the performance out of the nominal operating states that are commonly the only ones specified.

The introductory part of the work has been dedicated to the state of the art, research motivation and objectives of the work. In the second part, the attention has been paid to single pump systems. It has been described the mathematical model of hydraulic system and centrifugal pump including derivation of mathematical models representing flow control algorithms – i.e. especially the pump performance under variable speed flow control in comparison to passive and/or fixed speed flow control methods – throttling, bypass and on-off control. Then it has been presented derived mathematical models of drive components – from gearbox, over electrical motor to hydrodynamic coupling, frequency converter and transformer. Special attention has paid to approximation techniques of especially induction machine and transformer.

The second part of this thesis deals with single fan systems. It has been described mathematical model of pneumatic system and fan considering compressible medium. Then it has been presented the way of evaluation of the most common flow control techniques – flow control by inlet guide vanes, inlet damper, outlet damper, on-off control and variable flow speed control - employed for both axial and radial fans. Furthermore, a special methodology for pitch-controlled axial fans has been also presented.

Finally, based on the presented theoretical background, sophisticated tools for energy efficiency optimization of single pump and fan applications have been developed – MVD Pump Save 2012 and MVD Fan Save 2012 in their latest versions. The performance of developed mathematical models, methodology and software tools have been widely presented on evaluated case studies. Moreover, several case study variants have been elaborated to present the effect of selected important factors significantly influencing case study technical or economical results. A typical performance curves for application components have been also included as a referenced one to provide a complex set of relevant data for poorly specified case studies.

The last part of the thesis is dedicated to optimal control strategy of multiple pumps operating in parallel into common hydraulic system. It is presented the unique algorithm and/or methodology for generation of an optimal control strategy of these systems for both variable speed controlled and fixed speed controlled pumps. The presented algorithm is based on numerical optimization method using brute force approach, which enabled to solve the non-linear multidimensional optimization task. A special solution, which significantly speed-up the calculation process, for the cases of restricted space of freedom is also presented. The performance of the algorithm has been in detailed graphically presented on elaborated case studies. Additionally, the influence of a static head of a hydraulic system and the effect of variable sizing of pump in a pump group on an optimal control strategy have been presented.

The results of this thesis – especially the developed software tools MVD Pump Save 2012 and MVD Fan Save 2012 and the solution for optimal control of multiple pumps working in parallel - has been already successfully applied in practice to solve a real cases for mainly ABB and ČEZ company, which have cooperate on a testing and verification process.

5.1   Main contribution of this thesis

- Design, development and verification of a complex set of methodology and mathematical models for energy efficiency optimization of single pump applications.
- Design, development and verification of a complex set of methodology and mathematical models for energy efficiency optimization of single fan applications.
- Design, development and verification of a unique algorithm for optimal control strategy of multiple pumps operating in parallel into common hydraulic system.
- Development of special approximation techniques to improve the precision of mathematical models out of the nominal operating state using just commonly available data and nominal performance curves (i.e. non-laboratory measurements) for single pump and single fan applications.
- Collection of a complex set of typical performance curves which can be used as a referenced one to provide the relevant data in case of poorly specified case studies.
- Widely presented case studies of the typical high-power pump and fan applications.
- The developed sophisticated software tool MVD Pump Save 2012, which is used for design, optimization and technical and economical evaluation of single pump applications.
- The developed sophisticated software tool MVD Fan Save 2012, which is used for design, optimization and technical and economical evaluation of single fan applications.

5.2   Challenges for future research

- **Steam turbine drive for pump systems.** In the thesis, it has been developed mathematical models of fixed speed and/or variable speed electrical drive for pump systems. However, especially in thermal power or heating plants high power steam turbines are often employed on the site of drive. This solution is in general suitable especially for very high powers and low operating power range variation. Nevertheless, the turbine drive should be considered as an alternative and in-detail evaluated while making decision on the best possible drive as well.

- **Complex system for multiple pump applications.** The presented developed algorithm for optimal control of multiple pumps operating in parallel should be extended about the drive part to be able to perform a complex design and evaluation of both technical and economical parameters of these systems including the whole drive chain. Next way of possible research is in the task of optimal sizing and/or composition of group of pumps. Finally, the other perspective way is a research focused on the alternative algorithm for optimal control based on a continuous space using gradient and/or Newton's Raphson optimization methods. This approach would potentially decrease the computational power demand, which would enable direct implementation of the algorithm into PLC without the necessity of an offline pre-calculation. The real time evaluation would be suitable also for dynamic processes. However, the main drawbacks are especially the questionable reliability and calculation precision, which are the most important factors in high-power applications.

- **Optimal control of multiple turbines in hydro power plants.** The perspective way of the research is the extension of developed algorithm for optimal control of multiple pumps to the case of optimal control of multiple turbines, which are identical in many aspects. According to our experience, the parallel turbine control is similarly to pump systems often based just on empiric knowledge and test measurements and this area has a very significant energy efficiency optimization potential for both "grid coupled" turbine-generators and variable speed turbine-generators which have been recently employed in new and retrofit hydro power plants.

List of Figures

List of Tables

References

[1]   BP, *BP Statistical Review of World Energy 2012, Energy Charting Tool.*

[2]   ABB, Energy Efficient Design of Auxiliary Systems in Fossil-Fuel Power Plants, ABB, Inc. in collaboration with Rocky Mountain Institute.

[3]   US DoE, "Energy Efficiency and Renewable Energy, Assessment Study on Sensors and Automation in the Industries of the Future: Reports on Industrial Controls, Information Processing," 2004.

[4]   B. Ramesh, "Auxiliary Power Consumption Reduction in Thermal Power Stations," Schneider Electric, 12 2010. [Online]. Available: http://www.emt-india.net/Presentations2010/32-Power_2930Nov2010/03APC_Reduction_in_ThermalPowerStations.pdf.

[5]   WorldEnergy.org, [Online]. Available: http://pgp.worldenergy.org:8244/GraphSummary_LF.

[6]   I. J. Karassik , J. P. Messina, P. Cooper and C. C. Heald, Pump Handbook, 3rd ed., McGRAW-HILL, 2001.

[7]   S. Wang and S. Wang, Handbook of air conditioning and refrigeration, McGraw-Hill, 1993.

[8]   W. G. Taylor, "Motor Equipments for the Recovery of Petroleum," *Transactions of the American Institute of Electrical Engineers,* Vols. XXXV, no 1, pp. 539-554, Jan 1916.

[9]   E. Douville, "Selection and Application of Variable Speed Motor Drive Systems," *Industry Applications, IEEE Transactions on,* no. 6, pp. 698-702, 1982.

[10]   R. Hanna and S. Prabhu, "Medium-voltage adjustable-speed drives-users' and manufacturers' experiences," *Industry Applications, IEEE Transactions on,* vol. 33, no. 6, pp. 1407-1415, nov/dec 1997.

[11]   H. Hickok, "Adjustable Speed---A Tool for Saving Energy Losses in Pumps, Fans, Blowers, and Compressors," *Industry Applications, IEEE Transactions on,* no. 1, pp. 124-136, 1985.

[12]   D. Rice, "A suggested energy-savings evaluation method for AC adjustable-speed drive applications," *Industry Applications, IEEE Transactions on,* vol. 24, no. 6, pp. 1107-1117, 1988.

[13]   W. Stebbins, "Are you certain you understand the economics for applying ASD systems to centrifugal loads?," in *Textile, Fiber and Film Industry Technical Conference, 1994., IEEE 1994 Annual*, 1994.

[14]   S. Mircevski, Z. Kostic and Z. Andonov, "Energy saving with pump's AC adjustable speed drives," in *Electrotechnical Conference, 1998. MELECON 98., 9th Mediterranean*, 1998.

[15] R. A. Dent and Z. Dicic, "Adjustable speed drives improve circulating water system," *IEEE Transactions on Energy Conversion,* Vols. 9, no. 3, pp. 496-502, September 1994.

[16] V. Kogan, J. Provanzana and J. Michalec, "An indirect approach for evaluating the availability of adjustable speed drive systems applied to large power plant motors," *Energy Conversion, IEEE Transactions on,* vol. 9, no. 1, pp. 115-125, 1994.

[17] R. A. Dent and Z. Dicic, "Adjustable speed drives improve circulating water system," *IEEE Transactions on Energy Conversion,* vol. 9, no. 3, pp. 496-502, 1994.

[18] E. Turner and C. Lemone, "Adjustable-speed drive applications in the oil and gas pipeline industry," *Industry Applications, IEEE Transactions on,* vol. 25, no. 1, pp. 30-35, 1989.

[19] J. Armintor and D. Connors, "Pumping applications in the petroleum and chemical industries," *Industry Applications, IEEE Transactions on,* no. 1, pp. 37-48, 1987.

[20] R. Carlson, "The correct method of calculating energy savings to justify adjustable frequency drives on pumps," in *Petroleum and Chemical Industry Conference, 1999. Industry Applications Society 46th Annual*, 1999.

[21] *Vorecon - Variable Speed Planetary Gear,* 2010.

[22] *MagnaDrive ASD,* http://www.magnadrive.com/magna_asd.html, 2012.

[23] H. Weiss, "Adjustable speed AC drive systems for pump and compressor applications," *Industry Applications, IEEE Transactions on,* no. 1, pp. 162-167, 1974.

[24] B. Schmitt and R. Sommer, "Retrofit of fixed speed induction motors with medium voltage drive converters using NPC three-level inverter high-voltage IGBT based topology," in *Industrial Electronics, 2001. Proceedings. ISIE 2001. IEEE International Symposium on*, 2001.

[25] J. Rodriguez, S. Bernet, B. Wu, J. Pontt and S. Kouro, "Multilevel voltage-source-converter topologies for industrial medium-voltage drives," *Industrial Electronics, IEEE Transactions on,* vol. 54, no. 6, pp. 2930-2945, 2007.

[26] S. Kouro, M. Malinowski, K. Gopakumar, J. Pou, L. G. Franquelo, B. Wu, J. Rodriguez, A. M. Perez and J. I. Leon, "Recent Advances and Industrial Application of Multilevel Converters," *Transaction on Industrial Electronics,* vol. 57, pp. 2553-2580, 2010.

[27] A. Bocquel and J. Janning, "Analysis of a 300 MW variable speed drive for pump-storage plant applications," in *Power Electronics and Applications, 2005 European Conference on*, 2005.

[28] L. Frenning, Pump life cycle costs: A guide to LCC analysis for pumping systems, Europump and Hydraulic Institute, 2001.

[29] Europump and H. Institute, Variable Speed Pumping: A Guide to Successful Applications, Elsevier Science, 2004.

[30] P. S. Matter and H. Institute, Optimizing Pumping Systems: A Guide to Improved Energy Efficiency, Reliability, and Profitability, Pump Systems Matter and Hydraulic Institute, 2008.

[31] Siemens, *SinaSave,* 2013.

[32] ABB, *Energy Saving Tools,* 2012.

[33] P. S. Matter, *PSIM - Pump System Improvement Modeling Tool,* 2006.

[34] Z. Yang and H. Borsting, "Energy efficient control of a boosting system with multiple variable-speed pumps in parallel," in *Decision and Control (CDC), 2010 49th IEEE Conference on*, 2010.

[35] Z. Yang and H. Borsting, "Optimal scheduling and control of a multi-pump boosting system," in *Control Applications (CCA), 2010 IEEE International Conference on*, 2010.

[36] E. da Costa Bortoni, R. de Almeida and A. Viana, "Optimization of parallel variable-speed-driven centrifugal pumps operation," *Energy Efficiency,* vol. 1, no. 3, pp. 167-173, 2008.

[37] M. Massoud, Engineering Thermofluids, Thermodynamics, Fluid Mechanics, and Heat Transfer, Sp, 2005.

[38] ČEPS a.s., *Databáze - výroba elektrické energie v ČR.*

[39] J. Tuzson, Centrifugal Pump Design, John Wiley & Sons, 2000.

[40] P. S. Georgilakis, Spotlight on modern transformer design, London: Springer, 2009.

[41] M. McPherson, "Introduction of fluid mechanics," in *Subsurface Ventilation and Environmental Engineering*, Springer Netherlands, 1993, pp. 15-49.

[42] G. K. Batchelor, An introduction to fluid dynamics, Cambridge university press, 2000.

[43] G. Ludwig, S. Meschkat and B. Stoffel, "Design Factors Affecting Pump Efficiency," in *Energy Efficiency in Motor Driven Systems*, F. Parasiliti and P. Bertoldi, Eds., Springer Berlin Heidelberg, 2003, pp. 532-538.

[44] VOITH, *Hydrodynamic coupling,* 2010.

Author's publications

List of author's publications presented at international conferences

[A1] M. Sirovy, Z. Peroutka, „Energy efficient pump systems for high power industrial applications: VSDs for group control of multiple pump units in parallel," *IECON 2014 - 40th Annual Conference on IEEE Industrial Electronics Society*, Dallas, USA, 2014 [submitted for review].

[A2] M. Sirovy, Z. Peroutka, M. Byrtus a J. Michalik, „Medium voltage drive fan save: Energy efficient fan systems in power engineering, Part 2: Variable Pitch Flow Control versus Variable Speed Flow Control," *IECON 2013 - 39th Annual Conference on IEEE Industrial Electronics Society*, Vienna, Austria, 2013.

[A3] M. Sirovy, Z. Peroutka, J. Michalik a M. Byrtus, „Medium voltage drive fan save: Energy efficient fan systems in power engineering, Part 1: Radial fans," *IECON 2012 - 38th Annual Conference on IEEE Industrial Electronics Society*, Montreal, Canada, 2012.

[A4] M. Sirovy, Z. Peroutka, J. Molnar, J. Michalik a M. Byrtus, „Variable speed pumping in thermal and nuclear power plants: Frequency converter versus hydrodynamic coupling," *Power Electronics and Drive Systems (PEDS), 2011 IEEE Ninth International Conference on*, Singapore, 2011.

[A5] M. Sirovy, Z. Peroutka, J. Molnar, J. Michalik a M. Byrtus, „Sophisticated software for design and optimization of variable speed drives for high-power pumps: Hydrodynamic coupling versus frequency converter," *IECON 2011 - 37th Annual Conference on IEEE Industrial Electronics Society*, Melbourne, Australia, 2011.

[A6] M. Sirovy, Z. Peroutka, J. Molnár, J. Michalik a M. Byrtus, „Flow control methods in thermal power plants: Energy efficiency evaluation," *17th International Conference on ELECTRICAL DRIVES and POWER ELECTRONICS Proceedings*, Stará Lesná, Slovakia, 2011.

[A7] M. Sirovy, Z. Peroutka, J. Molnar, J. Michalik, M. Byrtus a P. Wikstroem, „Sophisticated software for design and optimization of VSDs for high-power pumps: Variable speed drive with frequency converter," *Power Electronics and Motion Control Conference (EPE/PEMC), 2010 14th International*, Ohrid, Macedonia, 2010.

[A8] M. Sirovy, J. Zak a Z. Peroutka, „Educational project of an interactive model of a photovoltaic power plant," *IPEC, 2010 Conference Proceedings*, Singapore, 2010.

[A9] A. Frick, A. Messner, F. Rüdiger a M. Sirovy, „Thermodynamic monitoring of rotating machines for the optimization of the electrical balance of plant (eBoP)," *Power-Gen Europe 2009*, Cologne, Germany, 2009.

List of author's proceedings presented at national conferences

[A10] J. Sadský a M. Sirový, „Využití simulačního programu Dymola v elektrotechnice,"
Elektrotechnika a informatika 2012, Nečtiny, 2012.

[A11] M. Sirový a Z. Peroutka, „Metody řízení průtoku pro čerpací systémy v tepelných
elektrárnách: Evaluace případové studie," *Elektrické pohony, XXXII. Konference*, Plzeň, 2011.

[A12] M. Sirový, „Educational project of an interactive model of a photovoltaic power plant: Solar
tracker versus fixed position station," *Elektrotechnika a informatika 2011*, Nečtiny, Czech
Republic, 2011.

[A13] M. Sirový a D. Vošmik, „Simulátor fotovoltaických článků: Laboratorní měření účinnosti
měničů pro FVE," *Elektrotechnika a informatika 2010*, Nečtiny, 2010.

[A14] D. Vošmik a M. Sirový, „Simulátor fotovoltaických článků: Hardwarové řešení a
implementace algoritmu řízení do DSP," *Elektrotechnika a informatika 2010*, Nečtiny, 2010.

[A15] M. Sirovy, „Regulace vybraných pohonů v energetice," *Elektrotechnika a informatika 2009*,
Nečtiny, 2009.

[A16] M. Sirovy, „Příprava a vypracování projektové dokumentace MVE," *řehlídka studentských
odborných prací na FEL, ZČU*, Plzeň, 2008.

[A17] M. Sirovy, „Optimalizace skupinového regulátoru turbín pro malé vodní elektrárny,"
Elektrotechnika a informatika 2008, Nečtiny, 2008.

[A18] M. Sirovy, „Moderní způsoby projektování a řízení MVE," *Cena ČEZ*, Praha, 2008.

List of author's functional samples and prototypes

[A19] M. Sirový, J. Sadský, *Funkční vzorek systému pro řízenou distribuci výkonu z FVE stanice,
2013.*

[A20] M. Sirový, J. Sadský, *Funkční vzorek automatizované stanice pro měření elektrických veličin
ve výkonovém rozsahu 3x 10 - 1000W, 2013.*

[A21] M. Sirový, *Funkční vzorek fotovoltaické mikroelektrárny se systémem sledování slunce, 2012.*

[A22] M. Sirový, *Funkční vzorek automatizovaného měřicího systému pro určení provozních
charakteristik vodních turbín, 2012.*

[A23] M. Sirový, *Zapojení obvodů pro automatizované měření evropské účinnosti fotovoltaických
měničů, 2011.*

[A24] M. Sirový, *Funkční vzorek vyhodnocovací jednotky pro měření účinnosti polohovatelných FVE systémů,* 2011.

[A25] M. Sirový, *Funkční vzorek řídící jednotky pro skluzovou váhu,* 2011.

[A26] D. Vošmik, M. Sirový a J. Molnár, *Výkonový emulátor fotovoltaických článků,* 2010.

[A27] M. Sirový, *Funkční vzorek systému pro analýzu účinnosti FVE systémů v kooperaci s volitelnými typy zátěže,* 2010.

[A28] M. Sirový, *Funkční vzorek pro měření a srovnání účinnosti jednoosých horizontálních FVE systémů,* 2010.

List of author's pilot plants

[A29] M. Sirový, *Univerzální řídící systém pro MVE Husinec, Šebelův mlýn,* 2009.

List of author's software

[A30] M. Sirový, Z. Peroutka, J. Michalík a M. Byrtus, *MVD Fan Save 2013,* 2013.

[A31] M. Sirový, Nástroj pro výpočet optimálního řízení paralelně pracujících čerpadel, 2013.

[A32] M. Sirový, Nástroj pro výpočet optimálního řízení paralelně pracujících čerpadel - specializace na 2D systémy, 2013.

[A33] M. Sirový, Z. Peroutka, J. Michalík, J. Molnár a M. Byrtus, *MVD Pump Save 2012,* 2012.

[A34] M. Sirový, Z. Peroutka, J. Michalík, J. Molnár a M. Byrtus, *MVD Fan Save 2012,* 2012.

[A35] M. Sirový, Z. Peroutka, J. Michalík, J. Molnár a M. Byrtus, *Medium Voltage Drive Pump Save,* 2010.

[A36] M. Sirový, Z. Peroutka, J. Michalík, J. Molnár a M. Byrtus, *Medium Voltage Drive Fan Save,* 2010.

[A37] M. Sirový, Z. Peroutka, J. Michalík, J. Molnár a M. Byrtus, *VSD Calc,* 2009.

List of author's research reports

[A38] M. Sirový, Z. Peroutka, J. Michalík a M. Byrtus, *MVD Fan Save User Guide - Advanced version,* 2013.

[A39] M. Sirový, Z. Peroutka, J. Michalík a M. Byrtus, *MVD Pump Save User Guide - Advanced version,* 2013.

[A40] M. Sirový, *Preliminary analysis and optimal control diagram algorithm for parallel pump operation,* 2012.

[A41] Z. Peroutka, J. Michalík, M. Byrtus, J. Sadský a M. Sirový, *MVD Pump Save 2012 - Visual Standards,* 2012.

[A42] Z. Peroutka, J. Michalík, M. Byrtus, J. Sadský a M. Sirový, *MVD Pump Save 2012 - Functional specification of user interface for testers & developers,* 2012.

[A43] Z. Peroutka, J. Michalík, M. Byrtus, J. Sadský a M. Sirový, *MVD Pump Save 2012 - Case Study Testing Specification,* 2012.

[A44] Z. Peroutka, J. Michalík, J. Molnár, M. Byrtus a M. Sirový, *MVD Pump & Fan Save: User Guide - Basic Version,* 2012.

[A45] Z. Peroutka, J. Michalík, J. Molnár, M. Byrtus a M. Sirový, *MVD Pump & Fan Save: Calculation Background ,* 2012.

[A46] Z. Peroutka, J. Michalík, M. Byrtus, J. Sadský a M. Sirový, *MVD Fan Save 2012 - Visual Standards,* 2012.

[A47] Z. Peroutka, J. Michalík, M. Byrtus, J. Sadský a M. Sirový, *MVD Fan Save 2012 - Functional specification of user interface for testers & developers,* 2012.

[A48] Z. Peroutka, J. Michalík, M. Byrtus, J. Sadský a M. Sirový, *MVD Fan Save 2012 - Case Study Testing Specification,* 2012.

[A49] Z. Peroutka, J. Michalík, J. Molnár, M. Byrtus a M. Sirový, *Comparative Study Of Variable Speed Drives In Power Systems; Part 4: VSD Calc - User Guide,* 2009.

[A50] Z. Peroutka, J. Michalík, J. Molnár, M. Byrtus a M. Sirový, *Comparative Study Of Variable Speed Drives In Power Systems; Part 3: Case Studies,* 2009.

[A51] Z. Peroutka, J. Michalík, J. Molnár, M. Byrtus a M. Sirový, *Comparative Study Of Variable Speed Drives In Power Systems; Part 2: Metodology Of Drive Design,* 2009.

[A52] Z. Peroutka, J. Michalík, J. Molnár, M. Byrtus a M. Sirový, *Comparative Study Of Variable Speed Drives In Power Systems; Part 1: General Problems,* 2009.

Appendix 1 – MVD Pump Save 2012

The software tool Medium-Voltage Drive Pump Save 2012 has been developed in order to provide sophisticated comparison of operational and economical features (e.g. operational costs, payback period or lifetime energy calculations) for various types of pump flow control methods. The tool takes into account the whole application chain - from hydraulic system and pump over a drive to power supply network – to provide a complex analysis of selected variants. As a standard variant, it is considered variable speed flow control driven by electrical motor supplied from frequency converter, which is being compared to other flow control techniques. In the latest version, it is implemented variable speed control realized by fixed speed electrical motor and hydrodynamic coupling and collection of passive flow control methods – throttling, bypass and on-off control. The important feature of the software tool is the ability to approximate behavior under variable speed control using just nominal performance curves or even nominal operating points for poorly specified cases. Moreover, a default case study is integrated in the tool to guide user over the case study evaluation process. Below see the interesting numbers from the software development. More in-detailed description is available especially in [A33] and [A39 − A45].

- Number of scalar variables between the user interface and calculation core: 2 440
- Number of rows of code: 33 889
- Development history: 5 years
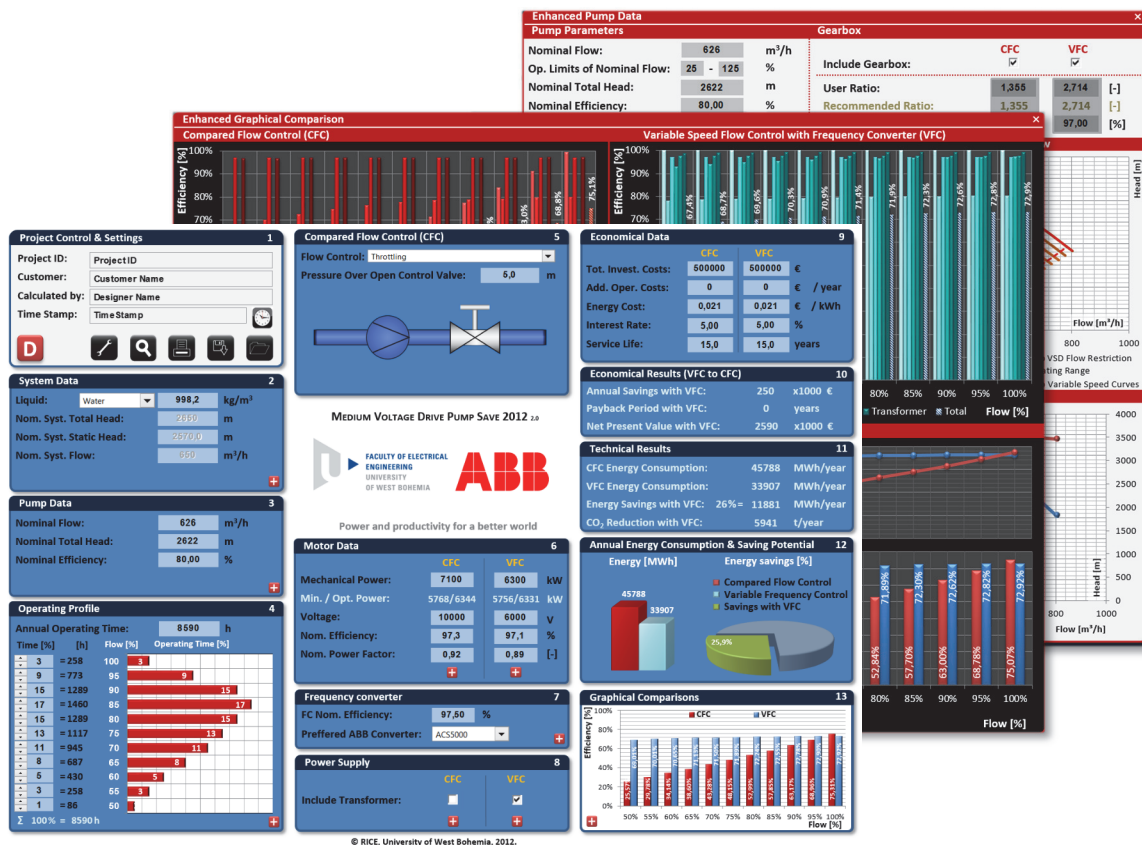
Illustrative screenshots of MVD Pump Save 2012

Appendix 2 – MVD Fan Save 2012

The software tool Medium-Voltage Drive Fan Save 2012 has been developed in order to provide sophisticated comparison of operational and economical features (e.g. operational costs, payback period or lifetime energy calculations) for various types of fan flow control methods. The tool takes into account the whole application chain - from pneumatic system and fan over a drive to power supply network – to provide a complex analysis of selected variants. As a standard variant, it is considered variable speed flow control driven by electrical motor supplied from frequency converter, which is being compared to other flow control techniques. In the latest version, it is implemented variable speed control realized by fixed speed electrical motor and hydrodynamic coupling and collection of passive flow control methods – inlet guide vanes, inlet damper, outlet damper and on-off control for radial fans and additionally pitch control for axial fans. The important feature of the software tool is the ability to approximate behavior under variable speed control using just nominal performance curves or even nominal operating points for poorly specified cases. Moreover, a default case study is integrated in the tool to guide user over the case study evaluation process. Below see the interesting numbers from the software development. More in-detailed description is available especially in [A34] and [A38, A44 – A48].

- Number of scalar variables between the user interface and calculation core: 3 060
- Number of rows of code: 42 797
- Development history: 3 years
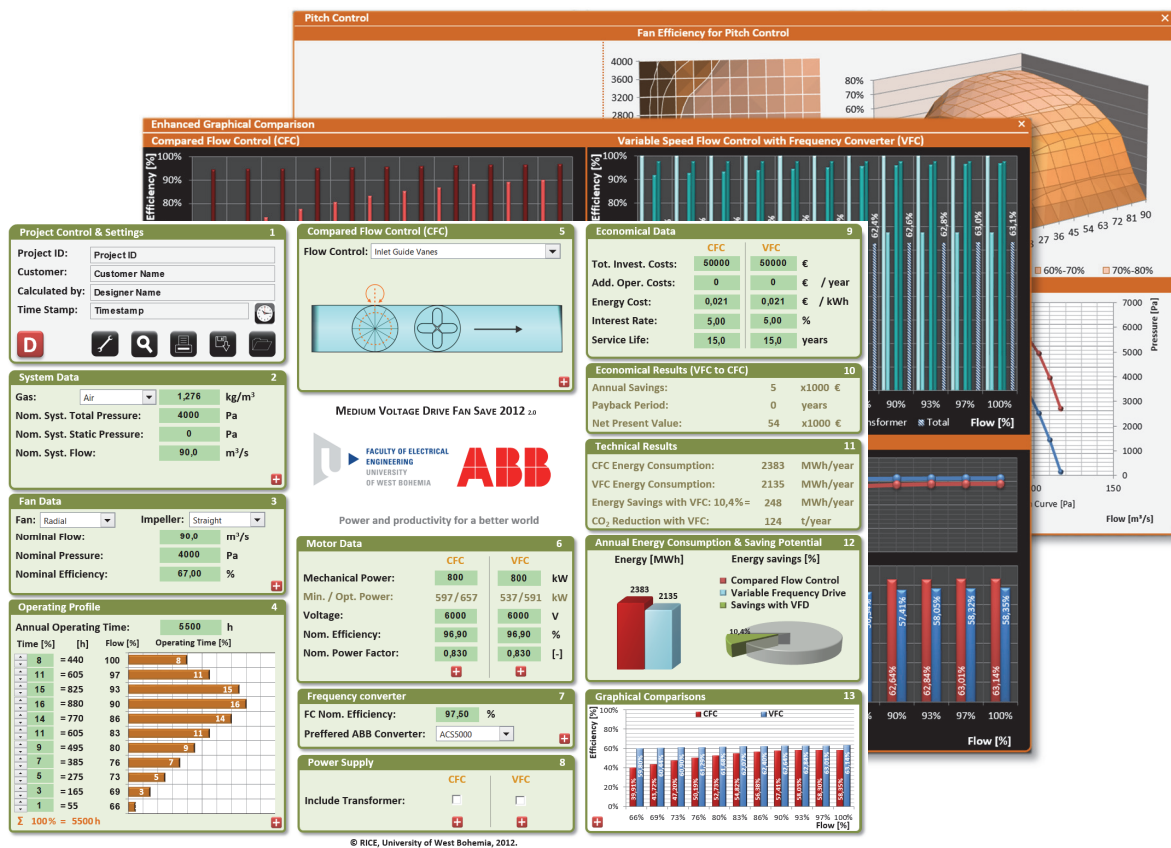
Illustrative screenshots of MVD Fan Save 2012